Functional Genomics of Bacterial and Fungal Biocontrol Agents

for Biotechnological Applications

by

Albert Remus R. Rosana

A thesis submitted in partial fulfillment of the requirements for the degree of

Doctor of Philosophy

Department of Chemistry
University of Alberta

Abstract

Microbial-based biotechnologies were developed using combinations of functional genomics, biochemical tools, and a tripartite pine tree-beetle-fungal infection model. Several bacterial and fungal species were probed for natural product biosynthesis potential using whole genome sequencing while mycoinsecticides formulations were developed for the biocontrol of the epidemic of invasive mountain pine beetle, *Dendroctonus ponderosae*.

The novelty of six environmental *Bacillus* isolates were established using whole genome sequencing and comparative genomics. The isolates were phylogenetically classified as *Bacillus thuringiensis* DNG9, *Bacillus velezensis* F11, *Bacillus cereus* E41, *Bacillus anthracis* F34, *Bacillus paralicheniformis* F47, and *Bacillus licheniformis* SMIA-2. Functional genomics revealed an arsenal of gene inventories supporting the production of putative bioactive molecules such as lanthipeptides, sactipeptides, lassopeptides, thiopeptides, and lipopeptides. The antimicrobial potential of the organic extracts of the isolates revealed potent activity against several indicator pathogenic microorganisms, especially relevant members of the WHO's ESKAPE bacterial group associated with antimicrobial resistance. Targeted antibacterial activity-guided purification and tandem mass spectrometry revealed two fengycin lipopeptides, supported by the *fenABCDE* operon in *B. velezensis* F11. Evolutionary comparative genomics further supported the phylogenetic placement of the six isolates in either the *B. cereus* or *B subtilis sensu lato* group.

The extremophilic novel actinobacterium, *Streptomyces* sp. AI-08, was isolated from volcanic soils. The antimicrobial assay of the ethyl acetate extract from spent fermentation medium supports a wide spectrum of antibacterial, antifungal and anti-colorectal cancer activity. The draft genome sequence was established and whole genome sequence-based phylogenetic analysis

supported a novel species closely related to *Streptomyces olivaceus* NRRL B-3009^T. Functional genomics revealed a total of 48 biosynthetic gene clusters were predicted which may support the observed biological activity. The speciation of *Streptomyces* sp. nov. A1-08 was proposed.

Morphological and biochemical characterization of ~93 strains of *Beauveria bassiana,* representing Canada- and world-wide collections, was established for evaluation of virulence against the mountain pine beetle (MPB). The fungal strains were screened for UV-light resistance, monoterpene tolerance, and desiccation tolerance to account for the major abiotic factors that could potentially limit the efficacy of the fungal species in the environment. The strains were categorized based on virulence factor production, conidial density, and myceliation rate. Although the fungus can colonize other non-target insects, *in-vivo* honeybee infection model revealed ~5% mortality, representing the natural death rate of the hive population. Conversely, laboratory results indicated 100% killing effect and mycosis against laboratory-reared and field-collected MPBs.

Beauveria bassiana-based mycoinsecticide formulations were tested under relevant *in planta* and *in natura* conditions. An industrial level biphasic liquid-solid fermentation was employed to access suitable conidial biomass for large scale MPB infection assays. Greenhouse-based MPB *in planta* infection assays supported a strain- and concentration-dependent killing and mycosis while *in natura* field pine forest application significantly reduced the reproductive success of MPB, perturbing the life cycle for at least one season. The mechanism of efficacy of the mycoinsecticides, under *in planta* and *in natura* conditions, was probed using functional genomics and *in vivo* fungal community interaction challenges. This is the first account supporting the efficacy of field application of *B. bassiana* as a biological control agent of MPB in Western Canada.

Preface

The contents of Chapter 2 were published as Daas*, Rosana*, et al. *Stand. Gen. Sci.* **2018**, *13*, 1-10. This was a collaborative project with declared equal contributions (*) from myself and the visiting PhD student, Mohamed Seghir Daas. Dr. Daas was responsible for isolating the bacterium and jointly worked with me on its purification. I performed all the experiments with assistance from the other authors, specifically the whole genome sequencing, morphological and biochemical analysis, comparative genomics and database curation. I wrote the manuscript.

Studies described in Chapter 3 were published as Daas*, Acedo*, Rosana*, et al. *FEMS. Microbiol. Lett.* **2018**, *365*, 1-9. This is collaborative project with declared equal contributions (*) from Dr. Mohamed Seghir Daas, Dr. Jeella Acedo, and myself. Dr. Daas isolated the bacterium while Dr. Acedo was responsible for the lipopeptide purification and elucidation. I performed the molecular identification of the bacterial isolate, morphological and biochemical assays, whole genome sequencing, comparative genomics, and functional genomics. I helped in the antimicrobial screening assays and wrote the manuscript sections pertaining to the above experimentals.

The studies in Chapters 4 were published in three separate manuscripts, namely: 1) Daas*, Rosana*, et al. *Genome Announc.* **2017**, *5*, e00383-17; 2) Daas*, Rosana*, et al. *Genome Announc.* **2018**, *6*, e00190-18; and 3) Bernardo, Rosana†, et al. *Microbiol Res Annouc*. **2020**, 9*, e00106-20. These are collaborative projects with declared equal contributions (*) with Dr. Mohamed Seghir Daas or corresponding authorship (†) with Dr. Samara Pinto Custodio Bernardo. I performed the isolate purification, DNA purification, whole genome sequencing, functional genomics, antimicrobial screening with the aid of the other authors. I wrote the manuscripts.

Parts of the studies in Chapter 5 have been published as Oliveros*, Rosana*, et al. *Phil. J. Sci,* **2021**, *150*, 1351-1377. This is a collaborative project with declared equal contributions (*)

and co-corresponding authorship with Kristel Mae P. Oliveros. Ms. Oliveros isolated the actinomycetes and performed antimicrobial and anti-cancer screening under my direction. I performed the whole genomes sequencing, functional genomics, comparative genomics. I helped secured the project funding and wrote the manuscript sections pertaining to the above experimentals.

The studies in Chapter 6 were published as Rosana et al. *Appl. Microbiol. Biotechnol*. **2021**, *105*, 2541-2557. This is a collaborative project with the research groups of Drs. Nadir Erbilgin, Joerg Bohlmann, and Allan Carroll. The live mountain pine beetle (MPB) was supplied by Dr. Jennifer Klutsch (Erbilgin Lab). The parallel large-scale MPB infection assay was performed with Dr. Stanley Pokorny (Caroll Lab). I performed most of the experimental work including the global collection of fungi, culture maintenance, conidial production and infection assays with the aid of the other authors. I wrote the manuscript.

Lastly, Chapter 7 is an unpublished work. This is a collaborative project with the research groups of Drs. Allan Carroll, Nadir Erbilgin, Joerg Bohlmann, Silvia Todorova and Tarryn Goble. I designed, led and executed the greenhouse and fermentation works with the assistance of Kleinberg Fernandez and Guncha Ishangulyyeva. The field experimental work was led by Dr. Stanley Pokorny with the assistance of myself, Kleinberg Fernandez, Lucas Feng, Amanda, Wayne Vuong, and Dr. Bethan Donelly.

Acknowledgement

I would like to extend my deepest appreciation and sincerest gratitude to the many individuals who contributed to the successful completion of this chapter in my life. These individuals deserved my humble gratitude that made this thesis possible.

First and foremost, to Dr. John C. Vederas, for providing the opportunity to conduct research under his guidance. His unreserved support and encouragement allowed me to continue the program and culminate this endeavour. The research environment and laboratory resources provided in the Vederas group ensure research productivity as well as learning and professional growth. My supervisory committee members, Drs Julianne M. Gibbs and Matthew S. Macauley, for their valuable suggestions and advice. I am also thankful to Drs. Michael Gänzle, Lynn McMullen and Robert Jordan for serving in my candidacy and/or defense committee. I am also grateful to Dr. Bradley S. Moore for serving as my external examiner in the final defense. I am also grateful to Kleinberg Fernandez, Dr. Bethan Donnelly, and Dr. Marco J. van Belkum for proofreading this thesis. All their suggestions and inputs were highly appreciated for the improvement and timely completion of this thesis. I am forever grateful to the following fellowship and scholarship bodies for supporting my graduate studies: Vanier NSERC Canada Graduate Scholarship, Alberta Innovate -Technology Futures, NSERC CGS-D3 Alexander Graham Bell Award, UA President's Doctoral Prize, UA Doctoral Recruitment, Izaak Walton Killam Memorial Scholarship, and Dorothy J. Killam Memorial Graduate Prize.

At this junction, I would also like to acknowledge several individuals who, in one way or another, became instrumental in the success of my graduate studies. To Dr. George W. Owttrim for lending me several of your molecular biology tools as well as providing personal and professional advice. To Drs. Mohammed Seghir Daas, Jeella Z. Acedo, and Samara Pinto Custodio Bernardo, as well as Prof. Kristel Mae P. Oliveros, I am very grateful for the opportunity to collaborate and work with all of you on several extremophilic bacterial isolates. Merci, Salamat, Obrigado, Dios mabalos!

Table of Contents

List of Tables

List of Figures

List of Abbreviations

16S	16 Svedberg
AAI	Average Amino acid Identity
AF	Alignment Fraction
AMR	Antimicrobial resistance
ANCOVA	ANalysis of COVAriance
ANI	Average Nucleotide Identity
ANOVA	Analysis of Variance
ANT	Anatis Bioprotection
antiSMASH	antibiotics and Secondary Metabolite Analysis Shell
API	Analytical Profile Index
ARSEF	Agricultural Research Service Collection of Entomopathogenic Fungal Cultures
asb	petrobactin (gene loci)
ASTM	American Society for Testing and Materials
ATCC	American Type Culture Collection
BAGEL	BActeriocin GEnome mining tooL
BASys	Bacterial Annotation System
BGC	Biosynthetic Gene Cluster
BHI	Brain Heart Infusion
BIOTECH	National Institute of Molecular Biology and Biotechnology
BLASTP	Basic Local Alignment Search Tool Protein
bp	base pairs
BPGA	Bacterial Pan Genome Analysis

BSF	Blue Stained Fungus(i)
Bt	*Bacillus thuringiensis*
CASSIS	Cluster ASSignment by Island Sites
CDAYE	Czapek Dox Agar Yeast Extract
CDBYE	Czapek Dox Broth Yeast Extract
CDS	coding sequence
CFM	Croatian Fermentation Medium
CFU	Colony Forming Units
CGViewer	Comparative Genomics Viewer
CHE-CNRCB	Coleccion de Hongos Entomopatogenos del Centro Nacional de Referencia de Control Biologico
CLSI	Clinical and Laboratory Standard Institute
C/N	Carbon to Nitrogen ratio
COG	Clusters of Orthologous Genes
CRISPR	Clustered Regularly Interspaced Short Palindromic Repeats
cry	Crystal (gene loci)
CVM	Croatian Vegetative Medium
DDBJ	DNA Data Bank of Japan
dDDH	digital DNA:DNA hybridization
DNA	Deoxyribonucleic acid
DSM	Deutsche Sammlung von Mikroorganismen
EDTA	ethylene diamine tetra acetic acid
EHBA	European Honeybee Agar
ENA	European Nucleotide Archive

EPF	Entomopathogenic Fungus(i)
FA	Formic Acid
FAD	Flavin Adenine Dinucleotide
fen	fengycin (gene loci)
FTIR	Fourier Transform Infra Red
G+C	Guanine + Cytosine
gANI	genome-wide Average Nucleotide Identity
GBDP	Genome Blast Distance Phylogeny
gcs	germicidin (gene loci)
GGDC	Genome-to-Genome Distance Calculator
GO	Gene Ontology
GRAS	Generally Recognized As Safe
GTR	General Time Reversible
HSD	Honest Significant Difference
IC50	Inhibition Concentration 50
ICP-OES	Inductively-Coupled Plasma – Optical Emission Spectroscopy
IDA	Inferred from Direct Assay
IDBA-UD	Iterative De Bruijn graph *de novo* Assembler for short reads sequencing data with highly Uneven sequencing Depth.
IMG	Integrated Microbial Genomes
IMG/M	Integrated Microbial Genomes and Microbiomes
IPA	isopropanol
ISP	International *Streptomyces* Project
JGI	Joint Genome Institute

kab	kanosamine (gene loci)
kbp	kilo base pairs
LAB	Lactic Acid Bacteria
lan	lanthionine (gene loci)
LAP	Linear Azol(in)e-containing Peptides
LB	Luria-Bertani (broth)
LC-MS	Liquid Chromatography-Mass Spectrometry
lch	lichenysin (gene loci)
log	logarithmic
LT	Lethal Time
MALDI-TOF	Matrix Assisted Laser Desorption Ionization – Time of Flight
masl	meter above sea level
Mbp	Mega base pairs
MDP	Master Dilution Plate
MEA	Malt Extract Agar
MEDUSA	Multi Draft based Scaffolder
MFS	Major Facilitator Superfamily
MH	Mueller Hinton
MIBiG	Minimum Information about a Biosynthetic Gene cluster
MIC	Minimum Inhibitory Concentration
MiGA	Microbial Genome Atlas
MIGS	Minimum Information about a Genome Sequence
MiSI	Microbial Species Identifier

MOD-ACTINO	Modern Actinobacteria
MPB	Mountain Pine Beetle
MPBA	Mountain Pine Beetle Agar
MRSA	Methicillin-Resistant *Staphylococcus aureus*
MS/MS	tandem Mass Spectrometry
MST	Mean Survival Time
MTT	4,5-Dimethylthiazol 2-yl)-2,5-diphenyltetrazolium
MUCL	Mycothèque de l'Université Catholique de Louvain
NA	Nutrient Agar
NAS	Non-traceable Author Statement
NCBI	National Center for Biotechnology Information
ncRNA	non-coding ribonucleic acid
NeuRiPP	Neural Network Identification of RiPP Precursor Peptides
NRRL	Northern Regional Research Laboratory
NRPS	Non-Ribosomal Peptide Synthetase
OD	Optical Density
opS	oosporein (gene loci)
ORF	Open Reading Frame
PCR	Polymerase Chain Reaction
PDA	Potato Dextrose Agar
PDB	Potato Dextrose Broth
Pfam	Protein families
PGAP	Prokaryotic Genome Annotation Pipeline

PHA	polyhydroxyalkanoate
PHASTER	PHAge Search Tool Enhanced Release
PKS	Polyketide Synthase
PRISM	PRediction Informatics for Secondary Metabolomes
PRJNA	BioProject Number
psi	pound per square inch
RAST	Rapid Annotation Subsystems Technology
RAxML	Randomized Axelerated Maximum Likelihood
RiPP	Ribosomally-synthesized Post-translationally modified Peptides
RNA	Ribonucleic acid
RODEO	Rapid ORF Description and Evaluation Online
rpm	revolution per minute
RP-HPLC	Reverse Phase-High Performance Liquid Chromatography
rRNA	ribosomal ribonucleic acid
RRE	RiPP Recognition Element
SANDPUMA	Specificity of Adenylation Domain Prediction Using Multiple Algorithms
SAMN	BioSample Number
SDA	Sabouraud Dextrose Agar
SDS	Sodium Dodecyl Sulfate
SEM	Scanning Electron Microscopy
SPR	Subtree Pruning and Regrafting
SRA	Sequence Read Archive
srf	surfactin (gene loci)

ssp	sub species
T	type strain
T1PKS	Type I Polyketide Synthase
T2PKS	Type II Polyketide Synthase
T3PKS	Type III Polyketide Synthase
TAGC	The Applied Genomic Core
TAS	Traceable Author Statement
TEM	Transmission Electron Microscopy
TFA	trifluoroacetic acid
TGA	Thermal Gravimetric Analysis
ths	thusin (gene loci)
TIGRfam	The Institute of Genomic Research family
TM	trade mark
tRNA	transfer ribonucleic acid
TSB	Tryptic Soy Broth
TYGS	TYpe strain Genome Server
UAMH	University of Alberta Microfungus Collection and Herbarium
USTHB	University of Science and Technology Houari Boumediene
WHO	World Health Organization
zam	zwittermicin A (gene loci)
ZOI	zones of inhibition

Chapter 1

Functional Genomics for Bacterial and Fungal Biotechnology

1.1. Introduction

1.1.1 Definitions and General Overview

The field of genomics has driven a new era for microbial research. The deposition of a huge quantity of DNA or RNA sequencing data generated from all forms of life in publicly accessible databases is exponentially increasing.[1] The availability of such data sets can be explored, exploited and drive hypotheses to generate new knowledge via the process called genome mining. This approach can be applied in a wide variety of fields including the characterization of physiological processes and metabolic pathways, identification and correlative validation of new drug targets, as well as the discovery of bioactive molecule from natural resources, which may also serve as lead for new drugs.[1-3] The genomics-driven pipelines in small molecule discovery tap the vast genetically encoded small molecules in draft or complete genomes. These small bioactive molecules play a fundamental role in several biological aspects such as signaling, gene regulation, nutrient cycling, self-preservation and defense.[2] All members of the three domains of life, Archaea, Bacteria, and Eukarya, have been the source of these specialized metabolites, or otherwise known as natural products.[2-3] Ecologically-speaking, and more importantly as an evolutionary adaptative mechanism, these natural products offer the organism with competitive advantage in their fluctuating abiotic environments and dynamic symbiotic interactions. Furthermore, with the wide variable bioactivities, we, humans have also tapped many

of these signaling molecules for our own use such as antibacterial, antifungal, chemotherapeutics, and insecticides.[2]

Natural products and their analogues sit at the foundation of many important chemotherapeutics which have made their way in widespread clinical application.[1] This includes, but is not limited to, a huge selection of molecules including the functional groups of antibacterial compounds like vancomycin, erythromycin, and penicillin[1]; antifungal agents like amphotericin, benomyl, and nystatin[2-3]; biosurfactants like fengycin and surfactins[4]; anticancer compounds like doxorubicin and paclitaxel[5]; and insecticidal agents such as Cry proteins, beauvericin (**1**), oosporein (**2**), tenellin (**3**) and bassianin (**4**) (Figure 1.1).[6]
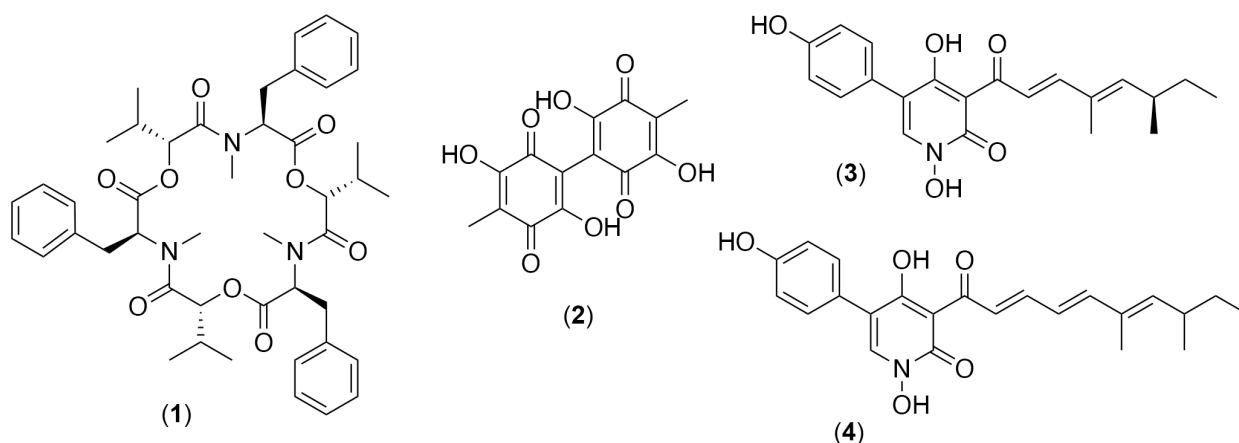
Figure 1.1. Insecticidal agents produced by *Beauveria bassiana*. Insect virulence factors include the cyclic hexadepsipeptide, beauvericin (**1**), the dibenzoquinone red pigment, oosporein (**2**), the yellow hydroxpyridone class with dienone side chain, tenellin (**3**) and tenellin analogue, bassianin (**4**).

Although the number and functional diversity of these natural products keeps on increasing, most large pharmaceutical companies are not as actively engaged in finding new drug leads from such sources.[1,7] A few key players were proposed for the decline, such as the increased efforts in combinatorial chemistry (possibly, robotic parallel syntheses), the high chance of rediscovering natural products from convergent evolutionary sources, limited metabolic choices

in laboratory fermentation conditions and difficulty in activating silent gene clusters.[8-9] Despite the ease of directly identifying biosynthetic gene clusters (BGCs) from the vast quantities of genomic sequence data available in public databases, genome annotation often limits the functionality of conversed and unique genetic loci and clusters.[2] The use of automated predictive algorithms in the discovery of natural products led into the extensive use of computer programs such as antiSMASH[10], BAGEL[11], and RODEO[12], including the use of machine learning in creating predictive neural networks, NeuRiPP.[13]

Undeniably, many of the genome-encoded and metabolically expressed biosynthetic pathways producing natural products had innate challenges. These include instability of small molecules which are simply undetected due to incompatible processing or extraction and/or analytical chemistry techniques,[14] or lack of known biological activity.[8] On the other hand, activity-guided fractionation, a classical functional approach, provides a robust method to analytically optimize the fermentation efforts that lead to the production, isolation, and structural characterization of novel natural products with an associated array of biological properties. Although a large majority of the secondary bioactive molecules and metabolic pathways predicted in genomic analyses are designated as cryptic, orphan or silent, the gene loci are associated with the absence of correlation with a known biosynthetic pathway.[15] This important junction offers a key opportunity of converging symbiotic natural systems for bioactives discovery. The strategic experimental conditions, targeted gene activation, and the evaluation of screening parameters can be leveraged within the ecological, evolutionary population genetics, and physiological contexts of a given symbiotic microbial interaction.[14]

Fundamental evolutionary mechanisms and phylogenetic diversity should be considered both to support a synergistic approach for genome mining, natural product drug discovery and

population chemical ecology.[14] Microbial genomes are evolutionary and ecologically dynamic. Microgeographical, spatio-temporal and diurnal environmental factors contribute to major phenotypic variations between and among related species and strains. This often drives the genotype-phenotype conundrum resulting in malleable secondary bioactive metabolic pathways. In bacterial and fungal kingdoms, the genes responsible for the regulation, biosynthesis, transport and even resistance from the autochthonous metabolite are often encoded on a contiguous section of the DNA. Functional genomic analysis coupled with comparative phylogeny and analytical chemistry tools will help in facilitating the discovery of genotype-to-phenotype correlations and the discovery of functional gene cluster-specific small molecules in complex bacterial and/or fungal symbiosis.[14, 16-17]

In this thesis, projects on novel strains of *Bacillus* comparative genomics, functional antimicrobial genomics of extremophilic *Bacillus* and *Streptomyces*, and mycoinsecticide evaluation and development in perturbing a tripartite tree-insect-fungal symbiosis are presented. Chapter 2 presents the comparative genomics of the insecticidal bacterial species, *Bacillus thuringiensis* DNG9. Chapter 3 describes the functional genomics of the lipopeptide antibiotic, fengycin, isolated from halophilic-oil slough isolate *Bacillus amyloliquefaciens* subsp. *plantarum* (now updated to *B. velezensis*) F11. Chapter 4 is a project on the whole genome sequencing of four novel extremophilic *Bacillus* species isolated from rare environments. Chapter 5 is a functional genomics association of an antibiotic and antitumor-producing novel species of *Streptomyces* from a volcanic soil. Chapter 6 is an evaluation and selection of the entomopathogenic fungus, *Beauveria bassiana,* as a biocontrol agent to combat the mountain pine beetle epidemic. And lastly, Chapter 7 discusses the efforts in developing and field-testing of *B. bassiana* mycoinsecticide formulations, as well as efforts in comparative genomics of the fungal natural product. The

succeeding sections of this chapter will provide background information on the above-mentioned projects in the same order the projects are presented in the thesis.

1.2. Bacterial Comparative and Functional Genomics

1.2.1 *Bacillus*

The genus *Bacillus* is a large, phylogenetically mosaic group of rod-shaped, endospore-forming bacteria in the phylum Firmicutes.[18] Members of the group are generally defined as Gram-positive, low guanine-cytosine (G+C) DNA content, representing approximately 293 species/subspecies with complex genetic diversity,[18-19] although several *sensu lato* groupings made their nomenclature chimeric resulting in unresolved polyphyly.[19-20] The genus was first described by Ferdinand Cohn in 1872 with *Bacillus subtilis* as the first representative type species.[21-22] Historically, most species are considered GRAS or generally recognized as safe. *B. subtilis* was considered as one of the most important species among industrially relevant microorganisms, second to the group of lactic acid bacteria which dominates food processing and preservation.[20-22] The classical 16S rRNA gene phylogeny combined with biochemical phenotypic characterizations categorized the *Bacillus* genus into six groups.[23]

Traditionally, all six groups of *Bacillus* represent a range of species and strains of human interest. The interest is linked to three major aspects, including, 1) food and industrial microbiology applications such as production of biotechnological products (e.g. enzymes for laundry detergent, lipopeptide antibiotics, and insecticidal toxins)[23]; 2) utilization of dormant and resistant endospores as model system for cellular differentiation, longevity and resistance to decontamination[24]; and lastly, 3) the pathogenicity model for human beings.[25] The bacterial

disease models date back to the 19th century with the studies of Louis Pasteur utilizing heat-treated *Bacillus anthracis* as the precursor for the first antibacterial vaccine, and Rober Koch's elucidation of specific disease-causing human microorganisms.[25]

To access further exploitation and development of *Bacillus* species for industrial processes, the complete genomes of several species of *Bacillus* have been continuously sequenced in order to understand their physiology, taxonomy, biochemistry, and genetics.[20] The explosion of genomic sequencing efforts opened an era that helped contribute significantly to the reclassification of the genus *Bacillus*, which now harbours 293 species/subspecies.[19] The historical absence of reliable means of classifying known *Bacillus* species into distinct clades, has led to challenges in the phylogenetic placement of new species into this genus.[19, 26]

The increasing availability of *Bacillus* genome sequences offers a wealth of knowledge related to classical and novel gene inventories, diversity among current and future isolates systematics, and evolutionary phylogeny, which cannot be obtained by any other approach.[27] The understanding of the genetics and biochemistry of the genus *Bacillus* also provides targeted direction regarding their environmental adaptation and ecological significance under extreme environmental conditions.[28] The access to an organism's whole genome sequence can be applied to genotyping studies, comparative genomics for resolving phylogenetic and evolutionary systematics, mutation screening and environmental profiling.[29-31] Lastly, genome sequencing has provided genetic insights into the metabolic framework of the microbial world and directed natural product discovery,[32] including the genus *Bacillus*,[33] thus reinvigorating microbial bioactives molecule research.[20] The exponential increase of publicly accessible *Bacillus* genomic sequences continuously drives functional genomic studies centered on the exploration of novel industrially-

important *Bacillus* species which possess novel genes, which encode hitherto novel products for a variety of applications.[34]

1.2.2. Actinomycetes

The bacterial phylum Actinobacteria represent a large group of Gram-positive bacteria with a high guanine-cytosine (G+C) DNA content. Representative members have a wide ecological distribution, including both terrestrial and aquatic habitats, significantly contributing to the recycling of organic matter.[35] This group of bacteria exhibits extensive variations in cellular and colony morphologies as well as physiologies and metabolic inventories that make it feasible to colonize a wide array of ecosystems, including extreme environments.

The demand for antibiotics is steadily increasing worldwide. The need for new antibiotics is rising because of the development of antibiotic-resistant pathogens, the emergence of new diseases, and the toxicity of current bioactive compounds.[36] Among these pressing concerns, antimicrobial resistance (AMR) is one of the most significant global public health challenges in our modern time.[37] Many people are still dying from untreatable infections due to AMR. When treating infections caused by multidrug-resistant pathogens, currently available antibiotics can be ineffective due to their lack of specific inhibitory activities or adverse side effects.[38] Therefore, there is still a pressing need to continue to bio-prospect alternative sources for novel microorganisms capable of producing bioactive compounds that can counteract existing and emerging resistant infectious pathogens.

To access a novel metabolite, ideally with antibiotic properties, a diverse and less exploited environment may present rare and unique actinomycete. The isolation and subsequent feasibility of fermentation scale-up for the production of rare actinomycetes, presents the first and crucial

step towards novel actinomycete resource development for novel drug discovery.[39] Alternatively, the term "Modern Actinobacteria" (MOD-ACTINO) which refers to a group of actinobacteria capable of producing compounds that can be explored for modern applications such as novel drug leads and cosmeceutics.[40] Members of this group are designated as novel actinobacteria isolated from special and less explored environments which can be valuable sources for different industries that seek to improve people's lives. Rare actinomycetes diversity, phylogeny and associated antimicrobial molecules are discussed in greater details in Chapter 5.

The successful recovery, isolation and fermentation of rare actinomycetes requires a sound understanding of eco-taxonomy and physiology and combination of this knowledge with the available whole genome sequences.[39] More recently, interdisciplinary approaches provide powerful knowledge platform with the aid of molecular information (genomics, transcriptomics, epigenomics), species concepts (evolutionary systematics) and natural product discovery (proteomics, metabolomics) in a post genomic era.[41-46]

1.3. Entomopathogenic Fungi in Insect Pest Management

1.3.1. Entomopathogenic Fungi

Global forest ecosystem health and food security are constantly being threatened by arthropod pests. In response, chemical pesticides have been used frequently over the last few decades.[6] This issue is further exacerbated by a geographical shift in arthropod colonization of novel and naïve habitats, predicated as a function of climate change.[46-49] Diversification of insect population, driven by perturbations caused by global environmental changes, especially temperature, provide an excellent opportunity for evolution of species boundaries.[48] Such a

phenomenon is particularly true for insects, as their life cycle and historical phenotypic traits are mainly dependent on temperature. The species altered gene flow is expected to respond rapidly, leading to a complex cascade at rapid evolutionary timelines. Climatic environmental changes can then direct evolutionary opportunistic events, which then select for either population collapse, persistence, hybridization or combinations of both.[47-48] The continuous large-scale perturbations resulting from climate change can also catalyze novel oscillation cycles of host-parasite interactions.[50] Such global dilemma will continue to affect the complex dynamics of insect-host evolution so long as rapid global warming and latitudinal climate changes continue. Therefore, the historical management of arthropod pests, as well as in this era, is continuously dominated in both agricultural and forest ecosystem practices. This is mainly attributed to the ease of applying synthetic pesticides resulting in an immediate responsive pest population control.[51-52]

Synthetic pesticides have been frequently used to manage arthropod pests throughout the world. However, these chemicals are often hazardous to off-target eukaryotic hosts, including humans, and the ecosystem in general.[6, 53] Their environmental persistence and physico-chemical- and biological transformation of these pesticides may negatively affect the entire ecosystem in an immeasurable scale.[53-55] Therefore, exploring environmentally friendly and sustainable alternatives has numerous researchers to use autochthonous biocontrol agents such as entomopathogenic fungi (EPF).[6,56] Although EPF's bioremediation potential is underexplored, recent efforts revealed their untapped capacity to transform select recalcitrant xenobiotic toxic contaminants including alkylphenols, organotin compounds, synthetic estrogens, pesticides and hydrocarbons.[57] EPF may contribute to not just to their mycoinsecticidal potential but also xenobiotic resiliency brought about by climate change-driven host insect range expansion and anthropogenic mitigation efforts.[57-59]

Entomopathogenic fungi include members of various genera that infect, reproduce, and efficiently kill arthropod pests, including insects.[6,51] Furthermore, these fungal species have a relatively high host specificity with a narrow effect on non-arthropod organisms (e.g. domesticated avian species like turkey, ducks, chicken).[51] However, several of these EPF have a broad-spectrum pathogenicity and variable virulence effects on several insect target species . Therefore, insights into the biodiversity, pathogenicity and virulence, especially the mechanisms of action are of prime significance for their efficient but safe utilization as a biocontrol agents[6] in agro-industrial and forest ecosystems.[51,58] This further includes their utilization for unconventional, recombinant DNA and omics-driven technologies.[59-61]

Members of these diverse invertebrate pathogenic fungi are generally classified as parasitic microbes under several groups, namely, Basidiomycota, Ascomycota, Deuteromycota, Entomophtoromycota and a few others under Chytridiomycota, Microsporidia and Oomycota.[6, 62] Although the nomenclature of these pleomorphic fungi is often unresolved and evolving, the halting of dual nomenclature systems has been slowly reconciled with the increasing availability of DNA-based molecular data (whole genome sequences, multilocus concatenated gene phylogenies, etc).[62] Commercially available EPF formulations are often centered in the order Hypocreales, in the division Ascomycota, and the majority of the high conidia-yielding species are representatives of the families, Ophiocordycipitaceae, Clavicipitaceae and Cordycipitaceae.[62] Moreover, although significant ecological and morphological phylogenetic variations exist in and between EPF species and strains, the most notable members used in mycoinsecticide preparations include the genera, namely: *Beauveria, Metarhizium, Cordyceps, Akanthomyces, Hirsutella*, and *Nomuraea.*[62-63]

Although biological agents like EPF may have environmental advantages against recalcitrant synthetic chemicals, potential safety concerns and other uncontrolled and unpredicted consequences may also place them at a disadvantage. These environmental safety concerns include (1) cross-pathogenicity to off-target hosts, (2) cascade of toxigenicity to non-target organisms in several trophic levels, (3) competitive local and geographical displacement of autochthonous microorganisms, and (4) general biotic allergenicity to name a few.[64-65] The paramount issue of introducing an allochthonous and often geographically exotic microbial agent is a sustained risk to off-target beneficial insects (e.g. pollinators), because once the entomopathogenic agent becomes established, it is most likely difficult to eradicate.[65] However, if indigenous and locally-isolated or better an autochthonous strains of EPF are utilized, the perturbation risk for damaging the insect pest ecosystem may be reversible and has reduced long-term detrimental effects.[64]

1.3.2. *Beauveria bassiana*

The discovery of the white muscardine fungus, *Beauveria bassiana*, came about from the investigation of a mysterious silkworm disease by Agostino Bassi in Italy. The "extraneous germ", which was later determined to be a fungus, caused devastating epizootic collapse of domesticated larval silkworms in Southern Europe in the 18-19th century.[66] The discovery of this contagious entomopathogenic fungus contributed to an important antecedent to the germ theory of disease.[67]

Taxonomically, the white muscardine fungus has several systematic reclassification events. It was first named *Botrytis bassiana* by Balsmamo-Crivelli in 1835 but later was reclassified into the genus *Beauveria* by Vuillemin in 1912, which was then designated *Beauveria bassiana* as the type species.[66] Until the recent advancement in genotypic, molecular and genomics-based taxonomic approaches, the sole anamorphic or asexual mode of reproduction

placed *B. bassiana* under the imperfect fungal phylum Deuteromycota, within Cordycipitaceae of the order Hypocreales.[65] The discovery of the sexual, teleomorphic stage, *Cordyceps bassiana*[62] prompted the taxonomic reclassification into the phylum Ascomycota.[65-66] Although the sexual stage has been discovered, the molecular cascade of signal for its anamorphic to teleomorphic shift is elusive and *B. bassiana* cultures often maintain a mitotically reproducing fungal propagule called conidium.

The anamorphic *B. bassiana* conidia has a wide insect host range, infecting multiple insect groups.[68] This cosmopolitan entomopathogenic fungus is not limited to insect hosts, as is also isolated from soil and as a foliar endophyte.[62] For the insect host, the conidia infect members of the orders, Coleoptera (beetles), Lepidoptera (moths), Orthoptera (grasshoppers), Phasmatodea (stick insects) and Blattodea (cockroaches, termites).[62]

1.3.3. *Beauveria bassiana* formulations

Integrated *B. bassiana*-based mycoinsecticides have been shown to elicit synergistic effect targeting an effective control of insect pest. Several documented examples support an increased *B. bassiana* efficacy when used in conjunction with insecticides, herbicide, and other microbial agents.[69] The commercial formulation, Mycotrol™ WP, demonstrated synergistic effect when mixed with imidacloprid (a neonicotinoid), against field populations of the tarnished plant bug, *Lygus lineolaris*, protecting cotton plantations.[70] *B. bassiana* pathogenicity is also enhanced when combined with sublethal doses of imidacloprid against the citrus root weevil, *Diaprepes abbreviates*.[71-72] A similar result was further demonstrated in field biocontrol of the migratory grasshopper, *Melanoplus sanguinipes*, using a combination of the insecticide, dimilin (diflubenzuron) and the commercial product *B. bassiana* strain GHA.[64] The synergistic use of

systemic insecticides with *B. bassiana* formulations shows promise in reducing dosages of synthetic chemicals through lower application rates.

The compatibility of a wide array of chemical fungicides and herbicides, more commonly used under greenhouse conditions, was also shown to interfere with *B. bassiana* effectivity.[73] Inhibition of *B. bassiana* mycelial growth and conidiation was reported for the following greenhouse-relevant fungicides: zined, chlorothalonil, thiophante-methyl, mancozeb and manen.[73] On the contrary, a synergistic effect was observed with the herbicide, diquat dibromide although the above results were limited under in vitro conditions and may respond variably under *in natura* field conditions.

Currently, there is very limited combinatorial utilization of two or more entomopathogenic microbes (fungi, bacteria, microsporidium, etc) with the objective of increasing the efficacy through synergistic interaction for insect biocontrol.[73] The common entomopathogenic bacterium, *B. thuringiensis*, showed synergistic interaction with MycotrolTM WP in the field biocontrol of the Colorado potato beetle, *Leptinotarsa decemlineata*, population.[74] Similarly, synchronous coinfection of *B. thuringiensis* and *B. bassiana* resulted in 95 – 100% mortality in *L. decemlineata* larvae, without signs of microbial antagonism or plant defoliation.[75] Another *B. bassiana* synergism was demonstrated using two entomopathogenic bacteria, *Photorhabdus temperata* and *Xenorhabdus nematophila*, in controlling the chickpea pulse beetle, *Callosobruchus chinensis*.[76] It was hypothesized that the bacterial component contributed to the arrestment of insect nutrition while the germinated fungal conidia kill the nutritionally-deprived and weakened larvae.[75-76] The combined use of the microsporidian parasite, *Paranosema l*ocustae and *B. bassiana*, supported an effective seasonal biocontrol of the migratory locust, *Locusta migratoria*.[77] These microbial cocktails, combining synergistic bioinsecticidal properties, could circumvent limitations of high

B. bassiana effective dose requirement, interspecies antagonism and abiotic limiting factors (e.g. effective water activity, temperature optima), therefore increasing the mycoinsecticidal general efficacy.

1.4. Mountain Pine Beetle, *Dendroctocus ponderosae*

1.4.1. MPB Epidemic, Climate Change and Perturbed Forest Ecosystem

The epidemic of mountain pine beetle (MPB) started in British Columbia in the early 1990s affecting a vast portion of the Western Canadian pine forest. To date, the magnitude of the epidemic far exceeds any previously recorded bark beetle outbreak, with more than 18 million hectares of pine stands affected, predominantly lodgepole pine (*Pinus contorta*). Economically, it is estimated that 50% of the affected forests are matured, harvestable lodge pole pines costing the Canadian government a combined financial and welfare value of $90 Billion.[78] In recent years, MPB was considered as an invasive bark beetle as it migrated well beyond its natural and historic host range, expanding into northern British Columbia and crossed eastward into the Rocky Mountains and prairie of north-central Alberta.[79] The host expansion was thought to be protected by the northern Canadian Rockies (e.g. Jasper and Banff National Parks) as an effective geographical barrier.[80] The MPB host range expansion was defined as an infestation of evolutionarily naïve populations of lodgepole pine, jack pine (*Pinus banksiana*), and its hybrid (*P. contorta* × *P. banksiana*).[82-83] The epidemic posed even greater continental threat, as *P. banksiana* is the predominant pine tree species extending across the entire boreal forest, into the Great Lakes and the Atlantic coast (Figure 1.2). The epidemic showed clear perturbation of the ecosystem including understory plant communities, avian species and high-elevation forest ecosystems.[83-85]

The potential for MPB to spread further eastward of Canada is a serious, major environmental, ecological and economic problem,[80, 86] especially being feed continuously by climate change.[87]
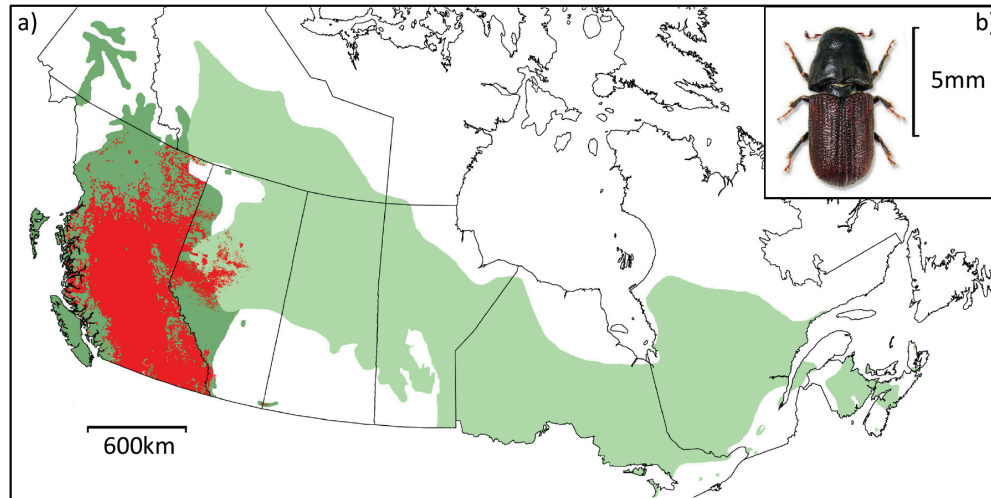
Figure 1.2. Geographical distribution of the ongoing *Dendroctonus ponderosae* outbreak (red) in relation to *Pinus contorta* (dark green) and *P. banksiana* (light green) population in Canada (A). A mountain pine beetle adult (B). Mountain pine beetle data from the governments of British Columbia and Alberta. Photo by K. Bolte.

1.4.2. Mountain Pine Beetle Biology

The mountain pine beetle, *Dendroctonus ponderosae* (Hopkins), a wood-boring coleopteran insect is the most serious native insect pest causing continental-scale damage to the Western North American boreal forest.[88] The beetle attacks a wide range of pine tree host species (*Pinus* sp.) including lodgepole (*P. contorta*), ponderosa (*P. ponderosa*), western white (*P. monticola*), whitebark (*P. albicaulis*), limber pine (*P. flexilis*) and lastly jack pine (*P. banksiana*).[88-89] One exception is the Jeffrey pine (*P. jeffreyi*) which is attacked by a different species of bark beetle, *D. jeffreyi*.[90] Although MPB is a rapidly expanding invasive species and currently threatening the boreal forest ecosystem, natural population control measures are limited, including dependence on extended cold winters and natural competition and predators including

parasites, insects and woodpeckers. Unfortunately, these natural enemies have very negligible impact towards the effective control of the current epidemic as well as future outbreaks.[91] Climate changes especially have driven massive outbreaks and eruptive impact to the conifer forest ecosystem.[92]

The mountain pine beetle spends most of its life cycle underneath the host pine tree bark. Developing stages of MPB, such as larvae, are around the cambium region where it feeds on phloem elements.[89, 93] The short time it is found outside the host is when the adults emerge, which is shortly followed by a flight period for adult beetles' dispersion to infect new pine tree hosts to reproduce. The complete reproductive cycle of a mountain pine beetle has a one-year lifespan in its current environment and host range (Figure 1.3).[94] This average lifespan may vary by a few months, being shorter or longer, depending on the local average temperatures.[95] Furthermore, predictive modeling of MPB phenological events like emergence and flight periods depends on the accumulated degree days, the time that a certain optimum temperature threshold is cumulatively attained.[96] The emerging adult MPB will colonize new host trees in early July to mid-August, as driven by optimum temperature. The female MPB bores tunnels into the bark by consuming the wood thereby creating maternal galleries for laying eggs. The newly hatched larva further create larval galleries, perpendicular to the maternal galleries. The larvae then spend the winter underneath the bark of the tree, protected from the freezing temperature of winter and continue their development in the following spring. Pupal development commences in June to July and adult emergence will completes the life cycle.[89]
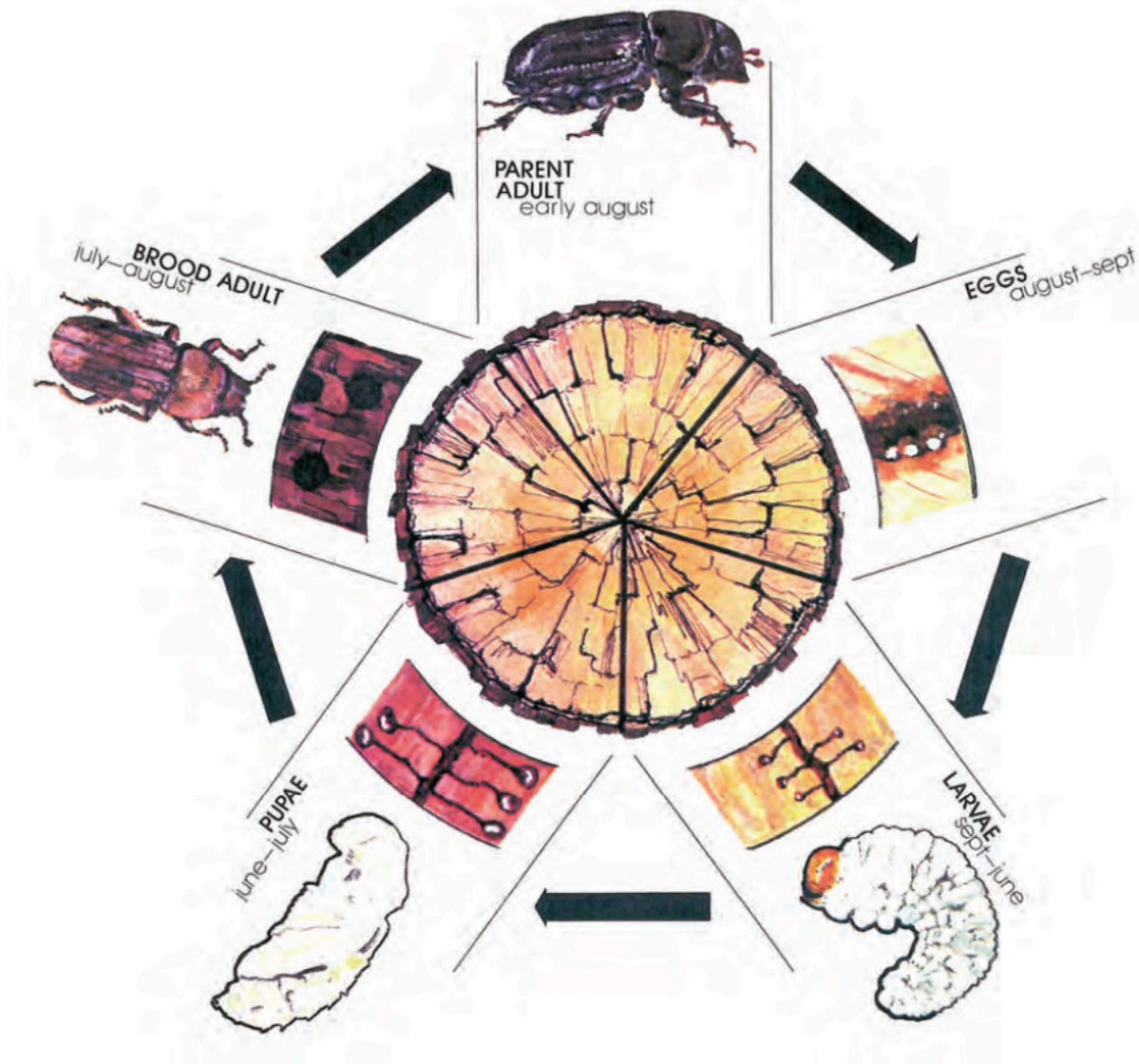
Figure 1.3. Life cycle of *Dendroctonus ponderosae*. Photo obtained from K. E. Gibson, USDA Forest Services, 2010.

Emerging population of beetles have two possible attack patterns depending on the density of emerging adult survivors during the overwintering cycle. First, low population density of emerged adult MPBs will selectively attack slowly deteriorating, repressed, and small-girth host pine trees which have been chosen under the premise of compromised tree defenses.[93, 97] This attack type often will not support outbreaks as the reproductive doubling rate may be less than one

due to low brood production in such marginal tree hosts. Alternatively, in the second type of attack, dense MPB populations overwhelm the host tree defenses of a mature, large, healthy tree through an aggregation pheromone-coordinated mass attack. This in turn results in an increased brood production capacity supported by a higher host tree vigor which then results in a cycle of positive reproductive feedback loop and therefore an unregulated MPB population outbreak.[96-98]

Most MPB massive attacks are capable of killing their conifer host over a wide latitudinal range, adapted to a wide temperature ranges and fairly diverse conifer hosts.[99] Such tree killer ability was evolved using an ancestral state phylogenetic reconstruction of extant *Dendroctonus* species life history traits and ecological developmental phenotypes supporting the ability to colonize a host tree via massive-concerted attacks and gregarious larval development. The long-standing and balancing ecological notion of continuous adaptive interactions between the conifer hosts and MPB give way to an arms race evolutionary battle between the two species,[99] which is now tipped in favour of the MPB, suggestibly driven by climate change.[92] Furthermore, climate change-driven host range expansion may substantially affect the planet's future carbon cycles as MPB-killed pine trees decay or burn easily to release their stored carbon.[80] Therefore, timely and effective mitigation efforts are now highly sought after to control this epidemic that continuously threaten the Western North American boreal pine forest and affects carbon dioxide capture in our planet.

1.4.3. Blue Stained Fungus

The mountain pine beetle bark system is a tripartite interkingdom interaction involving the host pine tree (Kingdom Plantae), the bark beetle (Kingdom Animalia) and a third player, the symbiotic, genetically heterogenous, collective phenotypic group, blue stained fungi (BSF)

(Kingdom Fungi). Prior to MPB emergence in the months of July to August, enclosed adults in pupal chambers typically graze on bark tissues (frass) while storing some fungal spores in their mycangia (mouth part) as well as their guts and exoskeletons.[100] Such unique bark beetle behaviour is considered a form of evolutionary mutualistic adaptation as both players benefit from the relationship for the successful attack on the host pine trees.[101] The known blue stained fungal symbionts belong to the teleomorphic ascomycetous genera, *Grosmannia*, *Ophiostoma* and *Leptographium*, phenotypically characterized by the production of melanin that stain the wood bluish black. Both spore types, asexual and sexual, are produced in slimy masses that adhere to insect bodies, ingested and actively stored in the mycagia and are dispersed to new hosts that represent fresh nutrient sources.[102-103] Two fungal species, *G. clavigera* and *O. montium* have been consistently isolated from the MPB's mycangia, exoskeletons as well as from the infested pine trees.[100-101] Recently, *L. longiclavatum* associated with mountain pine beetle has also been reported.[104] Interestingly, with or without the MPB, these symbiotic fungi have the capability to overcome the pine tree innate defenses (terpenes and alkaloids). Unlike the MPB localization, which is restricted just below the bark (cambium-phloem interface), BSF will colonize up to the heart and sapwood regions, plugging the xylem and tracheid elements, which then disrupts the water transport to the crown ultimately contributing to the death of the host tree. Economically, the discoloration due to melanin reduces the commercial value of the lumber as well as other by-products like wood fiber and pulp.[105]

The complexity of the tripartite interaction makes the bark beetle mycobiome research an excellent avenue for symbiosis research, as it represents diversity, common and shared resource management, competition and antagonism as well as replication of evolutionary origins.[101] The perturbation of this fungal ecosystem, by means of a targeted eradication of the mutualistic

symbiosis, can serve as another potential mitigation approach for the control of the MPB epidemic and other emerging bark-beetle-fungal-tree interactions.[107]

1.4.4. Mitigation Approaches Against the MPB Epidemic

Efforts to mitigate the spread of the mountain pine beetle epidemic and its impacts in North America, including Western Canada, have been hampered by the lack of effective and efficient direct control tactics.[108] One strategy is in silviculture treatment called a thinning mechanism.[109] The procedure entails either one of or combination of the following: 1) thinning from above or diameter-limit cutting which then removes trees over a certain diameter, 2) thinning for basal area reduction which reduces forest basal area, and 3) selective removal of thick-phloem trees. This procedure hopes to increase the tree vigor which then increases the tree's natural defenses (e.g. resins), therefore resisting MPB attacks. A second strategy, called prescribed burning, has been used not only to attempt mitigating MPB expansion but also to reduce forest fire build up.[110] In such fire adapted forest ecosystems, a balance must be maintained between the tree species composition, MPB and BSF pathogen build-up. The fall-and-burn treatment is a direct approach where trees with confirmed live MPB broods will be felled, and infested portions piled and burned. The third and most common strategy for the control of MPB population is the use of beetle semiochemicals like attractants, repellants, and insecticides. MPB attractants utilized in various studies include aggregation pheromones like *trans*-verbenol, exo-brevicomin, frontalin as well as aggregation enhancers like myrcene, ipsdienol, and lanierone (Figure 1.4). Conversely, the two repellents studied were verbenone and 4-allylanisole (Figure 1.4). Lastly, insecticides include carbaryl, chlorpyriphos, cyfluthrin, fenitrothion, permethrin and esfenvalerate.[109]
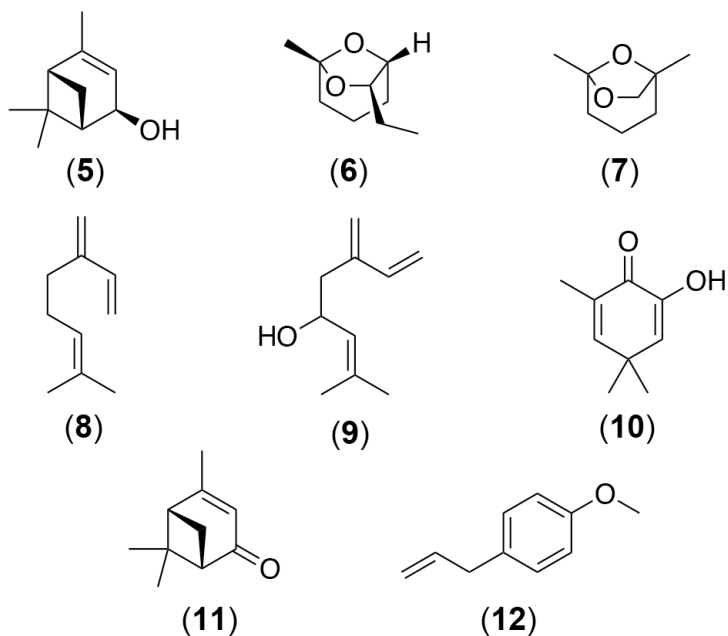
Figure 1.4. Semiochemicals utilized in MPB biocontrol strategies. Semiochemical attractants include the aggregation pheromones (–)-*trans* verbenol (**5**), *exo*-brevicomin (**6**), and frontalin (**7**). Aggregation potentiators include myrcene (**8**), ipsdienol (**9**) and lanierone (**10**). Anti-aggregation pheromones include (–)-*trans* verbenone (**11**) and 4-allylanisole (**12**).

Several important aspects of the beetle's life cycle and biology (Figure 1.3.) preclude conventional approaches in the management of MPB populations.[108] First, given that MPB spend all but a few days beneath the bark of their host trees, they are largely not affected by exogenous pesticide application. Second, blockage of the tree's vascular system by BSF (e.g. ophiostomatoid fungi) introduced into host tree during colonization by MPB, limits the efficacy of systemic insecticides in extended field seasons. Third, of the few pesticides registered for use in forestry in Canada,[111] no effective pesticide has been applied in lodgepole pine stands to control the MPB epidemic.[112]

Currently, the detection and physical removal of infested pine trees (felling, burning, or salvage harvesting) remains the current tactic available to manage MPB populations.[108] However, mechanical treatment of infested trees is costly, logistically difficult for some areas that are

inaccessible, and prone to failure. Given that successful suppression of any MPB population requires consistent, long-term application of direct control tactics, development of novel, ecologically viable, and cost-effective tools is critical to minimize the continued spread and impacts of invasive populations of this insect within vast pine forests east of the Rocky Mountains in Canada.

1.5. Thesis Overview

The projects presented in this thesis focus on the genomics of novel *Bacillus* strains isolated from extreme environments with emphasis on the bioinformatic prediction of secondary bioactive metabolites and the associated biosynthetic gene clusters. The functional association of the elucidated bioactive molecules with the genome inventories as well as proposals for phylogenomic, systematic and evolutionary re-classification of the isolates are presented. This thesis also includes pioneering work on the selection, evaluation and formulation of a *B. bassiana* mycoinsecticide for the biocontrol of the epidemic and invasive mountain pine beetle in Western Canada.

Chapter 2 describes the functional genomics analysis of a novel isolate of *Bacillus thuringiensis*, strain DNG9, from an oil contaminated Algerian soil-slough. The high-quality draft genome was established using an Illumina pair-end sequencing technology. The genome encodes several gene inventories for the biosynthesis of bioactive compounds such as zwittermicin A, petrobactin, insecticidal toxins, polyhydroxyalkanoates and multiple bacteriocins. Antimicrobial assays supported functional genomics potential for antibacterial and antifungal activities as well as biosurfactant properties. The availability of the genome will contributes to the study of

pathogenicity against insect pests, phyto-fungal diseases, and antimicrobial compound mining and comparative phylogenesis among the *Bacillus cereus sensu lato* group.

Chapter 3 describes the fengycin biosynthetic gene cluster elucidation in the novel isolate *Bacillus velezensis* strain F11. Functional genomic analysis and activity-guided purification reveals two lipopeptides, fengycin A and B, with antimicrobial activity against Gram-positive and -negative bacteria, as well as fungal phytopathogens. Genome mining supports a complete cluster for fengycin biosynthesis, under a five-gene member operon, *fenABCDE*. Comparative phylogenomics also supports a re-classification of *B. amyloliquefaciens* subsp. *plantarum* clade to *B. velezensis* providing evolutionary insights in the *Bacillus subtilis* species complex.

Chapter 4 describes the genomic analysis of four novel *Bacillus* species isolated from extreme environments in Algeria or Brazil. The draft genome sequences of the halophilic, salt lake isolates, *B. cereus* E41 and *B. anthracis* F34, encoded biosynthetic gene clusters for the siderophore petrobactin, polyhydroxyalkanoate (bioplastic pre-cursor) and the antimicrobial bacillibactin production. Similarly, functional genomic analysis of the draft genome of *B. paralicheniformis* F47 reveals the genetic potential to produce several lipopeptides, bacitracin, siderophores and bacteriocins supporting the antibacterial and antifungal phenotypes. Lastly, functional genomics of the thermophilic isolate, *B. licheniformis* SMIA-2, supports the established anti-methicillin-resistant *Staphylococcus aureus* activity as well as the candidate thermophilic enzyme loci.

Chapter 5 describes the comparative phylogenomics, functional genomics, and bioactivity analysis of the novel volcanic soil isolate, *Streptomyces*. A1-08. Comparative analysis of the closest *Streptomyces* type strains suggests A1-08 is a new species yet to be classified under this genus. The antimicrobial assay of the ethyl acetate extract from spent fermentation medium

supports a wide spectrum of antibacterial, antifungal and anti-colorectal cancer activity. Functional genomics analyses allow identification of 48 biosynthetic gene clusters that may support the observed bioactivity.

Chapter 6 describes the selection and evaluation of internationally collected strains of the entomopathogenic fungus *Beauveria bassiana* for the biocontrol of the invasive mountain pine beetle (MPB), *Dendroctonus ponderosae,* affecting the epidemic collapse of the Western Canadian pine forest ecosystem. *In vitro* MPB fungal infection assays suggest an effective lethal time and mycosis of laboratory raised MPB. Three morpho-phenotypic classes, as defined by mycelial-conidial density and pigmentation, suggest that the high diversity may contribute to the variations in the pathogenicity and virulence level in MPB. *B. bassiana* resistance to abiotic factors such as ultraviolet light and reconstituted pine tree monoterpenes provide insights to field trial response and mycoinsecticide product development. Lastly, *in vivo* fungal infection assays on potential secondary insects like honeybees, reveal a mortality rate comparable to hive daily population turnover rate.

Chapter 7 presents the development and field-testing of mycoinsecticide formulations containing conidia from select *B. bassiana* strains for targeted *in planta* bioassays under relevant *in natura* conditions. A biphasic liquid-solid fermentation yielded a semi-industrial scale conidial titer comparable with commercially available *B. bassiana* formulations. Conidial stability, as measured by viability in the reconstituted mycoinsecticide carrier, showed wide tolerance range under cold storage, *in planta* bark surface and pine forest stand environments. Emerging MPB infection assays under greenhouse conditions supported both strain- and concentration-dependent lethal times and *B. bassiana*-specific mycosis. Moreover, field bioassays, using infested bolt-exiting or healthy bolt-entering MPB populations, revealed a significant reduction in maternal

gallery lengths and larval density in the gallery. An attempt to probe the ecological and mechanistic virulence of the isolates was conducted. *In vitro* competition between the symbiotic BSF, *G. clavigera*, and the entomopathogen, *B. bassiana*, revealed effective inhibition by the latter, supporting an ecological advantage that perturbed the tripartite bark beetle system. Lastly, genomics of several *B. bassiana* strains supported an extensive inventory of virulence factors, as well as a proposal to reclassify the red pigmented, oosporein-producing strains to *B. pseudobassiana.* To our knowledge, this is the first account showing evidence of the efficacy of a *B. bassiana* formulation for the biocontrol of MPB population in relevant field environment.

Chapter 8 presents the summary and conclusions of the six different projects described in Chapters 2 – 7.

Lastly, Chapter 9 summarizes the experimental procedures utilized in the research projects presented in this thesis.

Chapter 2

Functional Genomics of *Bacillus thuringiensis* DNG9

2.1 Project Background

2.1.1. *Bacillus thuringiensis* DNG9

    Bacillus thuringiensis is a rod-shaped, Gram-positive bacterium that has been isolated from a variety of ecological niches including soil and aquatic environments and dead insects, among many others.[113] *B. thuringiensis* is known for its use as a bioinsecticide due to its ability to produce parasporal crystals that contain protein toxins (e.g. Cry proteins, also called δ-endotoxins) during its sporulation and stationary growth phase.[114] These protein toxins have also been successfully introduced to genetically modified crops, as exemplified in *Bt* corn, rendering these crops resistant to specific insect pests.[115] The protein toxins have been shown to be safe to plants, beneficial insects, and mammals due to the absence of specific receptors that are normally only found in the target organisms such lepidopterans (moths), coleopterans (beetles) and nematodes.[116,117] The potential of *B. thuringiensis* to serve as an alternative to chemical insecticides has driven the discovery of new *B. thuringiensis* strains that may lead to the identification of novel protein toxins with potential uses in pest management.[113,118] Aside from the insecticidal properties of *B. thuringiensis*, it has also been reported to exhibit antibacterial, antifungal, antibiofilm and emulsifying activities.[119-120] In general, *Bacillus* species is known to be rich sources of antimicrobial compounds.[121-14] For *B. thuringiensis*, its antibacterial effects can be attributed to a wide range of compounds including bacteriocins and lipopeptides.[125] On the other hand, its

antifungal activity has been attributed to the production of compounds such as zwittermicin, chitinase, and lipopeptides.[119]

2.1.2. Objectives

In this study, the whole genome sequence of *B. thuringiensis* DNG9, isolated from an oil-contaminated slough in Baraki-Algiers, Algeria was determined. This strain was chosen for sequencing due to its strong antimicrobial and emulsifying properties. It was the aim of this work to obtain a better understanding of the observed bioactivities based on the genes encoded in its genome.

2.2 Results and Discussion

2.2.1 Phenotypic and Genomic Characterization of *B. thuringiensis* DNG9

B. thuringiensis DNG9 was found to be flagellated, sporulating with a subcentral endospore and producing the insecticidal parasporal bodies (Figure 2.1ABC). These phenotypes are supported by gene inventories found in the genome of DNG9 (Figure 2.2). The RAST annotation has allocated these genes into 490 subsystems, the most abundant of which are genes that are associated with the metabolism of amino acids and derivatives (15.5%), followed by carbohydrate (11.7%), and protein metabolism (7.6%). The PGAP and JGI-IM annotated genomes were deposited to the DDBJ/ENA/GenBank databases under accession numbers MSTN00000000 and Ga0180945, respectively.

2.2.2 Functional Genomics of *B. thuringiensis* DNG9

B. thuringiensis DNG9 was found to be most active against *Lactococcus lactis* ssp. *cremoris* HP (Figure 2.1D), and was also active against *Carnobacterium divergens* LV13, *Salmonella enterica* Typhimurium ATCC 23564, and *Micrococcus* sp. ATCC 700405 but not against *Escherichia coli* JM109, *Pseudomonas aeruginosa* ATCC 14217, and *Enterococcus faecalis* 710C. Conversely, *B. thuringiensis* DNG9 was also found to be active against the fungus *Galactomyces geotrichum* MUCL 28959 but not *Aspergillus niger* ATCC 9142 and *Candida albicans* ATCC 10231. The antiSMASH 4.0 server predicted that DNG9 genome carries the gene
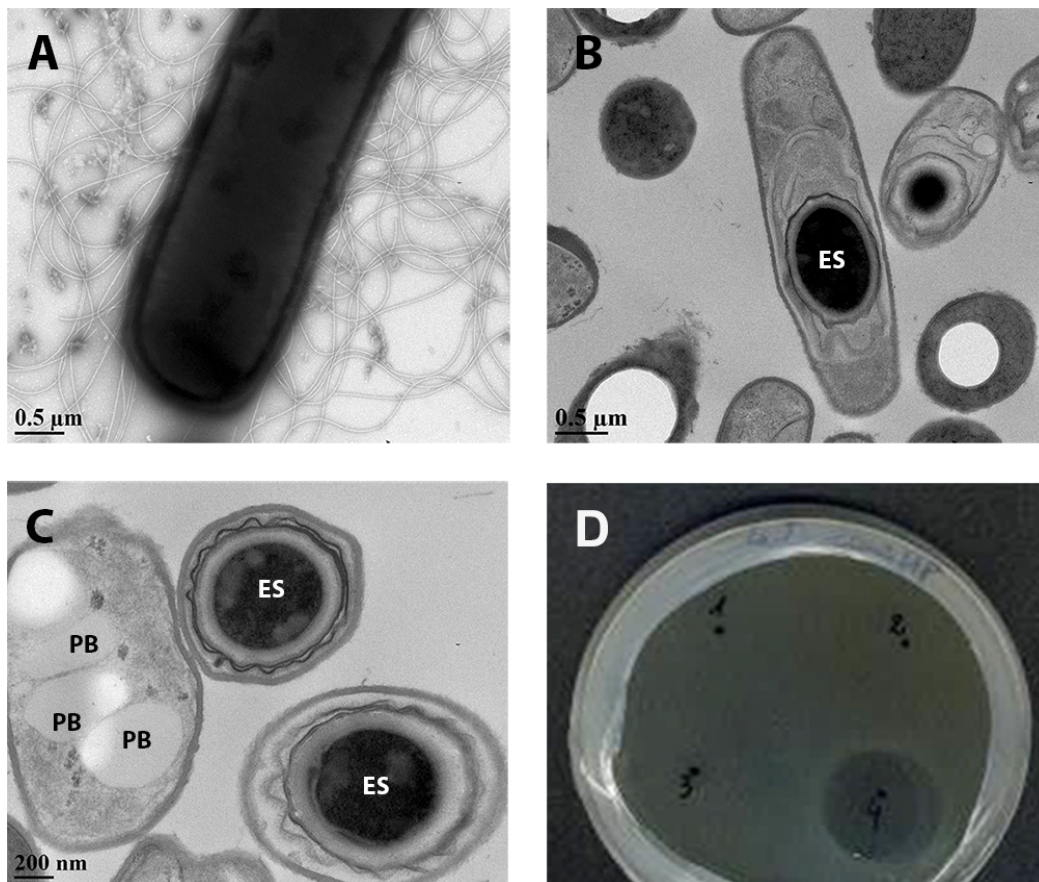
Figure 2.1. General morphological characteristics of *Bacillus thuringiensis* DNG9. Transmission electron micrograph (TEM) of DNG9 showing (A) flagellated cell, (B) subcentral endospore, ES, and (C) parasporal bodies, PB. (D) Spot-on-lawn assay showing the activity of DNG9 supernatant (labelled as 4) against indicator strain *Lactococcus lactis* subsp. *cremoris* HP.

clusters responsible for the production of several secondary metabolites including antibiotics, siderophores, and biopolymers. The genome was found to encode gene clusters with complete homology to the biosynthetic gene clusters of the antifungal compound, zwittermicin A (Figure 2.3A), the iron-siderophore, petrobactin (Figure 2.3B), and the bioplastic precursor, polyhydroxyalkanoates (PHAs) (Figure 2.3C). The aminopolyol compound zwittermicin A was previously shown to suppress fungal-oomycete diseases in plants,[126,127] suggesting that the antifungal activity of DNG9 could be attributed to this secondary metabolite. The presence of siderophores, like petrobactin and bacillibactin, in the genome of DNG9 suggests its iron acquisition abilities.
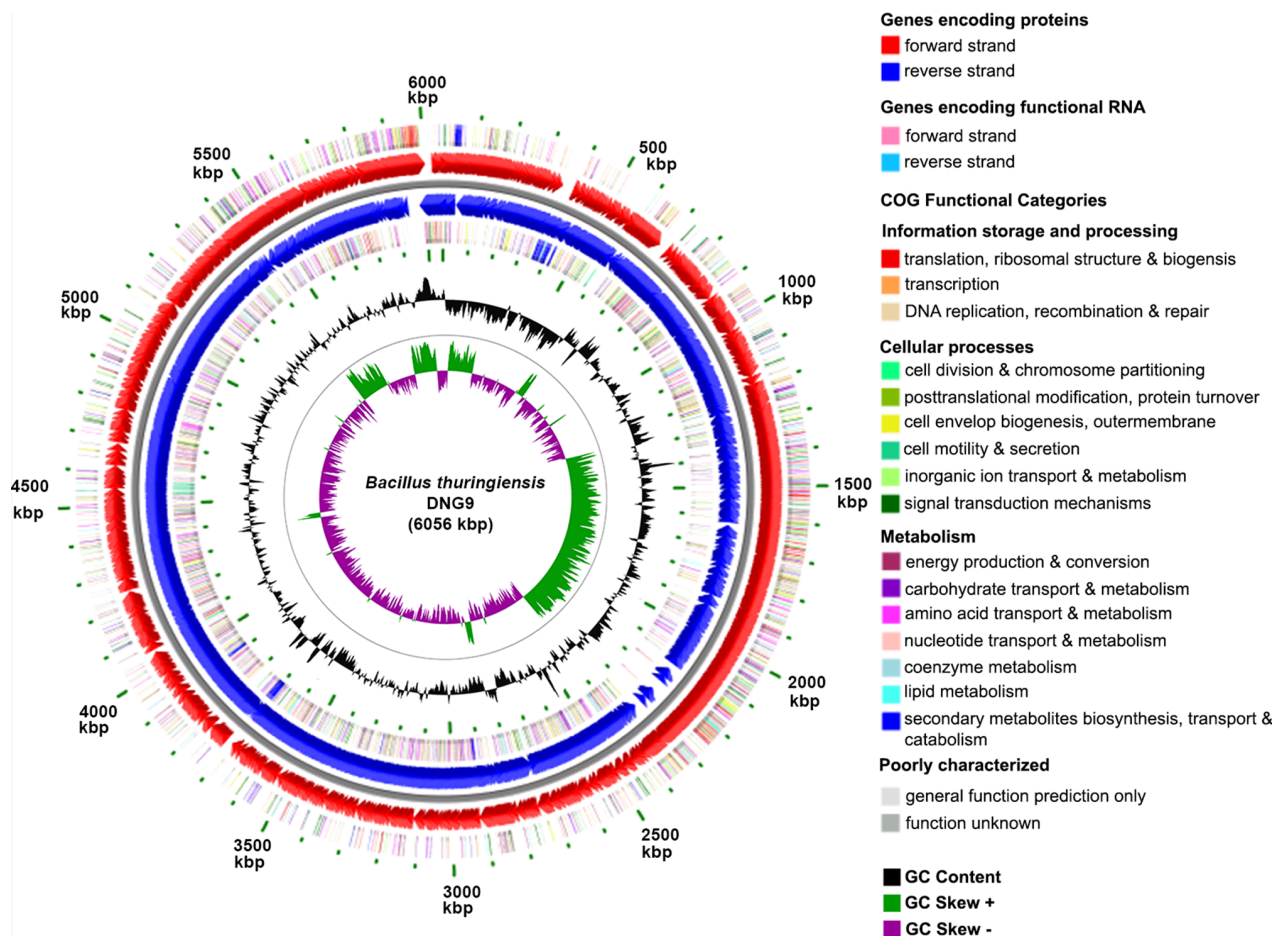
Figure. 2.2. Circular representation of the draft genome of DNG9 representing relevant genome features. The draft genome was aligned into one scaffold using *B. thuringiensis* Berliner ATCC 10792[T] genome. The outer most circle shows COG functional categories of coding regions in the clockwise direction. The lines in each concentric circle represent the position of the indicated feature; the color legend is shown to the right of the map. The second circle shows predicted coding regions transcribed on the forward (clockwise) DNA strand. The third circle shows predicted coding regions transcribed on the reverse (counter clockwise) DNA strand. The fourth circle shows COG functional categories of coding regions in the counter clockwise direction. The fifth and sixth circles show the percent GC content of the genome and the percent GC deviation (skewness) by strand, respectively. The genome map was created from a *de novo* assembled, BASys annotated, MEDUSA-rearranged scaffold contigs and viewed using CG Viewer.
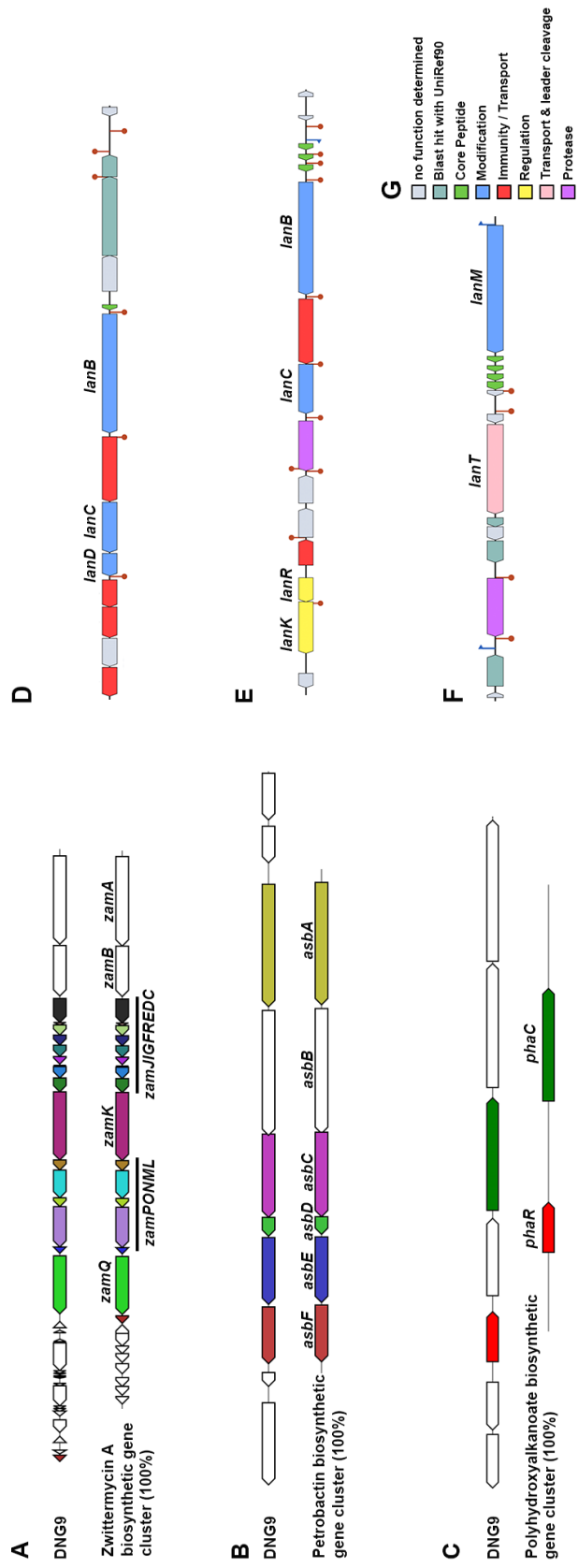
Figure 2.3. Secondary metabolite biosynthetic gene cluster organization in *B. thuringiensis* DNG9. Gene clusters for zwittermicin A (A), petrobactin (B), and polyhydroxyalkanoate (C) biosynthesis as predicted by antiSMASH 4.0. The DNG9 biosynthetic gene cluster is color coded with respect to its homology (%) to the known biosynthetic gene cluster. Gene cluster for three lanthipeptide class I (D), lanthipeptide class I (E) and lanthipeptide class II (F) biosynthesis as predicted by BAGEL 4.0. Color legend for Fig 2.3D, -E, -F is presented in G.

31

2.2.3 Comparative Genomics of *B. thuringiensis* DNG9

The biosynthetic gene clusters are not exclusive in *B. thuringiensis* but are also found in the genomes of other members of the *Bacillus cereus sensu lato* group.[128,129] Both antiSMASH 4.0 and BAGEL 3.0 servers also predicted a number of novel bacteriocins, mainly belonging to the class referred to as lanthipeptides (Figure 2.3D-F). Lastly, Bt_toxin scanner revealed that *cry* genes encoding the insecticidal crystal protein associated with *B. thuringiensis* are present in DNG9 genome, two homologs of *cry41* and one homolog of *cry6* genes. The wide biological target range of DNG9, including its antibacterial, antifungal, and insecticidal properties, could be attributed to these bioactive compounds. The genome of DNG9 is highly similar to those of *B. thuringiensis* Berliner ATCC 10792[T], *B. thuringiensis* YBT-1518, and B. *thuringiensis* Bt407, based on the phylogenetic analyses of the 16S rRNA gene (Figure 2.4), average nucleotide identity (ANI0 (>99%) and digital DNA:DNA hybridization (dDDH) (>95%) (Table 2.1) and shared gene content (Figure 2.5). Intra-species phylogeny showed the limitations of the 16S rRNA-based phylogenetic tree in resolving the *B. cereus sensu lato*, as many bootstrap values are < 80%.
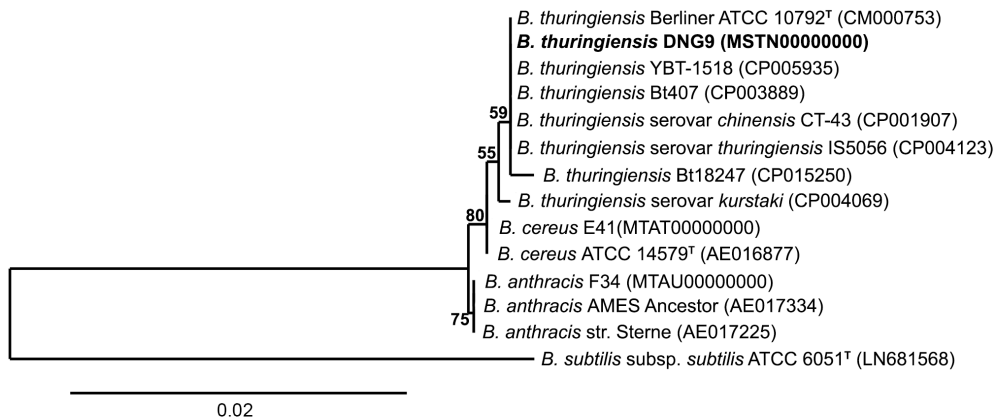
Figure 2.4. Maximum likelihood phylogeny of *B. thuringiensis* DNG9 16S rRNA gene. Nucleic acid sequences were aligned using Geneious and the tree was compiled using RAxML. Numbers above the branches refer to bootstrap values. The tree was rooted using *Bacillus subtilis* subsp. *subtilis* ATCC 6051[T]. Type strains are indicated with [T]. All strains represent sequenced

genomes. Scale bar indicates 2 nucleotide substitutions for each 10 nucleotide sequences. Accession numbers of publicly available sequences are given in brackets.

Table 2.1. Average nucleotide identity (ANI) and digital DNA:DNA Hybridization (dDDH) between the genome of DNG9 and closely related species in the class Bacillales.

Genome 1	Genome 2	ANI	dDDH
Bacillus thuringiensis Berliner ATCC 10792[T]	*Bacillus thuringiensis* DNG9	98.93	95.00
Bacillus thuringiensis YBT-1518	*Bacillus thuringiensis* DNG9	99.14	96.10
Bacillus thuringiensis Bt407	*Bacillus thuringiensis* DNG9	99.07	95.58
Bacillus thuringiensis serovar chinensis CT-43	*Bacillus thuringiensis* DNG9	99.05	95.50
Bacillus thuringiensis serovar *thuringiensis IS5056*	*Bacillus thuringiensis* DNG9	99.04	95.59
Bacillus thuringiensis Bt18247	*Bacillus thuringiensis* DNG9	99.10	92.20
Bacillus thuringiensis serovar *kurstaki*	*Bacillus thuringiensis* DNG9	96.28	72.95
Bacillus cereus ATCC 14579[T]	*Bacillus thuringiensis* DNG9	96.97	80.73
Bacillus cereus E41	*Bacillus thuringiensis* DNG9	96.78	80.89
Bacillus anthacis AMES Ancestor	*Bacillus thuringiensis* DNG9	91.05	6.90
Bacillus anthacis F34	*Bacillus thuringiensis* DNG9	91.09	6.76
Bacillus anthracis str. Sterne	*Bacillus thuringiensis* DNG9	91.02	6.80
Bacillus subtilis subsp. *subtilis* strain 168	*Bacillus thuringiensis* DNG9	76.95	0.02

The functional comparison of DNG9 genome composition with closely related *Bacillus* species (i.e. *B. thuringiensis, B. cereus* and *B. anthracis*)[130] is presented in Figure 2.5. *Bacillus subtilis* subsp. *subtilis* ATCC 6051[T] was used as an outgroup in the map. Comparison of the genomes of DNG9 and seven closely related *Bacillus* species by uni- and bidirectional best BlastP implemented in RAST, cross-validated with IMG annotations and viewed in IslandViewer v4 server,[131] revealed strain-specific genes that encode hypothetical proteins, which are grouped into genomic islands (Figure 2.5). These ORFs in DNG9 include a high proportion of mobile genetic elements, phage-like proteins, transposases, and hypothetical proteins in five distinct genomic

islands including an intact prophage in region A which is further supported by PHASTER server[132] analysis.

2.2.4 Genome Properties of *B. thuringiensis* DNG9

The size of the genome of DNG9 was estimated at 6,057,430 bp with 34.9% GC content, similar to the genomes of other *Bacillus thuringiensis* strains,[134-135] and contains 38 scaffolds with N_{50} of 347,259 bp. A total of 135 RNA genes and 284 pseudogenes were annotated by IMG/M and PGAP, respectively (Table 2.2). Annotation using the DOE-JGI IMG/MER pipeline revealed 6,109 total coding sequences of which 4,463 have functional predictions. Conversely, RAST annotation pipeline predicted 6,055 coding sequences; NCBI-PGAP revealed 6,213 coding genes; and lastly, BASys annotated 6,102 coding sequences. The 4,463 coding sequences predicted in IMG/M pipeline were placed in 25 general clusters of orthologous (COG) functional gene catalogs. The distribution of these protein-coding genes based on COG function is listed in Table 2.3. The 6.06 Mbp draft genome map of DNG9, as aligned against the type strain *B. thuringiensis* Berliner ATCC 10792, is presented in Figure 2.4.

Protein sequence identity (%)

	100	99.9	99.8	99.5	99	98	95	90	80	70	60	50	40	30	20	10
Bidirectional best hit	100	99.9	99.8	99.5	99	98	95	90	80	70	60	50	40	30	20	10
Unidirectional best hit	100	99.9	99.8	99.5	99	98	95	90	80	70	60	50	40	30	20	10
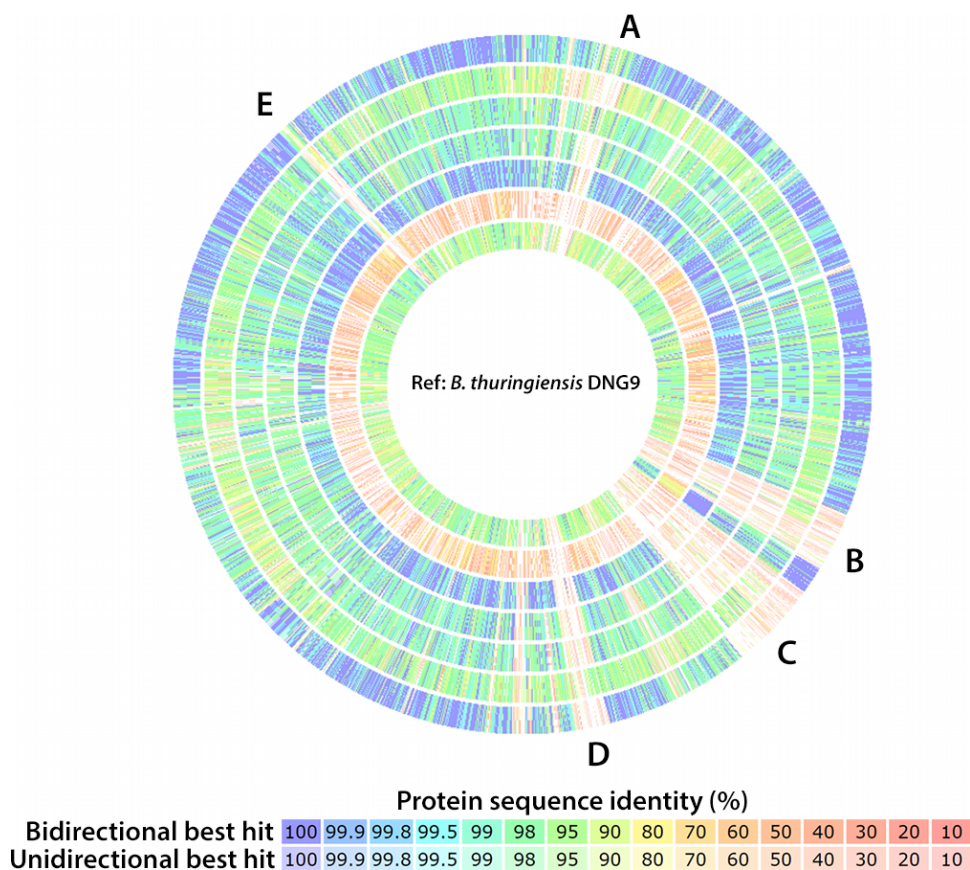
Figure 2.5. Genomic comparison of *B. thuringiensis* DNG9 to other *Bacillus* sp. genomes conducted using RAST. Each track represents pair-wise BLAST comparison between the open reading frames in query genome against those in *Bacillus thuringiensis* DNG9 (Ref = reference genome), with percentage of similarity represented with different colors shown in the legend. Query genomes used in this analysis (outer ring to inner ring): *B. thuringiensis* Berliner ATCC 10792[T], *B. anthracis* F34, *B. cereus* ATCC 14579, *B. cereus* E41, *B. thuringiensis* YBT-1518, *B. subtilis* subsp. *subtilis* ATCC 6051[T] and *B. anthracis* AMES Ancestor.

Table 2.2. Genome statistics of *B. thuringiensis* DNG9.

Attribute	Value	% of Total
Genome size (bp)	6,057,430	100.00
DNA coding (bp)	5,053,197	83.42
DNA G+C (bp)	2,107,907	34.80
DNA scaffolds	38	100.00
Total genes	6,109	100.00
Protein coding genes	5,974	97.79
RNA genes	135	2.21
Pseudo genes	284	4.65

35

Genes in internal clusters	2,024	33.13	
Genes with function prediction	4,463	73.06	
Genes assigned to COGs	3,633	59.47	
Genes with Pfam domains	4,883	79.93	
Genes with signal peptides	284	4.65	
Genes with transmembrane helices	1,741	28.50	
CRISPR repeats	4	0.07	

Table 2.3. Number of genes associated with general COG functional categories in *B. thuringiensis* DNG9.

Code	Value	%-age	Description
J	262	6.38	Translation, ribosomal structure, and biogenesis
A	0	0	RNA processing and modification
K	388	9.44	Transcription
L	135	3.29	Replication, recombination, and repair
B	1	0.02	Chromatin structure and dynamics
D	60	1.46	Cell cycle control, cell division, chromosome partitioning
V	124	3.02	Defense mechanisms
T	213	5.19	Signal transduction mechanisms
M	236	5.74	Cell wall/membrane biogenesis
N	55	1.34	Cell motility
U	36	0.88	Intracellular trafficking and secretion
O	160	3.89	Posttranslational modification, protein turnover, chaperones
C	210	5.11	Energy production and conversion
G	250	6.09	Carbohydrate transport and metabolism
E	400	9.74	Amino acid transport and metabolism
F	130	3.16	Nucleotide transport and metabolism
H	228	5.55	Coenzyme transport and metabolism
I	146	3.55	Lipid transport and metabolism
P	233	5.67	Inorganic ion transport and metabolism
Q	109	2.65	Secondary metabolites biosynthesis, transport, and catabolism
R	3.96	9.64	General function prediction only
S	301	7.33	Function unknown
-	2476	40.53	Not in COGs

2.3 Conclusion and Future Directions

In conclusion, here we report a 6.06 Mbp draft genome of *B. thuringiensis* DNG9, isolated from an oil-contaminated soil-slough in Baraki-Algeirs, Algeria. The final *de novo* assembly is based on 306.5 Mb of Illumina data, which provided an average coverage of 317×. The assembled genome contains 6,120 coding sequences (average of 4 annotation pipelines), of which the most abundant are genes that are associated with amino acid (15.5%), followed by carbohydrate (11.7%), and protein metabolism (7.6%). The antimicrobial properties of *B. thuringiensis* DNG9 against several Gram-positive and Gram-negative bacteria, as well as fungal phytopathogens, could be inferred in part with a number of gene inventories in encoded in the draft genome. The comparative analysis with closely related bacterial genomes, alignment of the 16S rRNA sequences and prediction of gene inventories for the insecticidal Cry protein biosynthesis placed strain DNG9 under *B. thuringiensis.* This indicated that strain DNG9 could have several potential use as an insect biocontrol agent, a fungal phytopathogen control agent, and a source of biopolymers (PHA) and antibacterial compounds. Lastly, the genome sequence of DNG9 may provide another model system to study pathogenicity against insect pests and plant diseases, and for antimicrobial compound mining and phylogenesis among *B. cereus sensu lato* group.

Chapter 3

Functional Genomics of Fengycin Lipopeptides from

Bacillus velezensis F11

3.1 Project Background

3.1.1. *B. velezensis F11*

    Bacillus species are rod-shaped, aerobic or facultative anaerobic, Gram-positive bacteria that produce robust endospores, which facilitate their survival in various habitats such as soil, aquatic environments, food, plants, and digestive tracts of animals and insects.[136] They have great potential in various biotechnological and biopharmaceutical applications due to their ability to produce an extensive range of antimicrobial compounds including bacteriocins and lipopeptide antibiotics.[137-138] In an era where there is an increasing threat posed by bacterial resistance to conventional antibiotics, *Bacillus* spp. could serve as potential sources of alternative antibiotic compounds.[138]

    Bacteriocins are ribosomally-synthesized peptide antibiotics that are produced by bacteria to kill competing bacteria. Next to lactic acid bacteria (LAB), the *Bacillus* genus is considered as the second most common producer of bacteriocins.[139] There is an increasing interest in *Bacillus* spp. because several strains have been shown to exhibit broader inhibition spectra than LAB.[139] LAB are mostly active against Gram-positive bacteria, while several *Bacillus* strains were shown to inhibit both Gram-positive and Gram-negative bacteria, as well as fungal pathogens. The broader inhibition spectra of *Bacillus* spp. can be attributed to the production of metabolites aside from bacteriocins, among which are antimicrobial lipopeptides. The known classes of *Bacillus*

lipopeptides include polymyxins, polypeptins, surfactins, fengycins, and iturins.[138] These lipopeptides are biosynthetically created using non-ribosomal peptide synthetases.[138-139] Aside from acting as antimicrobial agents, *Bacillus* lipopeptides could serve as biosurfactants. Their biodegradability and low toxicity render them as promising alternatives to synthetic surfactants.[139]

3.1.2 Objectives

In this chapter, we report the novel *Bacillus* strain, *Bacillus amyloliquefaciens* subspecies *plantarum* F11, phylogenetically updated to *B. velezensis*, which was isolated from an Algerian salt lake and was found to be active against both Gram-positive and Gram-negative bacteria, as well as fungi. We present the draft genome of the strain, which revealed that it is capable of producing a number of biosurfactants and bioactive metabolites. Furthermore, we describe the purification of fengycin lipopeptides through a series of activity-guided hydrophobic interaction chromatographic techniques coupled with mass spectrometry.

3.2 Results and Discussion

3.2.1 Genome Features of *B. velezensis F11*

A bacterial isolate from a salt lake in Ain Baida-Ouargla, Algeria was initially identified at the genus level as *Bacillus* sp. F11 based on taxonomical characterization using the API 50 CHB bacterial identification system (Table 3.1). Whole-genome shotgun sequencing was performed for strain F11, and the resulting statistics are summarized in Table 3.2. *De novo* assembly revealed a draft genome with a total size of 4,016,659 bp and a G+C content of 46.18 % in 17 contigs (>1,400 bp). The assembled genome has a high sequence coverage (511×) and an N_{50} of 567,030 bp.

Table 3.1. Morphological, biochemical, and physiological characteristics of *B. velezensis* F11.

+ : Positive reaction; - : Negative reaction.

Test	Reaction
Gram's reaction	+
Anaerobic growth	-
Chains of cells	+
Motility	+
Catalase	+
Oxidase	+
Nitrate reduction	+
Spores ellipsoid	+
Spores central/paracentral	-
Spores subterminal	+
Spores terminal	-
API 20 NE & API 50 CHB tests	
ß-galactosidase	+
Arginine dihydrolase	-
Lysine decarboxylase	-
Ornithine decarboxylase	-
Citrate utilization	-
Hydrogen sulfide production	-
Urease	+
Tryptophan deaminase	-
Acetoin production	+
Gelatinase	+
Fermentation/oxidation	
Glucose	+
Mannitol	+
Inositol	+
Sorbitol	+
Rhamnose	-
Sucrose	+
Melibiose	-
Amygdalin	+
Arabinose	+

Table 3.2. Genome properties of *B. velezensis* F11.

Attribute	Value	% of Total
Genome size (bp)	4,016,659	100.00
DNA coding (bp)	3,606,511	89.79
DNA G + C (bp)	1,855,067	46.18
DNA scaffolds	17	100.00
Total genes	4,027	100.00
Protein coding genes	3,921	97.37
RNA genes	106	2.63
Pseudogenes	89	2.21
Genes in internal clusters	979	24.31
Genes with function prediction	3,182	79.02
Genes assigned to COGs	2,732	67.84
Genes with Pfam domains	3,360	83.44
Genes with signal peptides	262	6.51
Genes with transmembrane helicases	1,036	25.73

Morphological analysis by TEM showed that strain F11 is flagellated (Figure 3.1A), which is consistent with the genome-encoded gene clusters for motility and chemotaxis. The genome sequence also supports extensive gene inventories for dormancy and sporulation, although endospore formation was not observed (Figure 3.1B). This can be attributed to samples being taken during the mid-logarithmic (log) phase for microscopy, while endospores usually form in late-log or stationary phases (Figure 3.1B, inset).

3.2.2. Comparative Genomic Analysis of *B. velezensis* F11

Core genome phylogenetic analysis placed strain F11 in the same clade as *B. amyloliquefaciens* ssp. *plantarum* DSM 23117, the type strain for this subspecies,[29] which is distinct from the clade containing *B. amyloliquefaciens* ssp. *amyloliquefaciens* DSM 7, the type strain for this subspecies (Figure 3.2). Recent whole phylogenomics data reclassified F11 to *B. velezensis.*
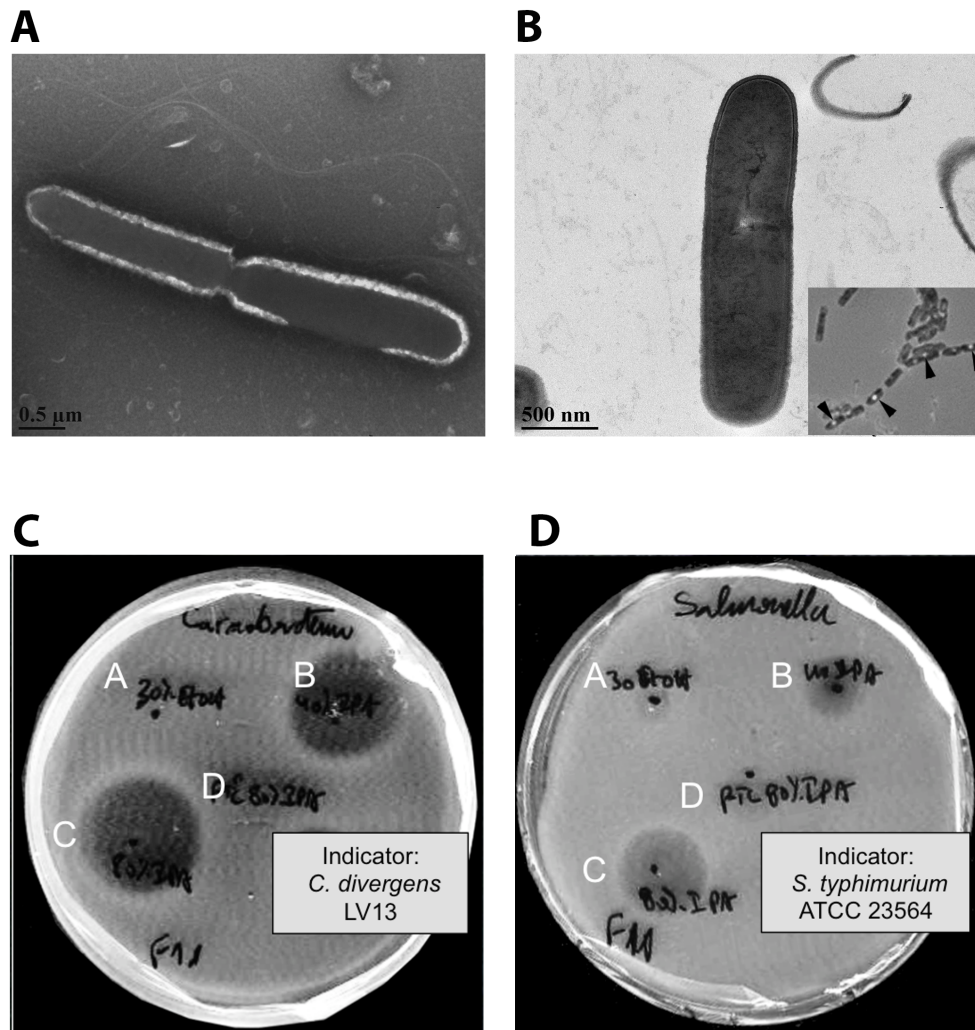
Figure 3.1. Cell structure and antimicrobial properties of *B. velezensis* F11. Transmission electron microscopy analysis of *B. velezensis* F11 showing (A) a negatively tungsten-stained flagellated dividing cell, and (B) a uranium-lead stained non-sporulated vegetative cell and Schaeffer-Fulton-stained endospores (triangle, inset). Spot-on-lawn assays showing zones of inhibition against (C) *Carnobacterium divergens* LV13 and (D) *Salmonella enterica* ssp. *enterica* serovar Typhimurium ATCC 23564. Fractions A, B, C, and D correspond to 30% ethanol, 40% isopropanol (IPA), 80% IPA with 0.1% trifluoroacetic acid, and sample flow-through, respectively, that were obtained from C_{18} solid phase extraction cartridge purification of the 80% IPA-0.1% TFA fraction from the Amberlite XAD-16 resin purification of the *B. velezensis* F11 culture supernatant.
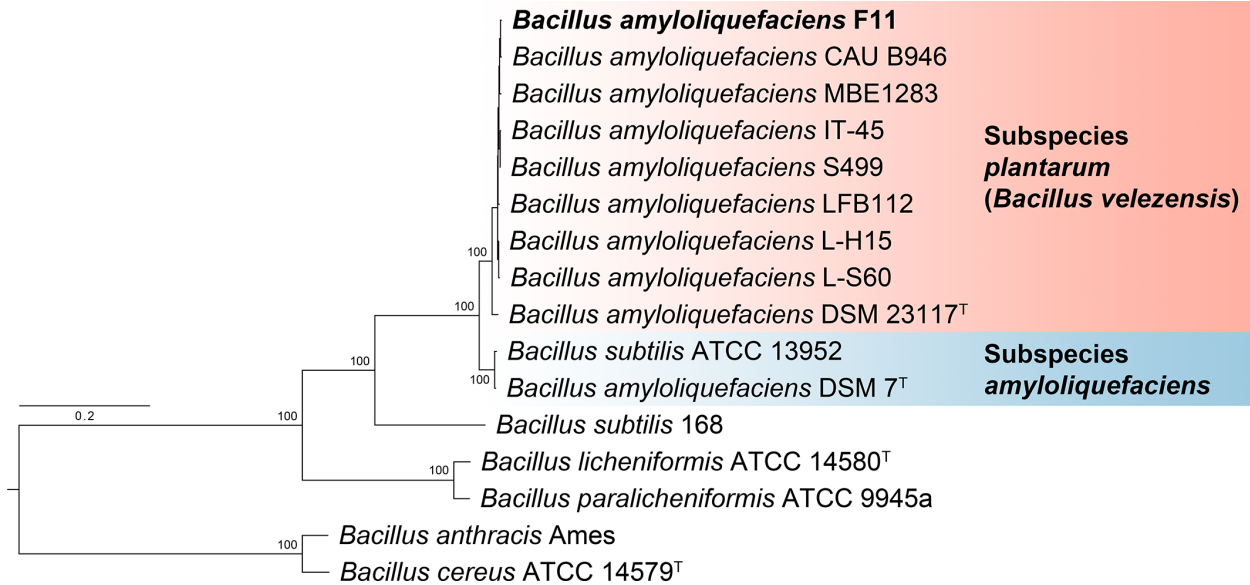
Figure 3.2. The phylogenetic relationship of *B. amyloliquefaciens* ssp. *plantarum* F11 (now *B. velezensis*) and selected closely related members of the genus *Bacillus*. The phylogenetic tree was reconstructed from the concatenated alignment of 1,313 core genes (1,192,958 bp). Relevant bootstrap values are indicated on the nodes. The scale bar represents nucleotide substitutions per site. The genome sequenced in this study (*B. amyloliquefaciens* ssp. *plantarum* F11) in bold. *B. amyloliquefaciens* ssp. *plantarum* is a later heterotypic synonym of *B. velezensis*.

Average nucleotide identity (ANI) and digital DNA:DNA hybridization (dDDH) confirm the identity of strain F11 to be *B. velezensis*, as indicated by values that were above the species cut-offs (95% and 70%, respectively)[140] against DSM 23117 (Table 3.3). On the other hand, comparison of the F11 and DSM 7 genomes displayed low similarity, sharing only 94% ANI and 55% dDDH (Table 3.3). Furthermore, DSM 7, when compared against DSM 23117, exhibits values of only 94% ANI and 56% dDDH. This indicates that DSM 23117 and F11 likely belong to a different species than DSM 7, not merely another subspecies. DSM 7 keeps the name as it was designated as *B. amyloliquefaciens* before DSM 23117. Dunlap and coworkers[141] suggest that *B. amyloliquefaciens* ssp. *plantarum* is a later heterotypic synonym of *Bacillus velezensis* (Figure

3.2). Incidentally, strain DSM 7 shares 99% ANI and 95% dDDH with *B. subtilis* ATCC 13952 (not a type strain for this species), suggesting that the latter was misidentified and is in fact a *B. amyloliquefaciens* ssp. *amyloliquefaciens*. Proper identification of our F11 strain was imperative to this study. Additionally, our work highlights the need to examine the reclassification of the *plantarum* and *amyloliquefaciens* subspecies into potentially two different species, which is an ongoing issue.[142-144]

Table 3.3. Pairwise whole-genome comparisons between various *Bacillus* sp. strains and *B. amyloliquefaciens* ssp. *plantarum* F11 (now *B. velezensis*). Average nucleotide identity (red, lower left) and *in silico* DNA-DNA hybridization (blue, upper right) are crossed compared.

	B. amyloliquefaciens F11	B. amyloliquefaciens CAU B946	B. amyloliquefaciens DSM 23117	B. amyloliquefaciens IT-45	B. amyloliquefaciens L-H15	B. amyloliquefaciens L-S60	B. amyloliquefaciens LFB112	B. amyloliquefaciens MBE1283	B. amyloliquefaciens S499	B. amyloliquefaciens DSM 7	B. subtilis ATCC 13952	B. subtilis 168	B. anthracis Ames	B. cereus ATCC 14579	B. licheniformis ATCC 14580	B. paralicheniformis ATCC 9945a
Bacillus amyloliquefaciens F11		95.10	80.20	95.30	95.20	95.20	95.80	94.50	95.30	55.00	54.50	20.60	28.90	29.60	18.90	19.10
Bacillus amyloliquefaciens CAU B946	99.36		80.20	95.30	94.70	95.00	96.00	94.80	95.30	55.30	54.90	20.80	34.50	34.50	19.90	20.10
Bacillus amyloliquefaciens DSM 23117	97.64	97.69		80.50	80.20	80.30	80.30	79.90	80.50	56.20	55.80	20.90	35.40	35.70	19.60	20.10
Bacillus amyloliquefaciens IT-45	99.35	99.45	97.69		95.10	95.20	95.80	95.20	100.00	55.50	55.20	20.80	34.50	34.80	19.70	20.10
Bacillus amyloliquefaciens L-H15	99.36	99.38	97.66	99.34		99.90	95.10	94.60	95.10	55.40	54.90	20.70	34.20	34.50	19.50	19.80
Bacillus amyloliquefaciens L-S60	99.34	99.38	97.65	99.31	99.99		95.10	94.90	95.20	55.30	54.90	20.80	34.50	34.80	19.40	19.80
Bacillus amyloliquefaciens LFB112	99.44	99.32	97.58	99.21	99.21	99.22		95.00	95.00	55.60	55.00	20.80	34.70	35.30	19.70	19.90
Bacillus amyloliquefaciens MBE1283	99.28	99.34	97.60	99.32	99.35	99.35	99.32		95.20	55.20	54.80	20.90	34.40	34.60	19.60	20.00
Bacillus amyloliquefaciens S499	99.37	99.43	97.69	99.97	99.40	99.40	99.35	99.39		55.50	55.10	20.70	33.70	34.00	19.50	20.00
Bacillus amyloliquefaciens DSM 7	93.95	93.92	93.99	93.89	93.91	93.91	93.86	93.94	93.93		95.40	20.90	34.60	35.80	19.90	20.00
Bacillus subtilis ATCC 13952	93.82	93.84	93.92	93.80	93.85	93.85	93.81	93.83	93.84	99.41		20.80	33.40	34.50	19.70	19.70
Bacillus subtilis 168	76.35	76.41	76.53	76.41	76.42	76.44	76.41	76.43	76.42	76.34	76.37		34.50	32.00	19.20	19.50
Bacillus anthracis Ames	66.38	66.56	66.61	66.57	66.59	66.61	66.57	66.60	66.57	66.77	66.70	67.20		45.00	30.20	32.20
Bacillus cereus ATCC 14579	66.80	67.01	67.06	66.92	66.86	66.89	66.94	66.91	66.90	67.01	66.98	67.51	91.52		32.40	32.90
Bacillus licheniformis ATCC 14580	71.88	71.99	71.92	71.94	71.95	71.96	71.93	72.00	71.92	71.94	71.96	72.13	66.07	66.12		58.30
Bacillus paralicheniformis ATCC 9945a	71.84	71.88	71.95	71.90	71.91	71.91	71.89	71.94	71.90	71.86	71.86	71.96	66.47	66.29	94.33	
Average nucleotide identity																

In silico DNA-DNA hybridization

3.2.3. BGC Genomic Analysis of *B. velezensis F11*

Analysis of the *B. velezensis* F11 draft genome for secondary metabolite production using the antiSMASH server revealed that the strain carries genes involved in the production of antibacterial polyketides (macrolactin, bacillaene, and difficidin), an iron-siderophore (bacillibactin), and an antibacterial dipeptide (bacilysin). Moreover, both antiSMASH and BAGEL predicted a gene cluster associated to a putative novel lanthipeptide. Lastly, biosynthetic machineries responsible for the production of cyclic lipopeptides surfactins, locillomycins, and fengycins are also present. The genome of F11 and other *B. velezensis* strains revealed the presence of the ~37.7 kb fengycin biosynthetic gene cluster (Figure 3.3A), consistent with our antiSMASH findings. Strains of the *velezensis* show an overall relatively high similarity (90%) to the curated fengycin cluster of DSM 23117 (Figure 3.3B). On the other hand, DSM7 and ATCC 13952 (ssp. *amyloliquefaciens*) show lower similarity (50 – 60%) against the DSM 23117 reference cluster (Fig. 3B).

(A)

Strains:
1) *B. amyloliquefaciens* **F11**
2) *B. amyloliquefaciens* CAU B946
3) *B. amyloliquefaciens* IT-45
4) *B. amyloliquefaciens* L-H15
5) *B. amyloliquefaciens* L-S60
6) *B. amyloliquefaciens* LFB112
7) *B. amyloliquefaciens* MBE1283
8) *B. amyloliquefaciens* S499
9) *B. amyloliquefaciens* DSM 7^T
10) *B. subtilis* ATCC 13952
11) *B. subtilis* 168
12) *B. amyloliquefaciens* DSM 23117^T

CDS   tRNA
rRNA   Other

BLAST hit:
= 100% identical
≥ 90% identical
≥ 80% identical
≥ 70% identical
≥ 60% identical
≥ 50% identical
≥ 40% identical
≥ 30% identical
≥ 20% identical
≥ 10% identical
≥ 0% identical

COG categories:
A COG
B COG
J COG
K COG
L COG
D COG
O COG
M COG
N COG
P COG
T COG
U COG
V COG
W COG
Y COG
Z COG
C COG
G COG
E COG
F COG
H COG
I COG
Q COG
R COG
S COG
Unknown

(B)

Fengycin biosynthetic gene cluster

Figure 3.3. *B. amyloliquefaciens* ssp. *plantarum* (now *B. velezensis*) **F11 genome BLAST atlas.**
(A) The map compares sequenced genomes against the reference, *B. amyloliquefaciens* DSM 23117. The four outermost rings show the forward and reverse strand sequence features of the reference genome (two innermost; colored based on CDS, rRNA, tRNA, or other) and their corresponding predicted functions categorized based on the Cluster of Orthologous Groups of proteins (COG) database (two outermost). The next 12 rings show regions of sequence similarity detected by BLASTP comparisons between genes of the reference and query genomes. (B) A magnified region of the BLAST atlas showing the comparison of the fengycin biosynthetic gene cluster of strains against the *B. amyloliquefaciens* DSM 23117 reference.

46

3.2.4. Biosurfactant and Emulsifying Activities of *B. velezensis F11*

The biodegradability and lower toxicity of natural biosurfactants render them as appealing alternatives to synthetic surface-active compounds.[145] The potential of *B. velezensis* F11 to produce biosurfactants was assessed based on its emulsification index, as well as the results of drop collapse and oil displacement assays. The emulsification index of *B. velezensis* F11, calculated at different time points, revealed that the strain exhibits high emulsifying activity, with a maximum emulsification index of 81% during the mid-stationary growth phase at 50 h of bacterial growth at 27 °C with shaking at 200 rpm (Figure 3.4).
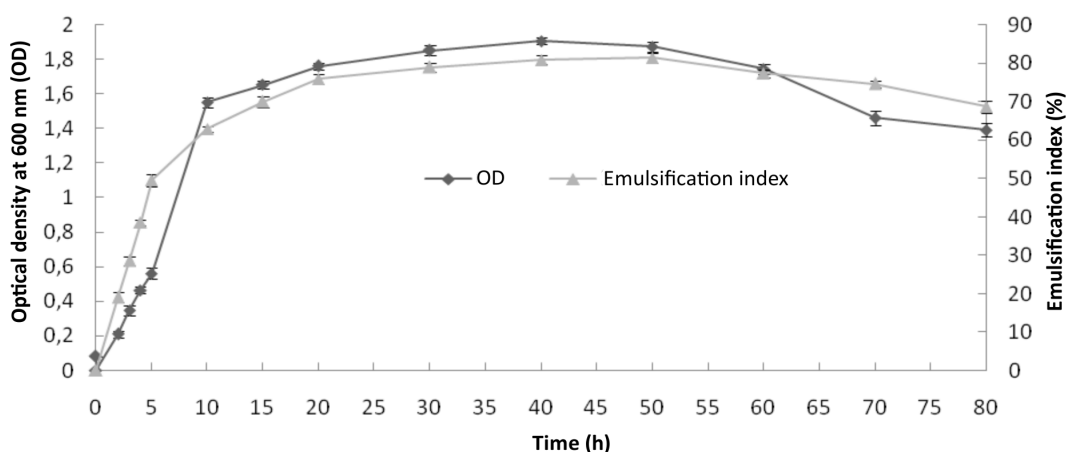
Figure 3.4. Time-course of growth and emulsification index of *B velezensis* F11 in LB medium at 27 °C. The experiments were performed in triplicate. Error bars are shown for standard deviation (P ≤ 0.05).

The formation of a stable emulsion is indicative of the presence of biosurfactants.[146-147] This was further supported by both the drop collapse and oil displacement assays. The drop collapse assay indicates that the maximum amount of biosurfactants was produced during the 40 to 60 h growth period (Table 3.4). Similarly, for the oil displacement assay, the maximum clearing zone of 2.2 cm was observed after 50 h of bacterial growth (Table 3.4).

Table 3.4. Drop collapse and oil displacement assays for *B. velezensis* F11. Scoring system of '+' to '+++' correspond to partial to complete spreading of bacterial culture droplet on the oil film surface. Rounded drops were scored as negative '-', indicative of the lack of biosurfactant production.

Time (hours)	Drop Collapse (Response level)	Oil spreading diameter (cm)
0	-	0
2	+	0.9
3	+	1.0
4	+	1.1
5	+	1.1
10	+	1.2
15	++	1.4
20	++	1.7
30	++	1.8
40	+++	2.0
50	+++	2.2
60	+++	2.1
70	++	1.9
80	++	1.8

3.2.5. Antibacterial and Antifungal Activities of *B. velezensis* F11

B. amyloliquefaciens strains have been reported to produce various antibacterial and antifungal compounds.[148-149] For instance, *B. amyloliquefaciens* RC-2 was shown to be an effective antagonistic agent against the fungal mulberry anthracnose pathogen due to the secretion of iturin lipopeptides.[148] *B. amyloliquefaciens* GA1 produces an anti-listerial lantibiotic, amylolysin, and antimicrobial lipopeptides surfactin, iturins, and fengycins.[150-151] More recently, *B. amyloliquefaciens* RX7 was reported to produce the novel broad-spectrum RX7 bacteriocin.[152]

B. velezensis F11 has potent activity against both Gram-positive and Gram-negative bacteria,

as well as various fungal species. Spot-on-lawn assays showed that the culture supernatant of *B. velezensis* F11 exhibits strong antagonistic activity against *C. divergens* LV13 and *L. lactis* subsp. *cremoris* HP, and moderate activity against *E. faecalis* 710C, *E. coli* JM109, *S. enterica* serovar Typhimurium ATCC 23564 and *P. aeruginosa* ATCC 14217. A plate diffusion assay revealed that *B. velezensis* F11 exhibits significant antifungal activity against *C. albicans* ATCC 10231*, A. niger* ATCC 9142 and *G. geotrichum* MUCL 28959. Altogether, the observed broad-spectrum of activity of *B. velezensis* F11 can be attributed to the production of a mixture of bioactive compounds as indicated in its genome.

3.2.6. Identification of Antimicrobial Lipopeptides by Mass Spectrometry

To further investigate the compounds responsible for the activity of *B. velezensis* F11, a large-scale fermentation was performed, and the culture supernatant was sequentially purified using Amberlite XAD-16 resin column chromatography, C_{18} SPE purification, and RP-HPLC. SPE fractionation revealed that the 80% IPA-0.1% TFA fraction was the most active fraction against both the Gram-negative (*S. enterica* serovar Typhimurium ATCC 23564) and Gram-positive (*C. divergens* LV13) indicator strains (Figure 3.1C, D). This fraction was consequently purified by RP-HPLC, and the active fraction was analyzed by mass spectrometry. LC-MS analysis revealed a cluster of peaks with *m/z* values of 1435.8 $[C_{70}H_{106}N_{12}O_{20} + H]^+$, 1449.8 $[C_{71}H_{108}N_{12}O_{20} + H]^+$, and 1463.8 $[C_{72}H_{110}N_{12}O_{20} + H]^+$ (Table 3.5).

Table 3.5. Fengycin lipopeptides from *B. velezensis* F11 as detected by mass spectrometric analysis.

Molecular formula	Observed *m/z*	Calculated *m/z*	Assignment
$[C_{70}H_{106}N_{12}O_{20} + H]^+$	1435.7731	1435.7719	C_{14} fengycin A
$[C_{71}H_{108}N_{12}O_{20} + H]^+$	1449.7881	1449.7876	C_{15} fengycin A
$[C_{72}H_{110}N_{12}O_{20} + H]^+$	1463.8027	1463.8032	C_{16} fengycin A
$[C_{72}H_{110}N_{12}O_{20} + H]^+$	1463.8027	1463.8032	C_{14} fengycin B

Through MALDI-TOF MS/MS sequencing, the peaks at 1435.8 and 1449.8 *m/z* were found to correspond to fengycin A lipopeptides with C_{14} and C_{15} saturated lipid tails, respectively (Figure 3.5C-E). Fengycins are lipodecapeptides that are cyclized through lactone formation between the phenolic hydroxyl group of Tyr^3 and the carboxylic acid group of the C-terminal Ile.[146] All known fengycin homologues consist of the same peptide sequence (L-Glu—D-Orn—D-Tyr—D-*allo*-Tyr—L-Glu—D-Ala/D-Val—L-Pro—L-Gln—L-Tyr—L-Ile), except at position 6, which could either be Ala or Val residue.[146] In turn, fengycins are classified as fengycin A or fengycin B for homologues with Ala or Val at position 6, respectively. For the lipid component, fengycins exhibit a β-hydroxy fatty acyl moiety at the N-terminus with a chain length of 14 to 17 carbon atoms that can be saturated or unsaturated.[151] Characteristic ions corresponding to the lactone ring (loss of [fatty acid—L-Glu—D-Orn]), and the lactone ring with D-Orn (loss of [fatty acid—L-Glu]) serve as fingerprint fragments that indicate the identity of the fengycins. For fengycin A, these fragments are 1080 and 966 *m/z*, respectively, while for fengycin B, the fragments are 1108 and 994 *m/z*, respectively (Figure 3.5A, 3.5B). MALDI-TOF MS/MS fragmentation of the peaks at 1435.8 and 1449.8 *m/z* showed the 1080 and 966 *m/z* fragments, which confirmed that both lipopeptides are fengycin A homologues (Figure 3.5D, 3.5E). Other fragmentation patterns that include internal cleavages on the lactone ring were analyzed by nano-LC MS/MS sequencing, which further

supported the identities of these lipopeptides. MS/MS fragmentation of the peak at 1463.8 *m/z*

showed that the peak corresponds to a fengycin A lipopeptide with C_{16} lipid tail, and a fengycin B

lipopeptide with a C_{14} lipid tail, since both sets of fingerprint fragments for fengycin A (1080 and

966 *m/z*) and fengycin B (1108 and 994 *m/z*) were observed (Figure 3.5F). The purification and

identification of the fengycin lipopeptides from *B. velezensis* F11 confirmed that the fengycin

gene clusters detected in the assembled genome sequence are functional.
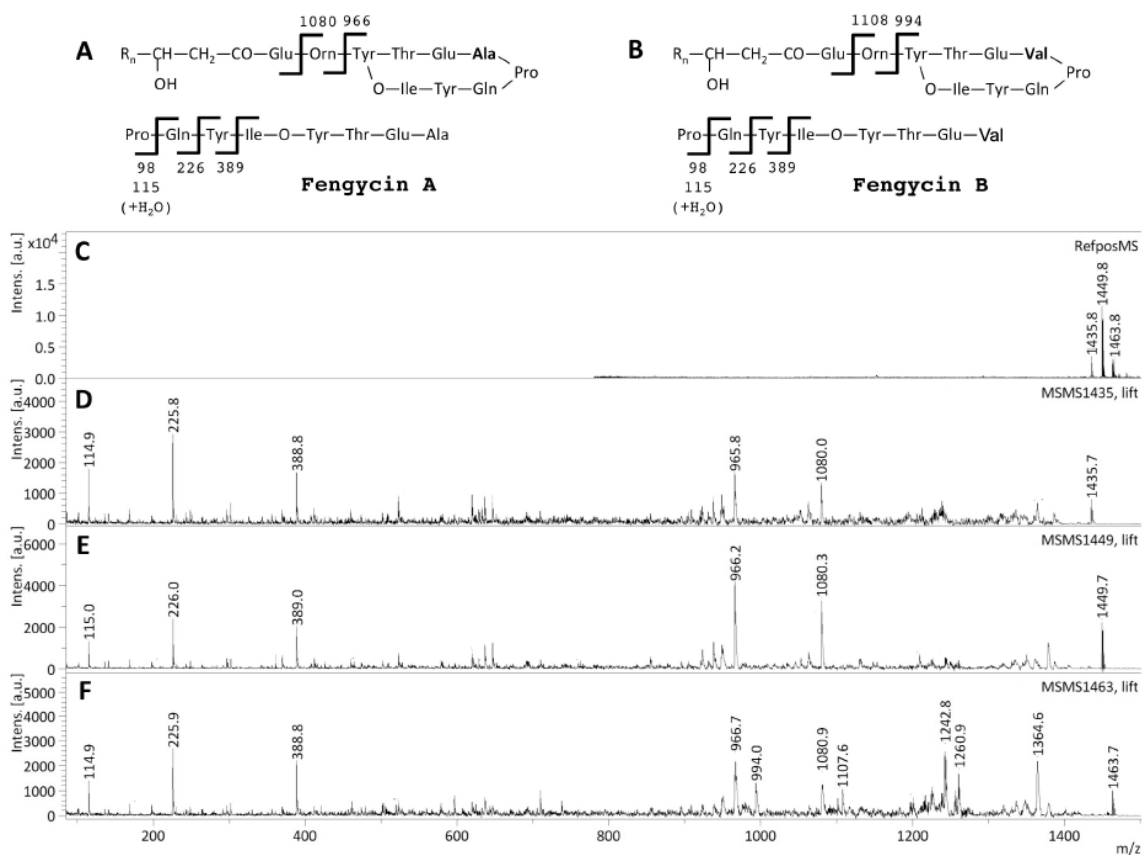
Figure 3.5 Mass spectrometry analysis of fengycin lipopeptides from *B. velezensis* F11. Structure and expected fragmentation patterns of (A) fengycin A and (B) fengycin B. (C) MALDI-TOF mass spectrum of fengycin lipopeptides from *B. velezensis* F11. MALDI-TOF MS/MS fragmentation of lipopeptides with *m/z* of (D) 1435.8, (E) 1449.8 and (F) 1463.8.

3.3. Conclusion and Future Directions

In conclusion, this chapter describes the isolation, characterization, and genome sequencing of strain F11, belonging to the species *B. velezensis*. This strain was shown to have excellent biosurfactant and emulsifying activities, and a broad inhibition spectrum against Gram-positive and Gram-negative bacteria, and fungi. Genome sequence analysis showed that *B. velezensis* F11 could serve as a promising source of surface-active compounds and antimicrobial agents. Among the genome-encoded secondary metabolites are fengycin lipopeptides, which we have isolated and purified, thereby demonstrating the functionality of the associated gene clusters. With the availability of the genome sequence of *B. velezensis* F11, future investigations on the other putative bioactive compounds encoded in the genome may be pursued.

Chapter 4

Genomics of *Bacillus* sp. from Extreme Environments

4.1 Project Background

4.1.1 *Bacillus cereus* E41 and *Bacillus anthracis* F34

Bacillus is a large and ubiquitous genus commonly isolated from soil and sediment habitats. *Bacillus* ssp. are aerobic or facultative anaerobic Gram-positive rod-shaped bacteria capable of forming spores, which allows them to persist and disperse in diverse habitats.[24] *Bacillus* ssp. also produce a variety of bioactive small molecules.[25-27] Two strains of *Bacillus*, *B. cereus* E41 and *B. anthracis* F34, were isolated from a salt lake in Aïn M'lila-Oum El Bouaghi, Eastern Algeria, and Ain Baida-Ouargla, Southern Algeria, respectively. *B. anthracis* F34 was ascertained after the detection of the virulence genes, pX01 and pX02. The genome sequences of the two isolates were sequenced to provide the genetic blueprint for the production of polyhydroxyalkanoate, iron siderophores, lipopeptides, and bacteriocins.

4.1.2. *Bacillus paralicheniformis* F47

Rhizophere-associated bacteria such as *Bacillus paralicheniformis* can suppress a variety of plant pathogens by producing antimicrobial secondary metabolites. For instance, *B. velezensis* F11 can inhibit several Gram-positive and Gram-negative bacteria and fungal plant pathogens which is ascribed to its production of multiple fengycin lipopeptides,[124,148,152] while members of the *B. cereus* and *B. subtilis sensu lato* groups produce a variety of bioactive small molecules such as lantibiotics and lipopeptides.[123] Here, we report the draft genome sequence of *Bacillus*

paralicheniformis F47 isolated from a salt lake in Southern Algeria, which encode multiple bacteriocins, lipopeptide, biosurfactants and siderophores.

4.1.3. *Bacillus licheniformis* SMIA-2

Bacillus sp. SMIA-2 is an important Brazilian strain for the production of industrially-relevant thermostable enzymes such as amylases,[153] xylanases,[154] proteases,[155] and cellulases,[156-157] used in diverse industrial fermentation substrates such as whey, sugarcane bagasse, corn steep liquor and food-waste.[158-159] SMIA-2 was isolated in 2001 from the soil of Campos dos Goytacazes, Rio de Janeiro, Brazil. The strain was phylogenetically categorized with thermophilic *Bacillus* group V with 94% similarity with *B. caldoxylolyticus* (Accession No. AH010483.2).[160] Re-sequencing of the 16S rRNA gene (Accession No. MN645931) revealed that SMIA-2 is 100% identical with the type strain, *Bacillus licheniformis* Gibson 46[T]. The genome of SMIA-2 was sequenced because it is an industrially important strain used in agricultural waste fermentation,[160] laundry detergent development,[161] and thermo-stable enzyme production for second generation bioethanol production in Brazil.[158-161]

4.2 Results and Discussion

4.2.1 Genomics of *Bacillus cereus* E41 and *Bacillus anthracis* F34

Genome annotation by the NCBI PGAP predicted 5,779 genes, including 5,492 coding sequences (CDSs), 12 rRNAs, and 98 tRNAs, in the genome of *Bacillus cereus* E41, and 6,265 genes, including 5,866 CDSs, 10 rRNAs, and 76 tRNAs, in the genome of *Bacillus anthracis* F34.

Both *Bacillus* ssp. have the complete gene cluster for polyhydroxyalkanoate biosynthesis that is used for the production of bioplastics. They are also predicted to produce the siderophore petrobactin (*asbABCDEF*).[162] In addition, they both contain the bacillibactin nonribosomal peptide synthetase (NRPS) operon *dhbACEF* and the corresponding iron-bacillibactin uptake cluster *feuABCD-yuiI*.[163]

The *B. cereus* E41 genome contains a complete gene cluster for the lantibiotic thusin (*thsA1TM1A2A2'M2FE*).[164] Furthermore, the genome contains biosynthetic gene clusters for surfactin, polyoxypeptin, as well as sugar compounds, such as S-glycan and exopolysaccharides. The whole-genome shotgun projects have been deposited in DDBJ/ENA/GenBank for *B. cereus* E41 (MTAT00000000) and *B. anthracis* F34 (MTAU00000000).

4.2.2. Genomics of *Bacillus paralicheniformis* F47

Genome annotation by the NCBI-PGAP predicted 4,117 genes, including 4,026 coding sequences (CDSs), while RNA genes were composed of 11 rRNAs, 75 tRNAs and 5 ncRNAs. The genome of *B. paralicheniformis* F47 exhibits 99.26% ANI, 0.94 AF and 70.54% dDDH (Formula 2) with the type strain *B. paralicheniformis* KJ-16$^\text{T}$,[165] supporting the placement of F47 in the species *B. paralicheniformis*. Conversely, the closest non-*B. paralicheniformis* species, *B. licheniformis* ATCC 14580$^\text{T}$ exhibits 94.69% ANI, 0.88 AF and 10.96% dDDH. Two putative CRISPR modules and one prophage were discovered while a total of three genomic islands were predicted with a total of 32 annotated coding genes identified.

The genome of F47 contains several gene clusters with homology to known lipopeptide biosynthetic operons including fengycin (*fenABCDE*),[124,155] surfactin (*srfADCB*),[166] and lichenysin (*lchAA*).[167] Furthermore, the operon for bacitracin biosynthesis (represented in scaffolds 11, 43 and

103) suggests a complete pathway for the synthesis of this antibiotic. Similarly, a complete tri-cistronic operon (*kabABC*)[168] for kanosamine biosynthesis was also detected in the genome. These bioactive molecules could contribute to the strong emulsifying and antimicrobial activity of F47 against the Gram-positive bacterium *Micrococcus* sp. ATCC 700405 and the fungal plant-pathogen *Verticillium dahlia* ATCC 44571. Two siderophore gene clusters were also predicted in the genome including bacillibactin and a putative anthrachelin.[169] One bacteriocin gene cluster with complete homology to a class IId cyclical uberolysin-like bacteriocin, circularin A, was identified. Lastly, gene clusters for terpene, citrulline and teichuronic acid biosynthesis were also detected. The whole-genome shotgun project has been deposited in DDBJ/ENA/GenBank and JGI-IMG/M under the accession numbers, MYFI00000000 and Ga0181491, respectively.

4.2.3. Functional Genomics of *Bacillus licheniformis* SMIA-2

Bacillus licheniformis SMIA-2 genome showed an ANI of 99.71% and alignment fraction of 0.97 with *Bacillus* sp. H15-1 whereas a comparison with the closest type strain *B. licheniformis* Gibson 46^T has an ANI of 99.57% (AF = 0.95) supporting the placement of SMIA-2 under the species *B. licheniformis*. SMIA-2 is a novel strain as revealed by dDDH comparative values <79% (formula 2). Paired-end sequencing yielded 46,616,926 reads (233× coverage). The draft genome is 4,292,816 bp in 34 contigs (N_{50} = 317,403 bp) and G+C = 45.85%.

NCBI-PGAP based genome annotation detected 4322 coding sequences, 11 rRNA genes and 79 tRNAs. The genome encodes gene inventories supporting thermostable enzyme production while a total of 13 gene clusters for putative biosynthetic secondary metabolites were predicted using antiSMASH version 5.[170] This includes lichenicidin A1/A2; non-ribosomal peptide synthetases (lichenysin-, bacillibactin-, fengycin-like), siderophore and a putative lassopeptide. A summary of the genome scan highlights five of the 10 gene clusters (Table 4.1). Experimental

evidence corroborated the antiSMASH *in silico* analysis results by agar-plug and butanol extract-disk diffusion inhibitory assays against *S. aureus* ATCC 6538, *B. infantis* strain 10Pi,[171] and *Pichia pastoris* strain X-33 using the spent medium of SMIA-2 (Figure 4.1). Lastly, the thermostable enzymatic activities of SMIA-2,[155-158] can be supported by gene inventories including six amylase genes; 13 loci for xylose metabolism, 55 protein degradation-associated loci and three cellulolytic enzyme loci (e.g. endoglucanase) under a putative cellulosome complex.

The whole-genome project for *Bacillus licheniformis* SMIA-2 has been deposited in DDBJ/ENA/GenBank under accession number JAACZZ000000000. The version described in this thesis is the first version (JAACZZ010000000), under BioProject number PRJNA602865, BioSample number SAMN13909444, and Sequence Read Archive (SRA) number SRX7638223.
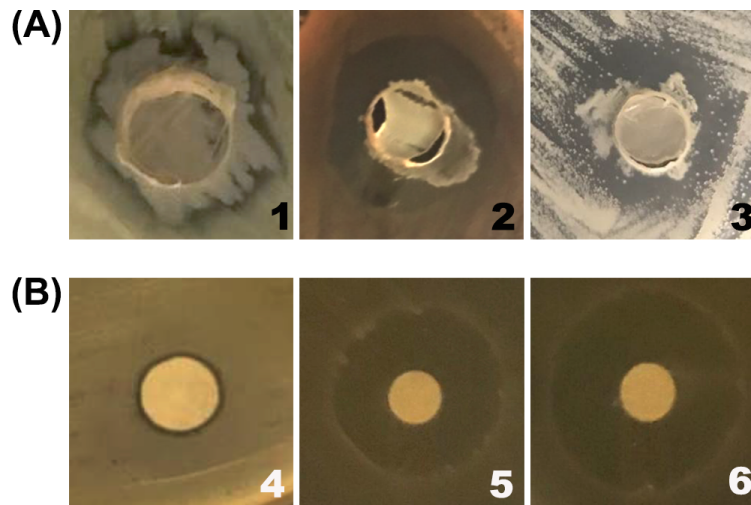
Figure 4.1 Antimicrobial activity of *Bacillus licheniformis* SMIA-2. (A) Agar-plug assay of 12 h-50 °C -grown SMIA-2 against *Staphylococcus aureus* ATCC 6538 (A1), *Bacillus infantis* 10Pi (A2), and *Pichia pastoris* X-33 (A3). (B) Disk diffusion assay using *n*-butanol extract of spent BHI medium of SMIA-2 against the indicator strain *B. infantis* 10Pi. Butanol solvent control, 10 μL (B4); SMIA-2 *n*-butanol extract, 10 μL (B5); and kanamycin, 10 μL (5 mg/mL) (B6).

Table 4.1. Summary of antiSMASH results for *Bacillus licheniformis* SMIA-2

Predicted biosynthetic metabolite	Contig Number	Coordinates within the contig	% Similarity to known cluster
NRPS	4	189027-243708	100 (lichenysin biosynthetic gene cluster)
NRPS	5	147101-175615	53 (fengycin biosynthetic gene cluster)
Lassopeptide	9	111876-134337	0 (no known biosynthetic gene cluster)
Lanthipeptide	9	198527-225488	100 (lichenicidin biosynthetic gene cluster)
NRPS	21	1-20181	46 (bacillibactin biosynthetic gene cluster)

4.3. Conclusion and Future Directions

Four novel environmental strains of *Bacillus* species were isolated from oil-contaminated lake in Algeria as well thermophilic *Bacillus* from the soils in Brazil. Whole genome phylogenetic analysis placed *B. cereus* E41 and *B. anthracis* F34 in the *Bacillus* cereus *sensu lato* group. Conversely, the two other species*, B. paralicheniformis* F47 and *B. licheniformis* SMIA-2, clustered into the *B. subtilis sensu lato* group. Bioinformatic analysis of the secondary bioactive gene inventories of the *Bacillus* genomes showed genetic potential for the production of lipopeptides, lanthipeptides, lasso peptide, lanthipeptides, biosurfactants and bacteriocins.

With the availability of the genome sequences, future investigations on the putative novel bioactive compounds encoded in the genome may be pursued. The encoded metabolites can be probed by several approached including but not limited to, 1) activity-guided purification, 2) heterologous expression in antimicrobial-resistant host strains, and 3 CRISPR-Cas activation of relevant biosynthetic gene clusters, to name a few.

Chapter 5

Functional Genomics of *Streptomyces* sp. nov A1-08

5.1 Project Background

5.1.1. Actinomycetes

Actinomycetes are known to be the most economically essential microbes mainly because they are capable of producing medically and pharmaceutically important products. Among the actinomycetes, *Streptomyces* species synthesize about 70% of the naturally available antibiotics and produce metabolites with anti-parasite, antimicrobial, antitumor, antiviral activity, and other pharmaceutically beneficial compounds.[172] *Streptomyces* species are also known to produce novel bioactive compounds such as cyphomycin,[173] lobophorin K,[174] uncialamycin, cladoniamide, and angucycline.[175-177] These promising *Streptomyces* species were recently suggested based on their environmental isolation sources as the "Modern *Actinobacteria*" (MOD-ACTINO) which refers to a group of actinobacteria capable of producing compounds that can be explored for modern applications such as new drugs and cosmeceutics.[178] Members of this group are categorized as novel actinobacteria isolated from special and less explored environments which can be valuable sources for different industries that seek to improve people's lives.[178]

5.1.2. Modern Actinomycetes and Novel Bioactive Natural Products

Continuous investigation of additional MOD-ACTINO is needed for the search for novel and effective secondary metabolites. Numerous studies have also been conducted in screening for actinomycetes with bioactive compounds in soil,[179-180] molluscs,[181] marine,[182-183] bat cave,[184] and

soil from urban green space environments.[185] Despite the efforts of studying antibiotic-producing *Streptomyces* species in different environments, poorly explored habitats such as volcanic soils were widely less investigated. Sulfur-rich volcanic soil is a potential source of naturally derived medicinal raw materials. Actinomycetes found in such extreme environment have adapted to utilize sulfur and other compounds as a nutrient source while at the same time using these sulfurous compounds as defense against other microorganisms.[186-187] Previous studies showed that volcanic environments are good sources of new bioactive natural products derived from *Streptomyces* species. Unique cyclic peptides ohmyungsamycins isolated from *Streptomyces* sp. SNJ042 from Jeju volcanic island in Korea showed potent cytotoxicity against various cancer cell lines and exhibited antibacterial activity against Gram-positive and Gram-negative bacteria.[187] Another study showed that *Streptomyces galbus* isolated from volcanic soils of Tangkuban Perahu Mountain revealed antibacterial activity against methicillin-resistant *Staphylococcus aureus*, methicillin-sensitive *Staphylococcus aureus*, methicillin-resistant coagulase-negative *Staphylococcus*, vancomycin-resistant *Enterococcus*, and *Escherichia coli*, antifungal (*Microsporum gypseum*), and anticancer (T47D breast cancer cell line) activity.[186]

5.1.3. Objectives

This study opens a vital opportunity to explore actinomycetes with antibiotic and cytotoxic activities from Mount Mayon, one of the most active volcanoes in the Philippines. The study aims to screen isolates for antimicrobial activity and eventually focuses on the isolate, with the greatest potential, *Streptomyces* sp. A1-08. Moreover, this study utilizes whole genome-based sequencing for species identification and prediction of secondary metabolite biosynthetic gene clusters.

5.2 Results and Discussion

5.2.1. Antimicrobial Screening of Isolated Actinomycetes

A total of 60% (18 out 30) of the morpho-phenotypically identified actinomycetes were isolated from the lowest elevation gradient at 500 meter above sea level (masl). This is also the region where the novel isolate A1-08 was detected. Approximately 27% (8 out 30) and 13% (4 out 30) of the actinomycetes were isolated from 1000 masl and 1500 masl, respectively (Table 5.1). Overall, 13 (43%) morphologically distinct isolates showed antagonistic activity against the selected test organisms (Table 5.2). Five isolates (A1-02, A1-14, A1-21, A1-30, and A3-02) inhibited only Gram-positive bacteria. Isolate A2-02 exhibited zones of clearing against fungi and Gram-positive bacteria. Furthermore, isolates A2-09 and A2-12 showed inhibition to yeast while A3-08 inhibited pathogenic molds like *Candida albicans* and *Fusarium* sp. Isolates A1-10 and A1-15 showed antifungal activities both to yeast and molds and isolate A3-07 was active against a mold and Gram-positive bacteria. Further studies will be conducted to elucidate the bioactive compounds also present in these isolates. Interestingly, the A1-08 isolate exhibited broad spectrum of antimicrobial activity against *Salmonella enterica* serovar Typhimurium BIOTECH 1756, *Klebsiella pneumoniae* BIOTECH 10283, *Staphylococcus aureus* BIOTECH 1823, methicillin-resistant *Staphylococcus aureus* (MRSA) BIOTECH 10378, *Candida albicans* BIOTECH 2219, *Aspergillus niger* BIOTECH 3080, and *Fusarium* sp. The broad-spectrum antibiotic property of the A1-08 isolate makes it a good candidate for exploring possible novel antimicrobial compounds. Succeeding tests and analyses were focused on the A1-08 isolate to further unravel other antimicrobial properties and describe potentially unique or novel bioactive compounds biosynthetically encoded in the genome. The data also suggest that the Philippine volcanic soil

could be an excellent niche for bioprospecting of antibiotic and anticancer producing actinomycetes.

Table 5.1. Phenotype of 30 actinomycetes isolated from Mt. Mayon.

Isolate code	Elevation gradient (masl)	Colony morphology	Color of aerial mycelia in ISP2 medium	Reverse side color of the substrate mycelia in ISP 2 medium	Presence of Arthrospores	Gram reaction
A1-01	500	concentric, powdery	light green to brown	white	yes	+
A1-02	500	round with radiating margin, powdery	cream white	yellow	yes	+
A1-03	500	irregular, powdery	light green to black	yellow	yes	+
A1-05	500	concentric	yellow	black	yes	+
A1-08	500	wrinkled, powdery	white to grey	yellow to brown	yes	+
A1-09	500	wrinkled	black to brown	black	yes	+
A1-10	500	wrinkled, powdery	white	white to brown	yes	+
A1-11	500	irregular, powdery	white to light purple	brown to black	yes	+
A1-12	500	wrinkled, powdery	black to brown	yellow to white	yes	+
A1-14	500	concentric, powdery	cream white	white to yellow	yes	+
A1-15	500	concentric, powdery	yellow	brown	yes	+
A1-16	500	wrinkled, powdery	grey	white to yellow	yes	+
A1-18	500	concentric, powdery	brown to black	grey to brown	yes	+
A1-20	500	concentric	white to light purple	brown	yes	+
A1-21	500	round with radiating margin, powdery	yellow	white	yes	+

A1-28	500	wrinkled, powdery	yellow to white	yellow	yes	+
A1-29	500	concentric, powdery	yellow to white	white	yes	+
A1-30	500	wrinkled, powdery	white to light orange	white	yes	+
A2-01	1000	wrinkled	grey to white	brown	yes	+
A2-02	1000	wrinkled, powdery	yellow	white to grey	yes	+
A2-03	1000	wrinkled, powdery	black	brown	yes	+
A2-05	1000	concentric, powdery	white	brown	yes	+
A2-07	1000	round with radiating margin, powdery	light orange	brown	yes	+
A2-09	1000	wrinkled, powdery	yellow to light green	brown to black	yes	+
A2-10	1000	concentric, powdery	brown to light green	white	yes	+
A2-12	1000	wrinkled, powdery	yellow to white	black	yes	+
A3-01	1500	wrinkled, powdery	white to dark brown	brown	yes	+
A3-02	1500	wrinkled	white to light brown	brown to black	yes	+
A3-07	1500	wrinkled, powdery	yellow to white	yellow to brown	yes	+
A3-08	1500	wrinkled, powdery	black	yellow	yes	+

Table 5.2. Evaluation of antimicrobial activity of 13 actinomycete isolates against selected test organisms using agar plug assay. Values are mean of three replicates and different letters indicate significant difference at $\alpha = 0.05$. nd-not determined, (-) no activity, MRSA - methicillin resistant *Staphylococcus aureus;* vancomycin, ampicillin, and nystatin at 100 ppm.

| | Diameter of Zones of Clearing (mm) | | | | | | | | | |
| Isolate Code | Gram-negative Bacteria | | | | Gram-positive Bacteria | | | Yeast | Mold | |
	Escherichia coli	Pseudomonas aeruginosa	Salmonella enterica	Klebsiella pneumoniae	Bacillus subtilis	Staphylococcus aureus	MRSA	Candida albicans	Aspergillus niger	Fusarium sp.
A1-08	-	-	14.2 ± 0.33^B	11.3 ± 0.20^B	-	11.5 ± 0.21^G	11.9 ± 0.14^C	13.9 ± 0.34^E	19.5 ± 0.41^C	13.2 ± 0.11^C
A1-02	-	-	-	-	18.3 ± 0.21^B	20.0 ± 0.11^B	-	-	18.3 ± 0.40^D	14.3 ± 0.10^B
A1-10	-	-	-	-	-	-	-	13.4 ± 0.10^F	-	-
A1-14	-	-	-	-	15 ± 0.43^C	-	-	-	-	-
A1-15	-	-	-	-	-	-	-	21.7 ± 0.31^A	21.3 ± 0.21^B	16.9 ± 0.10^A
A1-21	-	-	-	-	-	13.0 ± 0.11^F	-	-	-	-
A1-30	-	-	-	-	-	17.0 ± 0.26^C	-	-	-	-
A2-02	-	-	-	-	-	14.0 ± 0.17^E	10.5 ± 0.09^D	15.8 ± 0.34^D	22.3 ± 0.51^A	11.2 ± 0.02^D
A2-09	-	-	-	-	-	-	-	17.2 ± 0.22^C	-	-
A2-12	-	-	-	-	-	-	-	21.0 ± 0.38^B	-	-
A3-02	-	-	-	-	11.0 ± 0.01^E	15.0 ± 0.10^D	17.5 ± 0.34^A	-	-	-
A3-07	-	-	-	-	12.0 ± 0.03^D	14.0 ± 0.10^E	-	-	16.3 ± 0.21^F	-
A3-08	-	-	-	-	-	-	-	-	17.0 ± 0.21^E	-
Vancomycin	nd	nd	nd	nd	nd	nd	15.0 ± 0.21^B	nd	nd	-
Ampicillin	26.0 ± 0.10	20.0 ± 0.01	19.0 ± 0.31^A	21.0 ± 0.21^A	23.0 ± 0.11^A	40.0 ± 0.31^A	nd	nd	nd	-
Nystatin	nd	nd	nd	nd	nd	nd	nd	13.0 ± 0.10^F	14.7 ± 0.21^G	14.0 ± 0.11^B

5.2.2. Anti-MRSA Activity of *Streptomyces* sp. A1-08

Isolate A1-08 revealed promising anti-MRSA activity (MIC at ~2.50 mg/mL) (Figure 5.1), suggesting that A1-08 is a potential source of anti-MRSA compounds. Although the reported MIC values here represent a crude estimate of A1-08's anti-MRSA potential, the observed zones of inhibition corroborated the comparable contact-dependent inhibition clearing with that of vancomycin (Table 5.2), supporting a proposal that an unknown extractable anti-MRSA metabolite(s) has the vancomycin's anti-MRSA-like potential. The estimated MIC cannot exclude the potential contribution of an extended assay incubation period that could putatively create abiotic-induced formazan crystal formation as a result of persister MRSA cell's metabolism in the extract treated wells. Although partial formazan coloration was observed in the extract's lower concentration (1.25 mg/mL), this was not observed in any of the vancomycin treated controls, excluding a significant contribution of abiotic-induced and long assay time-dependent formazan formation. With the crude nature of the extract, the synergistic activity of multiple anti-MRSA metabolites in the ethyl acetate extract is yet to be determined.

Several studies showed that actinomycetes, specifically *Streptomyces* species, are known producers of anti-MRSA compounds. The endophytic *Streptomyces californicus* strain ADR1 showed promising antibacterial, antioxidant, and anti-biofilm activities.[188] Secondary metabolites such as alkaloids, phenolics, terpenes, terpenoids, and glycosides were produced and attributed to the said bioactivities of this strain. In another study, *Streptomyces* sp. strain MUSC 125 was isolated from a less explored mangrove soil habitat. This isolate also showed anti-MRSA, anti-biofilm, and antioxidant activities although attributed to known compounds such as 2,4-dihydroxy-6-propylbenzoic acid and thiophene, 2-butyl-5-ethyl.[189] The marine *Streptomyces* sp. MN41 showed a pyrrole-derivative bioactive compound which showed remarkable activity against MRSA with an

MIC of 2.80 μg/mL,[190] a value that is comparable with the ethyl acetate extract of *Streptomyces* sp. A1-08. A total of five soil *Streptomyces* species, namely, *Streptomyces* sp. CFJ2, *S. antibioticus* strain 1022-257, *S. flaveolus* strain NRRL B-1334, *S. psammoticus* strain NBRC 13971, and *Streptomyces* sp. b26, were also found to inhibit growth of all 10 clinical isolates of MRSA with zones of inhibition (ZOI) values ranging from 13.52 to 25.68 mm,[191] reminiscent of the
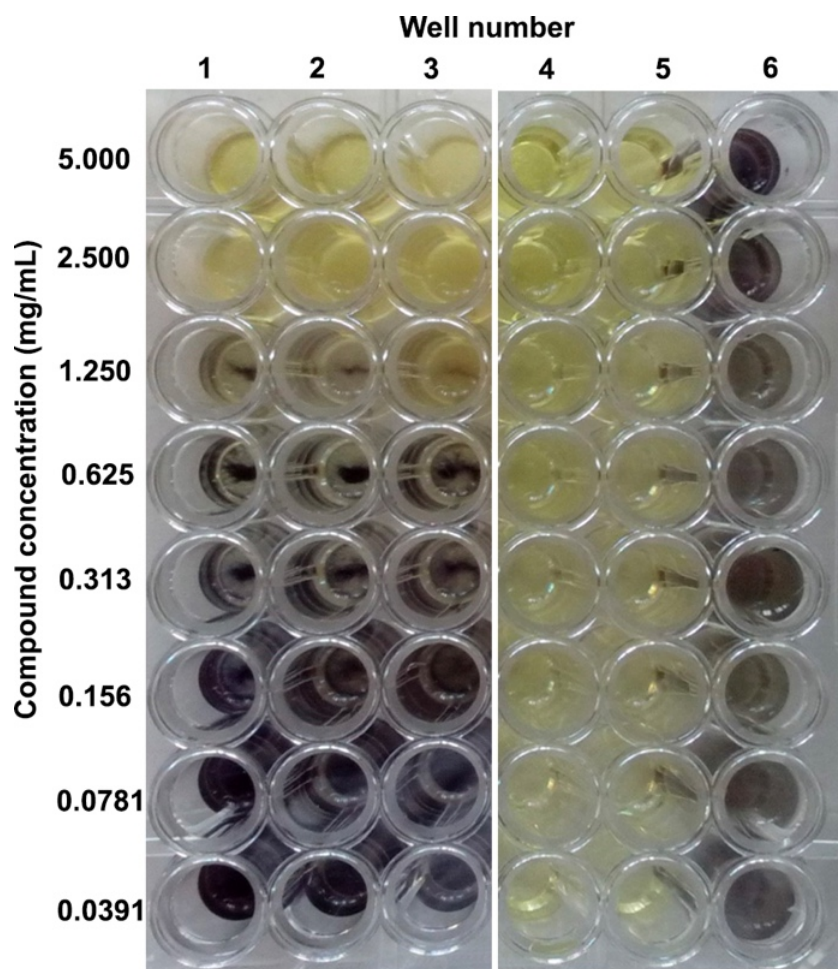
Figure 5.1. Determination of minimum inhibitory (MIC) concentration of ethyl acetate extract of *Streptomyces* sp. A1-08 strain against methicillin-resistant *Staphylococcus aureus* (MRSA) BIOTECH 10378 strain using MTT assay in 96-well microtiter plate. Well 1 to 3 - A1-08 ethyl acetate extract; well 4 to 5 - vancomycin at 100 ppm (positive control); well 6 - methanol solvent control (negative control). The image was a composite of two sets of photos obtained from the same micro-titer plate from the same assay.

three actinobacterial isolates reported here (Table 5.2). Interestingly, *Streptomyces* sp. SUK 25 was found to produce the natural metabolites chloramphenicol and *cyclo*-(L-valyl-L-prolyl) compounds which displayed promising effect in targeting multiple biological pathways in MRSA.[192] In a review by Kemung and co-workers,[193] all known potent anti-MRSA compounds isolated from *Streptomyces* species which exhibit lower MIC than clinically used antibiotics were discussed.

Despite previous efforts on discovering actinomycetes producing anti-MRSA compounds, the World Health Organization (WHO) reported that MRSA remains a critical antibiotic-resistant bacterium that urgently requires new drugs.[194] Published reports on the emergence of MRSA with reduced susceptibility to the first-line medications such as vancomycin,[195] daptomycin,[196] and linezolid,[197] that can lead to resistance will pose threats to future clinical treatments of MRSA infections. Therefore, continuous efforts to discover and identify novel compounds to inhibit MRSA would still be of great importance.

5.2.3. Cytotoxic Activity Against Human Colorectal Cancer Cell Line HCT 116

The ethyl acetate extract of isolate A1-08 showed lower potency as compared to doxorubicin (positive control) (Table 5.3) when tested against HCT 116 cell line (ATCC CCL-247). The ethyl acetate extract of A1-08, being a mixture of several metabolites, may have some lead compound(s) towards the development of an anticancer drug, given it will be purified and accessible for extensive cancer cell line bioactivity profiling. According to the American National Cancer Institute, the standard for IC_{50} values implying significant activity against cancer cell lines is <30 μg/mL.[198] However, it should be noted that there is a need for further fractionation and

purification of the compounds from the ethyl acetate extract to demonstrate more specific anticancer activity.

Table 5.3. IC$_{50}$ values of doxorubicin and ethyl acetate extract of *Streptomyces* sp. A1-08 isolate used to kill 50% of the HCT116 cell line using MTT assay. Values are mean of three replicates and different letters indicate significant difference at $\alpha = 0.05$.

Samples Tested	IC$_{50}$ (µg/mL)
Doxorubicin	1.9829[A]
A1-08	21.542[B]

In other studies, it was demonstrated *Streptomyces* species with cytotoxicity against HCT 116 and other cancer cell lines. Donghaecyclinones A – C, produced by volcanic island-derived marine *Streptomyces* sp. strain SUD119, exhibited cytotoxicity against several human cancer cell lines including colorectal cancer cell line HCT 116, breast cancer cell line MDA-MB231, gastric carcinoma cell line SNU638, lung cancer cell line A549, and liver cancer cell line SK-HEP1.[199] Ohmyungsamycins A isolated from volcanic soil isolate *Streptomyces* SNJ042 also showed potent cytotoxic activity against various cancer cell lines such as HCT-116, lung cancer cell line (A549), gastric cancer cell line (SNU-638), breast cancer cell line (MDA-MB-231), and human hepatic adenocarcinoma (SKHEp-1cells).[187] A deep-sea sediment isolate *Streptomyces* sp. CNR-698 strain was found to produce ammosamides A and B, which showed toxic activity against colorectal cancer cell line HCT 116.[200] Similarly, a sediment isolate *Streptomyces* sp. BCC 21795 showed cytotoxic activity against MCF7 and Vero cells which was attributed to quinazolinones.[201] *Streptomyces* sp. NTK 937 also produced a new antibiotic caboxamycin which displayed antitumor activity against stomach cancer cell line , breast cancer cell line (MCF7) and hepatocellular

carcinoma (HepG2).[202] A mangrove-derived *Streptomyces* sp. MUM256 showed its interesting ability to induce cell-cycle arrest and apoptosis in HCT 116 cell line while exerting no detectable toxicity against normal colon cells.[203] An extensive review by Law and co-workers[204] showed that mangrove-derived *Streptomycetes* are promising producers of new compounds with anticancer properties such as streptocarbazoles A and B, streptomyceamide C, neoantimycins A and B.

Similar to this study, a number of works[205-207] also investigated the use of crude extracts to perform bioactivity screening. The cytotoxic activity from these crude extracts is often considered a preliminary outcome that may not reflect true activity. However, the promising results produced by the crude extracts should not be neglected either. Performing additional experiments on these extracts should be done to further evaluate the compounds present responsible for such biological activity. Bioassay-guided fractionation of A1-08 ethyl acetate extracts and subsequent chromatographic purification will help in elucidating the chemical components responsible for the cytotoxic activity of A1-08 extracts against human colorectal cancer cell line HCT 116.

5.2.4. Morphological and Cultural Characterization of *Streptomyces* sp. A1-08

Colonies of *Streptomyces* sp. A1-08 grown on ISP-2 agar appeared as wrinkled, filamentous to irregular, opaque, rough, and chalky with brownish yellow substrate mycelium and white to gray aerial mycelium after 5 d. Isolate A1-08 grew luxuriously also on ISP-3, ISP-4, ISP-5, and ISP-7 culture media (Figure 5.2) but with variations on pigmentation, myceliation and arthrospore production. ISP 4 and 5 encouraged growth of mycelium but did not support sporulation. ISP 3 showed good growth of mycelium and has encouraged sporulation after 7 d. The gram-stained *Streptomyces* sp. A1-08 mycelia were Gram-positive, made up of long, filamentous and branching hyphae (Table 5.1).
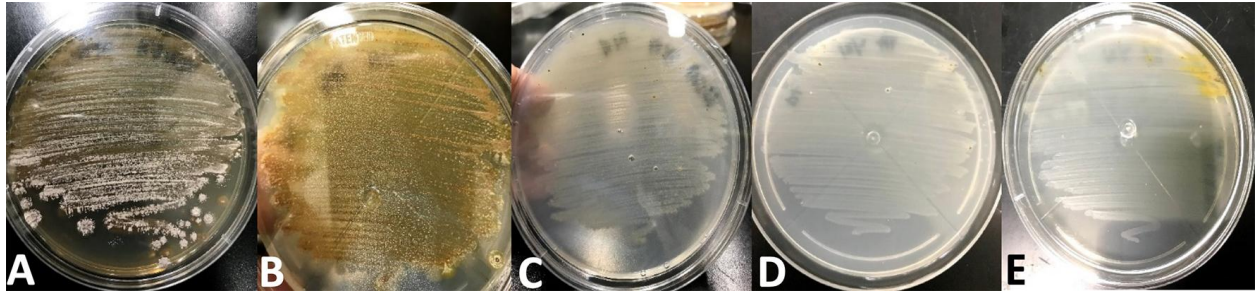
Figure 5.2. Differential growth phenotypes of *Streptomyces* sp. A1-08 on different ISP media after 7 d. Sporulated colonies on yeast extract malt extract agar (ISP 2) (A); pigmented and partially sporulated colonies on oatmeal agar (ISP 3) (B); myceliated, non-sporulated colonies on inorganic salts-starch agar (ISP 4) (C); myceliated, non-sporulated colonies on glycerol asparagine agar (ISP 5) (D), and myceliated, non-sporulated colonies on tyrosine agar (ISP 7) (E).

5.2.5. Whole Genome Phylogenetic Analysis of *Streptomyces* sp. A1-08

To establish the novelty of isolate A1-08, the genome was sequenced to probe its phylogenetic position. A total of 22,926,576 raw reads were obtained from Illumina NextSeq 500 sequencing runs. The resulting 3.24-Gb short paired-end reads (corrected to 100-150 bp per read) were used to generate a draft assembly with 286 contigs (57 contigs with length $\geq$ 50,000 bp) for a total length of 8,654,812 bp, N50 of 57,920 bp, GC content of 72.23%, and estimated coverage of 400× (Figure 5.3). NCBI PGAP predicted 7,572 protein-coding DNA segments. The whole-genome sequence for *Streptomyces* sp. A1-08 has been deposited in DDBJ/ENA/GenBank under the accession number JACBYP000000000.

The classical 16S rRNA gene-based phylogeny supports the placement of A1-08 in the genus *Streptomyces* as clustering appeared with validly-published and sequence-verified type strains member species (Figure 5.4A). Whole genome phylogenetic analysis of the A1-08 draft genome further revealed the closest type strain *Streptomyces olivaceus* NRRL B-3009[T] (57.80%

dDDH value) (Figure 5.4B). The 16SrRNA gene sequence was deposited in GenBank under the accession number MN121123.
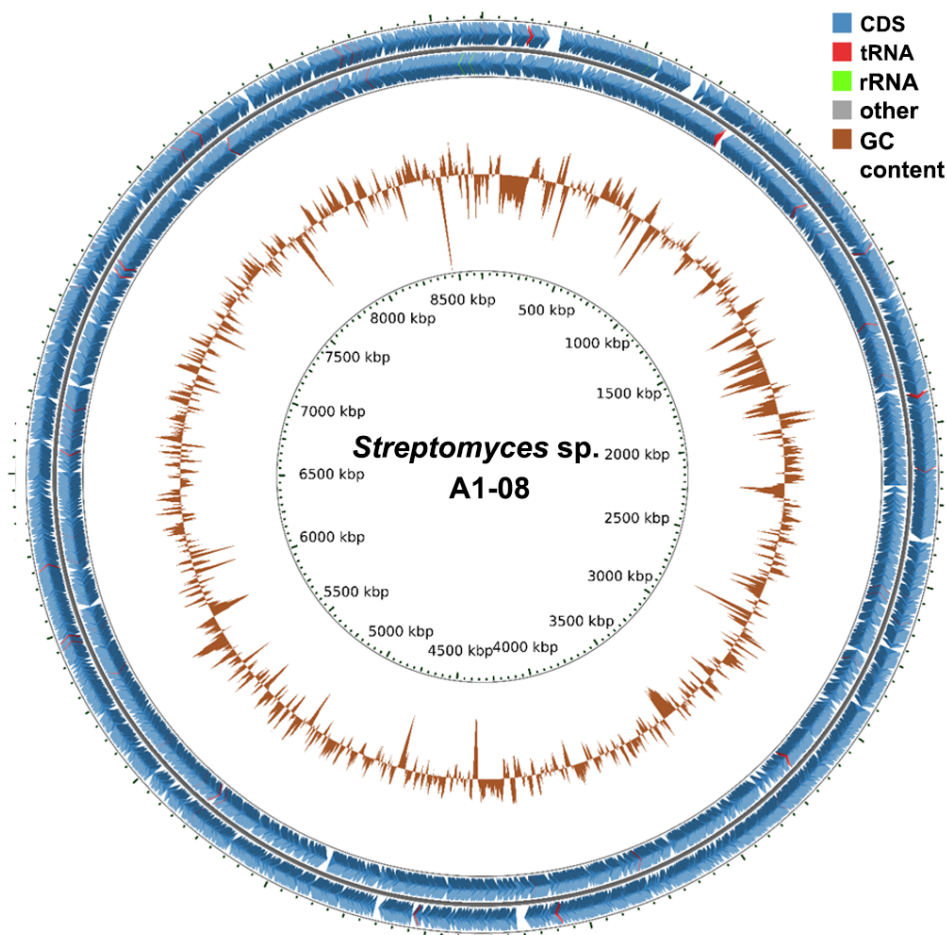
Figure 5.3. Genome map of *Streptomyces* sp. A1-08. From the outside to center ring: annotated genes (coding sequences, CDS) on the forward and reverse strands and the GC content. The genome map was created from a *de novo* assembled, BASys annotated, MEDUSA-rearranged scaffold contigs and viewed using CG Viewer.

The phylogenetic definition of a species would include strains with approximately 70% or greater DNA-DNA relatedness.[208-210] Given that *Streptomyces* sp. A1-08 has dDDH value lower than 70% strongly suggests that this isolate is a novel species. Interestingly, genome comparison using MiGA type strain and prokaryotic databases showed ANI values at 93.03% with the type strain *Streptomyces olivaceus* NRRL B-3009[T] and 92.92% with *Streptomyces* sp. VN1, both at

77% genome-aligned fraction. ANI values lower than 95% most likely represent a novel species.[211] Extensive comparative biochemical, morphological and genotyping analyses are required to propose the speciation of *Streptomyces* sp. nov. A1-08. The other 12 bioactive actinomycetes presented in this paper (Table 5.2) were not identified using 16S rRNA gene sequencing and whole genome sequencing and will be the focus of a future study. The isolates were putatively classified as actinobacteria based on cell morphology, Gram reaction, colony morphology, growth on selective media and arthrospore formation (Table 5.1).

5.2.6. Secondary Metabolite BGCs in *Streptomyces* sp. A1-08

The antimicrobial activities of *Streptomyces* sp. A1-08 may be correlated with the presence of secondary metabolite biosynthetic gene clusters. Gene prediction of secondary metabolites using antiSMASH version 6.0.0 revealed a total of 48 biosynthetic gene clusters (BGCs) (Table 5.4). The results were further corroborated by PRISM version 4.4.5, an independent predictive algorithm using Prodigal gene annotation. The analysis mapped 32 of the BGCs predicted by antiSMASH, strengthening the confidence in our list of secondary metabolites. Interestingly, the 16 BGCs predicted by antiSMASH, not mapped by PRISM, were mainly the terpene, betalactone and hybrid biosynthetic clusters. Although selective in mining ribosomally-synthesized post-translationally modified peptides (RiPPs), non-ribosomal peptide synthetases (NRPS) and polyketide synthase (PKS) clusters, PRISM was able to provide several combinatorial-based metabolite product predictions including the chemical structure and monoisotopic mass which may aid in future metabolite purification and structure elucidation.
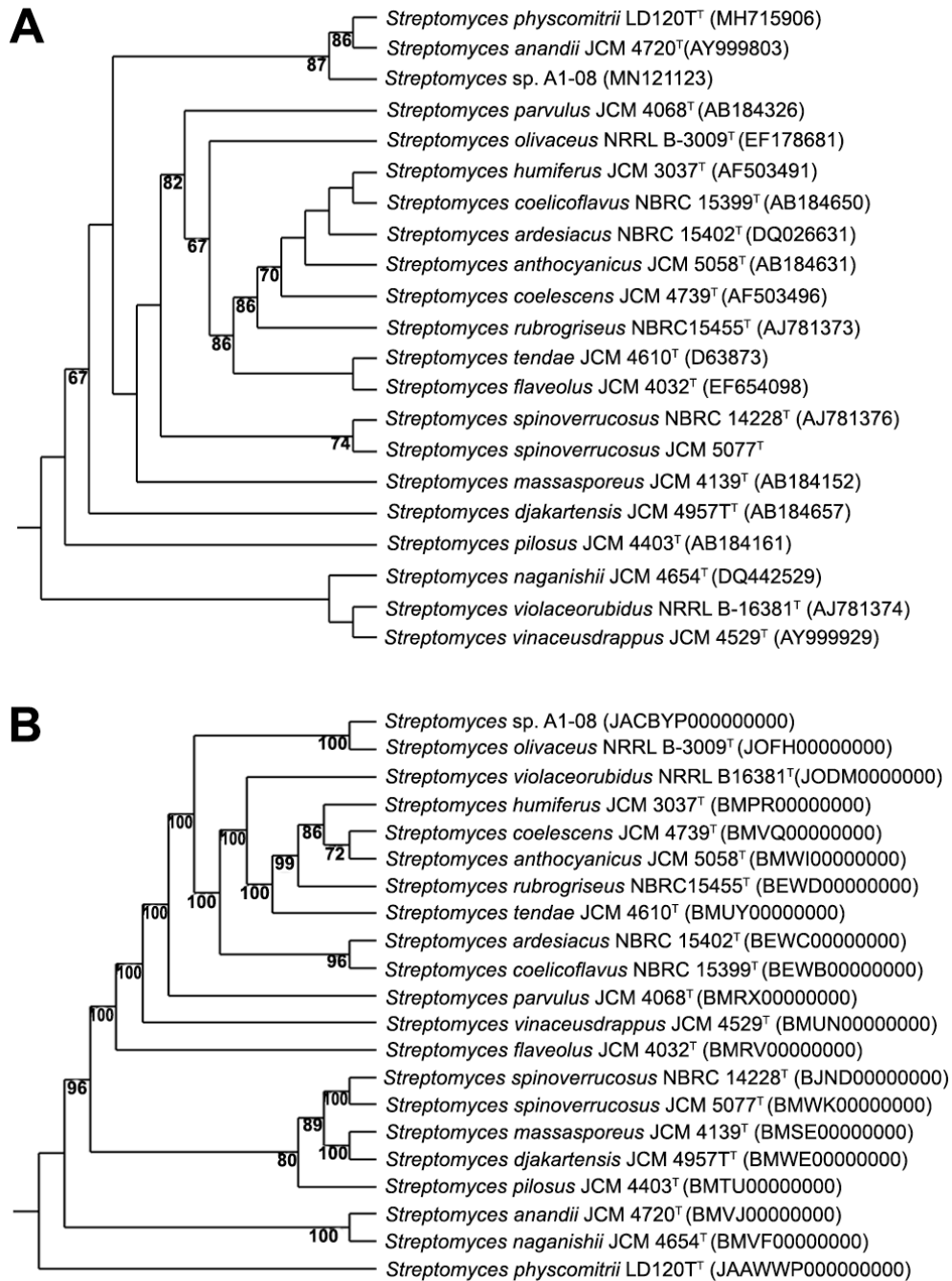
Figure 5.4. Cladogram tree based on 16S rRNA gene and whole genome sequence of *Streptomyces* sp. A1-08 and reference type strains. The tree was inferred using FastME 2.1.6.1 from GBDP distances calculated from either the 16S rRNA gene (A) or the whole genome sequences (B). The branch lengths are scaled in terms of GBDP distance formula d5. The numbers below the branches are GBDP bootstrap support values >60% from 100 replications, with average branch support of either 62.70 or 95.40% for 16S rRNA gene or whole genome tree, respectively. The accession numbers are indicated in parenthesis while [T] indicates type strains for each species.

Table 5.4. Predicted secondary metabolite biosynthetic gene clusters (BGCs) from the draft genome sequence of *Streptomyces* sp. A1-08 using antiSMASH ver 6.0.0.

No.	BGC Cluster Type*	Contig number	From	To	Most similar known cluster	% Amino Acid Similarity
1	Terpene	21	35,005	56,018	Albaflavenone	100
2	Ectoine	115	15,052	25,486	Ectoine	100
3	Terpene	33	52,070	73,317	Geosmin	100
4	T3PKS	8	76,637	117,821	Germicidin	100
5	Terpene	24	21,304	48,128	Hopene	92
6	NRPS-T1PKS	5	3	86,269	Mirubactin	78
7	NRPS	19	57,378	93,309	Coelichelin	72
8	NRPS-Indole	131	1	21,707	Ilamycins	71
9	NRPS	127	1	23,182	Coelibactin	63
10	PKS-like	48	1	39,063	Paulomycin	60
11	Melanin	15	37,008	47,631	Melanin	60
12	T1PKS	214	1	5,514	Piericidin A1	50
13	T2PKS	59	10,297	48,423	Spore pigment	50
14	NRPS	60	1	28,751	Totopotensamide A/B	46
15	RiPP-like	17	4,843	15,058	Informatipeptin	42
16	Terpene	93	17,902	32,499	Carotenoid	36
17	T2PKS, T1PKS	61	1	48,218	Murayaquinone	36
18	NRPS	2	1	59,804	Diisonitrile antibiotic SF2768	33
18	Indole	27	25,879	47,006	5-Isoprenylindole-3-carboxylate β-D-glycosyl ester	28
20	Butyrolactone	48	43,109	54,161	Scleric acid	23
21	Betalactone	21	56,121	81,674	Julichrome Q3-3/ Q3-5	22
22	NRPS	4	14,088	67,721	Rimosamide	21
23	NRPS, PKS, thioamide-Butyrolactone	49	7,793	54,159	A-47934	20
24	NRPS	24	55,531	82,313	Coelibactin	18
25	T1PKS, butyrolactone	153	1	16,279	4-hexadecanoyl-3-hydroxy-2-(hydroxymethyl)-2H-furan-5-one	18
26	T2PKS	30	32,164	78,042	Xantholipin	16

27	T1PKS	84	13,321	36,064	Ilamycins	14
28	PKA-like, T1PKS	87	9,286	33,975	Coelimycin P1	12
29	NRPS	120	1	25,443	Enduracidin	10
30	NRPS, T3PKS	156	1	15,186	Lobophorin A	10
31	T3PKS	119	1	25,958	Herboxidiene	8
32	NRPS, T1PKS	162	1	14,052	Totopotensamide	7
33	Betalactone	10	41,148	68,725	Divergolide A,B,C,D	6
34	T1PKS	7	102,624	125,994	Meilingmycin	5
35	Terpene	8	8,019	29,077	Ebelactone	5
36	Terpene	17	24,751	45,779	Versipelostatin	5
37	Lanthipeptide class III	31	27,768	50,554	Chrysomycin	5
38	PKS-like, butyrolactone	3	17,434	70,676	Asukamycin	4
39	T1PKS	67	14,238	44,197	Herboxidiene	4
40	NRPS	18	49,822	95,021	Phosphonoglycans	3
41	Lantipeptide class I	1	175,120	200,214	No hit	
42	NRPS	200	1	7,966	No hit	
43	Siderophore	246	1	2,725	No hit	
44	Siderophore	7	24,270	37,498	No hit	
45	Thioamitides	11	44,150	66,251	No hit	
46	Lantipeptide class I	23	63,428	83,231	No hit	
47	T1PKS	266	1	1,342	No hit	
48	RiPP-like	102	1	9,829	No hit	

*NRPS-non-ribosomal peptide synthetase cluster; LAP-linear azol(in)e-containing peptides; PKS-like-other types of PKS cluster; T1PKS-Type I polyketide synthase; T2PKS-Type II polyketide synthase; T3PKS-Type III polyketide synthase; RiPP-like-other unspecified ribosomally-synthesized and post-translationally modified peptide product

A *Streptomyces* genome typically consists of 20 to 40 types of BGCs, each responsible for producing one compound.[212] Thus, 48 different BGCs of *Streptomyces* sp. A1-08 may potentially yield a total of 48 individual bioactive compounds. Bacteria with a large number of gene clusters within the genome have high potential in synthesizing multiple types of compounds.[213] In *Streptomyces*, the production of secondary metabolites such as signal molecules or antibiotics is of particular interest mainly because these metabolites provide the organism with a competitive advantage, protection from unfavorable living conditions, and permit interspecies interactions.[214] Four out of 48 BGCs showed 100% similarity to genes of known BGCs where the majority are known to have antimicrobial activity (Table 5.4, Figure 5.5). These BGCs encode for the essential genes for the biosynthesis of the metabolites albaflavenone (*S. coelicolor* A3(2) BGC0000660), ectoine (*S. anulatus* BGC0000853), geosmin (*S. colelicolor* A3(2) BGC0001181.1), and germicidin (*S. argillaceus* BGC0001454) (Figure 5.5). Albaflavenone, a tricyclic sesquiterpene antibiotic (Figure 5.5E), was first isolated from *Streptomyces albidoflavus* and is known to exhibit antimicrobial properties and was found to be active against *Bacillus subtilis*.[215] Furthermore, albaflavenone has been reported to have an earthy, camphor-like odor and exhibits antibacterial activity.[216] Ectoines are commonly produced by *Streptomyces* species as compatible solutes to alleviate osmotic stresses (Figure 5.5B, 5.5E). A study by Sadeghi and co-workers[217] suggested that ectoines are osmoprotectants and can improve the structure and function of the cells in stressful environments. Ectoines may act as a protectant against desiccation or drought periods.[218] This may imply adaptive characteristics of ectoine-producing strains that allow them to thrive in challenging environments, such as volcanic soils. Geosmin, a volatile sesquiterpene metabolite (Figure 5.5C, 5.5E) responsible for the characteristic smell of moist soil or freshly plowed earth, is assumed to be responsible for the earthy smell of actinomycete detectable on agar plates

cultivated with *Streptomyces* sp. A1-08. The *gcsA* gene encoding for a type III polyketide synthase machinery, germicidin synthase, was also predicted in the genome of A1-08 (Figure 5.5D, 5.5E). Germicidin was first isolated from *Streptomyces viridiochromogenes* NRRL B-1551 and exhibited inhibitory effects on the germination of its own spores.[219]

The remaining BGCs of *Streptomyces* sp. A1-08 showing more than 70% similarities to known BGCs also revealed interesting antimicrobial properties. Hopenes are essential precursors for synthesizing bioactive hopanoids.[220-221] Hopanoids are natural products with crucial roles in stabilizing the structure of the bacterial membrane. Common examples of hopanoids are diploterol which have shown to display toxicity to mouse leukemia cells and bacteriophane-32,33,34,35-tetrol which exhibit potent anti-inflammatory and anti-oxidation activity.[222-223] Mirubactin is a siderophore showing powerful iron-binding affinity.[224] Bacterial siderophores exhibit specific antifungal or antibacterial activities.[225-226] Moreover, siderophore-antibiotic conjugates have been developed as drug leads that can reduce permeability-mediated drug resistance that is especially advantageous in multidrug-resistance pathogen control.[227] Coelichelin, like mirubactin, is an iron-chelating molecule that is involved in uptake of ferric iron.[228] Coelichelin has great potential in the study of metal acquisition pathways, bacterial responses to iron depletion, and host-pathogen interaction.[229]
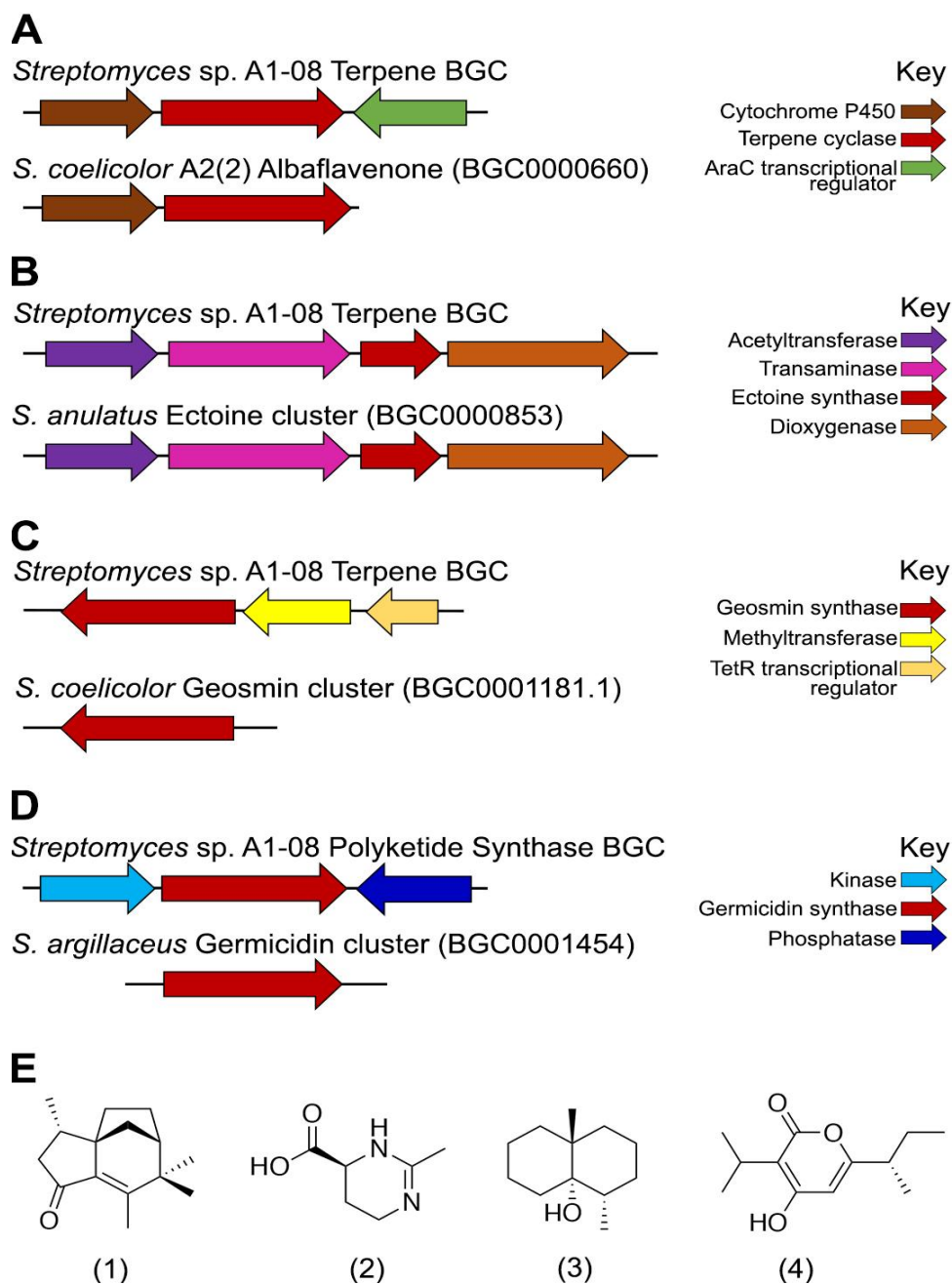
Figure 5.5 Selected secondary metabolite biosynthetic gene cluster (BGC) organizations in Streptomyces sp. A1-08. Biosynthetic gene clusters for albaflavenone (A), ectoine (B), geosmin (C) and germicidin (D) biosynthesis as predicted by antiSMASH and verified in MIBiG database. The core biosynthetic genes are indicated in red while other modifying, transport and/or transcriptional regulatory genes product homology are color coded to the known biosynthetic gene clusters in the MIBiG database. The BGC accession number is indicated in parenthesis. The associated chemical structures of the metabolites (E) were adapted from the MIBiG database structure and cross-validated in the literature: albaflavenone (1), ectoine (2), geosmin (3) and germicidin (4).

Ilamycin compounds were found to have cytotoxic activities against human tumor cell lines HeLa, HepG2, and A549. Ilamycins also showed strong tubercular activities against *Mycobacterium tuberculosis* H37Rv.[230] The reported cytotoxic and antitumorgenic properties of ilamycin and hopene above could contribute to the anti-colorectal cancer cell observed in the ethyl acetate extract of *Streptomyces* sp. A1-08, although an extensive activity-guided purification or BGC activation by heterologous expression is required to ascertain the bioactive anti-colorectal cancer molecule(s).

It is also worth mentioning that antiSMASH analysis showed a total of eight BGCs of *Streptomyces* sp. A1-08 which have no significant similar hits in the databases, hence *in silico* validation is necessary. BLASTP and MIBiG findings presented the potential function of these candidate biosynthetic gene clusters (Table 5.5). Identified core biosynthetic genes in contigs 1 and 23 are related to Class 1 lanthipeptide clusters of *Streptomyces* species. Furthermore, dehydratase and cyclase enzymes were also detected which supports the synthesis of Class 1 lanthipeptides. This was further supported by PRISM as the core precursor lanthipeptide was predicted. Interestingly, the precursor lanthipeptides were not detected in any publicly available genome sequences, including the closest phylogenetic type strain *Streptomyces olivaceus*, suggesting the novelty of these potential lanthibiotics. Among the commonly characterized lanthibiotics produced by *Streptomyces* species are cypemycin,[231] duramycin,[232] and ancovenin,[233] all of which are active against Gram-positive bacteria including MRSA. It is yet to be determined if the above lanthibiotics shared the (methyl)lanthionine rings structures which is also predicted in the lanthipeptides encoded in the BGCs of A1-08, which may contribute to the observed anti-MRSA activity.

Table 5.5. *In silico* validation of eight putative novel BGCs in *Streptomyces* sp. A1-08.

| Contig | Nucleotide Position | | Cluster Type | BlastP Analysis of Predicted Core Biosynthetic Genes | | | | | |
	Start	Stop		Description	Query Cover	E value	% amino acid ID	Acc. Len	Accession No.
1	185120	186082	Class I lanthipeptide clusters like nisin	Thiopeptide-type bacteriocin biosynthesis domain containing protein [Actinobacteria bacterium OK074]	96%	1.00E-140	67.2	325	KPI21871.1
	186064	187212	Class I lanthipeptide clusters like nisin	Lanthionine synthetase C family protein [*Streptomyces tsukubensis*]	99%	1.00E-175	68.06	380	WP_077972413.1
	187209	190214	Class I lanthipeptide clusters like nisin	Thiopeptide-type bacteriocin biosynthesis protein [*Streptomyces boluensis*]	99%	0	65.86	993	WP_161694976.1
7	29270	30799	Siderophore	Iron transporter [*Streptomyces olivaceus*]	100%	0	86.96	513	WP_031034548.1
	30963	32498	Siderophore	Iron transporter [*Streptomyces olivaceus*]	98%	0	87.7	509	WP_070389478.1
11	54150	55529	Thioamitides	YcaO-domain protein [Actinobacteria bacterium OK074]	85%	9.00E-114	50.38	429	KPI20077.1
	55526	56251	Thioamitides	TfuA-like core domain-containing protein [Actinobacteria bacterium OK074]	86%	2.00E-63	54.07	261	KPI20076.1
23	73428	75518	Class I lanthipeptide clusters like nisin	Methyltransferase, FxLD system [*Streptomyces coelicoflavus*]	100%	0	100	696	WP_108990583.1
	75537	76796	Class I lanthipeptide clusters like nisin	Lanthionine synthetase C family protein [*Streptomyces coelicoflavus*]	100%	0	100	419	WP_108990582.1
	76793	79885	Class I lanthipeptide clusters like nisin	Lantibiotic dehydratase [*Streptomyces coelicoflavus*]	100%	0	100	1030	WP_108990581.1
10	51148	52302	Betalactone	Isopropylmalate synthase [*Streptomyces fulvissimus*]	100%	0	97.14	384	WP_164355791.1
	57010	58725	Betalactone	AMP-binding protein [*Streptomyces* sp. YIM 132580]	100%	0	87.22	577	WP_161031271.1
200	3	7964	NRPS	Non-ribosomal peptide synthase [*Streptomyces atratus*]	100%	0	82.44	8022	WP_114243093.1
246	844	2724	Siderophore	Hypothetical protein [*Streptomyces olivaceus*]	99%	0	81.05	648	WP_195889435.1
266	1	1341	T1PKS	Type I polyketide synthase [*Streptomyces sioyaensis*]	100%	2.00E-136	51.89	517	WP_135796923.1

Biosynthetic gene clusters in contigs 7 and 246 are associated with iron transporter siderophores. They play a role in iron acquisition and oxidative stress protection.[234-235] Contig 11 cluster is related to thioamitides which are a group of ribosomally-synthesized and post-translational modified peptides (RiPPs) with potent cell anti-proliferative and pro-apoptotic activities. Furthermore, the thioamide containing metabolites showed great antibacterial activity against MRSA, surpassing the current standard drug against MRSA infection,[236] thus attracting more attention. The synthesis of such cluster is still largely unknown,[237] and in *Streptomyces* sp. A1-08, the large BGC (22 kbp) has a predicted 15 member gene loci, thus heterologous cluster activation could pose challenges. Contig 10 cluster is associated to β-lactones which are natural products that are integral features of many pharmacologically active compounds.[238] Within contig 200 is a cluster of non-ribosomal peptide synthetases (NRPS).[239] Antibiotics such as actinomycin, cephalosporin and vancomycin are examples of non-ribosomal peptide natural products.[239-240] Finally, a biosynthetic gene cluster in contig 266 is related to type 1 polyketide synthase (T1PKS) (*Streptomyces sioyaensis*, WP_135796923.1) (Table 5.5). Important polyketides with known antimicrobial and antitumor activities are erythromycin,[241] geldanamycin,[242] respectively.

Comparative genome analysis of the BGCs with the closest type strain, *Streptomyces olivaceus* NRRL B-3009[T] revealed a shared ~54% (n = 26) BGCs and ~46% (n = 22) unique BGC (Table 5.2). The two complete BGCs, coelibactin and coelichilin found in *S. olivaceus*, but fragmented in the contigs of A1-08, suggest the potential modifications in the latter isolate, hence could potentially results in different metabolites. Whole genome information and predicted BGCs of *Streptomyces* sp. A1-08 may potentially contribute to future research on the structure and function of bioactive compounds and their biosynthetic pathways and transport systems. On the other hand, many of the gene clusters may be weakly or silently expressed in laboratory

conditions.[212] Therefore, chemical analysis would be necessary to claim that the 48-secondary metabolite BGCs can all be synthesized by *Streptomyces* sp. A1-08. The limited full homology of gene clusters with known empirically verified metabolites and the low homology of unique clusters in *Streptomyces* A1-08 require comprehensive approach in elucidating the individual contribution of the predicted metabolites towards the anti-colorectal cancer cell line and anti-MRSA activity.

5.3. Conclusion and Future Directions

Streptomyces sp. A1-08 is a novel actinomycete species isolated from the volcanic soils of Mount Mayon and harbors antibiotic and anticancer activities. This study suggests that volcanic soils are promising sources of novel *Streptomyces* species exhibiting various biological activities such as broad-spectrum antimicrobial, anti-MRSA and anti-colorectal cancer activities. The genome sequence of *Streptomyces* sp. A1-08 was used to predict potentially novel bioactive secondary metabolites. Further work on metabolomics for the detection of new chemical scaffolds and functional genomics for in depth discovery of novel biosynthetic genes are needed to continue the search for natural products with promising use in medicine and pharmaceutical needs.

Chapter 6

Evaluation of *Beauveria bassiana* for the biocontrol of MPB

6.1 Project Background

6.1.1. Mountain Pine Beetle and the Current Epidemic in Western Canada

The mountain pine beetle (MPB), *Dendroctonus ponderosae*, has infested millions of hectares of lodgepole pine (*Pinus contorta*) forests in British Columbia, and Alberta, Canada, killing over 50% of mature lodgepole pine trees with an estimated cumulative economic and welfare loss of 90 Billion CAD.[78] At present, MPB is considered as an invasive species in Alberta,[243] as it crossed the Rocky Mountains,[244] killing and reproducing in evolutionarily naïve populations of lodgepole pine, jack pine (*Pinus banksiana)*, and their hybrids.[81] Its ability to attack and kill jack pine and cause outbreaks, has posed an alarming continental threat since this is a common pine species, extending across the entire boreal forest to the Great Lakes and the East Coast of Canada (Figure 1.2).[81, 245-248]

Several important aspects of the beetle's life cycle and biology preclude conventional approaches in the management of MPB populations.[108] First, given that MPB spend all but a few days beneath the bark of their host trees, they are largely not affected by exogenous pesticide application. Second, blockage of the tree's vascular system by ophiostomatoid fungi introduced into the host tree during colonization by MPB, limits the efficacy of systemic insecticides in extended field seasons, although a combined insecticide-fungicide mixture demonstrated effective pine tree protection for at least two field seasons.[249] Third, of the few pesticides registered for use in forestry in Canada (e.g. tebufenozide and azadirachtin),[111] no effective pesticide has been applied in lodgepole pine stands to control the MPB epidemic.[112] As a result, detection and

physical removal of infested trees (felling and burning, or salvage harvesting) remains the current tactic available to manage MPB populations.[108] However, mechanical treatment of infested trees is costly, logistically difficult for some areas that are inaccessible, and prone to failure. Given that successful suppression of any MPB population requires consistent, long-term, application of direct control tactics, development of novel, ecologically viable and cost-effective tools is critical to minimize the continued spread and impacts of invasive populations of this insect within vast pine forests east of the Rocky Mountains in Canada.

6.1.2. The Entomopathogenic Biocontrol Fungus, *Beauveria bassiana*

Beauveria bassiana is an entomopathogenic fungus that attacks and kills several bark beetle species. Although the species can colonize a wide variety of arthropods, including pollinating insects, some strains have narrow spectra of activity.[250-252] This fungus is already in use as a biological insecticide against some insect pests. For instance, *B. bassiana* was successful in field tests in controlling European spruce bark beetle (*Ips typographus*) due to its persistence in forest litter.[253] It was also used in Europe for the control of pine shoot beetle (*Tomicus piniperda*) using field trap logs,[254] and red palm weevil (*Rhynchophorus ferrugineus*) using an attract-and-infect system.[255] In North America, although *B. bassiana* is lethal to MPB[256] and several other bark beetle species in the laboratory,[250,252] field tests often fail to demonstrate propagation of the mycosis or control of beetle populations, often limited by ambient temperature, host tree monoterpenes[252] or impacts of drought and UV-susceptibility.[257-258] Likewise, a majority of studies often utilized fewer strains of *B. bassiana,* which in turn may limit plasticity and virulence

associated with geographically diverse origins of biocontrol potential of these phenotypically diverse and genotypically-mosaic entomopathogenic fungi.[259-261]

Being a phenotypically diverse species of entomopathogenic fungus, with a large number of target hosts ranging from several insect species to arachnids, it is critical to establish criteria that will determine its economic potential as a biocontrol agent.[262-263] The diverse morphological and physiological characteristics of *B. bassiana*, such as conidial yield, pigmentation, hyphal growth rate, mycelial density are related to its pathogenicity and virulence potential. Furthermore, *B. bassiana* varies in its tolerance to abiotic stresses such as fluctuations in temperature, humidity, UV-light and antifungal compounds (i.e. monoterpenes).[250] These virulence and abiotic factors tolerance criteria can directly guide its development as a flexible microbial biocontrol agent.

6.1.3. Objectives

The aims of this projects were to collect 93 *B. bassiana* strains from several culture collections worldwide and evaluate and select for their phenotypic characteristics and virulence towards MPB. From this evaluation, nine strains will be extensively characterized including colony morphology, growth rate, pigmentation, conidiation capacity and assessed for virulence against MPB in the laboratory. The extensive criteria for strain selection and screening are found in section 9.5.2. Secondly, the project aims to develop methods to assess insect-carcasses agar media for selecting virulent *B. bassiana* strains. Lastly, strains will also be screened for higher UV-resistance and tolerance to pine tree monoterpenes, providing competitive advantage in changing environmental conditions such as temporal and diurnal changes in UV intensity as well as variable monoterpene concentrations in constitutive and induced pine tree defenses. These

criteria will be used in identifying strains that are needed for future work to scale up as an insect biological control agent for the management of MPB in the wild.

6.2 Results and Discussion

6.2.1 Phenotypic Characterization of *B. bassiana* Isolates

Based on the growth characteristics on CDAYE agar medium, the 93 *B. bassiana* isolates were phenotypically classified into three morphotypes. Group I (n = 12) produced white mycelial, villous colony and red soluble pigments. Group II (n = 78) had a thin-powdery, cream-colored colonies and no soluble pigments were detected. Group III (n = 3) produced a felty, yellowish white colony with visible diffusible yellow pigment. Nine isolates were chosen for further study and the characteristic descriptions of these nine *B. bassiana* strains are summarized in Table 6.1.

Biomass growth was assessed based on mycelial growth rate and conidial yields in a 60 cm^2 0.25× SDA plates (Table 6.2). Generally, Group I isolates had the fastest mycelial growth rates fully covering the entire CDAYE agar plate within 7 d and producing a conidial yield ranging from 1.04×10^8 to 2.13×10^8 conidia per SDA plate ($F_{(8,18)} = 29.29$, $P<0.0001$). Group II strains had an intermediate colony growth rate covering ~2/3 of the agar surface in 7 d and highest conidial yields ranging from $4.39 – 11.8 \times 10^8$ conidia per SDA plate in 21 d ($F_{(8,18)} = 29.29$, $P<0.0001$). Group III strains grew the slowest, covering <1/4 of the agar surface after 21 d and producing the lowest conidial mass at $0.20 – 0.55 \times 10^8$ conidia per SDA plate ($F_{(8,18)} = 29.29$, $P<0.0001$), one log lower than the other groups. Although the malt extract agar (MEA) plate gave similar mycelial

growth response across the nine strains (Table 6.2), this media selectively screen for intense yellow pigmentation in Group III *B. bassiana.*

Table 6.1. Phenotypic characteristics of the nine *B. bassiana* strains.

Isolate Code	Group	Colony color	Colony texture	Pigment*	Isolation Host/Source	Geographic Source	Reference
UAMH 299	I	White	Villous	Red	European pine sawfly *(Neodiprion sertifer)*	Sault Ste. Marie, ON, CAN	UAMH[#]
UAMH 1076	I	White	Villous	Red	Soil under poplar tree	Edmonton, AB, Canada	UAMH[#]
UAMH 4623	I	White	Villous	Red	Twig of an unknown plant	Pennsylvania State College, USA	UAMH[#]
UAMH 1069	I	White	Villous	Red	Soil under spruce (*Picea* spp.)	Edmonton, AB, CAN	UAMH[#]
UAMH 4510	II	Creamy white	Thin powdery	Colorless	Bark of *Abies lasiocarpa* with *Dryocoetes confusus*	Smithers, BC, CAN	UAMH[#]
ANT-03	II	Creamy white	Thin powdery	Colorless	Anatis BioProtection	Laval, QC, CAN	ANT[$]
UAMH 9748	II	Creamy white	Thin powdery	Colorless	Soil	Ontario, CAN	UAMH[#]
110.25	III	Yellowish white	Felty	Yellow	Dutch Culture Collection	Netherlands	Eley et al. 2007
LFCC0167	III	Yellowish white	Felty	Yellow	Lallemand Plant Care	Sault Ste. Marie, ON, CAN	Lallemand[§]

[#] UAMH – University of Alberta Microfungus Collection and Herbarium
[$] ANT – Anatis Bioprotection
[§] Lallemand Plant Care Inc

Table 6.2. Growth rate and conidial yield of nine *B. bassiana* strains. Different letters denote significant difference at α = 0.05 with a Tukey's HSD adjustment.

Isolate Code	Group	Mycelial growth after 7 d			Conidial Yield ($\times 10^8$ conidia) in 60 cm^2 0.25× SDA after 21 d
		CDAYE	0.25× SDA	MEA	
UAMH 299	I	+++++	+++	+++	1.79 ± 0.27 bc
UAMH 1076	I	+++++	+++	+++	2.13 ± 0.20 bc
UAMH 4623	I	+++++	+++	+++	1.83 ± 0.24 bc
UAMH 1069	I	+++++	+++	+++	1.04 ± 0.18 c
UAMH 4510	II	+++	+++	+++	4.45 ± 1.24 b
ANT-03	II	+++	+++	+++	11.8 ± 1.76 a
UAMH 9748	II	+++	+++	+++	4.39 ± 2.65 b
110.25	III	+	+	+++	0.20 ± 0.04 c
LFCC0167	III	+	+	+++	0.55 ± 0.25 c

+++++, mycelial growth covered 100% of the plate
+++, mycelial growth covered ~67% of the plate
+, mycelial growth covered <25% of the plate

We found that phenotype, as defined by pigmentation, was related to virulence. Among the three types of media tested, CDAYE supported faster hyphal growth, conidiation yield and production of agar-diffusible pigments compared to a 0.25× SDA medium. The culture conditions responsible for the selective expression of the colored phenotypes have been reported,[264] which is dependent on: the carbon-to-nitrogen (C/N) ratio; the presence of organic or inorganic nitrogen sources; or the presence of divalent cations specifically, magnesium and zinc. The alteration of C/N ratio may shift the expression of specific pigmented compounds in *B. bassiana,* although this appears to be genotype-dependent and culture-time dependent. A low C/N ratio often leads to the production of the red pigment oosporein while a high C/N ratio supports the yellow pigments such tennelin or bassianin.[264-265] Glycerol was a better inducer than glucose for the induction of oosporein biosynthesis. On the other hand, increasing nitrate concentration did not limit oosporein

production while substituting asparagine as the nitrogen source induces the yellow pigment. Interestingly, for strains capable of producing both pigments, oosporein was formed first and until the nitrogen source was depleted, at which point bassianin started accumulating. Furthermore, the addition of trace metals in CDA base medium indicated that the red pigment oosporein was repressed by magnesium but was enhanced by zinc.[264]

Another set of criteria that are often considered for entomopathogen product development are mycelial growth rate, sporulation rate, and conidial area. Interestingly, the growth rate of *B. bassiana* appears to have variable correlation with virulence, sporulation rate, and conidial area. Previous studies on other bark beetle species have showed that isolates with a faster growth rate have the advantage of quicker infection in the laboratory or field,[250,252] but this was rarely supported for other insect-infection bioassays.[266-268]

6.2.2. Assessment of Insect Agar Media for *B. bassiana* Virulence Selection

The feasibility of using carcases of MPB was explored to develop an agar medium for growing and selecting for virulent and (hyper)virulent *B. bassiana* strains. Having an artificial media that can be used to select for virulence is especially important if live MPBs are unavailable during the winter season. This media development was also extended in another insect, the European honeybee (EHB), *Apis mellifera*, for a quick, large-scale, laboratory screening of entomopathogenic fungi virulence against agriculturally-beneficial insects. Mountain pine beetle agar (MPBA) and European honeybee agar (EHBA) media were made from lyophilized MPB powder and lyophilized honeybee powder, respectively. The two insect powders had no significant carbon-nitrogen ratio difference as revealed by elemental analyses (Table 6.3), and both supported the growth of the nine strains of *B. bassiana*.

Table 6.3. Elemental analysis of *Dendroctonus ponderosae* (DP) and *Apis mellifera* (AM) lyophilized powder.

Replicate	Wt. (mg.)	% N	% C	% H	% S	% O
DP1	1.5822	9.702306747	54.11302185	7.606041908	0.383168727	35.60139465
DP1	1.7096	9.650771141	53.84079361	7.602559566	0.323060006	35.22277832
DP1	1.6545	9.685803413	54.07806778	7.642033577	0.318551362	35.05156326
DP2	1.5964	9.718169212	53.99201965	7.645724297	0.354237318	35.26874924
DP2	1.6672	9.552751541	53.21146774	7.492612362	0.32952255	35.23487831
DP2	1.7293	9.690340996	54.01459122	7.644084930	0.314744025	35.06178259
AM1	1.7222	6.982572556	47.55653763	7.168415070	0.303668469	23.74513435
AM1	1.7324	6.988976955	47.59463882	7.170219421	0.317621738	23.57822037
AM1	1.5363	6.897191525	47.57046509	7.172136784	0.370771021	23.58425522
AM2	1.6174	6.727408886	47.07477188	7.044081688	0.313205957	23.37537003
AM2	1.5402	6.870326996	47.50792313	7.153573036	0.37463668	23.58821035
AM2	1.7287	6.863929272	47.55265045	7.186550140	0.368057072	23.57426722

Interestingly, all nine strains showed better average colonization in EHBA (30.4 ± 3.8 mm) (mean $\pm$ sd) than in MPBA (20.1 ± 1.5 mm) within 14 d ($F_{(1,34)} = 77.63$, $P<0.0001$), which is supported with visually denser myceliation in EHBA medium (Figure 6.1). No significant difference was established amongst the three phenotype groups in EHBA ($F_{(2,15)} = 2.32$, $P = 0.1322$) and MPBA ($F_{(2,15)} = 0.12$, $P = 0.8886$).
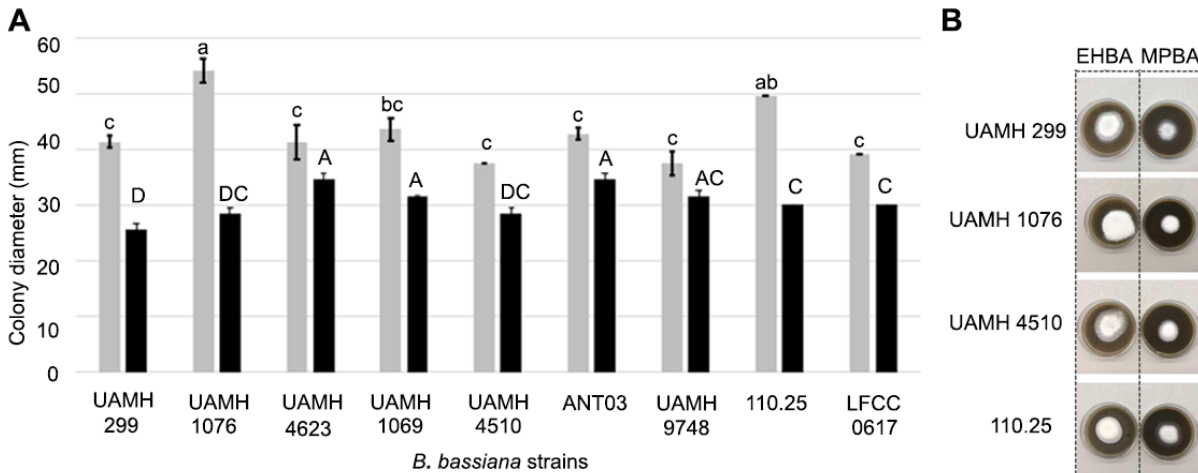
Figure 6.1 Colony diameter (mm) of *B. bassiana* strains grown on European honeybees agar (EHBA, gray bar) and mountain pine beetle agar (MPBA, black bar) incubated for 14 d at 25 °C (A). Representative plates of the three classes of *B. bassiana* strains grown on EHBA or MPBA media (B). Different letters denote significant differences at α = 0.05, with a Tukey's HSD adjustment.

6.2.3. Virulence Evaluation of *B. bassiana* against *D. ponderosae*

Infection of MPB by *B. bassiana* significantly impacted mean survival time (MST) of the beetles. The beetles treated with conidia died within 5 ± 1 d compared to the control treated with 0.01% Tween 80 that remained viable until 15 ± 1 d ($F_{(9,30)}$ = 64.480, $P<0.0001$). Similarly, the lethal time to kill 50% of the beetle population (LT_{50}) was significantly different between the experimental strains (4 ± 1 d) and control (9 ± 1 d) (Type I test $F_{(9,23)}$ = 16.00, P-value <0.0001) (Fig. 1). The same pattern was observed for LT_{100} (Type I test $F_{(9,23)}$ = 64.48, $P<0.0001$). The LT_{50} was significantly faster in Group I *B. bassiana* treatment (3 d) compared to Groups II and III (5 d and 4 d, respectively) (Figure 6.2), which did not differ from each other (Type I test $F_{(3,29)}$ = 49.06, $P<0.0001$). The established lethal times, LT_{50} and LT_{100}, support a precipitous death in the conidia-treated MPB, where the LT values are on the average, one day apart across the three groups of *B. bassiana* strains tested.
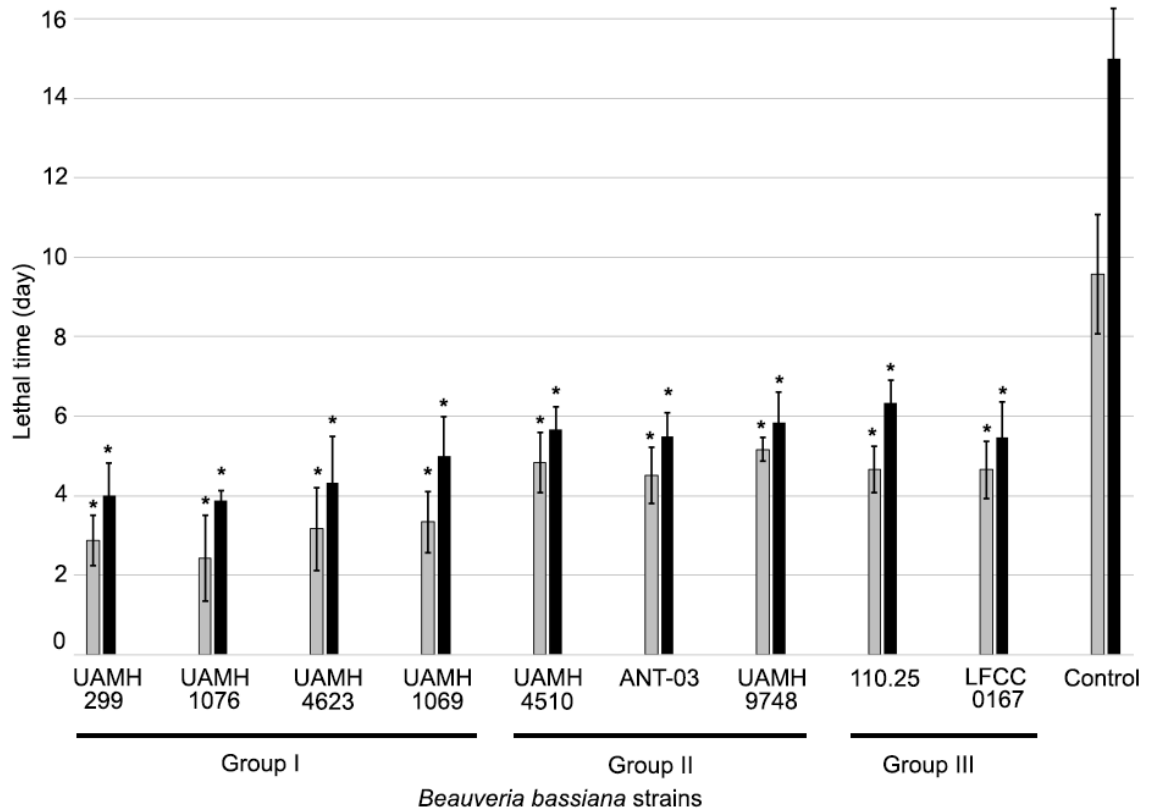
Figure 6.2 Lethal time (LT$_{50}$ in gray bar, LT$_{100}$ in black bar) *of D. ponderosae* **directly exposed to 1×10^8 CFU/mL** *B. bassiana* **conidia.** Nine strains of *B. bassiana* were grown in Czapek Dox Agar supplemented with 2% yeast extract for 14 d and conidia were harvested in 0.01% Tween 80 and the conidial concentration was determined using a haemocytometer. Control group is treated with 0.01% Tween. Values shown are mean and standard deviation of three biological experiments. Bars with * are not significantly different ($P<0.05$) from corresponding control, by ANCOVA followed by a post-hoc Dunnett's test.

Based on the results of the laboratory scale trials, all strains differed from control in both LT$_{50}$ and LT$_{100}$ within the Group I, Group II or Group III isolates (Figure 6.2), therefore, one strain for each group was chosen, namely: UAMH 299, UAMH 4510 and strain 110.25, respectively, to test on large-scale infection assay. The large-scale infection assay using three representative groups of *B. bassiana* showed a similar response to the first trial in that MST was significantly different among treatments ($F_{(59,600)} = 21.01$, $P<0.0001$). The survivorship curve (Kaplan-Meier non-parametric estimation, Figure 6.3) illustrates precipitous death of the beetles treated with *B.*

bassiana conidia compared to control beetles (MST = ~6 d) for strains UAMH 299 (MST = ~4 d, t value = 6.790, *P*<0.0001)) and 110.25 (MST = ~5 d, t value = 3.565, *P* = 0.0040), both of which support the small-scale laboratory trials (Figure 6.2). On the other hand, beetles treated with strain UAMH 4510 exhibited a similar survival curve (Figure 6.3) and nearly identical MST (MST=~6 d, t value = 0.097, *P* = 1.000) with the negative control group.

While strains of *B. bassiana* in Groups I and III grew slower and produced less conidia than Group II strains, both effectively killed MPB faster than the latter. This pattern is potentially due to the mycotoxic pigments found in strains in Groups I and III. For Group II strains, our results are in agreement with the previous work of Romon and co-workers on pine weevil (*Pissodes nemorensis*)[268] where the highly-sporulating Group II *B. bassiana* took the longest to elicit an effective lethal time for the large-scale infection MPB assays. This can be ascribed to the use of a lower conidial titer that potentially slows down the killing rate of Group II *B. bassiana* strains, similar to the extended mean survival time in European spruce bark beetle.[269] The effectivity of Group II strains appears to require higher conidial titer to elicit comparable lethal times as strains from Groups I and III. Alternatively, the virulence fitness of *B. bassiana* could also be ascribed to the possibility of Group II strains having a genotypic trade-off between the production of mycotoxic pigments and the production of high number of conidia that presumably increases the possibility of infecting a target host. Conversely, strains with mycotoxic pigments do not need as many conidia to effectively colonize their target host. As such, the negative correlation indicates that lower saprophytic competitiveness resulted in higher pathogenic and virulence potential.[268]
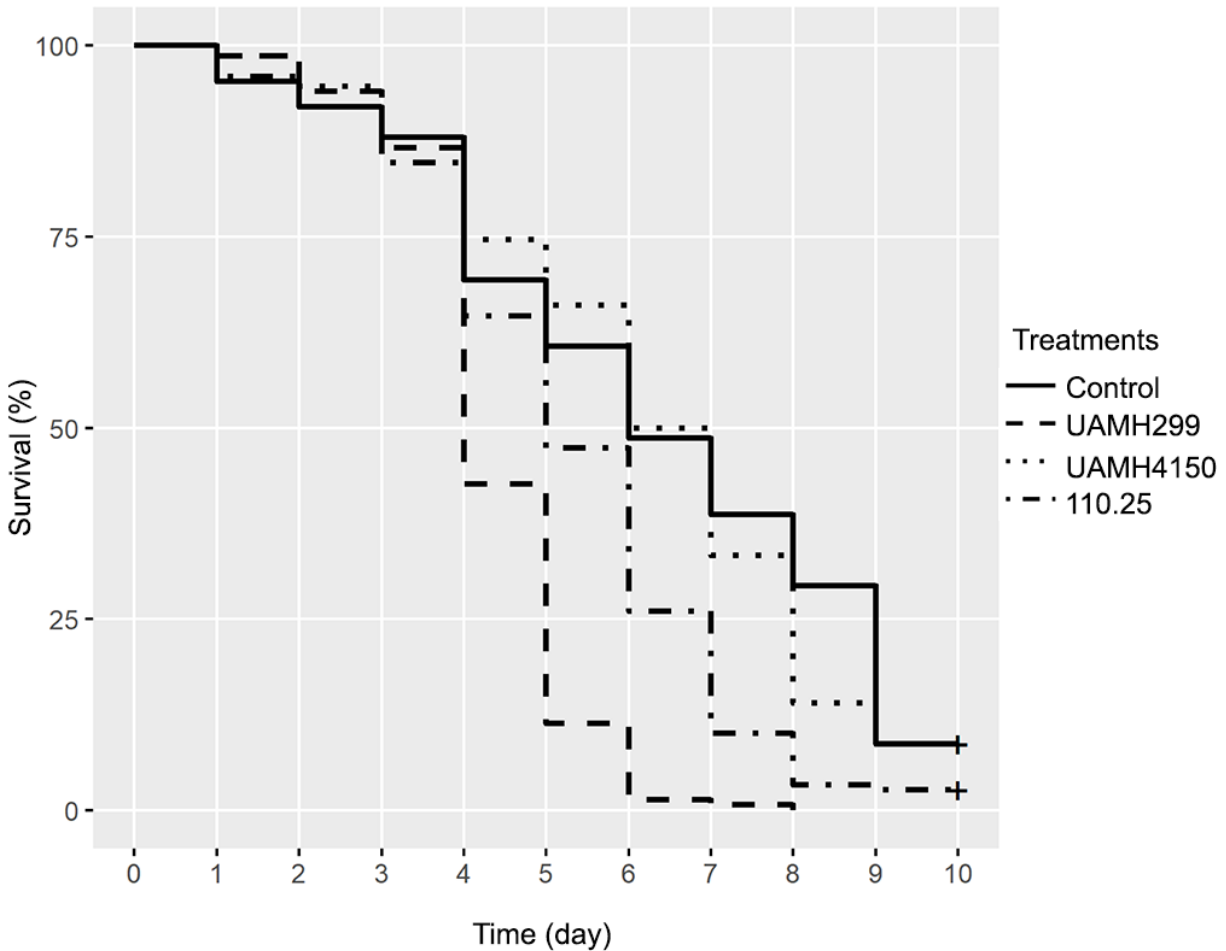
Figure 6.3. Kaplan-Meier survivorship curves of *D. ponderosae* treated with conidia of three *B. bassiana* strains (UAMH 299 ($LT_{50} = 4d$), UAMH 4510 ($LT_{50} = 6d$), 110.25 ($LT_{50} = 5d$) and negative control. Each curve depicts percent survival over time for 150 individuals per treatment. Individuals within each treatment were divided into groups of 10 and placed in plastic petri dishes lined with filter paper and exposed to 1.0×10^7 CFU/mL conidia diluted or distilled water for the control group. Each treatment was stored in a separate container at 21 °C and 70% humidity for 10 d. Every 24 h dishes were examined for fatalities and amended with an additional 5 mL distilled water. Dead individuals were removed upon detection.

The disparate lethal times of the Group II *B. bassiana* treatments from the two independent experiments could have arisen from a difference in the conidia titer (10^8 compared to 10^7 conidia /mL) used in the independent studies. Therefore, the linear survivorship curve of both Group II *B. bassiana* and the negative control prompted us to determine the possibility of a conidia dose-

dependent lethal time. Using a ten-fold dilution series of strain UAMH 4510 conidia, we showed

a concentration-dependent killing of MPB (Figure 6.4). The conidial concentration was inversely

proportional to the lethal time of the beetle resulting in LT_{50} ranging from $2 - 7$ d ($F_{(3,8)} = 48.28$,

$P<0.0001$) and LT_{100} ranging from $3 - 9$ d ($F_{(3,8)} = 26.83$, $P = 0.0002$). The highest conidial

concentration, 1×10^9 Colony Forming Units per mL (CFU/mL), resulted in LT_{50} and LT_{100} of 2 d

and 3 d, respectively. The conidial titer between treatments 1×10^8 and 1×10^7 CFU/mL, resulted

in LT_{50} and LT_{100} of 3 - 4 d and 4 - 6 d, respectively (Figure 6.4), which is reminiscent of Group I

and Group III conidial lethal times (Figure 6.2).
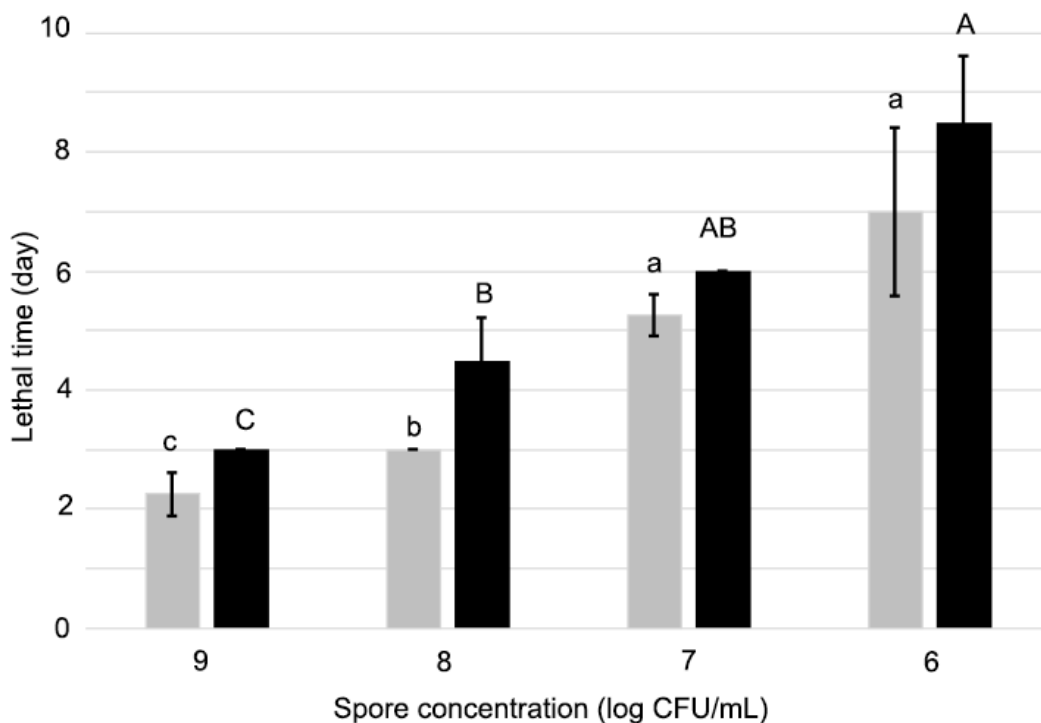
Figure 6.4. Dose-dependent killing time (LT_{50} in gray bar; LT_{100} in black bar) of *D. ponderosae* directly exposed to 1×10^9, 10^8, 10^7 and 10^6 CFU/mL Group II *B. bassiana* UAMH 4510 conidia. Values shown are mean and standard deviation of three biological experiments. Lower case lettering shows the results of post-hoc Tukey's HSD pairwise comparisons amongst the treatments. Mean values with different letters indicate a significant difference at $\alpha = 0.05$. The lowercase letters show the differences among the gray bars and capital letters show the differences among the black bars.

The observed lethal times of the large trial (UBC-based experiment) were further dissected at the level of the beetle age classes (Figure 6.5). The mean survival time was not significantly different across the five beetle age classes for the negative control and two of the *B. bassiana* treatments, strains UAMH 299 and 110.25 (Groups I and III, respectively) (Figure 6.5). Interestingly, strain UAMH 4510 (Group II), showed a decrease in beetle mean survival time in an age-dependent manner. The older beetles (exposed 20-25 d post emergence) died faster (MST = ~5 d) compared to younger beetles (exposed 0-10 d post emergence, MST = ~7 d, t value = 4.017, *P* = 0.048) (Figure 6.5).

The progressive development of an off-white mycosis in the dead MPB started on the tarsal appendages, followed by the head region, the thoracic area and ultimately covering the entire insect (Figure 6.6). The complete mycosis of the beetle body is variably observed in and between the three phenotypic groups, with no evidence of group-dependent sporulation (Figure 6.6F). The negative controls, the solvent and *Aspergillus nidulans* UAMH 9442 treatments, did not result in mycosis of MPB.
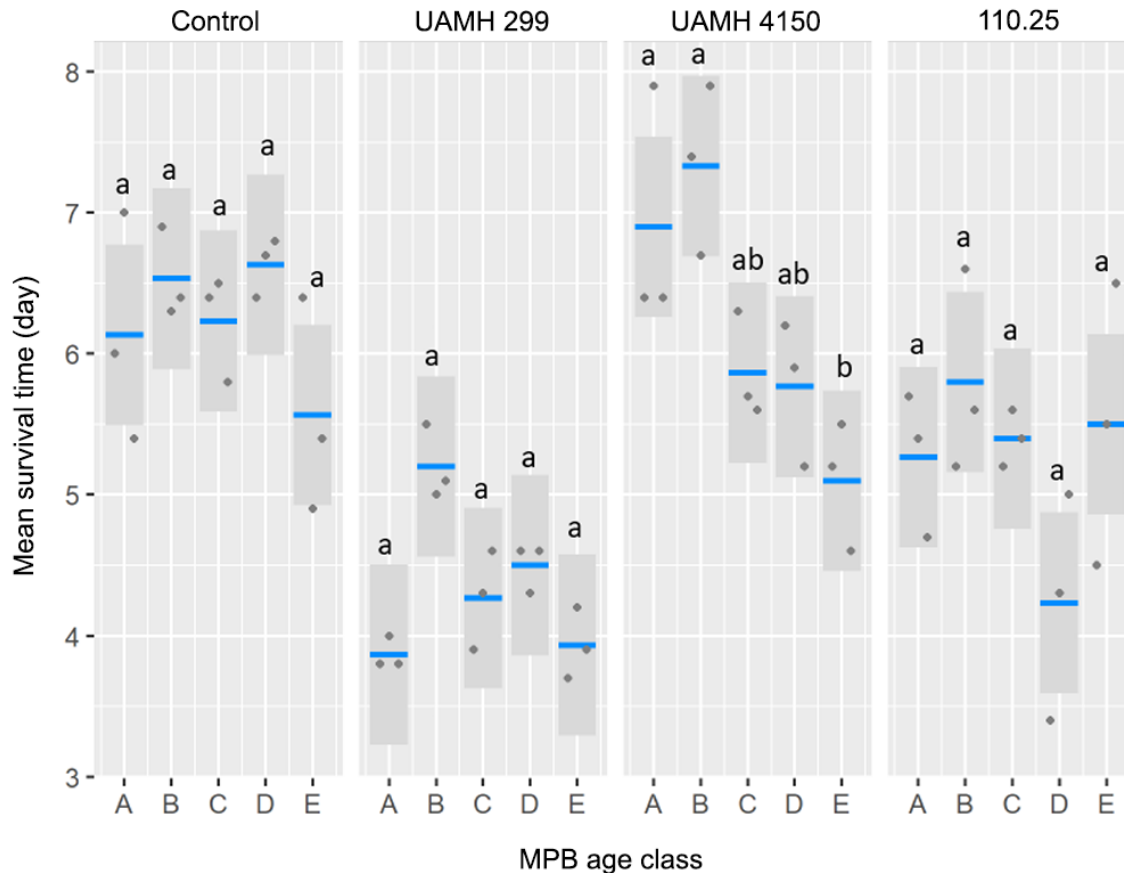
Figure 6.5. Visreg plot of mean survival time of five age classes of *D. ponderosae* treated with 1×10^7 CFU/mL *B. bassiana* conidia and a control group. Beetle age class was determined by the number of days between emergence from the bark and exposure to conidia: A (0-5 d), B (6-10 d), C (11-15 d), D (16-20 d) and E (21-25 d). Each point is the mean survival time of a group of 10 individuals from the same age class stored on the same petri dish. Each blue line is the mean of 3 petri dishes and the shading shows the 95% confidence interval of the mean survival time of each treatment by age class combination. Lower case lettering shows the results of post-hoc Tukey's HSD pairwise comparisons of age classes within treatment. Different letters indicate a significant difference at α = 0.05.

6.2.4. Virulence Evaluation of *B. bassiana* Against *A. mellifera*

Representatives of the three groups of *B. bassiana* were tested on worker European honeybees to assess their virulence potential. The effective dose to kill MPB (1×10^7 conidia /mL) was found to be ineffective against the worker honeybees. The average daily mortality (~5%) rate is similar across all the tested representatives of *B. bassiana* conidia and was not significantly different from the control ($F_{(3,10)} = 7.58$, p = 0.0133) (Figure 6.7). This mortality rate is comparable

to the estimated natural death turnover rate of a healthy colony.[167] Dead honeybees variably showed white mycosis after incubation for 14 d.
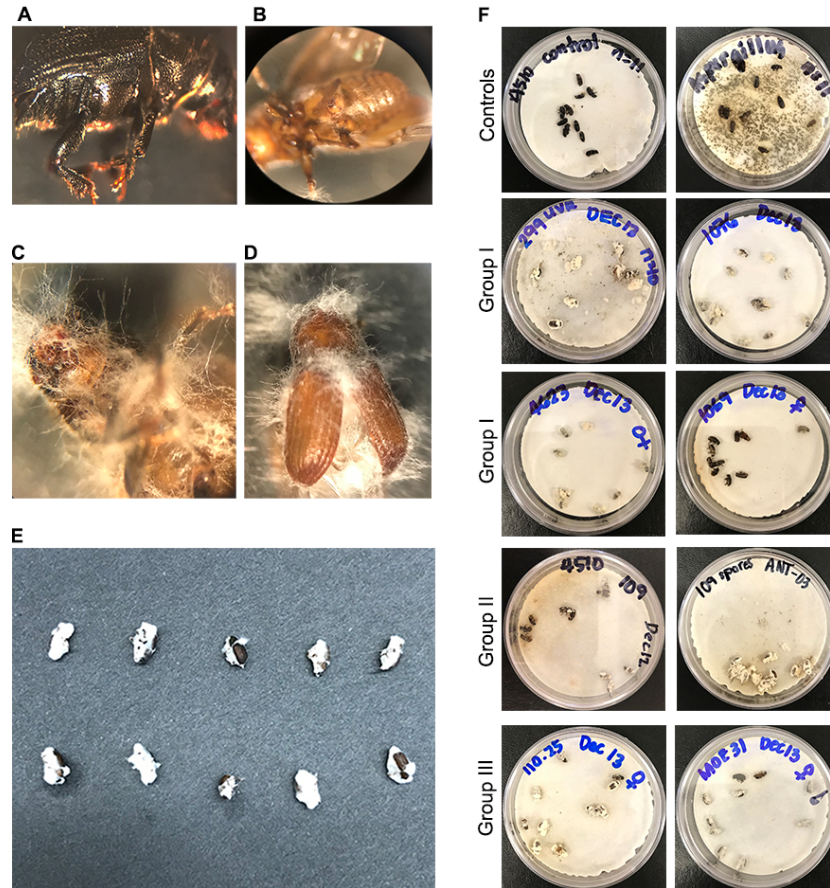
Figure 6.6 Mycosis in *D. ponderosae* after 14 d post exposure to *B. bassiana* conidia. (A) Uninfected *D. ponderosae* adult beetle. Progressive development of fungal mycoses in representative *D. ponderosae* treated with 1×10^7 CFU/mL conidia of *B. bassiana* strain UAMH 299 after day 3 (B), day 7 (C), and day 10 (D) viewed under a dissecting microscope and day 14 (E). Mycosis of *D. ponderosae* treated with either 1×10^7 (for Groups I and III) or 1×10^9 CFU/mL conidia (Group II) *B. bassiana* conidia after 14 d post infection (F). Control groups is treated with 0.01% Tween 80 or with 1×10^7 CFU/mL *Aspergillus nidulans* UAMH 9442 conidia.
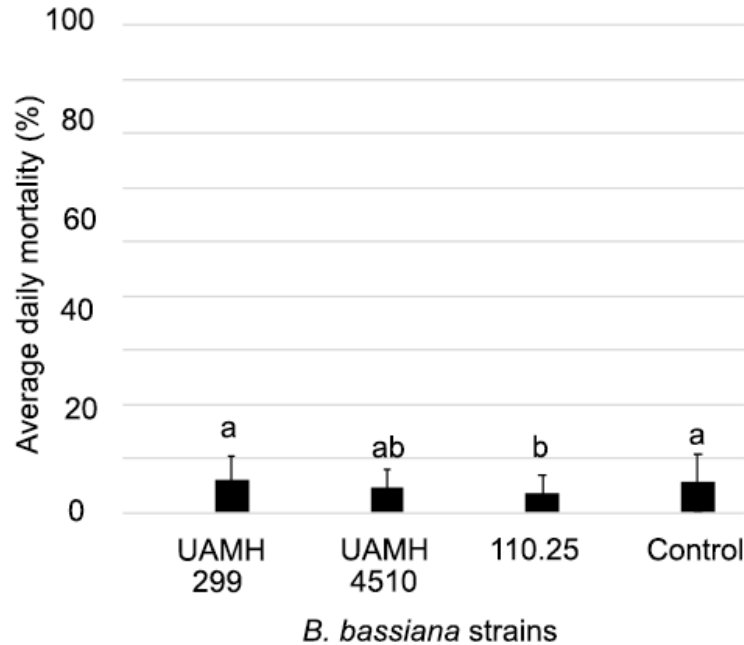
Figure 6.7. Average daily mortality of *A. mellifera* treated with 1×10^7 CFU/mL conidia of *B. bassiana* strains UAMH 299 (class I), UAMH 4510 (class II) and 110.25 (class III). Values shown are mean and standard deviation of three biological experiments. Dead individuals were removed upon detection. Different letters denote significant differences at $\alpha = 0.05$, with a Tukey's HSD adjustment.

As a generalist entomopathogenic fungus, *B. basssiana* has a broad range of host targets including, but not limited to, coleopterans (beetles), hemipterans (true bugs) and lepidopterans (butterflies and moths).[259] We found that honeybees did not exhibit the same infection profile by the *B. bassiana* conidia concentration that kill MPB, in agreement with earlier work.[270-273] The honeybee's hygienic behavioural responses towards pathogens may also explain their resistance to *B. bassiana* conidia infection, similar to the avoidance of the ectoparasitic mite *Varroa destructor*.[274] However, successful infection of honeybees appears to depend on conidial concentration and method of application.[270,272] Briefly, effective mycosis in *A. mellifera* was shown upon treatment of 1×10^{10} conidia/mL *B. bassiana* conidia or if the conidia were directly fed (through sugar solutions) instead of a passive contact before leaving the hive. Although the longevity of the worker honeybees may have been affected due to the absence of the queen

honeybee,[273] our trials showed no adverse effect on the honeybees as evident in their constant feeding. Although the conidia of *B. bassiana* showed conditional safety for European honeybees, immobile (dead) or direct-fed honeybees can still develop mycosis.[270] Although the selective and differential effect of the two insect agar media (MPBA or EHBA) did not support differentiation of virulence to the target insect, there could still be value in culturing *B. bassiana* strains in MPBA medium. Where passing of the fungus in a live insect host is not readily accessible,[272] or if multiple artificial commercial media passage may affect the virulence level of th strains,[275] the use of MPBA may maintain stability of virulence of the isolates against the MPB. However, this hypothesis is yet to be tested.

6.2.5. UV Resistance and Monoterpene Tolerance of *B. bassiana*

Two abiotic factors that may limit the growth of *B. bassiana* conidia were tested: UV resistance and monoterpene tolerance.[276-277] The three groups of *B. bassiana* showed variable UV tolerance (conidial growth after maximum time of UV treatment). Group I strains (red pigmented) showed significantly longest resistance (15-20 min), followed by the yellow pigmented Group III strains (15 min) and lastly the least UV-resistant were Group II (5-10 min) ($F_{(1,59)}$ = 151.09, P<0.0001) (Table 6.4). To test whether UV-resistance of *B. bassiana* could be increased, strain UAMH 299 was exposed to increasing time of UV light resulting in a fast-growing strain that survived UV exposure of 220 min.

Laboratory and field experiments often give incongruent results which may limit the efficacy of *B. bassiana* as a pest biocontrol agent in large areas of pine forest. This is largely attributed to various environmental factors, including exposure to UV light or pine monoterpenes, that restrict conidial survival, fungal colonization, and perpetuation of mycosis.[250,252] Our results

indicate that Group I *B. bassiana* conidia can tolerate UV-exposure longer. The higher UV tolerance of Group I strains may be attributed to the protective effect of colored pigments, such as oosporein, which can effectively absorb UV-light. Furthermore, tenellin or bassianin, presumably secreted by the yellow pigmented strains, acts as an iron-siderophore by scavenging iron that induced reactive oxygen species preventing cellular damage.[278] The conjugated bonds present in these pigments may support UV-light absorption, thereby helping in protecting the fungus. All these properties suggest that the diversity of UV-radiation tolerance amongst *Beauveria* sp. strains[279] require comprehensive screening of strain collections and should be accounted for selection and virulence evaluation.[280] The UV-tolerant wild type isolates or selected UV-resistant mutants thereof are good candidates for formulation with photoprotection advantage in the field.[258] Furthermore, UV tolerance and virulence can also be improved by the addition of natural substrates such as humic acid, lignin and sesame oil,[281] and potentially amendment of conidia preparations with their innate mycotoxic pigments (e.g. oosporein).

The three groups of *B. bassiana* revealed variable tolerance to the three tested monoterpenes and the simulated or reconstituted pine tree monoterpene profiles (Table 6.4). Tolerance to geraniol varied by group ($F_{(2,51)}$ = 330.56, $P<0.0001$), with Group II having greater tolerance than Groups I and III. While there was no variation in (–)-α-pinene tolerance for strains or strains within groups, we did find that the tolerance for monoterpene mixtures of either lodgepole pine or jack pine and the individual monoterpene, (–)-*trans* verbenol was greatest in groups II and III compared to group I (lodgepole pine: $F_{(2,51)}$ = 325.83, $P<0.0001$; jack pine had no variation within group; geraniol: $F_{(2,51)}$ = 29.61, $P<0.0001$). Interestingly, the fungal strains tolerated the simulated lodgepole pine monoterpene mix (undiluted) better than the jack pine monoterpene mix (100-fold dilution). Furthermore, concentrated (–)-α-pinene (700 mM)

Table 6.4. Monoterpene tolerance and ultra-violet resistance of nine *B. bassiana* strains. Monoterpene tolerance is defined as the maximum concentration of monoterpenes where mycelial growth was recorded. The monoterpene mixtures were ten-fold serially diluted and dilution factors were representation of total concentration for each pine tree species monoterpene treatment. UV resistance is the defined as the maximum time (min) where conidia germinated. Different letters denote significant difference at α = 0.05 with a Tukey's HSD adjustment.

Category	*B. bassiana* strain	Lodgepole pine monoterpene mix	Jack pine monoterpene mix *	Geraniol (µM)	(-)-α-Pinene (mM) *	(-)-*trans* Verbenol (mM)	UV-tolerance (min)
Class I	UAMH 299	0.1× a	0.001×	6.5 a	700	6.6 a	20 a
	UAMH 1076	0.1× a	0.001×	6.5 a	700	6.6 a	20 a
	UAMH 4623	0.1× a	0.001×	6.5 a	700	6.6 a	20 a
	UAMH 1069	0.1× a	0.001×	6.5 a	700	6.6 a	15 a
Class II	UAMH 4510	1× b	0.01×	650 b	700	660 b	5 b
	ANT-03	1× b	0.01×	650 b	700	660 b	10 c
	UAMH 9748	1× b	0.01×	650 b	700	660 b	5 b
Class III	110.25	1× b	0.01×	65 c	700	660 b	15 d
	LFCC0167	1× b	0.01×	65 c	700	660 b	15 d

*No variation in maximum concentration tolerance among replicates, therefore no statistics were performed.

was tolerated across all tested strains, although no statistical analysis was performed as no variation was observed across all strains (Table 6.4). On the other hand, geraniol tolerance was highest in Group II (650 µM), followed by Group III (65 µM) and lastly Group I (6.5 µM). The (–)-*trans* verbenol was tolerated the most by both Groups II and III strains (660 mM) and again the least by Group I (6.6 mM).

The pine monoterpenes (isoprenoids) landscape significantly influence the survival, proliferation and invasion of forest by the MPB.[248,282] As a host tree defence system, many of these monoterpenes were found to be toxic to MPB (e.g. (–)-limonene, (–)-α -pinene)[282] and have also been shown to suppress the growth of *B. bassiana* in defensively-induced Engelmann spruce (*Picea engelmannii*) trees (e.g., 3-carene, (–)-α-pinene).[252] Our results revealed that Group II *B.*

bassiana has the highest tolerance to monoterpenes tested as a mixture or individual components. Interestingly, the red-pigmented Group I *B. bassiana* conidia are the least resistant phenotype against the monoterpenes. This supports the notion that genetically similar, but phenotypically different *B. bassiana* isolates respond variably to abiotic stress and therefore the evaluation of different morphotypes is important due to within-haplotype phenotypic diversity.[277] Furthermore, the tolerance of *B. bassiana* to the individual effector monoterpenes involved in the MPB-aggregation pheromone biosynthesis may support synthetic engineering efforts in creating MPB pheromone-producing molds. The elucidated genes involved in the pathway[283-284] can be engineered into *B. bassiana* which can be explored as a recombinant tool for a selective and MPB-targeted biocontrol in the field. Although this result may serve as proxy for evaluating *B. bassiana* conidia against MPB, the current criteria for virulence selection is limited to laboratory-controlled assays. The pathogenicity of *B. bassiana* against *Dendroctonus rufipennis* in laboratory-based infection assay was shown to be ineffective unless *in planta* (presence of wood shavings, phloem, and monoterpenes) and *in natura* (cold temperature, lower water activity) conditions were considered.[277] Albeit, the three arbitrary classes reported here provided a range of phenotypes and MPB-virulence, further evaluation must be explored in field MPB infection experiments including *in planta* bioassays and *in natura* conditions.

6.4. Conclusion and Future Directions

Our study provides the first investigation comparing the efficacy of phenotypically diverse *B. bassiana* strains to kill MPB and evaluate their potential to control the spread of the invasive forest pest. The development of this entomopathogenic fungus into a biocontrol agent may contribute to the limited mitigation approach that is currently employed in controlling the spread

of the devastating effect by the MPB that is continuously threatening the western Canadian pine forest.

Several studies have tested and developed various techniques for the application of entomopathogenic *B. bassiana* against major forest insect pests including bark beetles.[182-185] Based on these earlier publications, we can briefly suggest several ways where we can potentially use *B. bassiana* as a biological control agent against MPB. Firstly, UV-protected microcapsules containing entomopathogen can be aerially sprayed over MPB infested forests. This application should coincide when beetles are actively flying and searching for new host trees from July and August in Western Canada. Secondly, regular flight intercept or multiple funnel traps baited with attractants (pheromones and/or host volatiles) could be used to contaminate beetles with *B. bassiana*. In this system, collection cups of such traps contain propagules of *B. bassiana* (ideally in the form of wettable powder) and could contaminate trapped insects. These insects should then be released to contaminate other individuals in the same or different populations. Thirdly, trap trees are commonly used to monitor and even control various bark beetles.[186] Bark surface of these trap trees can be contaminated by spraying with water suspension containing *B. bassiana* propagules. These trees can be baited with synthetic pheromones and used to attract and kill arriving beetles.

Chapter 7

Evaluation of *B. bassiana*

formulation for the population management of MPB

7.1 Project Background

7.1.1 *B. bassiana* Formulations

Mycoinsecticides are formulations containing fungal propagules employed as an active ingredient designed for inundative and inoculative applications targeting insect pests. Historically, the top commercially produced mycoinsecticides were based on three fungal species namely, *Beauveria bassiana*, *Metarhizium anisopliae*, and *Isaria fumosorosea*.[68] The extensive evaluation and prudent selection of geographically relevant and ecosystem-robust species are accounted for the efficacy towards the target insect. Development of mycoinsecticide formulation technology is of paramount importance for the successful implementation of a fungal biocontrol program. Depending on the technology, the approach offers a wide selection of processes for a robust facilitation of mycoinsecticide's handling, transport, and field application. Furthermore, the development strategies will also affect the temperature- and water activity-dependent stability and shelf-life; consistent insect-killing efficacy; ease of application and persistence in a wide range of abiotic environmental stresses.[65] Earlier efforts were directed towards dry formulations of dried fungal mycelial preparation using carriers such as sodium alginate, calcium chloride, or gelatinized cornstarch.[69] Similarly, conidial formulations used in field trials were based on diverse stabilizing agents such as oil, clay, silicon, wheat-bran, as well as emulsifiabale suspensions,[64] especially

agriculturally approved carriers for sustainable agriculture and environmental management.[65,70] Recently, other modes of fungal propagule stabilization include encapsulation technologies using spray dried-biocapsules, microencapsulating biopolymers, and nanocomposites.[71-73]

7.1.2 Field Trials and Current Applications

Several important aspects preclude conventional approaches to management of mountain pine beetle populations. First, given that beetles spend all but a few days beneath the bark of their host trees, they are largely unavailable to broadcast pesticide application. Second, blockage of the tree's vascular system by the blue stain fungi limits the efficacy of systemic insecticides. Third, in the event that a chemical tactic could be deployed effectively against mountain pine beetle, chemical pesticides are not presently registered for use in forestry in western Canada. As a result, detection and destruction of infested trees (felling and burning, processing) remains the only tactic available to manage mountain pine beetle populations. Unfortunately, mechanical treatment of infested trees is costly, logistically difficult and prone to failure. Given that successful suppression of any *D. ponderosae* population requires consistent, long-term, application of direct control tactics, development of novel, ecologically viable and cost-effective tools is critical to minimize the continued spread and impacts of invasive populations of this insect within vast pine forests east of the Rocky Mountains.

Despite the assortment of mycoinsecticide formulations, their efficacy was statistically limited in laboratory scale infection assays while commercially effective formulations are proprietary.[65] As such, the situation restricts our thorough understanding about the compositions or ingredients that holistically integrate into the success of a mycoinsecticide. Also, considering that genotypic and phenotypic variations within species and between strains of entomopathogenic

106

fungi, mycoinsecticide development is a vital parameter to consider in the successful management of targeted insect pests and their associated environmental limitations.[64]

7.1.3. Objectives

To perform a greenhouse and field tests on pine forest stands, *B. bassiana* strains, UAMH 299, UAMH 1076 and ANT-03 were developed and evaluated for conidial stability under storage, *in planta* (greenhouse) and *in natura* conditions (i.e. acreage). To access enough suitable and enough conidial biomass for MPB infection assays, a bi-phasic liquid-solid fermentation approach using commercial fungal broth (CDBYE) and parboiled rice substrate was developed. Greenhouse based MPB *in planta* infection assays were performed while field evaluation was executed in Hinton, Alberta pine forest stand. In an effort to support the mechanism of effectivity of the mycoinsecticide, under *in planta* and *in natura* conditions, we probed the *B. bassiana* perturbation of the tripartite interaction using functional genomics and *in vivo* fungal community interaction challenges.

7.2 Results and Discussion

7.2.1. Stability of *B. bassiana* formulation under storage, *in planta*, and *in natura* conditions

The stability of bioinsecticide formulations, especially those that are entomopathogenic fungus-based, are dependent on several abiotic factors including temperature, water activity and formulation carrier type.[277, 285-287] Using a proprietary kaolin clay-starch-calcium carbonate as carrier, we investigated the stability, as measured by time course conidial viability, of *B. bassiana*

conidial formulations at different abiotic regimes including long-term cold storage, *in planta* bioassay and/or *in natura* conditions (Figure 7.1).

The viable conidial titer did not significantly change across an eight-week storage at 4 °C for BioCeres, a commercially available mycoinsecticide containing *B. bassiana* strain ANT-03, maintaining a culturable conidial yield of 1.0×10^{10} CFU/g (Figure 7.1A). Furthermore, testing a 12 month-old batch of BioCeres stored at 4 °C resulted in a stable conidial titer of 1.0×10^{10} CFU/g. These results support the commercial claim of a minimum *B. bassiana* ANT-03 conidial concentration of 1.0×10^{10} CFU/g, the viable titer in BioCeres for 18 months (Anatis BioProtection, Inc). The in-house *B. bassiana* strains formulations containing UAMH 299, UAMH 4510 and 11.025, albeit started at a much lower titer than BioCeres ($\sim 1.0 \times 10^{7}$ CFU/g) also supported conidial formulation stability of at least eight weeks under storage at 4 °C (Figure 7.1A). Formulation UAMH 299 maintained a significantly stable titer without a noticeable decline in conidial yield throughout the eight-week time course. On the other hand, a one log and 1.5 log decreased in conidial titer was observed for formulations containing the strain UAMH 4510 and 110.25, respectively (Figure 7.1A). The lower conidial stability of the latter two formulations limited their further development for *in planta* and *in natura* insect bioassays. This limitation is further exacerbated by their lower fermentation yield capacity (conidia per CDAYE media plate) as well as higher dose requirement to elicit a comparable lethal time to kill MPB *in vivo*.[288] The subsequent stages of beetle infection assays were then focused on strains UAMH 299 and UAMH 1076 and the commercially available product containing strain ANT-03 (i.e. BioCeres).

The high conidial effective dose and long-term viability requirement for conidia powder development for *in planta* and *in natura* bioassays prompted us to explore a biphasic liquid-solid fermentation effort. Using a combined CDBYE medium and parboiled rice substrate, the conidial

yield increased significantly by 100-fold for *B. bassiana* UAMH 1076 and 10-fold for *B. bassiana* UAMH 299 (Figure 7.1B). The higher surface area of the individual rice grain provided better aeration during fermentation resulting in higher mycelial yield.[289] A higher mycelial biomass further leads to higher surface area for aerial conidiospore development and conidial yield.[289-290]
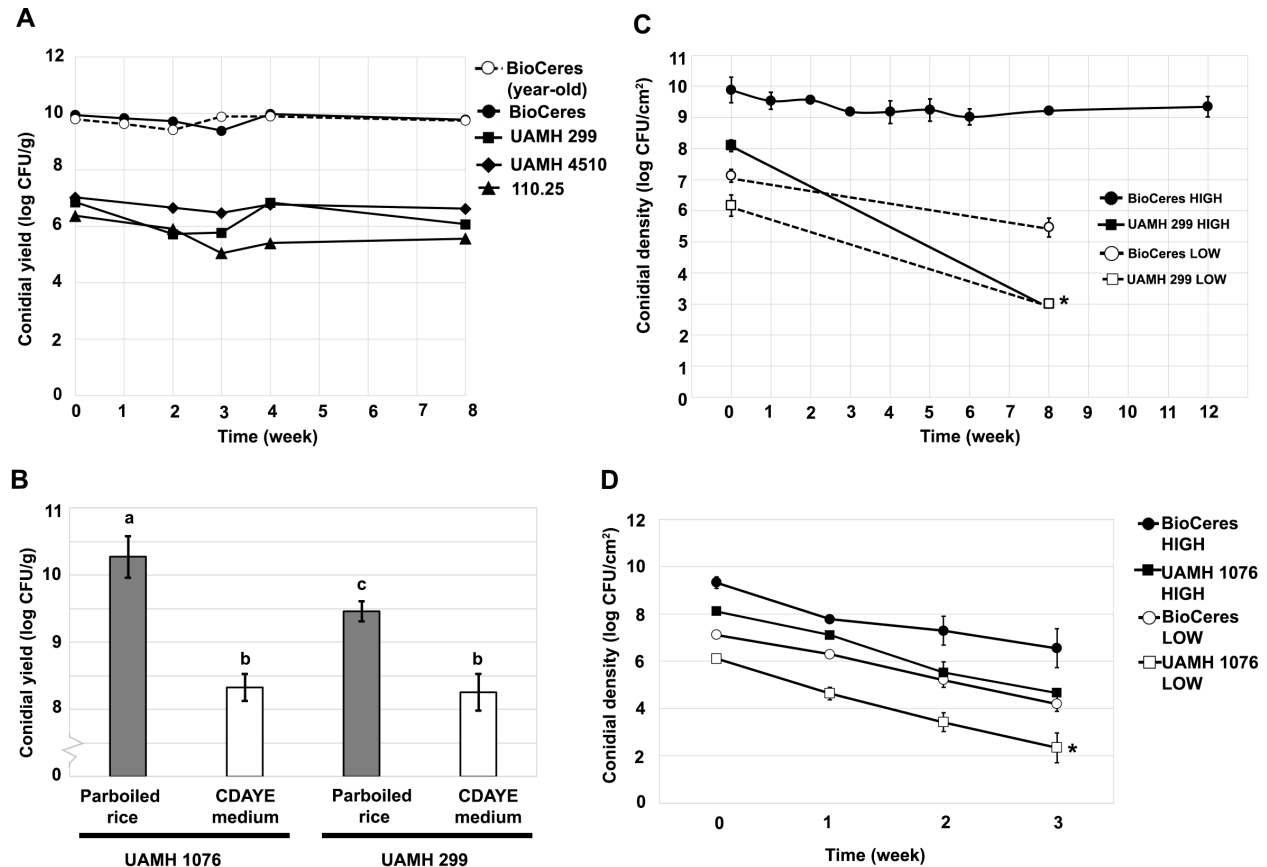
Figure 7.1. *Beauveria bassiana* **conidia production and viability under** *in vitro*, *in planta* **and** *in natura* **conditions.** *In vitro* stability of *B. bassiana* conidial powder formulations under storage at 4 °C for eight weeks. Viable conidial yield (log CFU/g) of commercially formulated BioCeres and three in-house CDAYE media-grown formulations containing conidia from strains UAMH 299, UAMH 4510, or 110.25. A year-old BioCeres formulation was tested in parallel with the new batch conidial products (A). Comparative conidial yield (log CFU/g) between *B. bassiana* strains UAMH 1076 and UAMH 299 grown under CDAYE media or parboiled rice substrate. Vertical bars showed the mean conidial yield while error bars represent the standard deviation of nine biological experiments. The letters show the results of post hoc Tukey's HSD pairwise comparisons among the treatments. Means with different letters indicate a significant difference at α = 0.05 (B). *In planta* viability of conidial powder formulations (BioCeres and UAMH 299)

applied on the bark of *Pinus contorta* bolts incubated under greenhouse condition at 25 °C for 12 weeks (C). *In planta* and *in natura* viability of conidial powder formulations (BioCeres and UAMH 1076) applied on the bark of *P. contorta* bolts incubated under field condition (farmed acreage) for three weeks. Asterisk (*) indicates fungal estimate below culturable limit of detection (D). Starting conidial titer (CFU/cm^2): BioCeres High – 1.0×10^9; BioCeres Low – 1.0×10^7; UAMH 299 High - 1.0×10^8; UAMH 299 Low - 1.0×10^6; UAMH 1076 High - 1.0×10^8; and UAMH 1076 Low - 1.0×10^6.

The result of the mycoinsecticide stability was further tested under an *in natura* conditions using an understory of a forest patch in a private acreage land in Sherwood Park, AB, Canada. The stability of BioCeres under greenhouse conditions prompted us to continuously test BioCeres performance in the field. On the other hand, the instability of UAMH 299 formulation (Figure 7.1C) prompted us to substitute UAMH 299 with a similar class I *B. bassiana*, UAMH 1076, especially since the conidial fermentation yield reached a comparable titer with BioCeres (Figure 7.1B). Furthermore, strain UAMH 1076 was also shown to have a comparable UV light resistance to UAMH 299.[288] An average of 10-fold reduction per week was observed for all formulations applied on the surface of the pine tree bolts (Figure 7.1D), suggesting that the fluctuating abiotic factors affected the treatments similarly. The rate of decline of the conidial viability was homogenously observed across all four treatments, with the high titer BioCeres treatment declining to 1×10^7 CFU/cm^2. This treatment also visually showed the residual powder formulation applied on the pine tree bolts. Conversely, the three other treatments, low BioCeres, high UAMH 1076 and low UAMH 1076, declined to less than 1.0×10^5 CFU/cm^2 after three weeks with no detectable powder observed. This suggest a maximum of one week field stability of the formulations to maintain a conidial concentration that is effective against MPB mortality.[285-288] This time-dependent dosage stability will affect the time constraint for effective MPB infection, as MPB mass flight happens in stages.[93] A situation where a constant exposure to high viable field *B.*

bassiana formulation must be ensured to provide maximum contact with stages of MPB emergence from the infected pine tree stands. Although no competing secondary autochthonous fungal colonization was visually observed on the bolts, the viability results may be negatively-compounded by the dynamic fluctuations in abiotic factors (e.g. precipitations, temperature, UV-index) during the testing period. These factors could potentially limit the formulation stability and conidial survival under the tested *in natura* conditions.[252, 277]

7.2.2. Virulence Evaluation of *B. bassiana* Formulations Against *D. ponderosae* Under *In Planta* Bioassays

The mean lethal time showed a conidial concentration-dependent effect for the BioCeres treatments, similar to the *in vitro* bioassay challenge using the pure conidia of *B. bassiana* ANT-03.[288] The fastest killing time was estimated at three days for both the high (T1) and low (T2) BioCeres treatments, although the lower dose treatment (T2) had greater variations (Figure 7.2A). The corresponding BioCeres *B. bassiana*-specific mycosis was also corroborated by the treatment dosage, with a 98% and 80% mycosis rate, for the high and low conidial treatments, respectively. The classical Koch's postulate of microbial infection was well supported in the above mycosis as the active *B. bassiana* ANT-03 was re-isolated from the mycosed MPB (Figure 7.3A). Furthermore, the dosages in the *in planta* treatments (1×10^9 and 1×10^7 CFU/cm^2) resulted in comparable mean lethal time with the *in vitro* direct application of conidia on the MPB integument.[256, 288, 291]
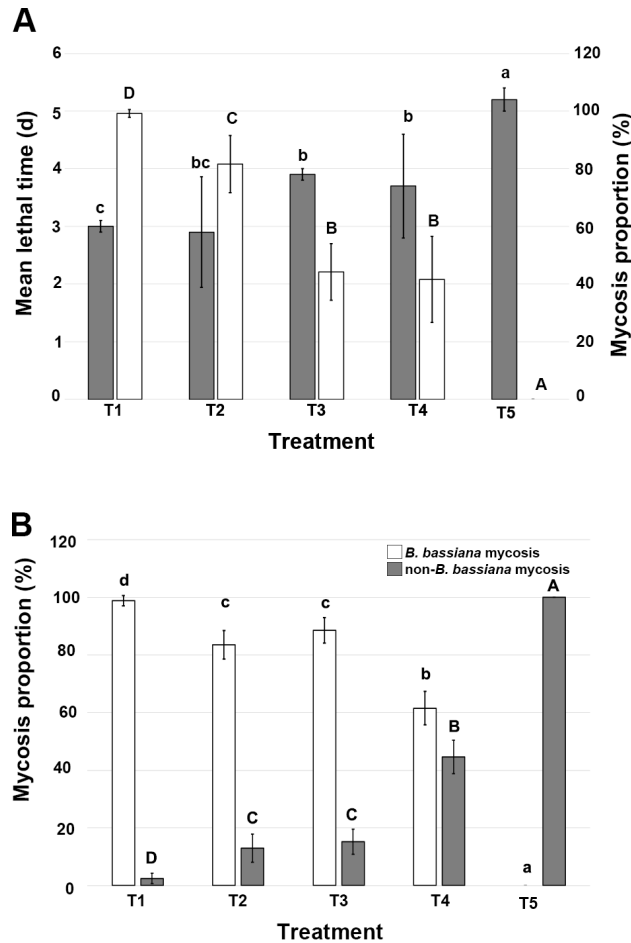
Figure 7.2. Mean lethal time and mycosis proportion of *B. bassiana* UAMH 299 and BioCeres formulation treated *P. contorta* bolts under greenhouse conditions. Mean lethal time (days, gray bars) and corresponding proportion of mycosed *B. bassiana* (%, white bars) MPB emerging the pine bolt and collected from the glass traps container (A). Mycosis proportion resulting from *B. bassiana* and non-*B. bassiana* mycosis from MPB that emerged from the pine bolt but remained in trapped in the plastic bins (B). *Pinus contorta* bolts containing developing MPB population were sprayed with *B. bassiana* powder formulations. Commercial BioCeres formulation containing *B. bassiana* ANT-03 was applied on the bark at either 1.0×10^9 CFU/cm^2 (T1) or 1.0×10^7 CFU/cm^2 (T2). In-house powder formulation containing *B. bassiana* UAMH 299 was applied on the bark at either 1.0×10^8 CFU/cm^2 (T3) or 1.0×10^6 CFU/cm^2 (T4). Control group was not treated with any formulation (T5). Live emerged MPBs were aseptically collected daily from the cages and transferred in Petri dishes lined with moistened filter paper. Each treatment was stored in a separate container at 25 °C and 70% humidity. MPB mortality was recorded daily while dead individuals were aseptically transferred to a 96-well titer plate containing CDAYE with 150 μg/mL chloramphenicol to assess for *B. bassiana*-specific mycosis proportion. Vertical bars showed the mean lethal time values while error bars represent the standard deviation of three biological experiments. The letters show the results of post hoc Tukey's HSD pairwise comparisons among the treatments. Means with different letters indicate a significant difference at α = 0.05. The lowercase letters show the differences among the gray bars, and the capital letters show the differences among the white bars.

112

On the other hand, MPB mean lethal time was extended by one day (i.e. 4 d), upon treatment with *B. bassiana* UAMH 299 formulation regardless of the conidial density although higher variation was observed in the lower dose treatments (Figure 7.2A). Both conidial treatments, 1×10^8 (T3) and 1×10^6 CFU/cm^2 (T4), also resulted in approximately 40% mycosed MPB population. The lower *B. bassiana* mycosis rate observed in the UAMH 299 formulation could be ascribed from a declining viable conidial titer as revealed by the time course culturable bioassays under *in planta* and *in natura* conditions (Figure 7.1C, 1D). A forest field application scenario is proposed where the contact-dependent successful infection will require long-term (e.g. three weeks) conidial-stability of the formulations to deliver a continuous effective dose.[285-287]
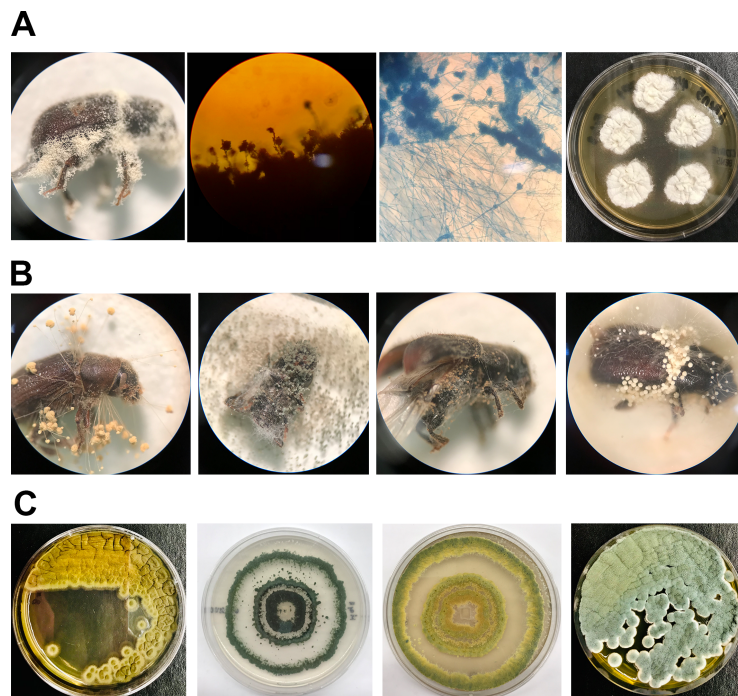
Figure 7.3. Mycosis of mountain pine beetle (MPB) resulting from the application of *B. bassiana* powder formulation on *P. contorta* bolts incubated under greenhouse storage conditions. (A) (L-R) *B. bassiana* mycosed MPB, clusters of conidiospores on the insect surface, lactophenol-blue stained of isolated *B. bassiana* mycelium and conidiospores, and re-isolated *B. bassisana* from the mycosed MPB grown on CDAYE medium. (B) Non-*B. bassiana* mycosed MPB showing four morphologically and visually different fungal conidiophores. (C) Selected axenic fungi isolated from non-*B. bassiana* mycosed MPB.

B. bassiana-specific mycosis were not detected in the control treatments (Figure 7.2A) although several autochthonous fungal species developed on the MPB during the *in vitro* CDAYE-titer plate incubation (Figure 7.3B). These autochthonous fungal species were not detected in any of the BioCeres-treated MPB (Figure 7.3B), potentially suggesting a competitive advantage of *B. bassiana* in altering the insect mycobiome. This microbiome alteration for competitive microbial growth was shown in the oosporein-producing *B. bassiana* phenotypes,[292-293] which may elude to the potential mycological competitiveness of the strains reported here.

The lethal time and MPB mycosis proportions may potentially be limited by the greenhouse cage set-up (i.e. bins) as well as the light-dependent daily harvesting method for the emerged MPB population.[294-295] Although such procedural limitation may affect the *in planta* greenhouse bioassays, the bolt-emerged but cage-trapped MPB population also revealed a similarly high infection rate resulting in *B. bassiana* mycosis (Figure 7.2B). Furthermore, the mycosis proportion followed a concentration-dependent and strain-dependent success rate, as previously reported.[288] BioCeres treatment's T1 and T2 provided ~100% and 85% *B. bassiana* mycosis, respectively. On the other hand, UAMH 299 treatment's T3 and T4 resulted in 90% and 60% mycosis rate, respectively. The untreated control did not show *B. bassiana* mycosis (Figure 7.2B) but other fungal species were detected, presumably part of the autochthonous fungal flora of MPB (Figure 7.3B, 7.3C), similar to the core mycobiome of related Scolytinae bark beetles,[296] including MPB.[100]

Variations in emerging population of MPB contributed to the variable level of success of the *in planta* greenhouse experiments. The two sources of emerging MPB, naturally infested and laboratory infested bolts, provided contrasting beetle emergence numbers; bark surface fungal status; parental, larval and pupal galleries; and the residual culturable *B. bassiana* from the applied

powder formulations (Table 7.1). In general, the laboratory infested bolts provided consistently robust emerging MPB population (100%) unlike the naturally infested bolts (73%). Approximately 27% of the naturally infested bolts (three of 11) did not successfully produce any F1 MPB generation. This was evident in the absence of emerged MPB as measured by the entrapment in the lighted glass traps, the holding sealed bins and upon debarking of the bolts after the 55 d treatment post application. Visible MPB frass was not detected although alternative frass formation from other unknown bark beetles were sporadically evident. The absence of F1 MPB offspring could be explained by the evident interruption of the parental MPB in creating parental galleries leading to the absence of the perpendicular larval galleries and subsequent pupal chambers. Furthermore, evidence of parental MPB gallery interruption was associated with either entrapment of the beetle in the pine resin or a fungal attack from non-*B. bassiana* fungal species.

Interestingly, the residual *B. bassiana* powder titer after 55 d of incubation in the greenhouse varied as a function of strain type and conidial concentration (Table 7.1, Figure 7.1). The high BioCeres treatment (T1) consistently supported high residual but viable and culturable conidia while the low BioCeres (T2) revealed a lower and ineffective conidial titer after two months of incubation in the greenhouse. Conversely, the high and low UAMH 299 formulations (T3 and T4) afforded an undetectable culturable *B. bassiana* titer which can possibly be masked by the autochthonous fungal community on the bark of the bolts. This suggests that the conidial viability, under the current application regimen, will provide an effective dosage to elicit killing effect if time-dependent application will ideally coincide with the emergence of MPB for maximum conidial contact.[285-287] A scenario where a single application of the *B. bassiana* powder formulation will coincide within the week (e.g 7-10 d) of massive MPB emergence event is recommended. Alternatively, a bi-monthly (every other week) application of the powder

formulation may be considered, especially if *in natura* conditions revealed a one log reduction in culturable conidial titer every week (Figure 7.1D).

Table 7.1. Status of debarked *Pinus contorta* bolts treated with *B. bassiana* dry formulations (T1, T2 = BioCeres) (T3, T4 = UAMH 299) under greenhouse incubation for 55 days. R indicate replications.

Treatment Code	*Pinus contorta* bolt MPB infection status	*Beauveria bassiana* conidia titer (CFU/cm^2)	MPB Presence			Fungal Status of the Bolt Outer Bark		Bolt and Gallery Fungal Status	Gallery MPB Status	Remarks
			Bins	Glass Trap	Debarked Bolt	*B. bassiana*	Other Fungi			
T1 R1	Naturally infested	1.0×10^9	Not detected	Not detected	Not detected	High	Minimal	Bark excellent, sapwood good, non-moldy	Parental galleries interrupted	Frass from non-MPB community
T1 R2	Naturally infested	1.0×10^9	Present	Present	Present	High	Minimal	White moldy galleries	Successful gallery development, many pupal chambers	MPB frass
T1 R3	Laboratory infested	1.0×10^9	Present	Present	Present	High	Average	White moldy galleries, Green moldy galleries	Successful gallery development, many pupal chambers	MPB frass
T2 R1	Naturally infested	1.0×10^7	Present	Present	Present	Average	Average	Moldy, variable moisture	Successful gallery development, many pupal chambers	MPB frass
T2 R2	Laboratory infested	1.0×10^7	Present	Present	Present	Average	Average	White moldy galleries	Successful gallery development, many pupal chambers	MPB frass
T2 R3	Laboratory infested	1.0×10^7	Present	Present	Present	Average	Average	White moldy galleries, Green moldy galleries	Successful gallery development, many pupal chambers	MPB frass

T3 R1	Laboratory infested	1.0×10^8	Present	Present	Present	Below limit of detection	High	Moldy, decaying bolt and white moldy galleries	Successful gallery development, many pupal chambers	MPB frass
T3 R2	Naturally infested	1.0×10^8	Not detected	Not detected	Not detected	Below limit of detection	Minimal	Bark excellent, sapwood good, non-moldy	Parental galleries interrupted	Frass from non-MPB community
T3 R3	Naturally infested	1.0×10^8	Present	Present	Present	Below limit of detection	High	Moldy, decaying bolt and white moldy galleries	Successful gallery development, many pupal chambers	MPB frass
T3 R4	Naturally infested	1.0×10^8	Present	Present	Present	Below limit of detection	High	Moldy and dried bolt	Successful gallery development, many pupal chambers	MPB frass
T4 R1	Laboratory infested	1.0×10^6	Present	Present	Present	Below limit of detection	High	Moldy, decaying bolt and white moldy galleries	Successful gallery development, many pupal chambers	MPB frass
T4 R2	Naturally infested	1.0×10^6	Present	Present	Present	Below limit of detection	High	Moldy and dried bolt	Successful gallery development, many pupal chambers	MPB frass
T4 R3	Naturally infested	1.0×10^6	Present	Present	Present	Below limit of detection	High	Moldy, variable moisture	Successful gallery development, many pupal chambers	MPB frass
T4 R4	Naturally infested	1.0×10^6	Not detected	Not detected	Not detected	Below limit of detection	High	Moldy and dried bolt	No galleries detected	MPB stuck in the resin
T5 R1	Naturally infested	0	Present	Present	Present	Below limit of detection	Average	Moldy and dried bolt	Successful gallery development, many pupal chambers	MPB frass
T5 R2	Laboratory infested	0	Present	Present	Present	Below limit of detection	High	Moldy, decaying bolt and white moldy galleries	Successful gallery development, many pupal chambers	MPB frass
T5 R3	Naturally infested	0	Present	Present	Present	Below limit of detection	High	Moldy, decaying bolt and white moldy galleries	Successful gallery development, many pupal chambers	MPB frass

7.2.3. Field Evaluation of BioCeres Against *D. ponderosae* Under *In Planta* Bioassay and *In Natura* Conditions

To assess the efficacy of BioCeres formulation in reducing the reproductive success of MPB infection, maternal and larval gallery traits were assessed. The mean MPB parental gallery length and mean MPB larvae per gallery were significantly higher in the control enclosures compared to those in the treated enclosures (Figure 7.4). Successful MPB reproductive cycle is often indicated by an extensive network of several vertical parental galleries tunneled by female MPB into which perpendicular larval galleries are created for laying eggs (Figure 7.4A). The larval gallery networks further expand as newly hatched larvae eat further into the pine tree phloem (Figure 7.4B). BioCeres treatment, regardless of concentration, resulted in a significant reduction of gallery length and abolition of an extensive larval gallery network (Figure 7.C). Additionally, the high BioCeres dosage treatments (i.e. IH, HH) had a significantly dramatic reproductive reduction effect ($F_{(4,13)} = 9.885$, $P<0.001$). Most of the galleries were less than 5 cm long with zero reproduction (Figure 7D, E). Furthermore, nearly all recovered parental MPB beetles from these galleries were covered in *B. bassiana* mycelia. Interestingly, the low BioCeres dosage treatment resulted in a shorter mean maternal gallery length for the MPB entry experiment (HL) (i.e. 10 ± 4 mm) compared to the MPB exit experiment (IL) (i.e. 20 ± 10 mm). MPB exit and entrance assays were described extensively in the experimental chapter 9.6.8. On the other hand, the type of MPB contact (exit or entry) with a high dose BioCeres treatment did not support a significantly different gallery reduction (HH, IH = 5 ± 1 mm) (Figure 7D). The mean larval density, the second indicator of MPB reproductive success, followed a similar trend as that of the maternal gallery length. The number of larvae per maternal gallery was significantly reduced by all

BioCeres treatments, in a concentration dependent manner ($F_{(4,13)}$ = 8.772, P = 0.0011). The untreated *P. contorta* bolts yielded an average of 48 ± 10 MPB larvae per log while virtually no larvae were detected in the high dose BioCeres treated bolts (i.e. IH, HH). On the other hand, larval yield dropped to 30% and 15%, on the low dose BioCeres treated bolts IL and HL, respectively. The absence of detectable larva in the high dose treatments can be ascribed to the stunted maternal galleries and efficient lethal time resulting in a dead-mycosed maternal MPB. The above data suggests that by utilizing a low BioCeres treatment, the effect seems to be better in reducing the reproductive rate that halted a tunneling MPB into healthy *P. contorta* bolt compared to an exiting MPB from an infested *P. contorta* bolt. A successful reproductive reduction can also be attained using a higher dose BioCeres, regardless of either treating an MPB-infested or protecting a healthy *P. contorta* bolt.

7.2.4. *B. bassiana* Competition with *Grossmania clavigera*

Several bark beetle systems have established symbiotic association with a phylogenetically heterogeneous fungal species collectively called blue stained fungus (BSF).[100, 297] In the MPB system, there are three known associated symbiotic BSF represented by the species *Grosmannia clavigera, Ophiostoma montium*, and *Leptographium longiclavatum*.[298-301] We focused our *in vitro* bioassays on *G. clavigera* as it is the most abundant BSF in the teneral adult stage of MPB, prior to its emergence,[297, 302] and the most invasive BSF pathogen in *P. contorta*.[303]

Two types of interaction responses were determined between the eight strains of *B. bassiana* and the two strains of *G. clavigera* (Figure 7.5). The first interaction included the inhibition of *G. clavigera* strains EL033 and EL035 by the red pigmented strains UAMH 299, UAMH 299[UVR], and UAMH 1076 as well as the yellow pigmented strain 110.25 (Figure 7.5A).
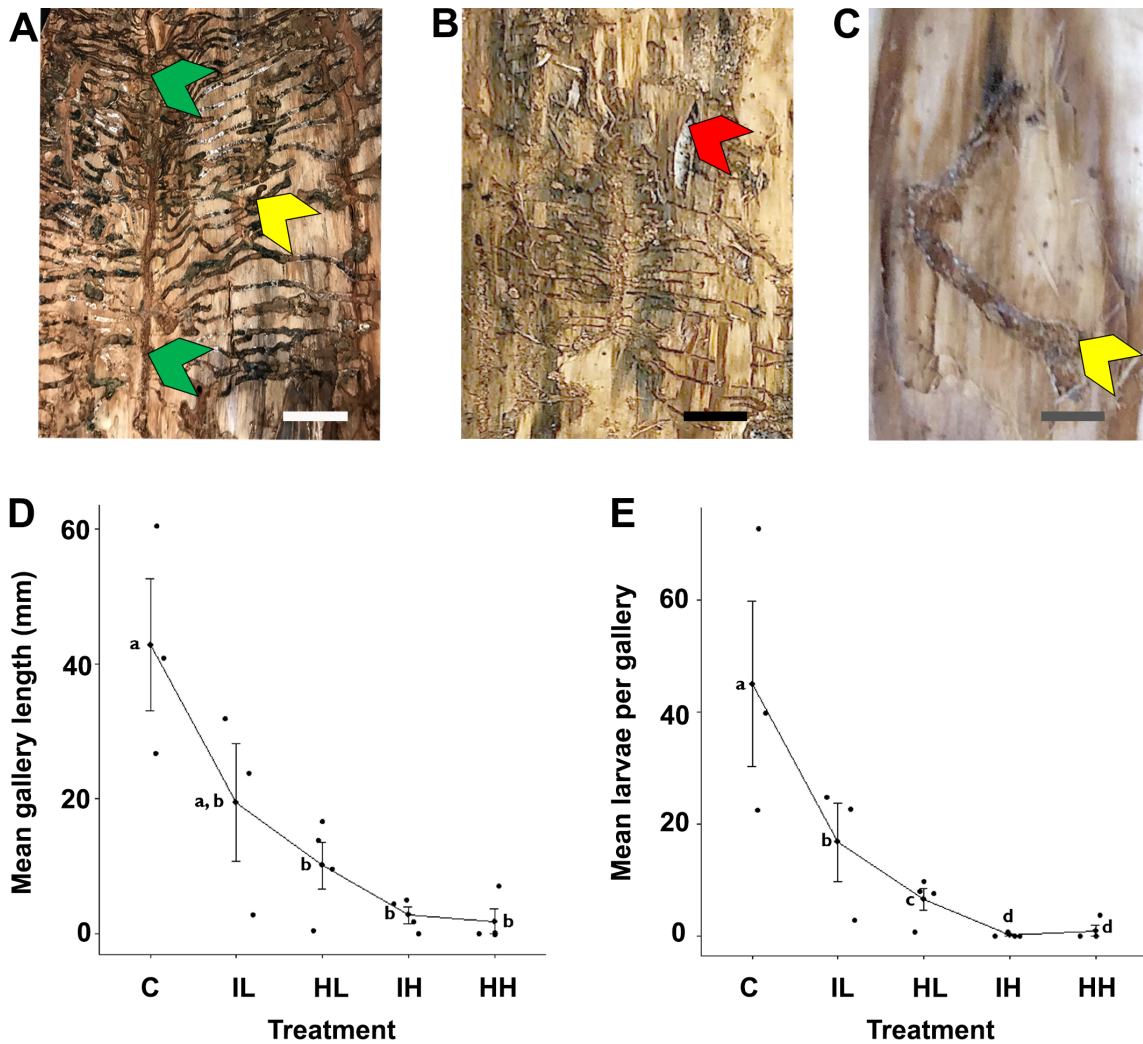
Figure 7.4. MPB reproductive indicators of *P. contorta* with or without treatment of BioCeres formulation. Successfully colonized *P. contorta* by MPB showing extensive network of vertical parental galleries (green arrow) and perpendicular larval galleries (yellow arrow), scale bar = 5 cm (A). Untreated control bolts successfully colonized by MPB showing developing larvae inside chamber (red arrow), scale bar = 5 cm (B). MPB infected bolts treated with high dose BioCeres formulation (IH) baited with healthy *P. contorta* food bolts. Shortened larval gallery (yellow arrow) evident of reduced MPB reproductive success in the baited healthy *P. contorta* bolts, scale bar 1 cm (C). Mean maternal gallery lengths of *P. contorta* bolts (D) and corresponding mean larvae per gallery (E). Treatment codes: C – control, untreated; IL – MPB infected bolt treated with low dose BioCeres, MPB exit inoculation; HL – healthy food bolt treated with low dose BioCeres, MPB entry inoculation; IH - MPB infected bolt treated with high dose BioCeres, MPB exit inoculation; and HH – healthy food bolt treated with high dose BioCeres, MPB entry inoculation. Each point is the mean length of maternal galleries or larvae per gallery observed in a 75 cm debarked log. Dots connected by lines are the treatment mean and SE. Different letters indicate a significant difference at α = 0.05.

Both *B. bassiana* and *G. clavigera* grew radially until a point where the growth stopped without the mycelial fronts touching and therefore forming a clear zone of inhibition (ZOI). Crescent-shaped ZOIs were evident on the high C/N media (e.g. PDA, MEA, SDA) supporting a radially-diffusible compound exuded by *B. bassiana* that prevented the further expansion and colonization of *G. clavigera*. As the high C/N media supported faster growth rate of *G. clavigera* than *B. bassiana*, the inhibition caused by *B. bassiana* strains slowed down the melanization of the *G. clavigera* mycelial front. (Figure 7.5A). On the other hand, when competition assays were performed using a low C/N media (e.g. CDAYE), comparable growth rate was observed between the two fungi, colonizing equal spaces on the agar surface (i.e. 50%). Furthermore, the medium did not induce melanization in *G. clavigera* until the zone of inhibition is formed at the interface of their respective mycelial fronts. Although the ZOI was consistently observed across the red-pigmented *B. bassiana* strains, attributing the inhibitory activity to oosporein is not fully supported yet, as the yellow-pigmented tenellin-producing strain 110.25 also showed significant ZOI. Furthermore, ZOIs were also evident across media conditions that did not support oosporein nor tenellin production.

The second interaction supported positive mycelial contact but non-inhibition of *G. clavigera* strains EL033 and EL035 by the red-pigmented *B. bassiana* strains UAMH 298 and 298[UVR] as well as the non-pigmented strains UAMH 4510 and ANT-03. There were no zones of inhibition detected and the mycelial front contact suggests a co-existing fungal profile, including the overlapping *B. bassiana* ANT-03 mycelia on top of the *G. clavigera* (Figure 7.5B). The contact of the two fungal mycelial fronts suggested that there was no radially-diffusible antagonistic molecules and that the available space occupied by either fungus is related to its innate media-

dependent growth rate alone. Interestingly, similar to the inhibitory *B. bassiana* strains, high C/N medium (e.g. PDA) interaction assay for the non-inhibitory *B. bassiana* also delayed the melanization of the mycelial front of *G. clavigera*.

The mycelial expansion growth rate of *G. clavigera* varied depending on the C/N ratio of the assay media (Figure 7.5C-E). PDA allowed for the fastest agar surface colonization of *G. clavigera* until a ZOI developed on day 4. The expansion rate dropped significantly with the corresponding maintenance of a clear inhibitory region up to 10 d. Conversely, in the absence of inhibition, *G. clavigera* mycelial expansion rate supported an exponential growth curve and plateaued only upon reaching the contact point with the test *B. bassiana* strain (Figure 7.5C). A shift in a low C/N ratio agar assay, CDAYE, revealed an overall similar response curve (Figure 7.5D). In both media assay types, the end of the logarithmic growth rate coincides well with the development of the zones of inhibition, regardless of media composition. This suggests that the *B. bassiana* strain-specific inhibitory potential against *G. clavigera* is not dependent on available nutritional content. Although, it is yet to be established if a similar inhibition will be relevant under *in vivo* and *in planta* conditions such as the phloem and xylem elements of a live *P. contorta* trees colonized by *G. clavigera*. Furthermore, the current phenotypic diversity of *B. bassiana* strains tested should be explored also on *G. clavigera* considering that the strain growth variation (Figure 7.5E) could also affect susceptibility and resistance.[277]
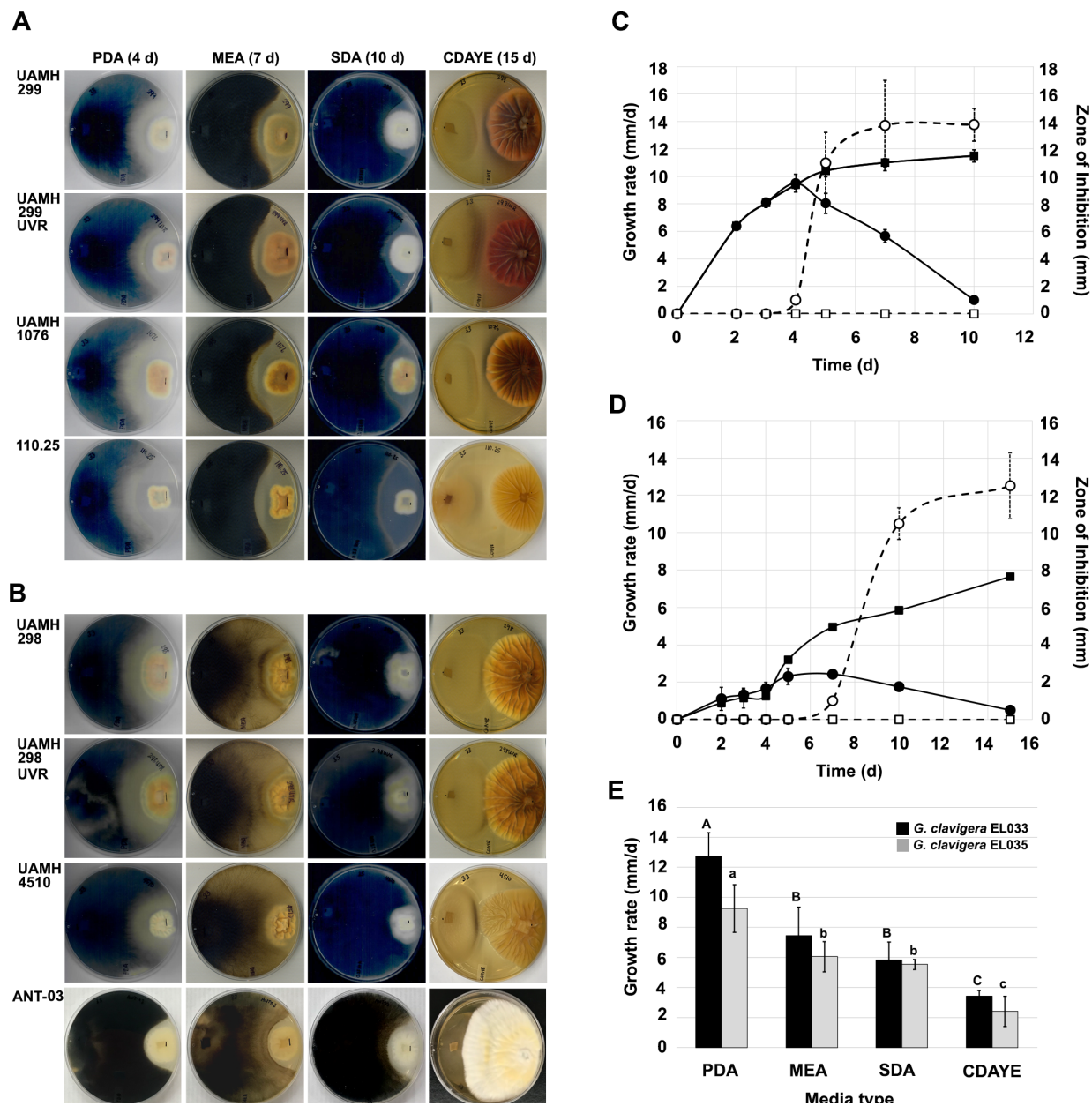
Figure 7.5. *In vitro* **interaction of the MPB symbiotic blue stained fungus,** *Grossmania clavigera* **(left) and the entomopathogenic fungus,** *Beauveria bassiana* **(right).** Inhibition (A) or non-inhibitory (B) mycelial expansion of representative *G. clavigera* strains under high (PDA, MEA, SDA) or low carbon-to-nitrogen ratio (CDAYE) media regimen for the indicated incubation time at 25 °C. Growth rate and zone of inhibition of *G. clavigera* strain EL033 under PDA (C) or CDAYE (D) media regimen in the presence of inhibitory (full circle) and non-inhibitory (full square) *B. bassiana* groups. Zone of inhibition values are indicated by empty circle and square. Comparative growth rate of *G. clavigera* strains EL033 or EL035 in different media regimen in the absence of *B. bassiana* (E). Vertical bars showed the mean growth rate values while error bars represent the standard deviation of three biological experiments. The letters show the results of post hoc Tukey's HSD pairwise comparisons among the treatments. Means with different letters

indicate a significant difference at $\alpha = 0.05$. The capital letters show the differences among the black bars, and the lowercase letters show the differences among the white bars.

On the other hand, the *in vitro* competition assay with *Leptographium abietinum,* a BSF symbiotically associated with the North American spruce beetle–Engelmann spruce system, revealed contrasting results.[277] All reported *B. bassiana* strains were found ineffective in competing nor inhibiting the symbiotic fungus *L. abietinum. In vitro* competition for resources resulted in a significantly better capture rate by *L. abietinum* placing *B. bassiana* at a colonization disadvantage. Furthermore, both fungal mycelial fronts were in contact and no zone of inhibition was formed. Although this is the case, the reported *B. bassiana* strains represent the class II white powdery phenotypes which corroborated our non-inhibitory results in G. *clavigera.*[277] Furthermore, the single assay medium (i.e. MEA) used in the competition assays perhaps may have limited the inferences,[277] as the expansion rate of the competing fungi could be affected by the media type (e.g. C/N ratio).[288] The inhibitory effects of the class I (red-pigmented) and III (yellow-pigmented) *B. bassiana* strains are yet to be established against *L. abietinum* as well as the related species *L. longiclavatum* or the other BSF, *O. montium*, which are both relevant in the MPB system.

7.2.5. Functional Genomics of *B. bassiana* Oosporein BGC

The three arbitrary colored phenotypes correlated well with the secondary metabolite effector molecules and culturing conditions. Group I *B. bassiana* all synthesize the red pigment, often associated with oosporein, albeit at variable intensity. Oosporein is a red dibenzoquinone compound reported to have limited insecticidal activity[293, 304] but can synergistically improve insect mortality when combined with *B. bassiana* conidia.[304] Recently, Fan and co-workers[292]

reported that oosporein virulence potential increases the colonization competitiveness of the fungus by reducing the microbiome of the insect host. The yellow pigments in Group III *B. bassiana* are potentially attributed to either tennellin and/or bassianin.[264] Interestingly, a direct gene knockout revealed that tenellin did not alter virulence towards insect larvae,[305] suggesting that it is not involved directly in killing insect larvae, although it exhibited limited biological activities such as inhibition of equine erythrocyte membrane ATPase activity[306] and iron chelation minimizing intracellular levels of the Fenton Reaction.[278] The entomotoxic properties of these yellow pigments are yet to be established in adult insects[307] including the MPB host. Lastly, the Group II phenotypes (white), although they did not produce any pigment in our culturing approach, provided the most conidia in any media (~5 - 10-fold more).[288]

The three phenotypic classes, as defined by pigmentation induced in low C/N ratio agar medium (Figure 7.6A),[288] may determine the inhibitory function of *B. bassiana* against the blue stained fungus. Whole genome sequencing of the eight *B. bassiana* strains revealed a clear phylogenetic divergence of the group into two distinct clades (Figure 7.6B). The red pigmented strains clustered together with high bootstrap support while the yellow pigmented and white powdery strains strain created a separate clade with a similarly high bootstrap value. Interestingly, the red pigmented clade clustered with a different species, *B. pseudobassiana* KACC 47484, the only sequenced genome available to date. On the other hand, the non-red pigmented strains, strongly co-localized with the type strain *B. bassiana* ARSEF 2860, while the third species *B. brongiartii* RCEF 3172 was separately and distantly related. Furthermore, the only closed whole genome of *B. bassiana* HN6, represented in 12 complete closed chromosomes, corroborated the phylogenetic placement of the non-red-pigmented *B. bassiana* and supported the proposed reclassification of the red-pigmented clade to *B. pseudobassiana*. The inclusion of the

teleomorphic sexual state of the genus *Beauveria*, *Cordyceps militaris* ATCC 34164, acted as the evolutionary outgroup of the phylogenetic tree, resulting as a distant branch from the analyzed phylogram.

The red pigmented strain observed in class I *B. bassiana* (heterotrophic synonym proposed as *B. pseudobassiana*) was associated with the dibenzoquinone molecule, oosporein.[292-293] Probing the genetic organization of the eight sequenced genomes revealed a highly conserved *opS* gene cluster (Figure 7.6C) with strong synteny regardless of the variable pigmented phenotype response in CDAYE medium (Figure 7.6A). The conserved seven-gene member *opS* operon included the catalytic polyketide synthase (*opS1*); a putative MFS multi drug resistance transporter (*opS2*); a GAL-4-like Zn2Cys6 transcription factor (*opS3*); an FAD binding domain-containing hydroxylase (*opS4*); a laccase-multicopper oxidase (*opS5*); a glutathione-*S*-transferase (*opS6*); and lastly a cupin 2 superfamily protein (*opS7*). A *de novo*, unbiased, and un-annotated genome cluster mining approach further revealed the conservation of several genes upstream of the *opS* biosynthetic operon which may provide insights into the phenotypic pigment variability observed in the eight *B. bassiana* strains. A conserved hydantoinase B/oxoprolinase, corA family metal ion transporter and a heat-labile enterotoxin IIB gene were shared across all sequenced *B. bassiana* genomes. Interestingly, the D-lactonohydrolase gene was found only in the yellow-pigmented *B. bassiana* strain 110.25. Furthermore, the white powdery strain, UAMH 4510, did not encode the heat-labile enterotoxin IIB and a hypothetical gene shared only amongst the red-pigmented strains. Similarly, the white strain ANT-03 had a gene insertion event found in-between the polyketide synthase and the MFS transporter genes *opS1-opS2* intron junction. The contribution of these anomalous gene deletion or insertion events towards the biosynthesis of the red pigment, oosporein, is yet to be determined either by mutagenesis or functional complementation analysis approaches.

The genetic composition and arrangement of the biosynthetic gene cluster responsible for the production of oosporein, tenellin and bassianin in *B. bassiana* has been elucidated,[293, 305, 308-309] although the same gene organization is yet to be elucidated in other fungal genera capable of producing the same effector pigmented molecules.[310-312] Furthermore, the strain-dependent pigment production and the relative differences in biosynthesis abundance level observed in *B. bassiana* could be attributed to several unknown mechanisms, acting either at the nutritional and culture conditions and/or combinations of genetic factors working at the complex interface of transcriptional, post-transcriptional or post-translational controls.[313] Whole genome sequencing and transcriptomics coupled with metabolomics approaches may shed light and research directions in elucidating these complex levels of controls. From an economic standpoint, our culturing condition that screens the strains can be considered an excellent criterion as it will minimize fermentation resources and time, and yet deliver a high titer of virulent strains for biocontrol agent product development and field application.

7.2.6. Functional Genomics of *B. bassiana* BGCs

The secondary bioactive metabolic profile encoded on the eight *B. bassiana* genomes revealed an arsenal of known and unknown biomolecules. The three major biosynthetic gene cluster types detected include polyketide synthases (PKS), non-ribosomal peptide synthetases (NRPS) and terpenoids (Table 7.2, Figure 7.7). On the other hand, a few hybrid BGC clusters are limited to NRPS-PKS clusters.

The oosporein BGC, a polyketide gene cluster, was detected across all sequenced *B. bassiana* genomes with cluster homology ranging from 71 to 85%. The gene variation, attributed to as much as 30%, was associated with the upstream genes which are not yet functionally linked

A

CDAYE valve view

| Upright | Underside |

UAMH 298
UAMH 298^UVR
UAMH 299
UAMH 299^UVR

CDAYE valve view

| Upright | Underside |

UAMH 1076
ANT-03
UAMH 4510
110.25

B

- *B. pseudobassiana* UAMH 298 — 99
- *B. pseudobassiana* UAMH 298^UVR — 100
- *B. pseudobassiana* UAMH 299 — 97 / 33
- *B. pseudobassiana* UAMH 299^UVR
- *B. pseudobassiana* UAMH 1076
- *B. pseudobassiana* KACC 47484 (LUDX00000000) — 100

B. pseudobassiana cluster

- *B. bassiana* HN6 (CP045877-CP045888) — 65
- *B. bassiana* ANT-03 — 100
- *B. bassiana* 110.25
- *B. bassiana* ARSEF 2860 (ADAH00000000) — 90
- *B. bassiana* UAMH 4510 — 100

B. bassiana cluster

- *B. brongniartii* RCEF 3172(AZHA00000000) — 86

C. militaris ATCC 34164 (CP023322-CP023328)

0.01

C

fungiSMASH BGC prediction; MIBiG BGC prediction

Proposed oosporein BGC (*opS1-opS7*)

BGC Legend

- Heat-labile enterotoxin IIB
- Hypothetical protein
- D-lactonohydrolase
- CorA family metal ion transporter
- Hydantoinase B/Oxoprolinase
- *opS1*, Polyketide synthase
- *opS2*, MFS multidrug resistance transporter, putative
- *opS3*, GAL4-like Zn2Cys6 fungal transcription factor
- *opS4*, FAD binding domain-containing hydroxylase
- *opS5*, Laccase 2/Multicopper oxidase
- *opS6*, Glutathione-S-transferase
- *opS7*, Cupin 2 superfamily protein
- Hypothetical protein

ARSEF 2860
UAMH 298
UAMH 298^UVR
UAMH 299
UAMH 299^UVR
UAMH 1076
UAMH 4510
ANT-03
110.25

128

D

Figure 7.6. Functional genomics of sequenced draft genomes of eight *Beauveria bassiana* strains and the oosporein biosynthetic gene cluster. (A) Phenotypic characteristics of eight *B. bassiana* strains grown on CDAYE medium showing surface mycelial-conidiation (upright valve view) and pigmentation (underside valve view). Variable degrees of oosporein (red) pigmentation intensity in class I *B. bassiana* strains UAMH 298, UAMH 298[UVR], UAMH 299, UAMH 299[UVR], and UAMH 1076. Undetectable pigmentation in class II *B. bassiana* strains ANT-03 and UAMH 4510 and yellow pigmentation in class III *B. bassiana* 110.25. (B) Phylogenetic relationship of the eight sequenced *B. bassiana* genomes supporting two distinct clusters, the red pigmented *B. pseudobassiana* and non-red pigmented *B. bassiana*. The neighbourhood-joining tree was estimated using the genomic distances between assemblies under 100 bootstrapping replicates. *Cordyceps militaris* ATCC 34164 was used as the outgroup. (C) The oosporein biosynthetic gene cluster (BGC) organization in the eight *B. bassiana* sequenced draft genomes. The core biosynthetic gene cluster, *ops1–ops7*, was predicted by MIBiG database using the reference type strain *B. bassiana* ARSEF 2860 while the putative upstream genes were predicted using fungiSMASH database. (D). Targeted metabolomics of oosporein using LC-MS. Oosporein was detected from the ethyl acetate extracts of class I *B. bassiana* strains while undetectable from class II and III *B. bassiana* strains. The limit of detection has a range of 100 – 10,000 ng/mL.

biosynthetically with the validated BGC in the reference species, *B. bassiana* ARSEF 2860 (Figure 7.6C). A similar red pigment, bikaverin, was also detected at 57% gene cluster homology. Interestingly, the PKS cluster is only restricted in the five red-pigmented class I *B. bassiana* which may potentially contribute also to the phenotypic separation from class II and III *B. bassiana* strains.[187] Four other known biosynthetic gene clusters encoding the production of the following fungal metabolites, dimethylcoprogen, beauvericin, clavaric acid and squalestatin S1, were detected in all eight sequenced genomes including the reference strain *B. bassiana* ARSEF 2860 (Table 7.2, Figure 7.7). The homologous BGC for emericellamide A biosynthesis was detected

across all five red-pigmented class I *B. bassiana* (60%) and non-red pigmented class II/III (40%), except UAMH 4510.

Strain-specific BGCs were also predicted in the eight sequenced *B. bassiana* draft genomes showing at least 40% homology with the core biosynthetic gene(s). This includes the desmethylbassianin in UAMH 299 and its UV resistant line, UAMH 299[UVR]; the antifungal ilicicolin H encoded in strains UAMH 1076 and ANT-03; pyranonigrin E and fumosorinone BGCs detected in the genomes of strains UAMH 298 and UAMH 298[UVR]; and lastly, the iron chelator, tenellin, a homologous BGC encoded only in strain 110.25 (Table 7.2, Figure 7.7) Other low homology BGCs (<40%) were represented by secalonic acid, trichodiene-11-one, bassianolide, and nivalenol, although the cluster gene comparison maybe limited to accessory biosynthesis genes (e.g. transport, modifying, transcriptional regulator).

Table 7.2. Bioinformatic predictions of known secondary metabolite biosynthetic gene clusters (BGCs) from the draft genome sequences of eight *B. bassiana* strains and the phylogenetically closest strain *B. bassiana* ARSEF 2860.

Biosynthetic Gene Cluster (BGC)	BGC Type	BGC Percentage Homology in *Beauveria bassiana* strains								
		ARSEF 2860	UAMH 299	UAMH 299[UVR]	UAMH 298	UAMH 298[UVR]	UAMH 1076	UAMH 4510	ANT-03	110.25
Oosporein	PKS	100	78	78	78	71	85	78	78	85
Beauvericin	NRPS	90	80	90	80	90	90	80	80	80
Clavaric Acid	Terpene	100	100	100	100	100	100	100	100	100
Dimethylcropogen	NRPS	100	100	100	100	100	100	100	100	100
Squalestatin S1	Terpene	40	40	40	40	40	40	40	40	40
Emericellamide A	NRPS	40	60	60	60	60	60	ND	40	40
Bikaverin	PKS	ND	57	57	57	57	57	ND	ND	ND
Desmethyl bassianin	NRPS-PKS	ND	40	40	ND	ND	ND	ND	ND	ND
Trichodiene-11-one	Terpene	18	18	18	ND	ND	ND	ND	ND	27
Secalonic Acid	PKS	ND	18	25	12+31	12+18	12	ND	ND	ND
Ilicicolin H	NRPS-PKS	ND	ND	ND	ND	ND	50	ND	50	ND
Pyranonigrin E	PKS	ND	ND	ND	100	100	ND	ND	ND	ND
Bassianolide	NRPS	60	ND	ND	ND	ND	ND	60	33	40
Tenellin	NRPS-PKS	100	ND	ND	ND	ND	ND	ND	ND	100
Fumosorinone	NRPS-PKS	ND	ND	ND	83	83	ND	ND	ND	ND
Nivalenol	Terpene	ND	ND	ND	12	8	ND	ND	22	ND

ARSEF – Agricultural Research Service Collection of Entomopathogenic Fungal Cultures
UAMH – University of Alberta Microfungus Collection and Herbarium
PKS – Polyketide synthase
NRPS – Non-Ribosomal Peptide Synthetase
UVR – Ultra-Violet light Resistant
ND – Not Detected

(**1**)

(**2**)

(**13**)

(**14**)

(**15**)

(**16**)

(**17**)

(**18**)

(**19**)

(**20**)

(**21**)

(**22**)

(**23**)

(**24**)

(**3**)

(**25**)

132
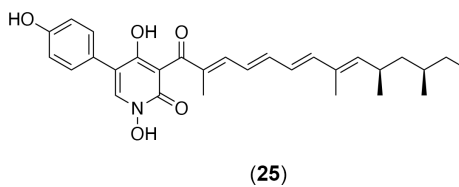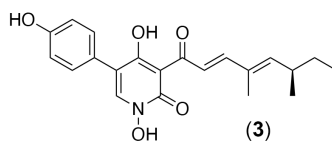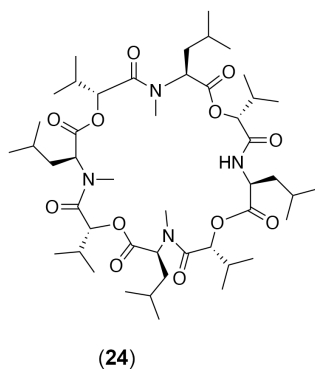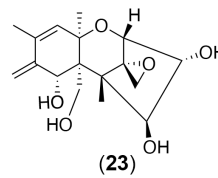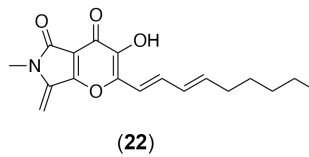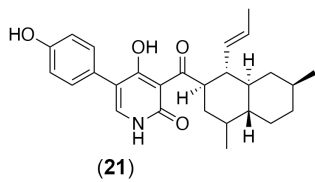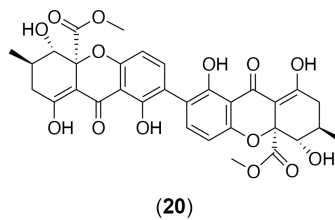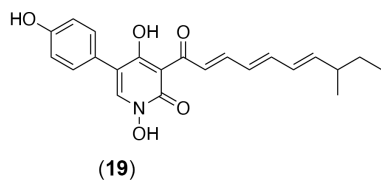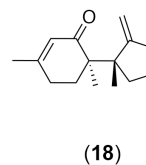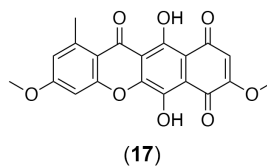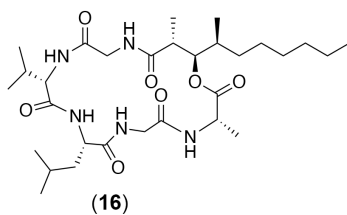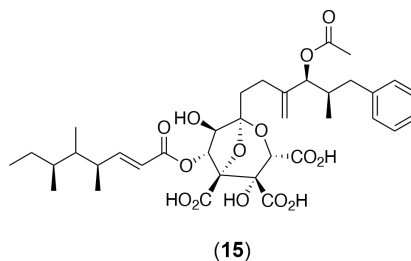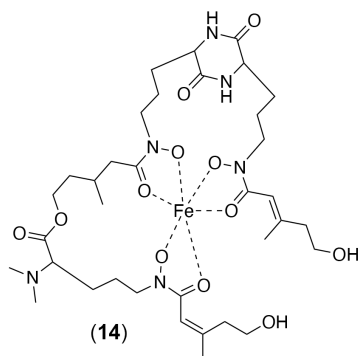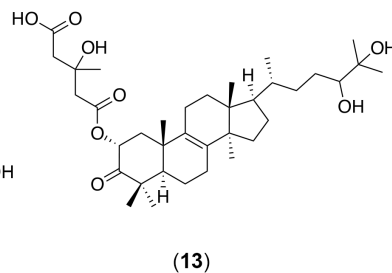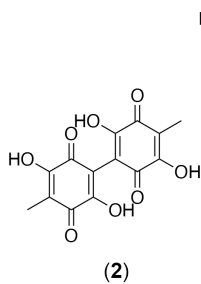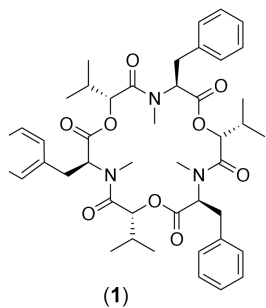
Figure 7.7. Chemical structures of the metabolites predicted from draft genome sequences of the eight *B. bassiana* pan genome. The predicted BGC supports the biosynthesis of the fungal metabolites beauvericin (**1**), oosporein (**2**), clavaric acid (**13**), dimethylcoprogen (**14**), squalestatin S1 (**15**), emericellamide A (**16**), bikaverin (**17**), trichodiene-11-one (**18**), desmethylbassianin (**19**), secalonic acid A (**20**), ilicicolin H (**21**), pyranonigrin E (**22**), nivalenol (**23**), bassianolide (**24**), tenellin (**3**) and fumosorinone (**25**).

7.3. Conclusion and Future Directions

This study provides the first evidence of the efficacy of *B. bassiana* powder formulations to kill MPB under relevant *in planta* bioassays and *in natura* conditions. The stability of the powder formulation, under long term cold storage, on the bark of *P. contorta* under greenhouse condition, and the marginal yet effective treatment dose coupled with critical beetle emergence timing contributed to the successful reduction of the MPB reproductive success in a forest stand.

Genotypic and phenotypic association of virulence and MPB-specific fungal secondary metabolites can be explored with the availability of the high-quality draft genomes of the eight *B. bassiana* strains. Furthermore, the development of genetic engineering tools for the synthetic manipulation of the strains for insect pheromone biosynthesis can be expedited. Antifungal selection and differential medium fungal responses can be tailored with the availability of the genetic blueprint.

On an economic application standpoint, forestry operational effectiveness of the *B. bassiana* formulations, like BioCeres, for large geographical landscape MPB control can be pursued. Likewise, a multi-year comparison, accounting for temporal and spatial variations in MPB mass attacks, can be considered in future experimental designs.

Chapter 8

Summary and Conclusion

This thesis presented the functional genomics of novel bacterial and entomopathogenic fungal species and strains. Whole genome sequencing and infection-challenge models were used in probing the encoded natural products biosynthetic gene clusters (BGCs) of several *Firmicutes* bacteria and the tripartite microbial interaction in mountain pine bark beetle system, respectively. The genomes of extreme environmental bacterial isolates from saline lakes,[123] oil-contaminated soils[124,314] thermophilic-[314] and volcanic soils,[316] and entomopathogenic fungi were sequenced and functional genome associations were established. It also involved the selection and evaluation of *Beauveria bassiana* as a potential mycoinsecticide for the targeted biocontrol of the mountain pine beetle, *Dendroctonus ponderosae*, in both laboratory and field relevant ecosystems.[288]

In the first study, the draft genome sequence of *Bacillus thuringiensis* strain DNG9 was sequenced.[314] *B. thuringiensis* DNG9 was isolated from an oil-contaminated slough in Algeria that showed strong antibacterial, antifungal and biosurfactant properties. The draft genome size was estimated at 6.06 Mbp and encodes several gene inventories for the biosynthesis of bioactive compounds such as zwittermicin A, petrobactin, insecticidal toxins, polyhydroxyalkanoates and multiple bacteriocins. The genome information of strain DNG9 will provide another model system to study pathogenicity against insect pests, plant diseases, and antimicrobial compound mining and comparative phylogenesis among the *B. cereus sensu lato* group.

In the second study, a novel *Bacillus* strain was isolated from Algerian salt lake that exhibits potent activity against Gram-positive and Gram-negative bacteria, as well as fungal pathogens.[124] The 4.02 Mbp draft genome sequence of the strain was established, and genome

sequence analysis identified the strain as *B. velezensis* F11. The functional genomics showed that the strain carries the genes for the production of various bioactive and surface-active compounds. These include the lipopeptides surfactin and fengycin, antibacterial polyketides macrolactin and bacillaene, and a putative novel lanthipeptide. Through an activity-guided purification method using hydrophobic interaction chromatographic techniques (Amberlite XAD-16 resin column chromatography, C_{18} solid phase extraction cartridge, and reverse-phase high-performance liquid chromatography), the strain was confirmed to produce fengycin lipopeptides. The identities of the isolated fengycin homologues were ascertained through tandem mass spectrometry.

In the third study, the draft genome sequences of four *Bacillus* species were established.[123] *Bacillus cereus* E41 and *B. anthracis* F34, were isolated from a saltlake in Aïn M'lila-Oum El Bouaghi, Eastern Algeria, and Ain Baida-Ouargla, Southern Algeria, respectively. Strains E41 and F34 have comparable draft genomes sizes of 5.39 Mbp and 5.84 Mbp, respectively, support genes for the production of several bioactive secondary metabolites, including polyhydroxyalkanoate, iron siderophores, lipopeptides, and bacteriocins. On the other hand, a third strain, *B. paralicheniformis* F47, was isolated from a salty lake in Aïn Baida-Ouargla, Southern Algeria. The 4.03 Mbp draft genome encodes genes for the production of several bioactive secondary metabolites, including the siderophore bacillibactin, the lipopeptides fengycin, surfactin and lichenysin, the antibiotics bacitracin and kanosamine and the bacteriocin, circularin A. Lastly, *B. licheniformis* SMIA-2, a thermophilic and thermostable enzyme-producing bacterium, was found to be active against several strains of *Staphylococcus aureus* and several *Bacillus* species. The 4.30 Mbp draft genome was established and bioinformatic prediction supporting gene inventories for amylase, protease, cellulase, xylanase and antimicrobial compound biosynthesis.

In the fourth study, the antimicrobial activity of actinomycetes isolated from volcanic soil collected from Mount Mayon, Albay, Philippines was reported.[316] A total of 13 out of 30 morphologically distinct actinomycete isolates showed antagonistic activity against test microorganisms. Isolate A1-08, the focus of the study, exhibited a wide spectrum of antimicrobial activity against *Salmonella enterica, Klebsiella pneumoniae, Staphylococcus aureus,* methicillin-resistant *S. aureus* (MRSA)*, Candida albicans, Aspergillus niger,* and *Fusarium* sp. Moreover, A1-08 was found to have anti-methicillin resistant *S. aureus* and anticancer activity against human colorectal cancer (HCT116) cell line. Whole genome sequence-based phylogenetic analysis supported a novel species of *Streptomyces* closely related to *S. olivaceus* NRRL B-3009. A total of 48 biosynthetic gene clusters were predicted in the 8.65 Mbp draft genome sequence that maybe responsible for the biosynthesis of known and potentially novel secondary metabolites.

In the fifth study, nine isolates of *B. bassiana* were examined for insect virulence characteristics, including conidiation rate, pigmentation, and infection rate in laboratory-reared *D. ponderosae*, to assess for their potential as biocontrol agents.[288] The strains were categorized into three phenotypic groups based on pigmentation, conidial density and myceliation rate. Virulence screening utilizing insect-based agar medium revealed no difference in selection of fungal growth. However, infection studies on *D. ponderosae* and *A. mellifera* showed contrasting results. *In-vivo A. mellifera* infection model revealed ~5% mortality, representing the natural death rate of the hive population, whereas laboratory-reared *D. ponderosae* showed 100% mortality and mycosis. The LT_{50} (lethal time 50) ranges from 2-5 $\pm$ 0.33 d and LT_{100} ranges from 4-6 $\pm$ 0.5 d. The selective advantages of the three phenotypic groups in terms of virulence, pigmentation, conidial abundance and tolerance to abiotic factors like UV and host tree monoterpenes were discussed. The results

can further provide insights into the development of several phenotypically diverse *B. bassiana* strains in controlling the spread of the invasive *D. ponderosae* in Western Canada.

In the sixth study, we established the *in vitro*, *in planta* and *in natura* stability of *B. bassiana* formulations, BioCeres and UAMH 299/1076, for assessment of efficacy in killing MPB under greenhouse and field relevant ecosystems. A biphasic fermentation approach, using CDBYE-parboiled rice, was performed to mass produce viable conidial formulations for strains UAMH 299 and 1076. A carrier mixture, kaolin clay-starch-calcium carbonate, was found to be suitable for creating wettable conidial formulations that maintained viable and culturable *B. bassiana* propagules. *In vitro* long-term cold storage (4 °C) stability test supported viable conidial formulations while greenhouse and field (acreage) stability studies suggest instability to fluctuation in abiotic factors, such as temperature and/or water activity. *In planta* application using *P. contorta* bolts under stable greenhouse conditions supported effective killing of emerging MPB population. Concentration and formulation (fungal strain) – dependent lethal times and mycosis rate (Koch's postulate) correlated well with the *in vitro B. bassiana* infection model. MPB mycobiome competition assays suggested that the pigmented phenotype (red and yellow) supports an inhibitory profile against the MPB-symbiotic fungus, *Grosmannia clavigera*. Functional genomics of eight strains suggested a conservation of the oosporein BGC, a potential candidate for a mycobiome (and microbiome) alteration and attenuation of MPB immune response. Field application using the commercial formulation, BioCeres, showed effective MPB biocontrol. Both mean MPB parental gallery length and mean MPB larvae per gallery were significantly higher in the control compared to those in the treated enclosures. Additionally, the higher conidial concentration treatments resulted in a more dramatic effect, where majority of the galleries were <5cm long with no detectable MPB reproduction. Furthermore, nearly all recovered parental MPB

from the galleries were covered in *B. bassiana* mycelia. Therefore, these results provided compelling evidence that BioCeres, and *B. bassiana* in general, can be used to drastically reduce the reproductive output of MPB in a natural pine forest setting.

In summary, this thesis covered the utilization of genomics, biochemical tools and insect-fungal bioassays in probing the wide microbial space for natural product biosynthesis and the development of a mycoinsecticide for the biocontrol of the invasive mountain pine beetle, *Dendroctonus ponderosae.* The availability of the established genome resources will contribute significantly to the phylogenomic and evolutionary studies of the *Bacillus sensu lato*, the complex and enormous secondary biosynthetic potential for antimicrobial discovery, and lastly the synthetic biology efforts in genetically engineering the MPB aggregation pheromone, (-)-*trans* verbenol, for a highly specific and targeted biocontrol of MPB epidemic in Western Canada.

Chapter 9

Experimental Procedures

9.1. General Experimental Details

9.1.1. Media preparation

The cultivation of microorganisms utilized microbiological media purchased from several companies including Sigma-Aldrich Inc (St Louis, MO, USA), Becton Dickinson and Company (BD, Franklin Lakes, NJ, USA), and Merck (Kenilworth, NJ, USA). Media preparation was carried out following the manufacturer's instruction for all dehydrated media. Similarly, compounded or modified microbial media were prepared using adjuvants/fortifiers/enhancers purchased from either Sigma-Aldrich or Thermo Scientific (Waltham, MA, USA). Agar based media were solidified using 1.5% (w/v) Bacto agar (BD, Ann Arbor, MI, USA) after the powdered or granulated media component(s) were completely dissolved in milliQ water. All heat-sterilization compatible media were autoclaved at 121 °C, 15 psi for 20 min. For heat labile media or its components, sterilization was performed using a 0.22 μm Stericup filtration unit (Millipore Sigma, USA). Antimicrobial supplements, like antibacterial or antifungal agents, were incorporated on a convection-incubator cooled down (50 °C) sterile solid or liquid media. Approximately 20 mL agar media solution was aseptically poured in each sterile Petri dish. Once the agar had solidified overnight, the plates were inverted and stored at 4-8 °C. Stocks of plates were warmed up to room temperature for 48 h and assessed for sterility prior to use for routine microbial culturing.

9.1.1.1 Bacterial Strains Glycerol Stocks

Single colony isolate was inoculated in broth medium and incubated overnight on their designated culture conditions following standard ATCC or DSM protocols, unless otherwise specified. The overnight, logarithmically growing bacterial culture (16 – 20 h) were cryopreserved in the presence of 20-30% glycerol and stored at –70 °C ultra-low freezer. Sterile 80% aqueous glycerol solution was used to prepare bacterial glycerol stocks. Liquid bacterial culture was thoroughly mixed with glycerol to a final volume of 1 mL. Starting culture was obtained from glycerol stocks by briefly scrapping the surface of the frozen stock using an inoculating loop or needle while adhering to aseptic conditions. Thawing of glycerol stocks was minimized using a – 20 °C bench top cooler (Thermo Fischer Scientific, Waltham, MA, USA).

9.1.1.2 Fungal Strains Preservation and Maintenance

Fungal propagules were preserved either as a cryo-stock culture under 20-30% glycerol (year-long storage), on a sterile carrier like glass beads at –20 °C (month-long storage) or agar slant at 4 °C (week-long storage). Fungal mycelia were grown to a dense liquid culture using Potato Dextrose Broth (PDB) for 48-96 h at 28 °C and amended with 80% aqueous glycerol solution to a final concentration of 30% for every 1 mL of stock. The fungal mycelial slurry was frozen at –70 °C as glycerol stocks. A second medium-term storage, carrier-conidial powder stocks, were prepared from 6-8 week old agar Petri dish culture. Conidial biomass was scrapped from agar surface using a sterile inoculating loop and transferred to a 5 mL glass vial, with half-filled with 5 mm glass beads (Sartorius, Germany) and kept at –20 °C. Lastly, maximally streaked 13 mm agar slats were grown aerobically to a dense mycelial-conidial biomass for at least 6 weeks at 28 °C. The agar slant test tubes were then sealed and kept upright at 4 °C for short term storage.

9.1.2. Antimicrobial Activity Assays

The antimicrobial potential of an isolate and its metabolites was assessed following the suggested guidelines by Clinical and Laboratory Standards Institute (CLSI).[317] Several inhibition assays and their combinations were utilized to assess the antimicrobial activity of environmental isolates reported here.

9.1.2.1 Deferred Microbial Inhibition Assay

For facultative anaerobic to microaerophilic microbial inhibition tests, a deferred inhibition assay was performed. A suitable agar assay medium was stabbed with a sterile inoculating needle or sterile toothpick dipped with a test bacterial colony of logarithmically grown liquid culture. The agar plate was incubated overnight at the optimal growth conditions for the species- and strain-specific requirements. In parallel to the test organism, the indicator strains (bacterial or fungal), were grown in the assay broth overnight. After the two parallel cultures had grown, a 5 mL molten soft agar (0.7% w/v) was inoculated with 100 μL of the indicator strain, briefly vortexed and aseptically poured on the stabbed-inoculated agar plate. The bioassay set up was incubated at the optimal temperature for the indicator strains for 16 – 24 h. Zones of inhibition were measured and characterized as follows: complete true clearing, gradient clearing, clearing with 'satellite' colonies and ambiguous marginal clearing.

9.1.2.2 Crossed-streak Inhibition Assay

The microbial strain of interest (i.e. putative antimicrobial producing isolate) was inoculated by a single streak in the center of the agar plate. After an incubation period depending upon the test microbial strain, the plate was inoculated with the indicator microorganisms tested by single streak perpendicular to the central streak. After further incubation, the antimicrobial interactions are analyzed by observing the inhibition zone size at the point of intersection.

9.1.2.3 Agar-Plug Inhibition Assay

To probe the *in vivo* antagonism and the potential contact-dependent inhibition, an agar plug diffusion method was employed. The indicator strains were tightly streaked on the surface of the assay agar medium using a sterile cotton swab or a broad inoculation loop (e.g. Drigalski spatula). In parallel, the test microorganism was grown on a different agar medium until a secondary growth or metabolic state is attained (e.g. conidiation, arthrospore or endospore formation). A 6 – 8 mm hole was cored or punched aseptically using a flame-sterilized metal cork borer from both the indicator and test microorganisms' lawn. A cored agar plug from the indicator plate was replaced by the putatively antimicrobial producing test organism. A zone of inhibition was measured for the bioactive-producing test microorganism while a potential microbial lawn lysis can happen in the indictor organism plug.

9.1.2.4 Agar Well Diffusion Inhibition Assay

An agar well diffusion method was employed on clarified spent medium of candidate microorganisms with potential antimicrobial activity. A lawn of indicator strains was prepared by either streaking (using a loop or cotton swab applicator) a bacterial colony for maximum coverage on the surface of agar plate, or alternatively by spread plating 100 µL of dense logarithmically

growing indicator strains. After the liquid culture was completely absorbed into the agar, a 6 – 8 mm hole was cored or punched aseptically using a flame-sterilized metal cork borer. An increasing volume of aliquot (20, 40, 60, 80, and 100 µL) of the culture extract was introduced into the well. The agar plate was incubated upright, under the indicator strains optimum growth conditions.

9.1.2.5 Spot-on-lawn Inhibition Assay

A crude or fractionated extract or purified compound was tested for antimicrobial activity using the spot-on-lawn inhibition assay. The indicator microorganism was grown overnight in 5 – 10 mL of suitable broth. The overnight, logarithmically-active growing indicator strains were inoculated (100 µL) in a 50 °C -tempered molten soft agar (0.7% w/v). The mixture was vortexed briefly and poured over an agar plate of similar media composition (agar at 1.5%). The soft agar was allowed to solidify and dried in a BioSafety cabinet or laminar flow hood for 10-15 min. The test fractions or purified compound(s), at 10 µL, were vertically spot-inoculated closed to the dried soft agar surface containing the indicator bacterial lawn. The spot samples were allowed to dry, incubated (inverted for bacterial lawn, upright for filamentous fungal lawn) at the optimal time and temperature for the indicator strain. Zones of clearing were measured and characterized as follows: complete true clearing, gradient clearing, and clearing with 'satellite' colonies.

9.1.3. DNA Molecular Biology Techniques

9.1.3.1. Genomic DNA Isolation

Genomic DNA extraction was performed using the Blood DNeasy blood and tissue kit (Qiagen, Germany), according to the manufacturer's suggestion. Modification in the extraction

procedure followed the suggested treatment according to the nature of the microbial isolate. For difficult samples such as sporulated *Bacillus* species or arthrosporulated *Streptomyces* (e.g. high exopolymeric substances, though cell walls, high humic acid containing), a phenol-glass bead isolation method was performed. Briefly, cells were resuspended in 100 µL of 50 mM Tris (pH 7.5) and treated with lysozyme (20 mg/mL, 37 °C for 30 min), followed by proteinase K (2 mg/mL, 56°C for 30 min), and RNase A (0.5 mg/mL, 37°C for 30 min). Cells were lysed in 500 µL cell breakage buffer (0.4% SDS, 0.5% N-lauroyl sarcosine, 0.5% Triton X-100, 50 mM Tris, 100 mM EDTA, pH 8.0) and 400 µL phenol using glass beads (0.5 mm diameter, Sartorius, Germany). The slurry was vortexed for 1 min and rested for 1 min on ice, for a total of 10 cycles. It was then clarified at $13,000 \times g$ for 5 min. The aqueous layer was repeatedly extracted with equal volumes of phenol, followed by phenol:chloroform (1:1), and chloroform:isoamyl alcohol (24:1). The DNA was precipitated with 0.1× 3 M sodium acetate (pH 5.2) and 2.5× absolute ethanol, washed with 70% ethanol, and resuspended in 10 mM Tris buffer (pH 8.0).

9.1.3.2. Polymerase Chain Reaction

DNA was amplified by polymerase chain reaction (PCR) using an Eppendorf MasterCycler Nexus thermal gradient cycler machine (Fisher Scientific Madison, WI, USA). Phusion high fidelity DNA polymerase (New England Biolabs; Ipswich, MA, USA) was used according to the manufacturer's instructions. When applicable, PCR products were purified either by using a QIAquick PCR Purification Kit Qiagen, Mississauga, ON, Canada) or a QIAquick Gel Extraction Kit Qiagen, Mississauga, ON, Canada).

9.1.3.3. Agarose Gel Electrophoresis

Agarose gels (1.5% w/v) were prepared using Ultra-Pure Agarose (Invitrogen) in 0.5× Tris-borate-EDTA (TBE) buffer. The gel was also pre-stained with SYBR Safe DNA gel stain according to the manufacturer's suggestions. (Life Technologies, CA, USA). Sample buffer (6×; Thermo Scientific, Waltham, MA, USA) was mixed with DNA samples prior to loading into the well of the agarose gel. The DNA fragments were resolved by running the BioRad Mini-Sub Cell GT (BioRad, CA, USA) at 90 – 110 V, tracked using a hand held UV lamp, and finally visualized on an ImageQuant RT ECL Imager (GE Healthcare Life Sciences, Little Chalfont, Buckinghamshire, UK). Thermal prints of inverted images were saved and analyzed using ImageJ software version 1.45 S (NIH, Washington, D.C, USA).

9.1.3.4. Assessment of DNA Quality and Quantity

Routine DNA quality control was determined using the NanoDrop 3300 spectrophotometer (ThermoFisher Scientific, USA) according to manufacturer's protocol. Alternatively, for high yielding DNA preparations, Implen NanoPhotometer P360 (Implen Inc., Westlake Village, CA, USA), was used specifically measuring DNA concentration at the absorbance of 260 nm. Nucleic acid purity from protein contamination used the A_{260}/A_{280} absorbance ratio (e.g. >1.8) while solvent and salt contamination relied on the A_{260}/A_{230} absorbance ratio (e.g. >2.2). DNA samples intended for whole genome sequencing were further assess using Qubit fluorometry ver 2.0 (Thermo Fischer Scientific, USA) and DNA Bioanalyzer (Agilent Genomics, USA).

9.1.3.5 DNA Dideoxy Sanger Sequencing

Routine DNA sequencing of PCR products or plasmid was performed at the Molecular Biology Service Unit, University of Alberta. Column of gel purified amplicons or plasmid template

were sequenced using the BigDye Terminator v3.1 Cycle Sequencing Kit (Applied Biosystems, Foster City, CA, USA) and an ABI 3730 DNA Analyzer (Applied Biosystems, Foster City, CA, USA).

9.2. Experimental Procedures for the Genomics Studies of five *Bacillus* species.

9.2.1 Genomics Studies of *B. thuringiensis* DNG9

9.2.1.1 *B. thuringiensis* DNG9 Identification and Database Comparison

Bacillus thuringiensis DNG9 was isolated from an oil-contaminated soil slough in Baraki-Algiers, Algeria. The samples were serially diluted in water, heat-shocked at 80 °C for 30 min to activate endospores, spread onto Luria Bertani (LB) agar and incubated at 35 °C for 24 h. Thirteen *Bacillus* strains and DNG9 were chosen for phylogenetic analysis. The chosen species represent the members of *B. cereus sensu lato* supergroup.[318] This includes the type strains *B. thuringiensis* Berliner ATCC 10792^T, *B. cereus* ATCC 14579^T and *B. anthracis* AMES Ancestor. The 16S rRNA gene sequence from the type strain *B. subtili*s subsp. *subtilis* ATCC 6051^T was selected as an outgroup. The maximum likelihood method was used to construct the phylogenetic tree.

The sequencing project information and associated MIGS (Minimum Information about a Genome Sequence) 2.0 compliance[319] are summarized in Table 9.1 and Table 9.2. This bacterium was selected for sequencing as it was determined to be one of the most promising strains for discovery of compounds with strong antibacterial, antifungal and biosurfactant abilities. The availability of the draft genome of DNG9 may contribute to the evolution and comparative genomics studies of the *B. cereus sensu lato* group. Furthermore, future investigations on its genome-encoded bioactive metabolites may be pursued. This work provided a standard draft genome and the assembled contigs have been deposited in public repositories.

9.2.1.2 *B. thuringiensis* DNG9 Genomic DNA Isolation

Genomic DNA was isolated from a combined 16 hr grown single colony isolate and a two mL 16 h grown liquid culture (150 rpm) from LB agar and LB broth, respectively. Total nucleic acid was extracted using the method described previously.[320] Briefly, cells were harvested at 5,000 × g for 2 min and resuspended in 100 µl 1× TE buffer (100 mM Tris-HCl, 50 mM EDTA, pH 8.0). The cell slurry was sequentially treated with 20 mg/mL lysozyme (37 °C, 30 min), 2 mg/mL proteinase K (56 °C, 30 min) and 0.5 mg/mL RNase A (37 °C, 30 min). The sphaeroplast suspension was lysed with 500 µl cell breakage buffer (0.4% SDS, 0.5% N-lauroyl sarcosine, 0.5% Triton X-100, 50 mM Tris, 100 mM EDTA, pH 8.0), 400 µl phenol and 150 µl glass beads (0.5 mm diameter, Sartorius, Germany). The slurry was vortexed for 1 min and rested for 1 min on ice, for a total of 10 cycles, and finally clarified at 13 000 × g for 5 min at room temperature. The aqueous layer was repeatedly extracted with equal volume of phenol, followed by phenol:chloroform (1:1) and finally with chloroform:isoamyl alcohol (24:1). The DNA was precipitated with 0.1× 3 M sodium acetate pH 5.2 and 2.5× absolute ethanol, washed with 70% ethanol and resuspended in 10 mM Tris buffer, pH 8.0. Quantity and quality were assessed using Qubit 2.0 fluorometry (Qiagen) and agarose gel electrophoresis, respectively.

Table 9.1. Classification and general features of *B. thuringiensis* strain DNG9

MIGS ID	Property	Term		Evidence code[a]
	Classification	Domain	Bacteria	TAS [321]
		Phylum	Firmicutes	TAS [322]
		Class	Bacilli	TAS [323]
		Order	Bacillales	TAS [324]
		Family	Bacillaceae	TAS [325]
		Genus	*Bacillus*	TAS [325, 326]
		Species	*Bacillus thuringiensis*	TAS [327]
		Strain	DNG9	
	Gram stain	Positive		IDA
	Cell shape	Rod		IDA
	Motility	Motile		IDA
	Sporulation	Spore (Subcentral)		IDA
	Temperature range	10 – 48 °C		TAS [328]
	Optimum temperature	28 – 35 °C		TAS [328]
	pH range; Optimum	4.9 – 8.0; 7.0		TAS [322, 329]
	Carbon source	Glucose		NAS
MIGS-6	Habitat	Soil		NAS
MIGS-6.3	Salinity	Salt tolerant		TAS [330]
MIGS-22	Oxygen requirement	Aerobic		IDA
MIGS-15	Biotic relationship	Free-living		IDA
MIGS-14	Pathogenicity	Insect pathogen		TAS [331]
MIGS-4	Geographic location	Algeria		NAS
MIGS-5	Sample collection	February 13, 2013		NAS
MIGS-4.1	Latitude	36° 40′ 9″ N		NAS
MIGS-4.2	Longitude	3° 5′ 43″ E		NAS
MIGS-4.4	Altitude	22 m		NAS

[a] Evidence codes - IDA: Inferred from Direct Assay; TAS: Traceable Author Statement (i.e., a direct report exists in the literature); NAS: Non-traceable Author Statement (i.e., not directly observed for the living, isolated sample, but based on a generally accepted property for the species, or anecdotal evidence). These evidence codes are from the Gene Ontology project.[332]

Table 9.2. Whole genome sequencing project summary for MIGS 2.0 compliance

MIGS ID	Property	Term
MIGS 31	Finishing quality	Draft genome
MIGS-28	Libraries used	Illumina paired-end
MIGS 29	Sequencing platforms	Illumina MiSeq100
MIGS 31.2	Fold coverage	317×
MIGS 30	Assemblers	CLC Genomic Workbench 7.5.2
MIGS 32	Gene calling method	GeneMarkS, Prodigal
	Locus Tag	BVF97
	Genbank ID	MSTN00000000
	GenBank Date of Release	9-Mar-17
	GOLD ID	Ga0180945
	BIOPROJECT	PRJNA359364
MIGS 13	Source Material Identifier	DNG9
	Project relevance	Agricultural, Biotechnological

9.2.1.3 *B. thuringiensis* DNG9 Whole Genome Sequencing, Assembly and Annotation

The genome of *Bacillus thuringiensis* DNG9 was sequenced at The Applied Genomic Core (TAGC), Department of Biochemistry, University of Alberta using Illumina paired-end sequencing platform and Nextera XT DNA library kit (Illumina, USA). Whole genome sequencing was performed in duplicates using the MiSeq Reagent kit v2. Sequencing of 250 bp paired-end modules gathered 3.69 M reads, which provided an average coverage of 317× resulting in 38 contigs. *De novo* assembly of the 6,057,430 bp paired-end sequences was created using CLC Genomics Worksbench v 7.5.2. (CLC bio, Aarhus, Denmark).

Gene prediction was performed using four automated genome annotation pipelines: (1) the NCBI Prokaryotic Genome Annotation Pipeline (PGAP)[333] using GeneMarkS+ and best-placed reference protein set; (2) the Joint Genome Institute – Integrated Microbial Genomes and Microbiomes (JGI-IMG/M) pipeline,[334] utilizing Prodigal gene caller;[335] (3) the Rapid Annotation

using Subsystem Technology (RAST) v2.0 server;[336] and (4) the Bacterial Annotation System (BASys) server.[337] CRISPR repeats were predicted by using CRISPRfinder.[338] The draft genome of DNG9 was aligned with the type strain *B. thuringiensis* Berliner ATCC 10792[T] closed genome to generate a single scaffold using Contiguator v2,[339] and Multi-Draft based Scaffolder (MEDUSA).[340] A chromosome map was generated from the single scaffold using BASys automated pipeline[337] and viewed using CGViewer.[341]

Species was established using genome-wide Average Nucleotide Identity (gANI) metric and alignment fraction (AF) calculated within the JGI-IMG/M server using the Microbial Species Identifier (MiSI) calculator.[342] Strain novelty was established using the Genome-to-Genome Distance Calculator (GGDC) 2.1 server employing digital DNA:DNA hybridization (dDDH) and DNA G+C content.[210]

9.2.1.4 *B. thuringiensis* DNG9 Microscopy Procedures: Scanning Electron Microscopy, Transmission Electron Microscopy and Schaeffer Fulton Endospore Staining

For scanning electron microscopy (SEM), early logarithmically growing 16 h-grown cells (McFarland = 0.3) in Nutrient Broth (BD Difco Laboratories, Sparks, MD, USA) were fixed overnight with 2% glutaraldehyde buffer. The overnight pellet was subjected to increasing ethanol series (50–100%) for dehydration. The dehydrated cells were gradually replaced with hexamethyldisilazane (HMDS) by a series of incubations in ethanol:HMDS (75:25, 50:50, 25:75, 0:100, 0:100). The samples were air dried overnight and mounted on SEM stubs. The sample was coated with a gold–palladium mixture using a Hummer 6.2 Sputter Coater (Anatech). The gold–palladium coated bacterial cells were viewed using a Philips Scanning Electron Microscope Model XL30 and analyzed using Scandium software as previously reported.[320, 343]

In parallel to SEM cell preparation, the same set of *B. thuringiensis* cells were prepared for transmission electron microscopy (TEM). Cells were rapidly frozen in liquid nitrogen under high pressure (2,100 bar) in a Bal-Tec HPM100. The freeze substitution procedure involved low temperature infiltration at –85 °C in 1% glutaraldehyde and 1% tannic acid (in acetone) for 72 h followed by three washes in anhydrous acetone for 1 h each at –85 °C. Frozen and fixed cells were stained with 1% OsO4 in acetone for 1 h at –85 °C. Cells were embedded in Spurr's resin after washing in anhydrous acetone. Samples were sectioned using an ultramicrotome (Reichert–Jung Ultra Cut E, Germany) and stained with 5% uranyl acetate–2.7% lead citrate at room temperature for 15 min. Sections were viewed using a Morgagni 268 TEM (Philips, FEI, Hillsboro, OR, USA) and Morgagni 268 version 3.0 software.[320]

Endospore staining was performed as reported by Schaeffer and Fulton.[344] An axenic microbial smear from a stationary phase, 120 h-grown *B. thuringiensis* DNG9 (McFarland >1.0) was air dried and heat fixed on a grease-free slide (Thermo Fischer Scientific, USA). The smear was covered with paper towel and flooded with 1% malachite green solution (HiMedia Laboratories, India). The slide was steamed using a water bath inside a fume hood for 10 min. The stain was continuously added dropwise preventing drying of the paper towel. The mordant-stained cells and endospores were washed gently by a stream of tap water. The unstained and colorless vegetative cells were counterstained with 0.5% aqueous safranin for 30 sec. The slide was washed with tap water, blot dried, and examined under an oil immersion objective using a Zeiss Axio Scope equipped with a digital camera and PictureFrame software version 2.3.

9.2.2. *B. cereus* E41 and *B. anthracis* F34 Whole Genome Sequencing, Assembly and Annotation

Genomic DNA was extracted from single-colony isolates of *B. cereus* E41 or *B. anthracis* F34 using the DNeasy blood and tissue kit (Qiagen), according to the manufacturer's protocol. Sequencing libraries from the genomic DNA extracts were prepared using the Nextera XT DNA library preparation kit (Illumina). Whole-genome sequencing was performed using the MiSeq reagent kit version 2 (2 × 250 cycles) and MiSeq sequencing technology (Illumina), generating 150-bp paired-end reads. De novo assembly of the reads into contiguous sequences (contigs) was carried out using the CLC Genomics Workbench version 7.5.2 (CLC Bio, Aarhus, Denmark). All of the genomes sequenced exceeded 300× coverage. The draft genomes of E41 and F34 yielded 29 and 66 contigs, respectively. The draft genomes were then annotated using RAST version 2.0[345] or PGAP.[333] Species identities were determined by an average nucleotide identity (ANI) of 97% using JSpecies version 1.2.1[346] with previously sequenced genomes in the GenBank database. Secondary metabolites were predicted using antiSMASH version 3.[347] The potential to produce bacteriocins was detected using BAGEL3.[348]

9.2.3 *B. paralicheniformis* F47 Whole Genome Sequencing, Assembly and Annotation

Genomic DNA was extracted using DNeasy blood and tissue kit (Qiagen) as described previously.[12] Sequencing libraries were created using the Nextera XT DNA library preparation kit and sequencing was performed using the MiSeq Reagent kit v2 (Illumina). *De novo* assembly of the 4,028,320 bp paired-end sequences (3.59 M reads) was generated using CLC Genomics Workbench v7.5.2. (CLC Bio, Aarhus, Denmark), which resulted in 119 scaffolds, providing a coverage of 167× and 46.2% G+C content. Gene prediction was performed using three automated annotation pipelines: (I) RAST v2.0,[345] (II) NCBI PGAP,[333] and (III) JGI-IMG/M.[334] Species identity was determined by calculating ANI and AF using the MiSI calculator employed in

IMG/M,[342] against previously sequenced genomes in IMG/M database. Strain identity was established by calculating the dDDH values using the GGDC v2.1 server.[210] Secondary metabolites were predicted using antiSMASH v4[350] while bacteriocins were predicted using BAGEL4.[244] Genomic islands were predicted using IslandViewer 4.0,[131] prophages using PHASTER,[132] and CRISPRs using CRISPRfinder servers.[338]

9.2.4. *B. licheniformis* SMIA-2 Whole Genome Sequencing, Assembly and Annotation

Genomic DNA was purified from a 12 h culture grown in Brain Heart Infusion (BHI) broth (50 °C, 200 rpm) using the DNeasy blood and tissue kit (Qiagen), following the manufacturer's protocol for Gram-positive bacterial DNA extraction. DNA were quantified using Qubit v2.0 and sequencing libraries (1 ng) were created using Nextera XT DNA library preparation kit (Illumina, San Diego, CA) and sequenced using the NextSeq reagent kit (2×150 bp). FastQC version 0.11.8 (http://www.bioinformatics.babraham.ac.uk/projects/fastqc/) was used to inspect quality of the sequences and quality trimming based on Phred quality scoring 20 and SolexaQA. Trimmed reads were *de novo* assembled using IDBA-UD with default parameters[351] implemented in MiGA pipeline v0.3.6.2.[211] The draft genome sequence was annotated using the NCBI PGAP version 4.8.[333] Taxonomic classification was established using MiGA;[211] calculation of the ANI nucleotide[352] and dDDH using the GGDC v2.1 server.[210]

9.3. Experimental Procedures for the Functional Genomics Studies of Fengycin-Producing *B. velezensis* F11

9.3.1. *B. velezensis* F11 Isolation and Identification

Water samples were collected from a salt lake in Ain Baida-Ouargla, Algeria. The samples were serially diluted with sterile water, thermally shocked at 80 °C for 30 min, spread onto LB agar (1% agar, w/v), and incubated at 37 °C for 24 h. Single colony isolates were obtained using successive streak plating. *Bacillus* sp. F11 was identified using an API 50 CHB test kit (BioMérieux, Marcy l'Etoile, France), according to the manufacturer's instructions.

9.3.2. *B. velezensis* F11 Genomic DNA isolation

Total nucleic acid was isolated from a combination of colonies of the pure culture on LB agar and biomass from liquid culture in LB broth grown overnight (16 h) from single colony at 37°C (160 rpm) (McFarland = 0.5). DNA was extracted using the method described previously with some modifications.[320] Briefly, cells were resuspended in 100 µL of 50 mM Tris (pH 7.5) and treated with lysozyme (20 mg/mL, 37 °C for 30 min), followed by proteinase K (2 mg/mL, 56 °C for 30 min), and RNase A (0.5 mg/mL, 37 °C for 30 min). Cells were lysed in 500 µL cell breakage buffer (0.4% SDS, 0.5% N-lauroyl sarcosine, 0.5% Triton X-100, 50 mM Tris, 100 mM EDTA, pH 8.0) and 400 µL phenol using glass beads (0.5 mm diameter, Sartorius, Germany). The slurry was vortexed for 1 min and rested for 1 min on ice, for a total of 10 cycles. It was then clarified at $13{,}000 \times g$ for 5 min. The aqueous layer was repeatedly extracted with equal volumes of phenol, followed by phenol:chloroform (1:1), and chloroform:isoamyl alcohol (24:1). The DNA was precipitated with 0.1× 3 M sodium acetate (pH 5.2) and 2.5× absolute ethanol, washed with 70%

ethanol, and resuspended in 10 mM Tris buffer (pH 8.0). Quality and quantity were assessed using agarose gel electrophoresis and Qubit 2.0 fluorometry (Qiagen, Mississauga, ON, Canada), respectively.

9.3.3. *B. velezensis* strain F11 Whole Genome Sequencing, Assembly, and Annotation

Whole-genome sequencing was carried out at The Applied Genomic Core (TAGC), Department of Biochemistry, University of Alberta (Edmonton, AB, Canada). The sequencing library was prepared using the Nextera XT DNA library preparation kit (Illumina Inc., San Diego, CA, USA). Sequencing was performed in duplicates using the MiSeq Reagent kit v2 (2×250 cycles) and MiSeq sequencing technology (Illumina Inc.), generating 150-bp paired-end reads. *De novo* assembly of the 4.02 Mbp genome was done using the CLC Genomics Workbench v7.5.2. (CLC bio, Aarhus, Denmark). Species identity was established by calculating ANI and *in silico* dDDH values, using JSpecies v1.2.1[346] and the GGDC v2.1,[210] respectively, against strains from the GenBank database (Table 9.3.). The draft genome sequence of *B. velezensis* F11 was annotated using three platforms, namely, the JGI-IMG/M annotation pipeline,[334] the RAST server,[345] and the NCBI PGAP.[333] The PGAP and JGI-IMG/M annotated genomes were deposited to DDBJ/ENA/GenBank under accession numbers MSTO00000000 and Ga0180326, respectively. Whole-genome sequences of reference strains (Table 9.3) were also annotated using RAST v2.[345] To determine the core genome, which refers to the set of genes present in all these strains, gene-clustering analysis was performed using the BPGA tool v1.3.0.[353] A 30% amino acid sequence identity cut-off was used. Nucleotide sequences from each of the 319 core gene clusters were then aligned using Clustal W v2.1,[354] and the alignments were concatenated, with positions with at least one gap stripped, using Geneious v8.1.8.[355] The resulting final alignment (303,234 bp) was used

to reconstruct a maximum likelihood phylogenetic tree with RAxML v8.2.8[356] using the GTR nucleotide substitution matrix and the gamma model of rate heterogeneity. Robustness of branching was estimated with 100 bootstrap replicates. *Clostridium botulinum* A ATCC 3502 (GenBank accession number AM412317) served as the outgroup. To align and visually compare whole genomes, the CGView Comparison Tool,[357] which employs BLASTP,[358] was used to construct a BLAST atlas. The *B. amyloliquefaciens* DSM 23117 genome (GenBank accession number, CP000560) was used as reference. The antiSMASH server v4.0.2[347] and BAGEL ver 3.0[348] were used to predict bioactive secondary metabolites and bacteriocins, respectively, that are encoded in the assembled draft genome of *B. velezensis* F11.

9.3.4. *B. velezensis* strain F11 Transmission Electron Microscopy

Cells were prepared for transmission electron microscopy (TEM) as described in Chapter section 9.2.1.2,[343] with some modifications. Actively growing cells were harvested and crosslinked in fixative solution (2% paraformaldehyde, 2.5% glutaraldehyde, 0.1 M phosphate buffer, pH 7.2) for 2 h at room temperature with shaking, and washed three times with 0.1 M phosphate buffer (pH 7.2) for 15 min. The cell pellet was post-fixed with 1% OsO_4 (in 0.1 M phosphate buffer, pH

Table 9.3. List of genomes used in the functional genomics of *B. velezensis*

Species and Strain	Accession Number
Bacillus amyloliquefaciens F11	MSTO00000000
Bacillus amyloliquefaciens CAU B946	HE617159
Bacillus amyloliquefaciens DSM 23117	CP000560
Bacillus amyloliquefaciens DSM 7	FN597644
Bacillus amyloliquefaciens IT-45	CP004065
Bacillus amyloliquefaciens L-H15	CP010556
Bacillus amyloliquefaciens L-S60	CP011278
Bacillus amyloliquefaciens LFB112	CP006952
Bacillus amyloliquefaciens MBE1283	CP013727
Bacillus amyloliquefaciens S499	CP014700
Bacillus subtilis ATCC 13952	CP009748
Bacillus subtilis 168	AL009126

Bacillus anthracis Ames	AE016879
Bacillus cereus ATCC 14579	AE016877
Bacillus licheniformis ATCC 14580	CP000002
Bacillus paralicheniformis ATCC 9945a	CP005965
Clostridium botulinum A ATCC 3502	AM412317

7.2) for 1.5 h, followed by three rounds of washing with the phosphate buffer for 15 min. Cells were gradually dehydrated for 15 min each in increasing ethanol concentrations: 1× 50%, 1× 70%, 1× 90%, and 3× 100%. Ethanol was then replaced with 1:1 Spurr:ethanol mixture and incubated at room temperature for 3 h, followed by an overnight incubation with 100% Spurr resin. The sample was cured in a Beem capsule at 80 °C for 18 h. Ultrathin sections (80 nm) were prepared using a Reichert–Jung Ultra Cut E microtome, placed in nickel-coated grids, and stained with a solution containing 5% uranyl acetate and 2.7% lead citrate at room temperature for 15 min. Sections were viewed using a Morgagni 268 TEM (Philips, FEI, Hillsboro, OR, USA) equipped with a GatanOrius CCD camera, and analyzed with Morgagni 268 v3.0 software.

A negative staining TEM was performed on unfixed cells to analyze surface structures (e.g. flagellation). An aliquot (50 µL) of bacterial suspension was deposited onto formvar-carbon coated grids for 30 sec, and stained with 2% phosphotungstic acid (pH 7.4) for 30 sec. Excess stain was wicked off and allowed to dry for 15 min before viewing under TEM. The fixed-negatively stained cells were viewed using a Morgagni 268 TEM (Philips, FEI, Hillsboro, OR, USA) equipped with a GatanOrius CCD camera, and analyzed with Morgagni 268 v3.0 software.

9.3.5. *B. velezensis* F11 Biosurfactant and Emulsification Assays

The emulsifying activity of *B. velezensis* F11 that was grown in LB broth at 27 °C (200 rpm) was evaluated using the emulsification index, drop collapse assay, and oil displacement assay. For the determination of the emulsification index, 2 mL mineral oil was added to 2 mL of bacterial

culture, and the mixture was shaken vigorously for 2 min. The emulsification index was calculated as the percentage of the height of the emulsified layer divided by the total height of the liquid column.[359] The emulsified solutions were allowed to stand at room temperature, and the emulsification index was calculated at different time points to assess the emulsion stability. For the drop collapse method, 2 µL of mineral oil was loaded into a 96-well microtiter plate, and 5 µL of bacterial suspension was added onto the oil surface.[360] The shape of the cell suspension was visually inspected after 1 min. Flat droplets were indicative of the presence of biosurfactants.[361] Bacterial suspensions grown at increasing time points (2 h to 80 h) were used for the abovementioned assay. Aliquots from the same bacterial cultures were centrifuged, and the supernatant was used for the oil displacement assay. For this assay, 20 µL mineral oil was placed on the surface of 50 mL sterile distilled water in a petri dish. The culture supernatant (10 µL) was carefully placed on the oil film surface. After 30 sec, the diameter of the clear halo on the oil surface was measured. The size of the halo is a measure of surfactant activity.[362]

9.3.6. *B. velezensis* F11 Antibacterial Activity Assay

Spot-on-lawn assays were used to test the antibacterial activity of *B. velezensis* F11. Three Gram-negative bacteria (*Escherichia coli* JM109, *Salmonella enterica* serovar Typhimurium ATCC 23564, and *Pseudomonas aeruginosa* ATCC 14217) and three Gram-positive bacteria (*Carnobacterium divergens* LV13, *Enterococcus faecalis* 710C, and *Lactococcus lactis* ssp. *cremoris* HP) were used as indicator strains. The Gram-negative strains were grown overnight in LB broth at 37 °C with shaking (250 rpm), while the Gram-positive strains were grown overnight in all-purpose tween (APT) broth at 37 °C for *E. faecalis* 710C, and at 25 °C for *C. divergens* LV13 and *L. lactis* ssp. *cremoris* HP. The indicator strain (100 µL) was added into 5 mL molten

soft agar (0.75%, w/v), which was consequently overlaid onto an LB/APT agar plate. An overnight culture of *B. velezensis* F11 that was grown in LB broth at 27 °C was centrifuged (5000 × *g*, 10 min), and 10 μL of the supernatant was spotted and dried onto the indicator lawn. The plates were incubated overnight at the optimal temperature for each indicator strain and examined for zones of clearing.

9.3.7. *B. velezensis* F11 Antifungal Activity Assay

A plate diffusion method was used to determine the antifungal activity of *B. velezensis* F11 against *Candida albicans* ATCC 10231, *Galactomyces geotrichum* MUCL 28959, and *Aspergillus niger* ATCC 9142 obtained from the Cellular and Molecular Biology Laboratory of USTHB, Algeria. *B. velezensis* F11 was grown in LB agar at 37 °C for 24 h. Agar discs (6 mm) containing fully-grown *B. velezensis* F11 were subsequently deposited on Mueller-Hinton (MH) agar plates that were inoculated with the indicator strains. *C. albicans* ATCC 10231 was grown in Sabouraud Dextrose Agar (SDA) containing 0.40 g chloramphenicol and 0.05 g cycloheximide, while *A. niger* ATCC 9142 and *G. geotrichum* MUCL 28959 were cultured on potato dextrose agar. The plates were kept at 4 °C for 2 h to allow the diffusion of any antifungal metabolites from *B. velezensis* F11. The plates were then incubated further at 30 °C and 25 °C for the yeast (*C. albicans* ATCC 10231) and molds (*A. niger* ATCC 9142 and *G. geotrichum* MUCL 28959), respectively. Inhibition zones were assessed after 24 and 48 h of incubation.

9.3.8. *B. velezensis* F11 Purification of Fengycin

Four liters of MH broth was inoculated with 10 mL of *B. velezensis* F11 overnight culture, and incubated at 27 °C with shaking (200 rpm) for 40 h. The culture was centrifuged (5000 × *g*,

20 min), and the supernatant was subjected to a series of hydrophobic interaction chromatographic techniques. A spot-on-lawn assay was used to monitor active fractions from each purification step using *S. enterica* serovar Typhimurium ATCC 23564 and *C. divergens* LV13 as indicator strains. The culture supernatant was loaded into a column with 40 g activated Amberlite XAD-16 resin (Sigma-Aldrich, St. Louis, MO, USA), and washed with 250 mL each of water, 20% isopropanol (IPA), 40% IPA, and 80% IPA with 0.1% trifluoroacetic acid (TFA) at a constant flow rate of 10 mL/min. The 80% IPA fraction was found to be the most active fraction and was in turn concentrated under vacuum for further purification using a C_{18} solid phase extraction (SPE) cartridge (Phenomenex, Torrance, CA, USA). The cartridge was activated with 50 mL methanol and 100 mL water prior to loading of the sample. After sample loading, the cartridge was washed with 50 mL each of 30% ethanol, 40% IPA, and 80% IPA with 0.1% TFA at a flow rate of 3 mL/min. The last fraction was found to be the most active fraction and was then subjected to reverse-phase high-performance liquid chromatography (RP-HPLC) using a Vydac C_{18} column (5 µm particle size, 300 Å, 4.6 × 250 mm) at 220 nm detection and 1 mL/min flow rate. Water (solvent A) and acetonitrile (solvent B) that were both acidified with 0.1% TFA were used as mobile phases. Solvent B was initially set at 20% for 5 min, increased to 55% for 30 min, and ramped up to 95% for 3 min. Active fractions were eluted at 33-35 min and were subjected to mass spectrometry analysis.

9.3.9. *B. velezensis* F11 Fengycin Mass Spectrometry

Determination of molecular masses and elemental compositions were accomplished through liquid chromatography-mass spectrometry (LC-MS) using an Agilent 1200 SL HPLC unit with a Phenomenex C_4 reverse-phase analytical column (5 µm particle size, 300 Å, 2 x 50 mm) that was

thermostated at 30 °C. A gradient system of 0.1% formic acid (FA) in water as solvent A, and 0.1% FA in methanol as solvent B was used. An aliquot of the sample was loaded onto the column at a flow rate of 0.20 mL/min, and an initial mobile phase composition of 95% solvent A. After sample injection, the column was washed with the initial loading conditions for 1 min to remove salts. Elution of the analytes was done using a linear gradient of 5% to 98% solvent B over a period of 9 min. Mass spectra were acquired in positive ionization mode using an Agilent 6220 accurate-mass time-of-flight (TOF) LC-MS system (Santa Clara, CA, USA) equipped with a dual sprayer electrospray ionization source with the second sprayer providing a reference mass solution. The drying gas flow rate was set at 10 L min^{-1} at 325 °C with the nebulizer at 25 psi. The mass range was 100-3000 Da at an acquisition rate of ~1.03 spectra per sec and instrument state of 4 GHz high resolution. The fragmentor was set at 175 V, skimmer at 65 V, and the capillary at 4000 V. Mass correction was performed for every individual spectrum using peaks at *m/z* 121.0509 and 922.0098 from the reference solution. Mass Hunter software package (ver. B.04.00) was used for data acquisition. Analysis of the LC-MS data was done using the Agilent Mass Hunter Qualitative Analysis software (ver. B.07.00, SP1).

Tandem mass spectrometry (MS/MS) was performed to confirm the sequence of the identified lipopeptides, specifically through matrix-assisted laser desorption ionization-time-of-flight (MALDI-TOF) MS/MS and nano-LC MS/MS. MALDI-TOF MS/MS was performed on an UltraflexXtreme^{TM} mass spectrometer (Bruker Daltonics, Billerica, MA, USA) in positive ion mode using α-cyano-4-hydroxycinnamic acid (CHCA) as the matrix. Nano-LC MS/MS analysis was performed using a RP-HPLC Easy-nLC II (Thermo Scientific, Waltham, MA, USA) system equipped with a C$_4$ Acclaim PepMap100 analytical column (3 μm particle size, 100 Å, 75 μm x 15 cm; Thermo Scientific, Dionex, USA) and an Acclaim PepMap100 trap column (5 μm particle

size, 100 µm x 2 cm). The LC system was coupled to a Q-TOF premier mass spectrometer (Waters, Milford, MA). A solvent system composed of 0.1% FA in water (solvent A) and in methanol (solvent B) was used. The sample (18 µL) was loaded onto the column and washed with 20 µL of solvent A to remove salts. Elution of the analytes was done with a flow rate of 350 nL/min and a solvent gradient of 1% to 98% solvent B in 16 min. The mass spectrometer was operated in positive ion mode with capillary voltage of 3.4 kV and source temperature of 100°C. Spectra were recorded with *m/z* ranges of 50-1990 in MS/MS mode. MassLynx software (Waters, Milford, MA) was used for instrumental control and data analysis. MS/MS data of the peptides were deconvoluted by MaxEnt 3 (a MassLynx processing tool), and the peaks were manually analyzed and compared with the theoretical fragments and internal fragments.

9.4. Experimental Procedures for the Functional Genomics Studies of *Streptomyces* sp. A1-08

9.4.1. Soil Sample Collection

Volcanic soil samples were collected from Mt. Mayon situated in Malilipot, Albay at three altitudinal gradients: Site 1 at 500 m above sea level (masl) (N 13°16'25.3", E 123°43'22.0"), Site 2 at 1000 masl (N 13°15'52.4" E 123°42'23.1"), and Site 3 at 1500 masl (N 13°14'47.5" E 123°42'56.0"). Each sampling site was situated 20 m away from the main trail. In each location, three areas that are 10 m away from each other were marked. In each of the three regions, soil samples were collected in 10 different points following a zigzag manner, wherein each point was one meter apart. Collected samples per elevation were mixed using sterile trowel and pail and three bags of soil were obtained as replicates for each sampling site. Samples were placed in autoclavable bags (5 × 12 in), sealed, and labeled appropriately. During transport, the soil samples were kept at ambient temperature. Samples were processed immediately or kept at 4 °C until testing.

9.4.2. Isolation of Actinomycetes

Ten grams of soil samples were diluted in 90 mL of 0.85 % NaCl solution. Serial ten-fold dilutions of 10^{-4} to 10^{-6} were spread-plated on actinomycete isolation medium (AIM, HiMedia Laboratories, India) supplemented with streptomycin (100 ppm final concentration) and nystatin (100 U/mL), to inhibit bacterial and fungal contamination, respectively. Inoculated plates were incubated at 37 °C for 10 d. To establish the morphological characteristics, pure culture of the selected isolate was inoculated to the following standard culture media: ISP (International

Streptomyces Project) -2, ISP-3, ISP-4, and ISP-5 following the protocol of Shirling and co-workers[363] and agar plates were incubated at 30 °C for 21 d.

9.4.3. Antimicrobial Screening of Actinomycete Isolates

Axenic culture of isolated actinomycetes was achieved by repeated streaking on ISP-2 plates. Each of the purified isolates were inoculated on ISP-2 plates and incubated for five to seven days at 30 °C for antibiotic assay using agar plug method. Agar plugs (~8 mm in diameter) were prepared from the resulting ISP-2 agar cultures and were placed in an inverted position on plates overlaid with test organisms (approximately 10^8 cells/mL).[364] After 48 h at 30 °C, diameters of zone of inhibition were measured using a Plasti-Cal Series 700 digital caliper (Mitutoyo, USA). Controls for the screening of antagonistic activity include filter paper discs impregnated with streptomycin or ampicillin (100 µg/mL) for Gram positive and Gram negative bacteria, vancomycin (100 µg/mL) for MRSA, and nystatin (100 U/mL) for yeasts and molds.

9.4.4. Indicator Bacterial and Fungal Strains for Antimicrobial Assay

Test organisms were provided by the Antibiotics Laboratory of the National Institute of Molecular Biology and Biotechnology (BIOTECH, Philippines) which included the following: *Escherichia coli* BIOTECH-1825*, Pseudomonas aeruginosa* BIOTECH 1824*, Bacillus subtilis* BIOTECH 1514*, Staphylococcus aureus* BIOTECH 1823*,* methicillin-resistant *Staphylococcus aureus* (MRSA) BIOTECH 10378*, Klebsiella pneumoniae* BIOTECH 10283*, Salmonella enterica* Typhimurium BIOTECH 1756*, Candida albicans* BIOTECH 2219*, Aspergillus niger* BIOTECH 3080*,* and *Fusarium* sp*.* The bacterial test strains were maintained on nutrient agar (NA) (HiMedia Laboratories, India) at 37 °C. The yeast species were maintained on ISP-2 agar at 37 °C. Mold

species were maintained on potato dextrose agar (PDA) (HiMedia Laboratories, India) at 30 °C until the cultures have sporulated.

9.4.5. Extraction of Bioactive Compounds from *Streptomyces* sp. A1-08

Ethyl acetate extract of A1-08 isolate was produced following the protocol of Zulaybar and colleagues.[365] The A1-08 isolate was heavily streaked on ISP-2 plates and incubated for 3 – 5 d at 30 ˚C. Agar plugs from these plates were used as inoculum in 20 mL Croatian vegetative medium (CVM) (dextrin 40.0 g/L, corn steep liquor 8.0 g/L, calcium carbonate 7.0 g/L, ammonium sulfate 2.0 g/L, lactic acid 1.4 mL/L at pH 7.5) as described previously[364-365] and incubated with shaking at 200 rpm in ambient temperature for 2 d. Contents of each CVM flask were transferred to 200 mL Croatian fermentation medium (CFM) and incubated with shaking at 200 rpm in ambient temperature for 5 d. To ensure that pure culture was maintained, a loopful of sample was taken from CFM flask and streaked on ISP-2 plates incubated at 30 ˚C for 1 d. Contents of the CFM flask were transferred to a sterile 1000 mL Erlenmeyer flask. An equal volume of ethyl acetate was added to the flask and incubated overnight with shaking at 200 rpm in ambient temperature. The clear part of the suspension was pipetted out, placed in a pre-weighed round flask, and was dried using a rotary evaporator and lyophilized. The lyophilized ethyl acetate extract was re-dissolved in an equivalent volume of methanol to obtain a 10, 000 ppm concentration as stock solution.

9.4.6. Minimum Inhibitory Concentration Determination

Methicillin-resistant *Staphylococcus aureus* (MRSA) was selected as the test organism for MIC analysis because not only it is one of the most clinically important pathogens listed in the

WHO high priority group that has also become endemic in hospitals today but because of its multi-drug resistance.[37] Stock solution (1000 µg/mL) of the lyophilized ethyl acetate extract of A1-08 isolate was serially diluted in two-fold. A mixture of 180 µL Mueller Hinton Broth (BD Difco Laboratories, Sparks, MD, USA) with MRSA at 0.5 McFarland turbidity (approximately 1.5×10^8 cells/mL), and 20 µL of sample in methanol was inoculated in the first row of the plate. To all other wells, 100 µL of MHB were added. To each well 10 µL of MTT indicator solution were added. The plate had two columns for vancomycin antibiotic (two-fold serial dilution) as positive control, and a column with methanol only as negative control. The plate was incubated at 37 °C for 24 h. The color change was assessed visually. The lowest concentration at which color change occurred was taken as the MIC value. The average of the three replicates was calculated and was considered as the MIC.

9.4.7. Cytotoxic Activity Assay

The cytotoxic activity of the ethyl acetate extracts from A1-08 isolate on the human colorectal cancer cell line HCT 116 (ATCC CCL-247) was investigated using MTT assay. The MTT cytotoxicity assay used in this study was adapted from Mosmann,[366] with some modifications. The HCT 116 cell line was seeded separately at 4×10^4 cells/mL in sterile 96-well microtiter plates. The plates were incubated overnight at 37 °C and 5 % CO_2. Lyophilized ethyl acetate extracts at 4 mg/mL in dimethyl sulfoxide (DMSO; RCI Labscan Limited, Thailand) were serially diluted to obtain 1000, 500, 250, and 125 µg/mL in a master dilution plate (MDP). From the MDP, 10 µL were obtained and dispensed onto the plated cells to achieve the final screening concentrations 50, 25, 12.5, and 6.25 µg/mL. Cells treated with doxorubicin served as positive control while those treated with DMSO served as negative control. Three replicate wells were used

per concentration. The treated cells were then incubated for 72 h at 37 °C and 5 % CO_2. After

incubation, the medium was removed carefully to not disrupt the adherent cells, and 20 μL MTT

at 5 mg/mL in 1× PBS (Amresco, Ohio, USA) were added. The cells were again incubated at 37

°C and 5 % CO_2 for 4 h, after which 150 μL DMSO was added to each well. Using a Bio-Rad

microplate reader (Munich, Germany), the absorbances were measured at 570 nm. The

concentration required to kill 50% of the cell population or the Inhibition Concentration 50 (IC_{50})

was computed using ICPIN Software ver 2 (USEPA, USA) from a toxtat program. Three trials

with three replicates per concentration were performed.

9.4.8. Molecular Identification of *Streptomyces* sp. A1-08

Total genomic DNA was purified from an A1-08 single colony grown for 72 h in yeast

malt extract broth (28 °C, 180 rpm) using Wizard genomic DNA purification kit (Promega, USA)

following the manufacturer's protocol. The quantity and quality of the extracted genomic DNA

were assessed using Nanodrop 3300 (ThermoFisher Scientific) and resolved through agarose gel

electrophoresis, respectively. DNA extracts were stored at −20 °C until further processing.

Amplification of 16S rRNA gene was carried out in a 0.2 mL thin-walled microfuge tube

containing 1× Phusion GC buffer, 10 mM dNTP mix, 3% DMSO, 10 μM each of primer pair, 1 U

Phusion high-fidelity DNA polymerase (New England Biolabs, Ipswich, MA, USA) and 50 ng

genomic DNA template. The universal 16S rRNA bacterial primer pair of 27F (5'

AGAGTTTGATCMTGGCTCAG 3') and 1492R (5' TACGGYTACCTTGTTACGACTT 3') was

utilized.[367] The amplification was carried out using a Veriti® thermal cycler (P/N 4375786, Life

Technologies) with the following conditions: heated lid (98 °C,); initial denaturation at 96 °C, 30

s; 25 cycles of denaturation (95 °C, 10 s), annealing (49 °C, 30 s), and extension (72 °C, 45 s); and

final extension (72 °C, 10 min). At the end of the thermal cycling, the amplicons were resolved through agarose gel electrophoresis (1% agarose, 0.5× TBE buffer), stained with ethidium bromide and visualized under ChemiDoc™ XRS Gel Documentation system (Bio-Rad, USA) light. PCR products were column-purified using the QiaQuick PCR purification kit (Qiagen, Germany) and quantified using Qubit fluorometry v2.0 according to manufacturer's protocol. The column-purified amplicons were sequenced using the BigDye Terminator v3.1 cycle sequencing kit in an ABI 3730 DNA Analyzer (Applied Biosystems, USA). Sequencing was carried in three regions using three primers targeting the 16S rRNA gene: 27F, 1492R and the internal primer 907R (5' CCGTCAATTCCTTTRAGTTT 3').[368] The 16S rRNA gene sequence was deposited in GenBank under accession number MN121123.

For whole genome sequencing, A1-08 was grown in tryptic soy broth (TSB) (Difco, Laboratories, Sparks, MD, USA) for 96 h at 28 °C, 180 rpm. Genomic DNA extraction and sequencing protocols were adapted from protocols described previously[123-124] with modifications. Briefly, cells were harvested using a 0.22 μm Stericup filtration unit (Millipore Sigma, USA) and actinobacterial biomass was washed twice with ice-cold 1× Tris-EDTA (100 mM Tris-HCl, 50 mM EDTA, pH 8.0) buffer. Cell biomass (10 mg) was transferred in a microcentrifuge tube and resuspended in 100 μL 100 mM Tris-HCl buffer pH 8.0. To efficiently extract high molecular weight DNA, the cell suspension was pre-treated with achromopeptidase (5 mg) – lysozyme (10 mg) (Sigma, St. Louis, MO, USA) combination and incubated at 37 °C for 20 min. This was followed by treatment with 2 mg/mL proteinase K (56 °C, 30 min) (Qiagen, Germany) and 0.5 mg/mL DNase-free RNase A (37 °C, 30 min) (Thermo Fisher Scientific, USA). The pre-treated cells' genomic DNA was extracted and purified using the DNeasy Blood and Tissue DNA extraction kit (Qiagen, Germany) according to manufacturer's protocol. DNA quality and quantity

were assessed using Nanodrop spectrophotometry, Qubit fluorometry, and microfluidics-electrophoresis (BioAnalyzer, Agilent). A Nextera XT DNA sequencing library (1 ng) was prepared as described previously[123] and sequencing was performed using NextSeq reagent kit (2 × 150 bp) as previously reported.[315]

9.4.9. Whole Genome Assembly and Annotation of *Streptomyces* sp. A1-08

Default parameters were used for all software unless otherwise specified. The read quality was checked with FastQC v0.11.8.[369] Raw reads were adapter-trimmed using BBDuk v38.35[370] with the parameters ktrim, r; k, 23; mink, 11; hdist, 1; tpe; tbo; minlen, 100; trimq, 10 and ref, adapters. Trimmed reads were then filtered to remove contaminants using BBDuk v38.35 (with the parameters k, 31; ref, artifacts, phix). Reads were error-corrected using BBDuk v38.35 (with the parameters ecc, t; keepall; passes, 1; bits, 16; prefilter). The resulting reads were trimmed by quality scores using BBDuk v38.35 with the following parameters: qtrim, r; trimq, 10; and minlen, 100. The resulting short paired-end reads (corrected to 100-150 bp per read), were *de novo* assembled into contigs using SPADES v. 3.11.1[371] with k = 21, 33, 55 up to 77. Assemblies were evaluated using Quast v3.1.[372] CG view software was used to construct the genome map.[373] Prokka annotation was used in genome annotation.[374]

9.4.10. Phylogenetic Analysis of *Streptomyces* sp. A1-08

The draft genome assembly was uploaded to the MiGA server ver 2.0[211] and was queried against the TypeMat and NCBI Prok databases. Results from this analysis gave information on the classification and the comparison to other related genomes based on ANI and AAI values. A phylogenetic tree, based on sequence alignment of closely related genomes was inferred using

TYGS server.[375] All pairwise comparisons among sets of genomes were conducted using GBDP approach and accurate intergenomic distances under algorithm "trimming" and distance formula d_5. Digital DDH values and confidence intervals were calculated using the recommended settings of the GGDC 2.1.[210] Assignment to species and subspecies is based on dDDH threshold which can be utilized for taxon delineation at the subspecific level.[376] The resulting intergenomic distances were used to infer a balanced minimum evolution tree with branch support via FASTME 2.1.6.1 including SPR postprocessing.[377] Branch support was inferred from 100 pseudo-bootstrap replicates each. The trees were visualized with PhyD3.[378]

9.4.11. Prediction of Secondary Metabolite Biosynthetic Gene Clusters (BGCs)

The observed antimicrobial properties of *Streptomyces* sp. A1-08 can be inferred from the secondary metabolites encoded in its genome. Genome sequence analysis for secondary metabolites encoded in biosynthetic gene clusters (BGCs) was done using the antiSMASH v6.0.0. genome server.[379] Identified clusters and their genes involved in scaffold assembly were verified against the MIBiG database.[380] AntiSMASH uses CASSIS algorithm for prediction of boundaries of gene clusters and SANDPUMA algorithm to enhance substrate specificity predictions of secondary metabolites. The predictions utilized the relaxed cluster mining mode and all features were configured to establish a comprehensive inventory of known and putative secondary metabolites and their associated biosynthetic gene clusters. Furthermore, the antiSMASH biosynthetic gene clusters predictions in A1-08 was compared in parallel with PRISM 4 (ver 4.4.5) using default parameters.[381] The draft genome of the closest type strain *Streptomyces olivaceus* NRRL B-3009[T] was bioinformatically mined in parallel with A1-08 to infer similar secondary metabolite gene clusters and contrast the unique biosynthetic gene clusters in *Streptomyces* sp. A1-

08. A natural product search using Antibase,[382] Norine,[383] Sci-Finder and Web of Science was performed on the metabolites with established biosynthetic gene clusters (100% homology) as supported by MIBiG database.[380] Low gene homology (e.g. <40%) or the absence of precursor peptide, core biosynthetic genes and/or modifying enzymes, and gene cluster predicted artifacts resulting from broken BGCs hanging in contig edges were excluded, as expected of draft genome's limitations.

9.5. Experimental Procedures for the *In Vitro* and *In Vivo* Studies of *B. bassiana* against MPB

9.5.1. *B. bassiana* Strains and Growth Conditions

Ninety-three isolates of *B. bassiana* were obtained from the following culture collections: (1) the UAMH Centre for Global Microfungal Biodiversity (University of Toronto, Toronto, ON, Canada), (2) the CBS Culture Collection (Delft, The Netherlands), (3) Anatis Bioprotection Inc. (Laval, QC, Canada), (4) Lallemand Plant Care Inc. (Sault Ste. Marie, ON, Canada), (5) El Colegio de la Frontera del Sur (Tapachula, Chiapas, Mexico) and (6) Coleccion de Hongos Entomopatogenos del Centro Nacional de Referencia de Control Biologico SENASICA (Tecoman, Colima, Mexico) (Table 9.4). The strains were maintained on Potato Dextrose Agar (PDA) (BD Difco, Ann Arbor, MI, USA) incubated at 25 °C for 14 – 21 d. Conidia were harvested using a Drigalski spatula and kept at –20 °C for long term storage or resuspended in 0.01% Tween 80 as wetting agent for biological assays and culture propagation.

Table 9.4. *B. bassiana* strains used in the *in vitro* and *in vivo* MPB infection assays

Strain Code	Culture Collection	Place of Isolation	Host or Sample	Pigment in CDAYE	Colony Texture	Colony Color	Phenotype Group
298	UAMH - University of Toronto	Sault Ste, Marie, Ontario, Canada	Forest tent caterpillar, *Malacosoma disstria*	Yellow	Felty	Yellowish white	III
299	UAMH - University of Toronto	Sault Ste, Marie, Ontario, Canada	European pine sawfly, *Neodiprion sertifer*	Red	Villous	Creamy white	II
1069	UAMH - University of Toronto	Edmonton, Alberta, Canada	Soil under spruce tree	Red	Villous	Creamy white	I
1076	UAMH - University of Toronto	Edmonton, Alberta, Canada	Soil under Poplar with heavy underbrush	Red	Villous	Creamy white	I
1384	UAMH - University of Toronto	Edmonton, Alberta, Canada	Sandy soil, badger paddock	Colorless	Thin powdery	White	II

173

4510	UAMH - University of Toronto	Smithers, British Columbia, Canada	Bark of *Abies lasiocarpa* with *Dryocoetes confusus*	Colorless	Thin powdery	White	II
4623	UAMH - University of Toronto	Pennsylvania State College, USA	Contaminant from twig	Red	Villous	Creamy white	I
4748	UAMH - University of Toronto	Edmonton, Alberta, Canada	Colorado potato beetle, *Leptinotarsa decemlineata*	Colorless	Thin powdery	White	II
8658	UAMH - University of Toronto	Edmonton, Alberta, Canada	Forest tent caterpillar, *Malacosoma disstria*	Colorless	Thin powdery	White	II
9748	UAMH - University of Toronto	Ontario, Canada	Soil, potential insect pathogen	Colorless	Thin powdery	White	II
110.25	CBS Culture Collection (Delft, The Netherlands)	Not reported	Not reported	Yellow	Felty	Yellowish white	III
992.05	CBS Culture Collection (Delft, The Netherlands)	Not reported	Not reported	Colorless	Thin powdery	White	II
ANT-03	Anatis Bioprotection, Inc	Not reported	Active component of BioCeres G WP	Colorless	Thin powdery	White	II
Bb15	El Colegio de la Frontera Sur, Mexico	CNAP, Goias, Brasil	*Chalcodermus aeneus*	Colorless	Thin powdery	White	II
Bb4	El Colegio de la Frontera Sur, Mexico	Ecuador	*Hypothenemus hampei*	Colorless	Thin powdery	White	II
Bb6	El Colegio de la Frontera Sur, Mexico	Ecuador	*Hypothenemus hampei*	Colorless	thin powdery	White	II
Bb7	El Colegio de la Frontera Sur, Mexico	Morelos	*Atta mexicana*	Colorless	thin powdery	White	II
Bb8	El Colegio de la Frontera Sur, Mexico	Texcoco, Estado de México	*Leptinotarsa sp.*	Colorless	thin powdery	White	II
Bb9	El Colegio de la Frontera Sur, Mexico	Puebla, Puebla, Mexico	*Lygus sp.*	Colorless	thin powdery	White	II
Bb12	El Colegio de la Frontera Sur, Mexico	Irapuato, Guanajuato, Mexico	*Nezara viridula*	Colorless	thin powdery	White	II
Bb18	El Colegio de la Frontera Sur, Mexico	Papantla, Veracruz, Mexico	No identification	Colorless	thin powdery	White	II
Bb19	El Colegio de la Frontera Sur, Mexico	Tabasco, México	No identification	Colorless	thin powdery	White	II
Bb25	El Colegio de la Frontera Sur, Mexico	Finca San Miguel, Tapachula, Chiapas, Mexico	*Hypothenemus hampei*	Colorless	thin powdery	White	II
Bb26	El Colegio de la Frontera Sur, Mexico	Ejido Ahuacatlán, Cacahoatán, Chiapas,	*Hypothenemus hampei*	Colorless	thin powdery	White	II
BbDc	El Colegio de la Frontera Sur, Mexico	Tapachula, Chiapas, Mexico	*Diaphorina citri*	Colorless	thin powdery	White	II
BBHy	El Colegio de la Frontera Sur, Mexico	Finca Alianza, Cacahoatán, Chiapas, Mexico	*Hypothenemus hampei*	Colorless	thin powdery	White	II
BbRhy	El Colegio de la Frontera Sur, Mexico	Tapachula, Chiapas, Mexico	*Rhysomatus nigerrimus*	Colorless	thin powdery	White	II
Granada	Lallemand Plant Care, Inc - Quebec, Canada	Brazil	Active component of Granada	Colorless	thin powdery	White	II
1538; Str20; MOE31, LFCC0167	Lallemand Plant Care, Inc - Quebec, Canada	Not reported	Not reported	Yellow	Felty	Yellowish white	III
1559, NAI-21; 9	Lallemand Plant Care, Inc - Quebec, Canada	Not reported	Not reported	Red	Villous	Creamy white	I
1543, Str12; KAE23	Lallemand Plant Care, Inc - Quebec, Canada	Not reported	Not reported	Red	Villous	Creamy white	I
1446, Str1:2B	Lallemand Plant Care, Inc - Quebec, Canada	Not reported	Not reported	Red	Villous	Creamy white	I

1458, Str15; KAF33	Lallemand Plant Care, Inc - Quebec, Canada	Not reported	Not reported	Red	Villous	Creamy white	I
1459, Str60; HLD32	Lallemand Plant Care, Inc - Quebec, Canada	Not reported	Not reported	Red	Villous	Creamy white	I
1454, Str10; NAH22	Lallemand Plant Care, Inc - Quebec, Canada	Not reported	Not reported	Red	Villous	Creamy white	I
1451, Str27; RUB31	Lallemand Plant Care, Inc - Quebec, Canada	Not reported	Not reported	Red	Villous	Creamy white	I
1546, Str32; APF13	Lallemand Plant Care, Inc - Quebec, Canada	Not reported	Not reported	Red	Villous	Creamy white	I
1459, Str16; PAE22	Lallemand Plant Care, Inc - Quebec, Canada	Not reported	Not reported	Colorless	Thin powdery	White	II
CHE-CNRCB 01	Coleccion de Hongos Entomopatogenos del Centro Nacional de Referencia de Control Biologico	ARSEF 3285	*Atta* sp.	Colorless	Thin powdery	White	II
CHE-CNRCB 02	Coleccion de Hongos Entomopatogenos del Centro Nacional de Referencia de Control Biologico	Colima, Mexico	*Hypothenemus hampei*	Colorless	Thin powdery	White	II
CHE-CNRCB 05	Coleccion de Hongos Entomopatogenos del Centro Nacional de Referencia de Control Biologico	Not reported	*Diabrotica balteata*	Colorless	Thin powdery	White	II
CHE-CNRCB 06	Coleccion de Hongos Entomopatogenos del Centro Nacional de Referencia de Control Biologico	Not reported	*Spodoptera frugiperda*	Colorless	Thin powdery	White	II
CHE-CNRCB 08	Coleccion de Hongos Entomopatogenos del Centro Nacional de Referencia de Control Biologico	Not reported	*Geraeus senilis*	Colorless	Thin powdery	White	II
CHE-CNRCB 11	Coleccion de Hongos Entomopatogenos del Centro Nacional de Referencia de Control Biologico	Not reported	Unknown	Colorless	Thin powdery	White	II
CHE-CNRCB 14	Coleccion de Hongos Entomopatogenos del Centro Nacional de Referencia de Control Biologico	Not reported	Unknown	Colorless	Thin powdery	White	II
CHE-CNRCB 15	Coleccion de Hongos Entomopatogenos del Centro Nacional de Referencia de Control Biologico	Not reported	*Diatraea sccharalis*	Colorless	Thin powdery	White	II
CHE-CNRCB 13	Coleccion de Hongos Entomopatogenos del Centro Nacional de Referencia de Control Biologico	Not reported	*Conotrachelus perseae*	Colorless	Thin powdery	White	II
CHE-CNRCB 17	Coleccion de Hongos Entomopatogenos del Centro Nacional de Referencia de Control Biologico	Not reported	*Oebalus mexicana*	Colorless	Thin powdery	White	II
CHE-CNRCB 26	Coleccion de Hongos Entomopatogenos del Centro Nacional de Referencia de Control Biologico	Oaxaca, Mexico	*Hypothenemus hampei*	Colorless	Thin powdery	White	II

CHE-CNRCB 29	Coleccion de Hongos Entomopatogenos del Centro Nacional de Referencia de Control Biologico	Colombia	*Hypothenemus hampei*	Colorless	Thin powdery	White	II
CHE-CNRCB 30	Coleccion de Hongos Entomopatogenos del Centro Nacional de Referencia de Control Biologico	Vera Cruz, Mexico	*Hypothenemus hampei*	Colorless	Thin powdery	White	II
CHE-CNRCB 31	Coleccion de Hongos Entomopatogenos del Centro Nacional de Referencia de Control Biologico	Colombia	*Hypothenemus hampei*	Colorless	Thin powdery	White	II
CHE-CNRCB 32	Coleccion de Hongos Entomopatogenos del Centro Nacional de Referencia de Control Biologico	Not reported	*Laspeyresia pomonella*	Colorless	Thin powdery	White	II
CHE-CNRCB 35	Coleccion de Hongos Entomopatogenos del Centro Nacional de Referencia de Control Biologico	ARSEF5740, USA	*Phyllophaga* sp.	Colorless	Thin powdery	White	II
CHE-CNRCB 42	Coleccion de Hongos Entomopatogenos del Centro Nacional de Referencia de Control Biologico	ARSEF5743, USA	*Phyllophaga* sp.	Colorless	Thin powdery	White	II
CHE-CNRCB 55	Coleccion de Hongos Entomopatogenos del Centro Nacional de Referencia de Control Biologico	Not reported	*Phyllophaga* sp.	Colorless	Thin powdery	White	II
CHE-CNRCB 57	Coleccion de Hongos Entomopatogenos del Centro Nacional de Referencia de Control Biologico	Not reported	*Phyllophaga* sp.	Colorless	Thin powdery	White	II
CHE-CNRCB 58	Coleccion de Hongos Entomopatogenos del Centro Nacional de Referencia de Control Biologico	Not reported	*Phyllophaga* sp.	Colorless	Thin powdery	White	II
CHE-CNRCB 63	Coleccion de Hongos Entomopatogenos del Centro Nacional de Referencia de Control Biologico	Not reported	*Phyllophaga* sp.	Colorless	Thin powdery	White	II
CHE-CNRCB 64	Coleccion de Hongos Entomopatogenos del Centro Nacional de Referencia de Control Biologico	Not reported	*Phyllophaga* sp.	Colorless	Thin powdery	White	II
CHE-CNRCB 76	Coleccion de Hongos Entomopatogenos del Centro Nacional de Referencia de Control Biologico	Not reported	*Phyllophaga* sp.	Colorless	Thin powdery	White	II
CHE-CNRCB 82	Coleccion de Hongos Entomopatogenos del Centro Nacional de Referencia de Control Biologico	Not reported	*Schistocerca piceifrons*	Colorless	Thin powdery	White	II
CHE-CNRCB 83	Coleccion de Hongos Entomopatogenos del Centro Nacional de Referencia de Control Biologico	Not reported	*Schistocerca piceifrons*	Colorless	Thin powdery	White	II
CHE-CNRCB 84	Coleccion de Hongos Entomopatogenos del Centro Nacional de Referencia de Control Biologico	Not reported	*Schistocerca piceifrons*	Colorless	Thin powdery	White	II
CHE-CNRCB 85	Coleccion de Hongos Entomopatogenos del Centro Nacional de Referencia de Control Biologico	Not reported	*Schistocerca piceifrons*	Colorless	Thin powdery	White	II

CHE-CNRCB 92	Coleccion de Hongos Entomopatogenos del Centro Nacional de Referencia de Control Biologico	Not reported	*Schistocerca piceifrons*	Colorless	Thin powdery	White	II
CHE-CNRCB 101	Coleccion de Hongos Entomopatogenos del Centro Nacional de Referencia de Control Biologico	Not reported	*Diabrotica* sp.	Colorless	Thin powdery	White	II
CHE-CNRCB 102	Coleccion de Hongos Entomopatogenos del Centro Nacional de Referencia de Control Biologico	Not reported	*Diabrotica* sp.	Colorless	Thin powdery	White	II
CHE-CNRCB 103	Coleccion de Hongos Entomopatogenos del Centro Nacional de Referencia de Control Biologico	Not reported	*Diabrotica* sp.	Colorless	Thin powdery	White	II
CHE-CNRCB 106	Coleccion de Hongos Entomopatogenos del Centro Nacional de Referencia de Control Biologico	Not reported	*Spodoptera frugiperda*	Colorless	Thin powdery	White	II
CHE-CNRCB 107	Coleccion de Hongos Entomopatogenos del Centro Nacional de Referencia de Control Biologico	Not reported	*Spodoptera frugiperda*	Colorless	Thin powdery	White	II
CHE-CNRCB 105	Coleccion de Hongos Entomopatogenos del Centro Nacional de Referencia de Control Biologico	Jalisco, Mexico	Unknown coleopteran beetle of pine tree	Colorless	Thin powdery	White	II
CHE-CNRCB 159	Coleccion de Hongos Entomopatogenos del Centro Nacional de Referencia de Control Biologico	San Luis Potosi, Mexico	*Hypothenemus hampei*	Colorless	Thin powdery	White	II
CHE-CNRCB 460	Coleccion de Hongos Entomopatogenos del Centro Nacional de Referencia de Control Biologico	Not reported	Unknown	Colorless	Thin powdery	White	II
CHE-CNRCB 483	Coleccion de Hongos Entomopatogenos del Centro Nacional de Referencia de Control Biologico	Not reported	*Galleria mellonela*	Colorless	Thin powdery	White	II
CHE-CNRCB 491	Coleccion de Hongos Entomopatogenos del Centro Nacional de Referencia de Control Biologico	Not reported	*Galleria mellonela*	Colorless	Thin powdery	White	II
CHE-CNRCB 493	Coleccion de Hongos Entomopatogenos del Centro Nacional de Referencia de Control Biologico	Not reported	*Galleria mellonela*	Colorless	Thin powdery	White	II
CHE-CNRCB 528	Coleccion de Hongos Entomopatogenos del Centro Nacional de Referencia de Control Biologico	ARSEF 3286, France	*Spodoptera littoralis*	Colorless	Thin powdery	White	II
CHE-CNRCB 529	Coleccion de Hongos Entomopatogenos del Centro Nacional de Referencia de Control Biologico	ARSEF 3312, USA	Unknown	Colorless	Thin powdery	White	II
CHE-CNRCB 546	Coleccion de Hongos Entomopatogenos del Centro Nacional de Referencia de Control Biologico	ARSEF 3289, USA	*Spodoptera frugiperda*	Colorless	Thin powdery	White	II
CHE-CNRCB 117	Coleccion de Hongos Entomopatogenos del Centro Nacional de Referencia de Control Biologico	Chihuahua, Mexico	Adult pine tree borer	Colorless	Thin powdery	White	II

CHE-CNRCB 157	Coleccion de Hongos Entomopatogenos del Centro Nacional de Referencia de Control Biologico	Not reported	*Hippodamia convergens*	Colorless	Thin powdery	White	II
CHE-CNRCB 160	Coleccion de Hongos Entomopatogenos del Centro Nacional de Referencia de Control Biologico	Not reported	*Schistocerca piceifrons*	Colorless	Thin powdery	White	II
CHE-CNRCB 173	Coleccion de Hongos Entomopatogenos del Centro Nacional de Referencia de Control Biologico	Not reported	*Hypothenemus hampei*	Colorless	Thin powdery	White	II
CHE-CNRCB 368	Coleccion de Hongos Entomopatogenos del Centro Nacional de Referencia de Control Biologico	Not reported	*Phyllophaga* sp.	Colorless	Thin powdery	White	II
CHE-CNRCB 408	Coleccion de Hongos Entomopatogenos del Centro Nacional de Referencia de Control Biologico	San Luis Potosi, Mexico	"Burrito de alfalfa"	Colorless	Thin powdery	White	II
CHE-CNRCB 409	Coleccion de Hongos Entomopatogenos del Centro Nacional de Referencia de Control Biologico	San Luis Potosi, Mexico	"Burrito de alfalfa"	Colorless	Thin powdery	White	II
CHE-CNRCB 417	Coleccion de Hongos Entomopatogenos del Centro Nacional de Referencia de Control Biologico	Puebla, Mexico	*Phyllophaga* sp.	Colorless	Thin powdery	White	II
CHE-CNRCB 420	Coleccion de Hongos Entomopatogenos del Centro Nacional de Referencia de Control Biologico	Puebla, Mexico	Adult beetle	Colorless	Thin powdery	White	II
CHE-CNRCB 606	Coleccion de Hongos Entomopatogenos del Centro Nacional de Referencia de Control Biologico	Not reported	Beetle	Colorless	Thin powdery	White	II
CHE-CNRCB 614	Coleccion de Hongos Entomopatogenos del Centro Nacional de Referencia de Control Biologico	Not reported	*Sphenarium purpurascens*	Colorless	Thin powdery	White	II
CHE-CNRCB 636	Coleccion de Hongos Entomopatogenos del Centro Nacional de Referencia de Control Biologico	Not reported	Not reported	Colorless	Thin powdery	White	II
CHE-CNRCB 637	Coleccion de Hongos Entomopatogenos del Centro Nacional de Referencia de Control Biologico	Not reported	Not reported	Colorless	Thin powdery	White	II

9.5.2. Assessment of Pigmentation, Conidiation Capacity, Colony Phenotype of *B. bassiana*

Frozen conidial suspension stocks were routinely spread-plated on PDA.[256] Qualitative assessment of soluble pigments was performed using media for the induction of red pigments using Czapek Dox Agar (CDA) (Sigma-Aldrich, St Louis, MO, USA) amended with 2% yeast extract (CDAYE) and yellow pigments using Malt Extract Agar (MEA) (BD Difco Laboratories, Sparks, MD, USA). Conidia production capacity was assessed using 0.25× strength Saboraud Dextrose Agar (SDA) (Sigma-Aldrich, St Louis, MO, USA). The growth rate of the fungal isolates was assessed by spot-inoculation of 1×10^7 conidia into the center of the Petri dish using three different media: CDAYE, 0.25× SDA and MEA. Agar plates were incubated upright at 25 °C and colony phenotype observations were carried out daily for 7 d for growth rate assessment or 14-21 d for conidia production. Fungal colony phenotype, texture and pigmentation were categorized qualitatively, based on the phenotypic classification scheme reported by Zhang and co-workers.[250] Group I *B. bassiana* has a white, villous, mycelial colony capable of producing red, agar-diffusible pigments in CDAYE in 3 – 7 d. Group II *B. bassiana* has a creamy white colony, thin-powdery texture and no detectable agar-diffusible pigments. Lastly, Group III is characterized to have a yellow-white mycelial colony with a felty texture and the ability to diffuse yellow pigment(s) in MEA medium. Based on the qualitative phenotyping efforts done on the 93 *B. bassiana* strains, nine strains were selected for targeted assays based on several combinations of criteria: 1) strains that are publicly available, accessible, and taxonomically validated cultures and/or with previously verified virulence gene cluster; 2) a range of phenotypes that will provide a range of insect virulence levels; 3) a range of conidial capacity that may directs product development (i.e. high titer, storage viability) and 4) strains registered and approved for agricultural insect pest managements.

To provide a consistently similar proportion of viable conidia in all our same-day assays, we have established harvesting time points that provided at least 95% viable conidia. Routine conidial viability was estimated for each *B. bassiana* strains utilizing a 7, 14, 21, or a 28 d old 0.25× strength SDA medium-grown *B. bassiana* with modification.[276, 384] Conidia were harvested from the agar medium using a Drigalski spatula and resuspended in 0.1% Tween 80. The conidia were serially 10-fold diluted and 100 uL aliquot was evenly spread-plated on germination medium (2% sucrose, 0.5% peptone, 1.5% agar) plates,[276] followed by incubation at 23 °C for 24 h. The proportion of un-germinated conidia was estimated from three field-of-visions of the duplicate Petri dish cultures under an inverted microscope (Model DM IL-LED, Leica Microsystems, Concord, ON, CAN). Percent germination of $95 \pm 2\%$ was established for the 21 d cultures, which is then used as default source of conidia for all assays, unless otherwise specified. The large differences in conidial viability from solid-powdered preparations necessitated the use of only freshly-harvested conidia, we estimate the conidial titer and proceed to infection of MPB all carried out on the same day.

9.5.3. Development of Insect Media for Selecting Virulent *B. bassiana*

To probe the virulence and insect selectivity of *B. bassiana* in laboratory settings, insect-based media selection approach was developed utilizing carcasses of MPB or European honeybee. Carcasses of MPB were obtained from West Fraser Timber Co. Ltd. (Vancouver, BC, CAN) whereas honeybees were obtained from Beaverlodge Research Farm, Agriculture and Agri-Food Canada (Beaverlodge, AB, CAN). The insects were frozen at –80 °C until processing. Insect powders were prepared by macerating frozen insect carcasses using a mortar and pestle and intermittently flash-frozen with liquid nitrogen until a homogeneous consistency was obtained.

The macerated insect slurry was further lyophilized for 48 h using a Virtis Freeze Dryer model 4K BTXL (SP Industries, Stone Ridge, NY, USA), re-grinded using a mortar and pestle and stored at − 20 °C until use. Six subsamples of each insect powders were analyzed for total carbon, hydrogen, nitrogen, sulfur and oxygen (CHNSO) using a Flash 2000 Organic Elemental Analyzer (Thermo Scientific, Cambridge, UK). Using the insect powders, the mountain pine beetle agar (MPBA) and European honeybee agar (EHBA) were prepared. The media contained 20 g/L insect powder, resuspended in milliQ water, amended with 1.5% agar and sterilized at 121 °C for 15 min. *B. bassiana* conidia were harvested using 0.01% Tween 80 and conidial concentration was estimated using a haemocytometer. A 100 μL aliquot (serially diluted to 1×10^3 conidia/mL) of conidia was spot inoculated on to the center of the agar delivering 100 conidia per spot. Colony diameter was measured after 14 d using a Vernier caliper (Model 316119, MTX) (Bearings Canada Inc, Woodbridge, ON, CAN).

9.5.4. UV Resistance and Monoterpene Tolerance of *B. bassiana*

B. bassiana conidial UV resistance was assessed using the methods of Wang and co-workers,[276] with modifications. The nine selected strains were harvested from a 21 d old CDAYE medium using a Drigalski spatula and resuspended in 0.1% Tween 80. Conidial suspension was filtered into a sterile cheesecloth and assessed qualitatively and quantitatively using a haemocytometer. The conidia were diluted to 1×10^7 conidia/mL and 100 μL was spread plated on germination medium. The opened plates were irradiated with ultraviolet light from a mercury lamp G30T8 (spectral peak = 253.7 nM, UV output = 13.9 W, intensity = ~600 mW/cm^2) (Ushio America, Inc, Cypress, CA, USA) in a Canadian Cabinet, model BM4-2A-49 (Caltec Scientific, Calgary, AB, CAN) for 5, 10, 15, 20, 25, 30, 45, and 60 min exposure. The plates were covered,

removed and photo-reactivated under white light (30 μmol photons m^{-2} s^{-1}) for 5 h and incubated in the dark at 25 °C for 7 d. UV tolerance is defined as the maximum time (min) of UV exposure where conidial growth was observed in the germination medium. To investigate whether UV-resistance in *B. bassiana* could be improved, colonies of strain UAMH 299 that survived the longest UV radiation exposure were transferred to new PDA plates and irradiated for 120 min to allow for the isolation of isolates with increased UV resistance. The process was repeated for two more cycles of increased UV exposure (180 and 220 min, respectively), and subsequent selection of colonies that were not inhibited in their growth by UV irradiation.

B. bassiana conidial growth and resistance in the presence of pine tree microbial defense molecules[277] such as monoterpenes were assessed qualitatively. Simulated monoterpene mixtures from lodgepole pine and jack pine were prepared accordingly to Burke and Carroll.[385] The lodgepole pine monoterpene mixture was simulated via distillation of a commercial lodgepole pine turpentine (Synergy Semiochemicals, Burnaby, BC, CAN) and was previously characterized and chemically-verified using GC-MS analyses while the jack pine monoterpene mixture was reconstituted based on previous assessments of jack pine monoterpene profiles.[243,386] The lodgepole pine distillate contained the following monoterpene ratios: 4.4% (–)-α-pinene, 3.6% (+)-α-pinene, 7% (–)-β-pinene, 22% (+)-3-carene, 5% α-phellandrene, 5% (–)-limonene, 40% (–)-β-phellandrene, and 13% unidentified several minor components. The minor components are terpinolene, myrcene, (+)-limonene, (+)-β-pinene, camphene, γ-terpinene, α-terpineol, and bornyl acetate.[142] Conversely, the reconstituted jack pine had the following component ratios: 12% (–)-α-pinene (99% purity), 45% (+)-α-pinene (99% purity), 10% (–)-β-pinene (99% purity), 27% (+)-3-carene (99% purity), 3% myrcene (90%), 3% (–)-limonene (96% purity).[243] All components of the reconstituted jack pine monoterpene mix were purchased from Sigma-Aldrich (St Louis, MO,

USA). Selected individual monoterpenes were further tested to establish *B. bassiana* strains that can tolerate monoterpenes, including geraniol, (–)-α-pinene and (–)-*trans*-verbenol, as part of the effector molecules involved in MPB aggregation pheromone biosynthetic pathway.[282-283] Commercial pure geraniol (9 % purity) was purchased from Acros Organics (Morris Plains, NJ, USA) while commercial (1S)-(–)-α-pinene (99% purity) was purchased from Sigma-Aldrich (Oakville, ON, CAN) and purified by silica plug using hexane as the eluent. (–)-*trans*-Verbenol was synthesized via oxidation of (1*S*)-(–)-α-pinene using lead tetraacetate, followed by treatment with glacial acetic acid to access the verbenyl acetate, then hydrolysis with potassium hydroxide to afford the crude product, which was purified by column chromatography (eluent system: 10% ethyl acetate in hexanes).[387] A ten-fold dilution of each individual monoterpene or reconstituted mixture was performed with dimethyl sulfoxide as diluent. The pine monoterpene mixtures were diluted in four test concentrations of 1×, 0.1×, 0.01× and 0.001×. Moreover, geraniol was diluted to 650 μM, 65 μM and 6.5 μM; (–)-α-pinene to 700 mM, 70 mM and 7 mM; and lastly (–)-*trans* verbenol to 660 mM, 66 mM and 6.6 mM. Dimethyl sulfoxide served as the solvent control. A spot-on-lawn assay was performed with 1×10^7 conidia for each *B. bassiana* strains pour plated into CDAYE medium. The classical spot-on-lawn assay was carried as described previously[124, 388] where 10-μL aliquots of diluted monoterpenes using a micropipette were spotted on a prepared lawn of conidial strains. Plates were incubated in the dark for 7 d at 25 °C and mycelial growth for monoterpene maximum concentrations tolerated by the fungus was recorded. The assay was performed in triplicates.

9.5.5. Mountain Pine Beetle Rearing

In order to perform bioassays on live MPB, beetles were reared in insect rearing rooms at the University of Alberta (UA) (designated as UA MPB) and University of British Columbia (UBC) (designated as UBC MPB). In late June 2019, UA MPB were reared from two naturally infested lodgepole pine trees felled in Western Alberta, cut into 35 cm long bolts, and sealed with melted wax to reduce moisture loss from cut edges. Infested bolts were stored at 4 °C for two months until placed at 24 °C in rearing bins to collect emerging adult beetles. Emerged beetles were stored at 4 °C on moistened paper towel and separated by sex using external characteristics on the seventh abdominal tergite of the male.[389] The poor MPB yield from naturally infested bolts necessitated us to rear the MPB for the infection assays which also provided a steady supply of MPB during months when beetles are not readily available (i.e. winter season in AB, Canada). On August 6, 2019, bolts were cut from two mature healthy lodgepole pine trees (i.e., without MPB infestation) and waxed the cut edges (bolt diameter >20 cm). These uninfested bolts were stored at 4 °C and moved to 22 °C before introduction of MPB. Each cut bolt was then infested with six pairs of female and male adult beetles. Females were placed into 0.8 cm diameter holes drilled through the bark and spaced equally around the lower section of each bolt followed by males after the females initiated gallery construction.[390] Infested bolts were placed in rearing chambers and stored at 22 °C for one month and then transferred to 4 °C for an additional month. After returning bolts to 22 °C, beetle emergence was monitored for two months. Emerged beetles were stored at 4 °C on moistened paper towel.

UBC MPB were reared in a two-step process. In April 2019, one naturally infested lodgepole pine tree was felled in Western Alberta, cut into 1 m bolts, and transported to UBC where cut edges were sealed with melted wax. Bolts were placed in an emergence cage at 21°C and checked daily for adult emergence for two months. Over a two-week emergence period

beginning in early June, ~150 adults were collected from the bolts and stored at 4 °C on moistened paper towel covered with pine shavings. In late June, when it became apparent that yield from the naturally infested logs would be too low for sufficient replication in upcoming assays, two healthy lodgepole pine trees from coastal British Columbia were felled, cut into 75cm bolts, sealed with melted wax, and placed in an emergence cage. On June 24, 2019, all adult MPB that emerged from the naturally infested logs were deposited in the cage containing uninfested logs and allowed to naturally colonize the material. These bolts were checked daily and emergence commenced in early September. This second emergence period lasted 24 d, after which no further adults were collected during daily checks, yielding ~1000 MPB which were stored at 4 °C on moistened paper towel covered with pine shavings.

9.5.6. Assessment of *B. bassiana* Virulence Against *D. ponderosae* and *A. mellifera*

The conidia were harvested from a 21 d old CDAYE plate culture and used to evaluate the efficacy of *B. bassiana* for causing mortality in three different tests: 1) completely randomized block design for small-scale population of MPB using nine strains of *B. bassiana*, 2) large-scale MPB trial using three representative selected strains UAMH 299, UAMH 4510 and 110.25 of *B. bassiana*, and lastly 3) worker honeybees using strains UAMH 299, UAMH 4510 and 110.25. All tests were done in the dark at 23 °C and relative humidity of ~70%.

In the first test (UA Experiments), the nine *B. bassiana* strains were tested on 10 laboratory-reared MPB with three biological replications. Individual beetles were randomly placed into Petri dishes (6 cm in diameter) lined with a 5.5-cm filter paper (P4) (Fisher Sci, Pittsburgh, PA, USA). The conidial suspension (1×10^8 conidia/mL) was directly applied on the dorsal surface of the beetle's thorax and abdomen in 10-µL aliquots using a micropipette delivering a total of 1×10^6

conidia per beetle. Three biological replicates of unexposed MPB to *B. bassiana* conidia (n = 3) were treated with 10-μL aliquots of either 0.01% Tween 80 or 1×10^7 conidia /mL *Aspergillus nidulans* UAMH 9442 as controls. Beetles were checked daily for mortality and white fungal mycosis, and the number of days until death were recorded for each treatment. The lethal time to kill 50% (LT_{50}) and 100% (LT_{100}) of the population were also recorded.

In the second test (UBC Experiment), three *B. bassiana* strains representing Groups I, II and III, namely: UAMH 299, UAMH 4510 and 110.25, respectively, were tested on 600 MPB. Here, the MPB were categorized into five age classes based on time between adult emergence from infested bolts and exposure to treatments: (1) 0-5 d, (2) 6-10 d, (3) 11-15 d, (4) 16-20 d, and (5) 21-25 d. Three experimental replicates of 10 beetles each placed into Petri dishes (6 cm in diameter) lined with a 5.5 cm filter paper (P4, Fisher Scientific, PA, USA) were made for each age class by treatment combination [n = 10, three replicates, 4 treatments (three *B. bassiana* strains and a control group), 5 age classes, total = 600 MPB]. For MPB exposed to *B. bassiana* strains [n = 10 MPB per plate, (three biological replicates), 5 age classes, 3 strains, total = 450 MPB], conidial suspensions, containing 1×10^7 conidia/mL, were directly applied on the dorsal surface of each MPB's thorax in 10 μL aliquots using a micropipette, delivering a total of 1×10^5 conidia per beetle (1×10^6 conidia per plate). The control beetles [n = 10 MPB per plate, (three biological replicates), 5 age classes, total = 150] were treated with 10 μL aliquots of 0.01% Tween 80. Beetles were checked daily for mortality until total cohort death was recorded for each replicate. Dead beetles were separated from survivors, sexed using a dissecting microscope, comparing the seventh abdominal tergite (heavy pigmentation and angular rear margin for male while homogeneous coloring and curved rear margin for female),[389] and checked daily for fungal mycosis. Mean survival time, LT_{50} and LT_{100} of each replicate were recorded.

In the third test (UA Experiment), *Apis mellifera* worker honeybees were kept in a fabricated flexi glass cage (Figure 9.1) approved by the Alberta Apiary Institute for the laboratory experiments and handling of European honeybees. The colony was fed ad libitum with 20% (w/v) sucrose solution in a slow drip-type feeding conical tube and were acclimated in each cage for at least 3 d prior to application of *B. bassiana* conidia. Representative strains of the three groups of *B. bassiana,* UAMH 299, UAMH 4510 and 110.25, were used for infection experiments utilizing a total of 1×10^7 conidia per cage. The conidial suspension was spread-plated using a Drigalski spatula into the removable base tray of the cage and was reintroduced into the cage for the worker honeybees (n = 50) to passively walk through. Negative control cage was spread with 100 ul 0.01% Tween 80. Cage set-ups were kept at 25 °C in the dark and only exposed to room light briefly during inspection and refilling of sugar solution. Mortality was recorded daily for 14 d. The honeybee infection assays were done in three biological replicates.
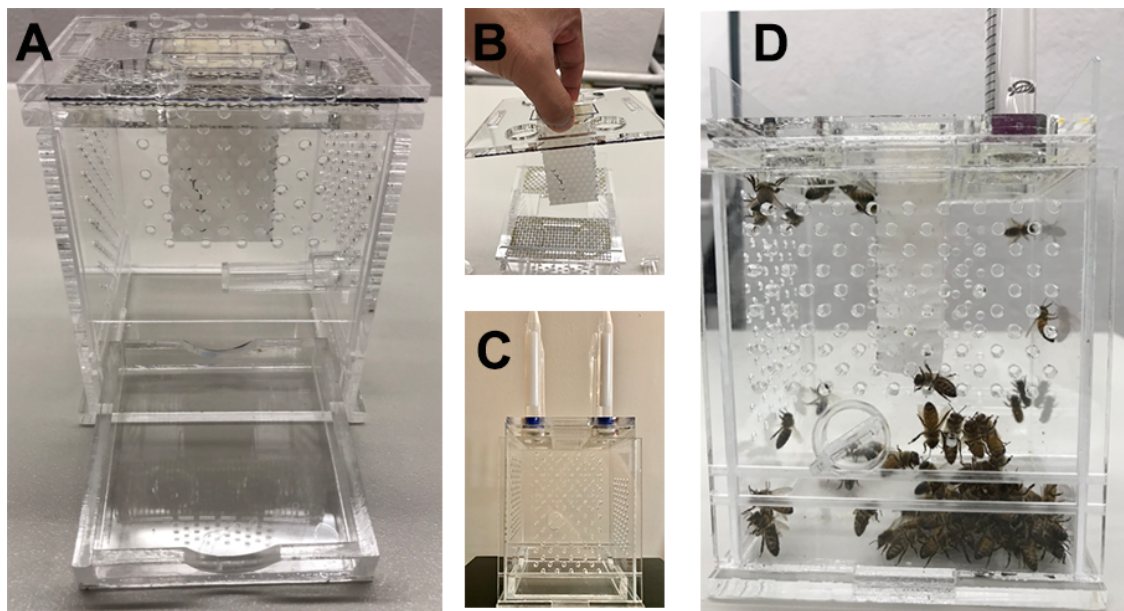
Figure 9.1. Honeybee cage used in *B. bassiana* infection assay. (A) Assembled cage with removable base tray and perforated removable walls, (B) removable top lid with hexagonal plastic hive cell mimics, (C) inverted 15 mL conical sucrose feeder tubes and (D) functional cage with European worker honeybees.

9.5.7. Statistical Analysis

To test whether there are differences in the conidial yield amongst the nine strains of *B. bassiana* grown in 0.25 × SDA for 21 d, analysis of variance (ANOVA) was conducted on the conidial concentration (conidia/mL), with a post hoc Tukey's test.

We tested the effect of insect media on *B. bassiana* growth with an ANOVA with the media type as the fixed effect. Furthermore, we tested whether the growth of each group phenotype differed within each insect media type with an ANOVA and post hoc Tukey's test for multiple comparisons.

To test the effect of each *B. bassiana* strain against the control on the time to LT_{50} and LT_{100} in the first experiment, analysis of covariance (ANCOVA) was used with strain as a main effect and replication as a covariate (lmer function in lmerTest package 3.1-0 in R). MPB LT_{50} and LT_{100} values were log transformed to fit assumptions of normality and homogeneity of variance. A Dunnett's post hoc test was conducted to compare each strain to the control (Dunnett Tests package 2.0). The same analysis to test whether time to mortality of MPB varied with phenotypic group classification (Groups) with a post hoc Tukey's test.

For data from the second experiment, which is the large-scale *B. bassiana* infection assay, age classes were initially not used as a grouping variable and ANOVA was used with treatment as the sole fixed effect (lm function in base R stats package) to test the effect of each *B. bassiana* strain on mean survival time of MPB (15 replicates per treatment). This model did not require data transformation to meet assumptions of normality and homogeneity of variance. Tukey's HSD tests were used to generate pairwise comparisons among treatments (Emmeans package 1.5). A second ANOVA model with treatment, age class, and their interaction as fixed effects was used to assess differences in mean survival time among age-classes within a treatment. The data did not require

transformation to meet assumptions and Tukey's HSD tests were used to make pairwise comparisons among all treatment by age class combinations.

For data from the third experiment, the honeybee infection assay, we performed an ANOVA to test whether the average daily percent mortality differed between three strains. We used a Tukey's post hoc test for multiple comparisons.

To test whether the class II *B. bassiana* has a dose-dependent killing effect on MPB, we used different concentration of strain UAMH 4510 and conducted an ANOVA on the lethal time, LT_{50} and LT_{100} with a post hoc Tukey's test.

To test whether tolerance to host tree monoterpene mixes or individual monoterpenes involved in MPB pheromone biosynthesis varied among strains, we conducted an ANOVA on the maximum concentration that conidia germinated. Similarly, UV tolerance (maximum time that conidia germinated) was tested the same way.

All analyses were performed in R 3.6.0.[391]

9.6. Experimental Procedures for *In Planta* and *In Natura* Studies of *B. bassiana* against MPB

9.6.1. *B. bassiana* Isolates for *In Planta* and *In Natura* Experiments

Several representative *B. bassiana* were selected for large conidial propagation based on the fastest lethal time against MPB, high UV tolerance, and high conidial titer production.[288] These parameters are critical for combined *in planta* bioassays and *in natura* conditions for *B. bassiana* survival and mycoinsecticide effectivity.[277] A proprietary, commercial and agriculturally-approved *B. bassiana* formulation, BioCeres G WP, was provided by Anatis Bioprotection, Inc, Quebec, Canada. Similarly, using an in-house dry powder formulation, *B. bassiana* strains representing the three pigmented phenotypic classes[250,288] were prepared. This include the red-pigmented class I *B. bassiana* (strains UAMH 299 and 1076), the non-pigmented powdery class II *B. basssiana* (strain UAMH 4510), and the yellow-pigmented class III *B. bassiana* (strain 110.25). The in-house *B. bassiana* strains were grown, harvested and tittered as previously reported.[288] The conidia were mixed with the proprietary-based BioCeres kaolin clay-starch-calcium carbonate powder formulation (Anatis BioProtection, QC Canada) at 1:10 conidia:powder ratio for the subsequent *in planta* bioassays and/or *in natura* conditions.

9.6.2. Conidia Production using Biphasic CDBYE-Parboiled Rice Fermentation

In order to access a massive but sustainable source of *B. bassiana* conidia for large-scale greenhouse and field infection assays, a biphasic liquid-solid state fermentation approach was carried out as described previously,[289] with modifications using parboiled rice substrate (C. Hauxwell, personal communication; S. T. Jaronski, personal communication). Three fermentation

trials were carried out from February 2021 to June 2021, namely: Batch 1 (February) – 2 kg rice substrate each for *B. bassiana* strains UAMH 299 and 1076; Batch 2 (April) – 10 kg rice substrate for *B. bassiana* strain UAMH 1076; Batch 3 (May/June) – 10 kg rice substrate with 150 μg/g chloramphenicol for *B. bassiana* strain UAMH 1076. The red pigmented isolates, *B. bassiana* strains UAMH 299 and 1076, were selected from the in-house culture collection as they provide (1) high conidial yield, (2) fastest lethal time against MPB, (3) longest UV resistance exposure time, and (4) ease of harvesting from solid fermentation substrates.[288]

Biphasic fermentation approach started from CDAYE agar-grown conidial inoculum. Conidia were harvested from 21 d old CDAYE medium using a Drigalski spatula and titered to 1.0×10^8 conidia/mL using a haemocytometer.[288] Liquid Czapek Dox medium (100 mL) was inoculated with titered conidia to a final concentration of 1.0×10^7 conidia/mL and incubated at 28 °C for 72 – 96 h at 175 rpm. Commercially bought parboiled rice (Grace Kennedy Inc, Walmart, Canada) was dry sterilized in several batches at 121 °C for 20 min. One-kg aliquot dry rice was autoclaved in a 2 L Erlenmeyer flask and cooled to room temperature for at least overnight. The cooled sterile rice was aseptically cooked with equal volume (1 g/mL) sterile 10% yeast water in a microwave for 6 – 8 min, or until all the liquid has evaporated. The dense mycelial liquid inoculum (72 h grown) was mixed with the room-tempered cooked rice at 100 mL mycelial suspension per 1,000 g cooked parboiled rice. The homogenized mixture was kept in sterile aluminum pans (one inch depth maximum) and incubated at 28 °C, 70% relative humidity under an equal light-dark cycle (12:12 HH) for 10 d. Parboiled rice-mycelial cake was visually inspected for non-white conidiation and pigmentation every three days. To limit bacterial growth throughout the fermentation pipeline, 150 μg mL or μg/g chloramphenicol was amended in each liquid-solid substrate for the third production batch. Subsamples from each batch were assessed for axenic

status by spread-plating a completely randomized collected samples with factorial arrangement (3 × 5).[289] Subsamples were cored using a sterile metal spatula and ten-fold serially-diluted using 0.05% Tween 80 diluent. An aliquot of 100 μL was spread-plated, in duplicate, on CDAYE medium amended with or without 150 μg/mL chloramphenicol. Fungal microcolonies were pre-counted after incubation at 25 °C for 72 h and red pigment-producing *B. bassiana* colony count was verified after 10 d. Conidial yield was compared between parboiled rice fermentation approach and commercial agar media Petri dish production method.

9.6.3. *B. bassiana* Conidia Drying and Harvesting

The conidia were harvested after a two-stage drying approach (S.T. Jaronski, personal communication). First, to induce conidiation of the 10-d old mycelial-rice biomass, the holding fermentation incubator's relative humidity was sequentially brought down from 70% to 50% for five days using a dehumidifier. The second stage drying was carried out for the next five days by bringing down the chamber humidity from 50% down to 20% using a dehumidifier and continuous air fanning. To obtain the conidia as powder, it was necessary to dry the fungal mycelia, and the rice substrate, thus allowing the mechanical separation of the conidia from the parboiled rice substrata.[289]

The dried *B. bassiana*-parboiled rice cake was aseptically hand-crushed to individual grains while being processed inside a sterile BioSafety Cabinet model BM4-2A-49 (Caltec Scientific, AB, Canada). The conidia were harvested as a powder by sieving through a metal mesh (0.25 mm^2) by repeatedly pressing the loosen rice grains against the mesh. Conidial viability was titered as described previously[288] and was used for the subsequent powder carrier development for

pine tree bolt application technology, long term storage viability and *in planta* and *in natura* experimental treatments.

9.6.4. Conidia Powder Formulation Development

The dry formulation reported here was created based on the compacted pesticide powder formulation of Anatis Bioprotection, Inc.[392] The BioCeres commercial powder composition was analyzed using Fourier transform infrared (FTIR) spectrometry and X-ray diffraction analysis. The powder was further subjected to thermal gravimetric analysis (TGA) while a sulfated furnaced-burned ash powder version was analyzed using inductively-coupled plasma – optical emission spectroscopy (ICP-OES) for metal composition. Reference standard chemical controls including kaolin clay, soluble starch, xantham gum and calcium carbonate were purchased from Sigma-Aldrich.

Fourier transform infrared (FTIR) spectra were recorded on a Thermo Fisher Scientific Nicolet™ Continuum™ Infrared Microscope (Madison, WI, USA, 2011) equipped with a range of 4000 cm^{-1} – 650 cm^{-1}, resolution of 4.000, number of scans of 32, an MCT/A detector, an XT-KBR beamsplitter, and a transmittance microscope. The spectra were acquired by the Analytical and Instrumentation Laboratory, Department of Chemistry, University of Alberta. OMNIC version 9.13 software was used for proprietary FTIR data acquisition and analysis.

BioCeres was converted to a sulfated ash using the standard test method described in ASTM for organic materials (ASTM International, 2021). Briefly, the powder was placed in a porcelain crucible and then heated using a Bunsen burner with several drops of concentrated sulfuric acid. The overnight blackened sulfated powder was placed in a muffled furnace and heated at 800 °C for 2.5 h to a gray ash powder for the subsequent analysis. ICP-OES analysis was done

at the Biogeochemical Analytical Service Laboratory at the University of Alberta using an Thermo Scientific ICAP 6300.

9.6.5. *B. bassiana* Conidial Stability Under Various Application Conditions

9.6.5.1. Long-term Conidial Viability at 4 °C Storage.

Five treatments were assessed for the conidial stability of *B. bassiana* under the Anatis BioProtection proprietary-based kaolin clay-starch-calcium carbonate powder formulation. Two batches of the commercial mycoinsecticide BioCeres, containing at least 1.0×10^{10} conidia/g *B. bassiana* strain ANT-03, were provided by Anatis BioProtection Inc (QC, Canada). The first batch was provided in January 2020 (year-old batch) while the second batch was obtained in January 2021 and were both kept at 4 °C until processing (labelled as year-old BioCeres). Conversely, the three in-house batches (strains UAMH 299, UAMH 4510 and 110.25) were harvested from CDAYE medium as previously described.[288] The conidia were mixed with the kaolin clay-starch-calcium carbonate powder targeting a minimum conidial density of 1.0×10^7 conidia/g using a hybridization oven system model 642 (Thermo Scientific, USA). All treatments were kept at 4 °C for weekly subsampling and conidial viability assessment. The five conidial treatments were aseptically sampled weekly for four weeks and after two months. One-gram subsamples were ten-fold serially-diluted using 0.05% Tween 80 diluents. An aliquot of 100 μL was spread-plated, in duplicate, on CDAYE medium amended with 150 μg/mL chloramphenicol. Fungal microcolonies were pre-counted after incubation at 25 °C for 72 h and sporulated *B. bassiana* count was verified after 10 d.

9.6.5.2. Greenhouse *In-Planta* Conidial Viability at 25 °C.

Four conidial treatments were assessed for the viability of conidia in the powder formulations after application on the surface of lodgepole pine tree (*Pinus contorta*) bolts kept in a greenhouse. The greenhouse condition was maintained at 25 °C, 15% relative humidity and under continuous illumination of 30 μmol photons $m^{-2} s^{-1}$. The BioCeres high dose (1.0×10^9 conidia/cm^2) treated bolts were aseptically sampled weekly for eight weeks and after three months. Three 1 cm^2 bark area was swabbed using a letheen broth quick swab kit (3M Inc, ON, Canada). The three other treatments, namely: BioCeres low dose (1.0×10^7 conidia/cm^2), UAMH 299 high dose (1.0×10^8 conidia/cm^2), and UAMH 299 low dose (1.0×10^6 conidia/cm^2) were sampled only at the beginning of the incubation period and after eight weeks, mainly restricted by the experimentally-sealed bins where the pine tree bolts were kept. Viable and culturable *B. bassiana* conidial density were statistically below 1.0×10^3 conidia/cm^2 after the eight-week incubation period and therefore was not tested on the third month. Advance stage of bolt decay on the eighth week incubation period also prompted non-testing on the third month for the three treatments described above.

9.6.5.3. *In Planta* and *In Natura* Conidial Viability in Semi-field Environment (Acreage).

Four conidial treatments were assessed for the viability of conidia in the powder formulations after application on the surface of lodgepole pine tree bolts (*in planta*) and kept in a field acreage farm with mixed tree foliage (*in natura*) for three weeks. The four other treatments, namely: BioCeres high dose (1.0×10^9 conidia/cm^2), BioCeres low dose (1.0×10^7 conidia/cm^2), UAMH 1076 high dose (1.0×10^8 conidia/cm^2), and UAMH 1076 low dose (1.0×10^6 conidia/cm^2) were sampled weekly for three weeks. Triplicate 5 cm^2 bark area was swabbed using a letheen

broth quick swab kit (3M Inc, ON, Canada). Swabbed fungal suspension were ten-fold serially-diluted and 100 μl aliquot was spread-plated in duplicates on a CDAYE agar with 150 μg/mL chloramphenicol. Viable and culturable *B. bassiana* conidial density below 1.0×10^6 conidia/cm^2 after the three-week incubation period was not further tested. Conidial density lower than 1.0×10^6 conidia/g may potentially result in low infection success in MPB as reported previously.[187] The two trials were carried out from May 7 – 28 and June 4 – 25, 2021 in a private acreage farm located at 52409, Range Road 223, Strathcona County, AB, Canada.

9.6.6. Assessment of *B. bassiana* Mycosis from Emerged MPB

To establish the *in planta* effectivity of the dry powder *B. bassiana* formulations, live mountain pine beetle (MPB) were accessed from both naturally- and laboratory-infested *P. contorta* pine tree bolts. The high *in vitro* MPB virulence[288] and long-term green-house stability of both class I and II *B. bassiana* conidia dry formulation prompted us to test BioCeres and UAMH 299 under greenhouse conditions. In September 2020, naturally infested trees were felled in White Court, Alberta, cut into one-m bolts, and transported to the Department of Renewable Resources, University of Alberta. MPB-infested bolts were sealed with melted wax and overwintered for MPB development for two months at 4 °C incubator, placed in an emergence bin at 25 °C. A portion of the naturally infested bolts provided the F1 generation MPBs were used to infest healthy bolts as described previously.[288]

Five bolt treatments (T) with three replication each were prepared and exposed to different concentrations of BioCeres (T1, T2), UAMH 299 (T3, T4), and a control (T5). The BioCeres or the harvested *B. bassiana* UAMH 299 were diluted using the reconstituted kaolin clay-starch-calcium carbonate powder: T1 – BioCeres at 1.0×10^9 CFU/g; T2 – BioCeres at 1.0×10^7 CFU/g;

T3 – UAMH 299 at 1.0×10^8 CFU/g; T4 – UAMH 299 at 1.0×10^6 CFU/g; and T5 – no powder control treatment. The *B. bassiana* powder was sprayed using a mechanical powder duster applicator pump (Amazon, Canada) under a sterile BioSafety Cabinet model BM4-2A-49 (Caltec Scientific, AB, Canada). The bolts were kept in sealed rearing bins with glass traps for emerging MPBs.[390] The bins containing the bolts were kept in a greenhouse in the BioTron Facility, Department of Biological Sciences, University of Alberta at 25 °C, 15% relative humidity and under continuous illumination of 30 µmol photons m^{-2} s^{-1}.

Daily emerged live and dead MPBs from the bolts and reached the glass traps (by phototropism)[390] were counted and collected. All beetles were transferred to a moistened filter paper-lined Petri dish and kept at 25 °C until death of all MPBs were reached (lethal time). Once all MPBs were dead, carcases were transferred individually into a 96-well titer plate (Costar, Corning, USA). The interior of the plates was covered with sterile water-moistened kimwipe paper to maintain a constantly high relative humidity (70 – 90%) and incubated for 14 d at 25 °C. MPB were collected from the bolts in the greenhouse for 55 d. Assessment of mean lethal time and corresponding *B. bassiana* mycosed proportion was reported.

9.6.7. Assessment of *B. bassiana* Mycosis from Debarked Pine Tree Bolts

The bolt-emerged MPBs that remained trapped in the sealed dark container bins (versus MPBs that did not segregate to the glass trap due to positive phototropism) were individually collected, counted and separated into a 96-well titer plate (Costar, Corning, USA) lined with 100 µL CDAYE medium with 150 µg/mL chloramphenicol. The interior of the plates was covered with sterile water-moistened kimwipes paper to maintain a constantly high relative humidity (70 – 90%) and incubated for 14 d at 25 °C. Individual wells containing mycosed MPB were assessed for *B.*

bassiana mycosis using three approaches. First, white powdery MPB surface with distinct granular conidiation[288] was assessed per well. Secondly, the beetles were viewed under a dissecting microscope (Stereomaster, model 12-563-411, Fisher Scientific, USA) and analyzed for distinct *B. bassiana* conidia cluster arrangement (i.e. staphylococcal-like conidial arrangement) at the perpendicular conidiophore's end. Thirdly, nichrome-wire swabbed, lactophenol blue-stained mycelial biomass was viewed under an inverted phase contrast microscope (Axiovert 25, Zeiss, Germany) for *B. bassiana* morphological mycelial assessment. To support the classical Koch's postulate of infection, the *B. bassiana*-infected MPB were touched-point using an inoculating needle and samples were spot-inoculated on a CDAYE media amended with 150 μg/mL chloramphenicol and 100 U/mL nystatin. Non-*B.bassiana* mycosed MPB were tested the same way using CDAYE media amended with 150 μg/mL.

9.6.8. *In Natura* Forest Stand Application of BioCeres Formulation

The robust *in vitro* and *in planta* stability of the commercial dry formulation BioCeres, prompted us to focus our efforts on field trials. This was to test the hypothesis that the active ingredient, *B. bassiana* ANT-03, support pathogenicity and virulence to field populations of MPB in its dynamic forest ecosystem and reduce the reproductive success of MPB for one seasonal cycle. The experimental site is located ~55 km northwest of the town of Hinton, AB, Canada (Figure 9.2).

Field-controlled MPB fungal infection challenge experiments were divided into two infection models, an exit and entry approach. First, an exit experimental model, designated as I (for infested), was designed that involved the use of MPB-infested *P. contorta* bolts incubated with an adjacent healthy *P. contorta* food bolt. The infested bolts were subjected to BioCeres

treatment. This system mimicked a scenario where a freshly emerging MPB from the source infested pine trees will passively pick up the bark-applied *B. bassiana* conidia as they exit the bolts before tunnelling and infesting the healthy food bolts. A second system, an Entry experimental model, designated as H (for healthy), involved the use of BioCeres-treated healthy food bolts and an adjacent MPB-infested pine bolt. The infested bolts will provide the emerging MPB which will attack the healthy food bolt covered in *B. bassiana* conidia. This scenario tested the protective effect of BioCeres on healthy pine trees against the MPB attacks and its reproductive success. The pair of infested and healthy bolts were placed inside a mesh enclosure tent which prevented the escape of any emerging MPB (Figure 9.3).

Two concentrations of BioCeres were chosen based on the *in vitro* effectivity of *B. bassiana* ANT-03, that elicit an effective mean lethal time of 3-5 d.[288] The first dose was titered to 1.0×10^9 CFU/cm^2, designated as H (H for high) while a second dosage at 1.0×10^7 CFU/cm^2, designated as L (L for low) and these were applied on either infested or healthy *P. contorta* bolts.

In, July 18, 2021, each pair of 1.8 m bolts were randomly assigned to five treatments, namely: 1) C – control, untreated bolts; 2) IL – infested bolt treated with a low dosage of BioCeres; 3) HL – healthy bolts treated with low dosage of BioCeres; 4) IH – infested bolts with high BioCeres dose; and lastly 5) HH – healthy bolts with high BioCeres dose. Experimental replications were set at four pairs per treatment. The BioCeres powder was sprayed using a mechanical, hand powered, powder duster applicator pump (Amazon, Canada). After the powder application, the mesh enclosures were sealed to prebent the emerged MPB from flying away and forcing them to attack the adjacent food bolts. A plastic sheet installed on top of the mesh enclosure to mimic the canopy of the pine trees (Figure 9.3) The bolts were left *in situ* until August 31 for a total incubation time of 50 d.

On August 31, 2021, the enclosures were re-opened to establish residual viable conidial titer and harvest 75 cm subsections of each healthy food bolts for debarking and assessment of mean gallery length and mean larval density. The subsections were transported and analyzed at the Department of Forest and Conservation Sciences, University of British Columbia.
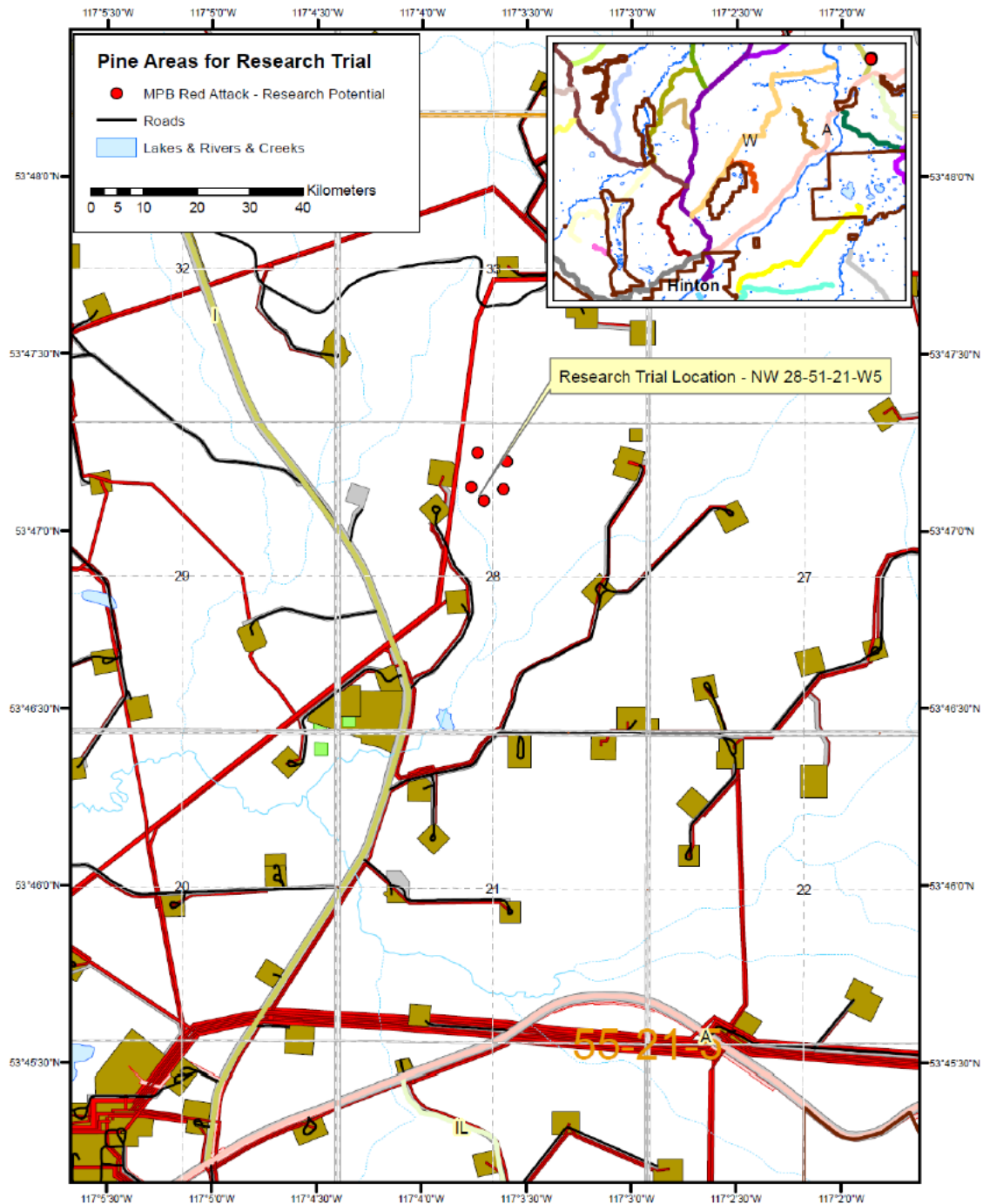
Figure 9.2. Map of field trial site in Hinton, AB, Canada. BioCeres treatments were applied on a pine area for research trial owned by West Fraser, Inc located ~55 km northwest of the town center of Hinton. The *P. contorta* population represent a 100-year-old pine forest stand.

Figure 9.3. Experimental set up for paired infested and healthy *P. contorta* bolts. Front bolt showed white powder application throughout the 1.8 m log section. Mesh enclosures prevented emerged MPB from leaving the tent and forcing them to attack the adjacent healthy food bolt. A plastic sheet installed on top of the mesh tent served as mimic for pine forest canopy shade.

9.6.9. *In Vitro Beauveria bassiana* Competition with *Grossmania clavigera*

Eight *B. bassiana* strains (UAMH 299, UAMH 299[UVR], UAMH 1076, UAMH 298, UAMH 298[UVR], UAMH 4510, ANT-03 and 110.25)[288] were evaluated in four culture media settings for

their ability to inhibit the growth expansion and compete for resource space against two *G. clavigera* isolates (EL 033, EL 035).[393-395] Here, we were testing the hypothesis that certain strains of *B. bassiana* inhibit the MPB symbiont, *G. clavigera* (n = 64 total experimental units). The four culture media representing variable carbon-to-nitrogen (C/N) ratio, namely: PDA (high C/N), MEA and SDA (medium C/N) and CDAYE (low C/N), were used to assess for potential media-dependent competition or inhibition effects. The *G. clavigera* fungal inoculum was grown on their respective media at 25 °C, for at least 10 d or until complete melanization was attained. Similarly, *B. bassiana* inoculum was grown at 25 °C for 2-4 d or until the mycelial mass occupied ~67% of the media without visually-discernable conidiation. Agar blocks (1 cm^2) were aseptically excised and invertedly placed on the surface of the same corresponding media. The two competing fungal species agar blocks were placed on opposite ends of the plate at 10 mm from the edge of a 95 mm Petri dish (Fisherbrand, Waltham, MA) and incubated upright at 25 °C. The growth rate, as defined as surface mycelial expansion per unit time, was recorded daily. Fungal pigmentation, such as melanin production in *G. clavigera* or oosporein/tenellin production in *B. bassiana* isolates, were visually inspected. The Petri plates were scanned (Epson Perfection, V39, USA) either when the two fungal front mycelial mass made contact (no competition) or when zone of inhibition (antagonism) remained constant. The images showing the ability of either fungus to maintain its occupied media resource space were analyzed using ImageJ software version 1.45 S (NIH, Washington, D.C).[396] Total Petri dish area occupied by *B. bassiana* for each replicate was treated as the response variable.[252]

9.6.10. Mycelial Production for Whole Genome Sequencing

Eight morphologically similar but variably pigmented *B. bassiana* strains[187] were selected and grown to establish high quality draft genome reference sequences. Starting fungal inoculum was obtained from frozen mycelial stocks and were re-activated using CDAYE medium and incubated at 25 °C for 4-6 weeks, or until conidial lawn is at its maximum. Conidia were harvested from the agar media, titered and inoculated a 100-mL CDAYE broth medium in baffled-500 mL Erlenmeyer flask to a final concentration of 1.0×10^7 conidia/mL and incubated at 28 °C for 72-96 h at 175 rpm. Mycelia were harvested by centrifugation using an Avanti J-E (Beckman Coulter, USA) with JLA-16.250 rotor at $5,000 \times g$ for 20 min at 4 °C. The resulting mycelial pellet was washed twice with ice-cold TE (10 mM Tris – 1mM EDTA) buffer, pH 8.0 and flashed frozen in liquid nitrogen, and stored at –80 °C until processing. Quality control analysis for bacterial contamination was carried out for all samples. An aliquot of the mycelial slurry was serially-diluted ten-fold up to 1.0×10^{-6} and all dilutions were spread-plated, in quadruplicate, on Standard Methods Agar (SMA, BD Difco Laboratories, Sparks, MD, USA) with 100 U/mL nystatin. The duplicate plates were incubated at either 28 or 35 °C for 48 – 72 h to check for bacterial load. Frozen mycelial pellets were sent to the Michael Smith Laboratories, University of British Columbia for DNA extraction followed by an Illumina HiSeqX 150 sequencing of a chromium genome library at the BC Cancer Genome Sciences Centre for a minimum genome coverage target of 15×. Genome assembly, annotation and analyses were performed at the BC Cancer Genome Sciences Centre.

9.6.11. Bioinformatic Analysis of Biosynthetic Gene Clusters in *B. bassiana*

The observed antifungal (*G. clavigera*) properties of *B. bassiana* can be inferred from the secondary metabolite biosynthetic gene cluster (BGC) encoded in its genome. Genome sequence

analysis for secondary metabolites encoded in BGCs was done using the fungiSMASH v6.0.0.[379] Identified clusters and their genes involved in scaffold assembly were verified against the MIBiG database[380] and in silico validated by BLASTP comparison.[358] FungiSMASH used the CASSIS algorithm for prediction of boundaries of gene clusters while SANDPUMA algorithm was employed to enhance substrate specificity predictions of secondary metabolites.[397] The predictions utilized the relaxed cluster mining mode and all featured algorithms were configured to "on" thus establishing a comprehensive inventory of known and putative secondary metabolites and their associated biosynthetic gene clusters. The inventory of featured algorithms included the following: (1) known cluster blast, (2) cluster blast, (3) sub cluster blast, (4) MIBiG cluster comparison, (5) active site finder, (6) RRE finder, (7) cluster Pfam analysis, (8) Pfam-based GO term annotation, and lastly, (9) TIGRfam analysis.[162]

9.6.12. Mycelial Production for RNA Extraction and Transcriptome Sequencing

The genetic conservation of the oosporein biosynthetic gene cluster detected in all the eight *B. bassiana* sequenced genomes raised the question of a potential transcriptional or post-transcriptional control in the expression of the gene cluster. The pleiotropic red phenotype reported in several *B. bassiana* global strain collection[288] prompted us to probe the transcriptomic profile of the eight *B. bassiana* strains in response to red pigmentation-dependent growth conditions (i.e. low C/N ratio). The fungal inoculum was reactivated from frozen mycelial stocks by spot-inoculation at the center of a PDA medium and incubated at 25 °C for 3 – 5 d. A one-cm^2 agar block was cored on the expanding mycelial culture and transferred to four differential pigment-inducing media, namely: CDAYE for red pigmentation, MEA for yellow pigmentation, PDA for yellow pigmentation and 0.25× SDA medium for induction of conidiation. After comparative

quality analysis of cultures based on morphology, condiation density and pigmentation response,[288] the conidia from the 0.25× SDA were harvest, tittered and inoculated in a 25-mL CDAYE broth medium in a 250 mL Erlenmeyer flask to a final concentration of 1.0×10^7 conidia/mL and incubated at 28 °C for 72 h at 175 rpm. The active mycelial culture was inoculated (10% v/v inoculum) then in a 100-mL CDAYE broth medium in a baffled-500 mL Erlenmeyer flask and incubated at 28 °C for 72 – 96 h at 175 rpm. The mycelial slurries were harvested using a Stericup Quick Release-GP vacuum filtration system (0.22 µm, polyethersulfone membrane) (Millipore-Sigma, USA). The mycelial mat was aseptically transferred to a 50 mL conical tube, flash frozen in liquid nitrogen, and stored at –80 °C until processing. Likewise, the corresponding filtrates were saved and frozen at –80 °C for oosporein analysis. Quality control analysis for bacterial contamination was carried out for all samples as described above. Frozen mycelial mats were sent to the Michael Smith Laboratories, University of British Columbia for RNA extraction followed by an Illumina HiSeq at the BC Cancer Genome Sciences Centre. Transcriptome assembly, annotation, mapping reads, and analyses were performed at the BC Cancer Genome Sciences Centre.

References

1. Challis, G.L. Genome mining for novel natural product discovery. *J Med Chem*. **2008**, *51*, 2618-2628.

2. Kenshole, E.; Herisse, M.; Michael, M.; Pidot, S.J. Natural product discovery through microbial genome mining. *Curr Opin Chem Biol*. **2021**, *60*, 47-54.

3. Xue, A.; Robbins, N.; Cowen, L.E. Advances in fungal chemical genomics for the discovery of new antifungal agents. *Ann N Y Acad Sci*. **2021**, *1496*, 5-22.

4. Shekhar, S.; Sundaramanickam, A.; Balasubramanian, T. Biosurfactant producing microbes and their potential applications: a review. *Crit Rev Environ Sci Technol*. **2015**, *45*, 1522-1554.

5. Bhanot, A.; Sharma, R.; Noolvi, M.N. Natural sources as potential anti-cancer agents: A review. *Int J Phytomed*. **2011**, *3*, e09.

6. Islam, W.; Adnan, M.; Shabbir, A.; Naveed, H.; Abubakar, Y.S.; Qasim, M.; Tayyab, M.; Noman, A.; Nisar, M.S.; Khan, K.A.; Ali, H. Insect-fungal-interactions: A detailed review on entomopathogenic fungi pathogenicity to combat insect pests. *Microb Pathog*. **2021**, 159, 1-16.

7. Foulston, L. Genome mining and prospects for antibiotic discovery. *Curr Opin Microbiol*. **2019**, *51*, 1-8.

8. Brakhage, A.A.; Schuemann, J.; Bergmann, S.; Scherlach, K.; Schroeckh, V.; Hertweck, C. Activation of fungal silent gene clusters: a new avenue to drug discovery. In: Petersen, F.; Amstutz, R. (eds) Natural Compounds as Drugs. Progress in Drug Research. **2008**, 66, 1-12.

9. Liu, Z.; Zhao, Y.; Huang, C.; Luo, Y. Recent advances in silent gene cluster activation in *Streptomyces*. *Front Bioeng Biotechnol*. **2021**, *9*, 1-10.

10. Medema, M.H.; Blin, K.; Cimermancic, P.; De Jager, V.; Zakrzewski, P.; Fischbach, M.A.; Weber, T.; Takano, E.; Breitling, R. antiSMASH: rapid identification, annotation and analysis of secondary metabolite biosynthesis gene clusters in bacterial and fungal genome sequences. *Nucleic Acids Res*. **2011**, *39,* W339-W346.

11. de Jong, A.; van Hijum, S.A.; Bijlsma, J.J.; Kok, J.; Kuipers, O.P. BAGEL: a web-based bacteriocin genome mining tool. *Nucleic Acids Res*. **2006**, *34*, W273-W279.

12. Tietz, J.I.; Schwalen, C.J.; Patel, P.S.; Maxson, T.; Blair, P.M.; Tai, H-C.; Zakai, U.I.; Mitchell, D.A. 2017. A new genome-mining tool redefines the lasso peptide biosynthetic landscape. *Nat Chem Biol.* **2017**, *13*, 470-478.

13. de Los Santos, E.L. NeuRiPP: Neural network identification of RiPP precursor peptides. *Sci Rep*. **2019**, *9*, 1-9.

14. Vizcaino, M.I.; Guo, X.; Crawford, J.M. Merging chemical ecology with bacterial genome mining for secondary metabolite discovery. *J Ind Microbiol Biotechnol*. **2014**, *41*, 285-299.

15. Medema, M.H.; Kottmann, R.; Yilmaz, P.; Cummings, M.; Biggins, J.B.; Blin, K.; De Bruijn, I.; Chooi, Y.H.; Claesen, J.; Coates, R.C.; Cruz-Morales, P. Minimum information about a biosynthetic gene cluster. *Nat Chem Biol*. **2015**, *11*, 625-631.

16. Gilchrist, C.L.; Li, H.; Chooi, Y.H. Panning for gold in mould: can we increase the odds for fungal genome mining? *Org Biomolec Chem*. **2018**, *16*, 1620-1626.

17. Kessler, S.C.; Chooi, Y.H. Out for a RiPP: challenges and advances in genome mining of ribosomal peptides from fungi. *Nat Prod Rep*. **2021**, 1-9.

18. Økstad, O.A.; Kolstø, A.B. Genomics of *Bacillus* species. In: Genomics of foodborne bacterial pathogens. Springer, New York. **2011**, 29-53.

19. Patel, S.; Gupta, R.S. A phylogenomic and comparative genomic framework for resolving the polyphyly of the genus *Bacillus*: Proposal for six new genera of *Bacillus* species, *Peribacillus* gen. nov., *Cytobacillus* gen. nov., *Mesobacillus* gen. nov., *Neobacillus* gen. nov., *Metabacillus* gen. nov. and *Alkalihalobacillus* gen. nov. *Int J Syst Evol Microbiol*. **2020**, *70*, 406-438.

20. Sharma, A.; Satyanarayana, T. Comparative genomics of *Bacillus* species and its relevance in industrial microbiology. *Gen Insights*. **2013**, *6*, GEI-S12732.

21. Cohn, F. Untersuchungen über Bacterien. Beitrage zur Biologie der Pflanzen. **1872**, *1*, 127–244.

22. Soule, M. Identity of *Bacillus subtilis*, Cohn 1872. *J Infect Dis*. **1932**, *51*, 191–215.

23. Priest, F.G. Systematics and ecology of *Bacillus*. In: *Bacillus subtilis* and other Gram-positive bacteria - Biochemistry, physiology, and molecular genetics. In: Sonenshein, A.L.; Hoch, J.A.; Losick, R. (eds.) ASM Press American Society for Microbiology, Washington, D.C. **1993**, 1-55581-053-5.

24. Nicholson, W.L.; Munakata, N.; Horneck, G.; Melosh, H.J.; Setlow, P. Resistance of *Bacillus* endospores to extreme terrestrial and extraterrestrial environments. *Microbiol Molec Biol Rev*. **2000**, *64*, 548-572.

25. Drobniewski, F.A. *Bacillus cereus* and related species. *Clin Microbiol Rev*. **1993**, *6*, 324–338.

26. Gupta, R.S.; Patel, S.; Saini, N.; Chen, S. Robust demarcation of 17 distinct *Bacillus* species clades, proposed as novel Bacillaceae genera, by phylogenomics and comparative genomic analyses: Description of *Robertmurraya kyonggiensis* sp. nov. and proposal for an emended genus *Bacillus* limiting it only to the members of the *Subtilis* and *Cereus* clades of species. *Int J Syst Evol Microbiol*. **2020**, *70*, 5753-5798.

27. Alcaraz, L.D.; Moreno-Hagelsieb, G.; Eguiarte, L.E.; Souza, V.; Herrera-Estrella, L.; Olmedo, G. Understanding the evolutionary relationships and major traits of *Bacillus* through comparative genomics. *BMC Gen*. **2010**, *11*, 1-7.

28. Earl, A.M.; Losick, R.; Kolter, R. Ecology and genomics of *Bacillus subtilis*. *Trends Microbiol*. **2008**, *16*, 269-275.

29. Rasko, D.A.; Altherr, M.R.; Han, C.S.; Ravel, J. Genomics of the *Bacillus cereus* group of organisms. *FEMS Microbiol Rev*. **2005**, *29*, 303-329.

30. Ibrahim, M.A.; Griko, N.; Junker, M.; Bulla, L.A. *Bacillus thuringiensis*: a genomics and proteomics perspective. *Bioeng Bugs*. **2010**, *1*, 31-50.

31. Zheng, J.; Gao, Q.; Liu, L.; Liu, H.; Wang, Y.; Peng, D.; Ruan, L.; Raymond, B.; Sun, M. Comparative genomics of *Bacillus thuringiensis* reveals a path to specialized exploitation of multiple invertebrate hosts. *MBio*. **2017**, *8*, e00822-17.

32. Katz, L.; Baltz, R.H. Natural product discovery: past, present, and future. *J Ind Microbiol Biotechnol*. **2016**, *43*, 155-176.

33. Cochrane, S.A.; Vederas, J.C. Lipopeptides from *Bacillus* and *Paenibacillus* spp.: a gold mine of antibiotic candidates. *Med Res Rev*. **2016**, *36*, 4-31.

34. Xu, B.H.; Lu, Y.Q.; Ye, Z.W.; Zheng, Q.W.; Wei, T.; Lin, J.F.; Guo, L.Q. Genomics-guided discovery and structure identification of cyclic lipopeptides from the *Bacillus siamensis* JFL15. *PloS One*. **2018**, *13*, e0202893.

35. Nett, M.; Ikeda, H.; Moore, B.S. Genomic basis for natural product biosynthetic diversity in the actinomycetes. *Nat Prod Rep*. **2009**, *26*, 1362-1384.

36. Demain, A.L. Importance of microbial natural products and the need to revitalize their discovery. *J Ind Microbiol Biotechnol*. **2014**, *41*, 185–201.

37. World Health Organization. Fact sheets on sustainable development goals: health targets. Antimicrobial Resistance. **2017**, Retrieved from https://www.euro.who.int/ on Oct 11 2021.

38. Cheeptham, N.; Sadoway, T.; Rule, D.; Watson, K.; Moote, P.; Soliman, L.C.; Azad, N.; Donkor, K.K.; Horne, D. Cure from the cave: volcanic cave actinomycetes and their potential in drug discovery. *Int J Speleol.* **2013**, *42*, 35-47.

39. Tiwari, K.; Gupta, R.K. Rare actinomycetes: a potential storehouse for novel antibiotics. *Cri Rev Biotechnol*. **2012**, *32*,108-132.

40. Law, J.W.; Letchumanan, V.; Tan, L.T.; Ser, H.L.; Goh, B.H.; Lee, L.H. The rising of "Modern Actinobacteria" era. *Prog Microbe Mol Biol*. **2020**, *3*, 1-6.

41. Foulston, L. Genome mining and prospects for antibiotic discovery. *Curr Opin Microbiol*. **2019**, *51*, 1-8.

42. Xu, M.; Wright, G.D. Heterologous expression-facilitated natural products' discovery in actinomycetes. *J Ind Microbiol Biotechnol*. **2019**, *46*, 415-431.

43. Mitousis, L.; Thoma, Y.; Musiol-Kroll, E.M. An update on molecular tools for genetic engineering of actinomycetes—the source of important antibiotics and other valuable compounds. *Antibiotics*. **2020**, *9*, 1-31.

44. Kurtböke, D.I. Biodiscovery from rare actinomycetes: an eco-taxonomical perspective. *Appl Microbiol Biotechnol*. **2012**, *93*, 1843-1852.

45. Baltz, R.H. Renaissance in antibacterial discovery from actinomycetes. *Curr Opin Pharmacol*. **2008**, *8*, 557-563.

46. Getahun, D. Predictions of climate change on agricultural insect pests vis-à-vis food crop productivity: a critical review. *Ethiopian J Sci Sust Develop*. **2020**, *7*, 18-26.

47. Wilson, R.J.; Fox, R. Insect responses to global change offer signposts for biodiversity and conservation. *Ecol Entomol*. **2021**, *46*, 699-717.

48. Larson, E.L.; Tinghitella, R.M.; Taylor, S.A. Insect hybridization and climate change. *Front Ecol Evol*. **2019**, *7*, 1-11.

49. Pato, J.; Illera, J.C.; Obeso, J.R.; Laiolo, P. The roles of geography, climate and sexual selection in driving divergence among insect populations on mountaintops. *J Biogeogr*. **2019**, *46,* 784-795.

50. Brooks, D.R.; Boeger, W.A. Climate change and emerging infectious diseases: Evolutionary complexity in action. *Curr Opin Syst Biol*. **2019**, *13*, 75-81.

51. Maina, U.M.; Galadima, I.B.; Gambo, F.M.; Zakaria, D. A review on the use of entomopathogenic fungi in the management of insect pests of field crops. *J Entomol Zool Stud*. **2018**, *6*, 27-32.

52. Rajmohan, K.S.; Chandrasekaran, R.; Varjani, S. A review on occurrence of pesticides in environment and current technologies for their remediation and management. *Indian J Microbiol*. **2020**, *60*, 125-138.

53. Özkara, A.; Akyıl, D.; Konuk, M. Pesticides, environmental pollution, and health. In Environmental health risk-hazardous factors to living species. *Intech Open*. **2016**, *1*, 1-31.

54. Ji, C.; Song, Q.; Chen, Y.; Zhou, Z.; Wang, P.; Liu, J.; Sun, Z.; Zhao, M. The potential endocrine disruption of pesticide transformation products (TPs): The blind spot of pesticide risk assessment. *Environ Inter*. **2020**, *137*, e105490.

55. Grabowski, P.; Musumba, M.; Palm, C.; Snapp, S. Sustainable agricultural intensification and measuring the immeasurable: Do we have a choice?. In Routledge Handbook of Sustainability Indicators. **2018**, 453-476.

56. Nechols, J.R. The potential impact of climate change on non-target risks from imported generalist natural enemies and on biological control. *BioControl*. **2021**, *66*, 37-44.

57. Skendžić, S.; Zovko, M.; Živković, I.P.; Lešić, V.; Lemić, D. The impact of climate change on agricultural insect pests. *Insects*. **2021**, *12*, 1-31.

58. Dara, S.K.; Montalva, C.; Barta, M. Microbial control of invasive forest pests with entomopathogenic fungi: A review of the current situation. *Insects*. **2019**, *10*, e341.

59. Litwin, A.; Nowak, M.; Różalska, S. Entomopathogenic fungi: unconventional applications. *Rev Environ Sci Biotechn*. **2020**, *19*, 23-42.

60. Karabörklü, S.; Azizoglu, U.; Azizoglu, Z.B. Recombinant entomopathogenic agents: a review of biotechnological approaches to pest insect control. World J Microbiol Biotechnol. **2018**, *34*, 1-12.

61. Harith-Fadzilah, N.; Abd Ghani, I.; Hassan, M. Omics-based approach in characterising mechanisms of entomopathogenic fungi pathogenicity: A case example of *Beauveria bassiana*. *J King Saud Uni Sci*. **2020**, *33*, 1-12.

62. Kepler, R.M.; Luangsa-Ard, J.J.; Hywel-Jones, N.L.; Quandt, C.A.; Sung, G.H.; Rehner, S.A.; Aime, M.C.; Henkel, T.W.; Sanjuan, T.; Zare, R.; Chen, M. A phylogenetically-based nomenclature for Cordycipitaceae (Hypocreales). *IMA Fungus*. **2017**, *8*, 335-353.

63. Humber, R.A. Identification of entomopathogenic fungi, In: Manual of Techniques in Invertebrate Pathology. **2012**, 151–187.

64. Goettel, M.S.; Jaronski, S.T. Safety and registration of microbial agents for control of grasshoppers and locusts. *Memoirs Entomol Soc Can*. **1997**, *129*, 83-99.

65. Mascarin, G.M.; Jaronski, S.T. The production and uses of *Beauveria bassiana* as a microbial insecticide. *World J Microbiol Biotechnol*. **2016**, *32*, 1-26.

66. Rehner, S.A.;Buckley, E. A *Beauveria* phylogeny inferred from nuclear ITS and EF1-α sequences: evidence for cryptic diversification and links to *Cordyceps* teleomorphs. *Mycologia*. **2005**, *97*, 84-98.

67. Ainsworth, G.C. Agostino Bassi, 1773 – 1856. *Nature*. **1956**, *177*, 255-257.

68. de Faria, M.R.; Wraight, S.P. Mycoinsecticides and mycoacaricides: a comprehensive list with worldwide coverage and international classification of formulation types. *Biol Contr*. **2007**, *43*, 237-256.

69. Rajput, S. *In vivo* and *in vitro* evaluation of *Beauveria bassiana* pathogenicity for western flower thrips, *Frankliniella occidentalis. Educ Res Arch*. **2006**. 1-218.

70. Steinkraus, D.C.; Tugwell, N.P. *Beauveria bassiana* (Deuteromycotina: Moniliales) effects on *Lygus lineolaris* (Hemiptera: Miridae). *J Entomol Sci*. **1997**, *32*, 79-90.

71. Quintela, E.D.; McCoy, C.W. Pathogenicity enhancement of *Metarhizium anisopliae* and *Beauveria bassiana* to first instars of *Diaprepes abbreviatus* (Coleoptera: Curculionidae) with sublethal doses of imidacloprid. *Environ Entomol*. **1997**, *26*, 1173-1182.

72. Quintela, E.D.; McCoy, C.W. Synergistic effect of imidacloprid and two entomopathogenic fungi on the behaviour and survival of *Diaprepes abbreviatus* (Coleoptera: Curculionidae) in soil. *J Econ Entomol*. **1998**, *91*, 110-122.

73. Todorova, S.I.; Coderre, D.; Duchesne, R.-M.; Côté, J.-C. Compatibility of *Beauveria bassiana* with selected fungicides and herbicides. *Environ Entomol*. **1998**, *27*, 427-433.

74. Wraight, S.P.; Ramos, M.E. Synergistic interaction between *Beauveria bassiana* and *Bacillus thuringiensis tenebrionis*-based biopesticides applied against field populations of Colorado potato beetle larvae. *J Invertebr Pathol*. **2005**, *90*, 139-150.

75. Kryukov, V.Y.; Khodyrev, V.P.; Yaroslavtseva, O.N.; Kamenova, A.S.; Duisembekov, B.A.; Glupov, V.V. Synergistic action of entomopathogenic hyphomycetes and the bacteria *Bacillus thuringiensis* ssp. *morrisoni* in the infection of Colorado potato beetle *Leptinotarsa decemlineata*. *Appl Biochem Microbiol*. **2009**, *45*, 511-516.

76. Iqbal, M.; Shaheen, F.A.; Mahmood, R.; Rafique, M.K.; Bodlah, I.; Naz, F.; Raja, M.U. Synergistic effect of entomopathogenic fungi and bacteria against pulse beetle, *Callosobruchus chinensis*. *Pakistan J Zool*. **2019**, *51*, 1-7.

77. Tan, S.Q.; Yin, Y.; Cao, K.L.; Zhao, X.X.; Wang, X.Y.; Zhang, Y.X.; Shi, W.P. Effects of a combined infection with *Paranosema locustae* and *Beauveria bassiana* on *Locusta migratoria* and its gut microflora. *Insect Sci*. **2021**, *28*, 347-354.

78. Corbett, L.J.; Withey, P.; Lantz, V.A.; Ochuodho, T.O. The economic impact of the mountain pine beetle infestation in British Columbia: provincial estimates from a CGE analysis. *Forestry*. **2016**, *89*: 100–105.

79. Janes, J.K.; Li, Y.; Keeling, C.I.; Yuen, M.M.; Boone, C.K.; Cooke, J.E.; Bohlmann, J.; Huber, D.P.; Murray, B.W.; Coltman, D.W.; Sperling, F.A. How the mountain pine beetle (*Dendroctonus ponderosae*) breached the Canadian Rocky Mountains. *Mol Biol Evol*. **2014**, *31*,1803-1815.

80. Keeling, C.I.; Yuen, M.M.; Liao, N.Y.; Docking, T.R.; Chan, S.K.; Taylor, G.A.; Palmquist, D.L.; Jackman, S.D.; Nguyen, A.; Li, M.; Henderson, H. Draft genome of the mountain pine beetle, *Dendroctonus ponderosae* Hopkins, a major forest pest. *Gen Biol*. **2013**, *14*, 1-20.

81. Lusebrink, I.; Erbilgin, N.; Evenden, M.L. The lodgepole × jack pine hybrid zone in Alberta, Canada: a stepping stone for the mountain pine beetle on its journey east across the boreal forest? *J Chem Ecol.* **2013**, *39*, 1209-1220.

82. Rosenberger, D.W.; Venette, R.C.; Maddox, M.P.; Aukema, B.H. Colonization behaviors of mountain pine beetle on novel hosts: Implications for range expansion into northeastern North America. *PloS One*. **2017**, *12*, e0176269.

83. Runyon, J.B.; Fettig, C.J.; Trilling, J.A.; Munson, A.S.; Mortenson, L.A.; Steed, B.E.; Gibson, K.E.; Jørgensen, C.L.; McKelvey, S.R.; McMillin, J.D.; Audley, J.P. Changes in understory vegetation including invasive weeds following mountain pine beetle outbreaks. *Trees For People*. **2020**, *2*, e100038.

84. Janousek, W.M.; Hicke, J.A.; Meddens, A.J.; Dreitz, V.J. The effects of mountain pine beetle outbreaks on avian communities in lodgepole pine forests across the greater Rocky Mountain region. *For Ecol Manag.* **2019**, *444*, 374-381.

85. Soderer, D.N. Susceptibility of high-elevation forests to mountain pine beetle (*Dendroctonus ponderosae* Hopkins) under climate change. *Utah State University Digital Commons*. **2021**, 1-226.

86. Audley, J.P.; Fettig, C.J.; Munson, A.S.; Runyon, J.B.; Mortenson, L.A.; Steed, B.E.; Gibson, K.E.; Jørgensen, C.L.; McKelvey, S.R.; McMillin, J.D.; Negrón, J.F. Impacts of mountain pine beetle outbreaks on lodgepole pine forests in the Intermountain West, US, 2004–2019. For Ecol Manag. **2020**, *475*, e118403.

87. Levesque, K.D. The effect of climate change on mountain pine beetle (*Dendroctonus ponderosae* Hopkins) in Western Canada. *Lakehead University Knowledge Commons*. **2021**, 1-42.

88. Safranyik, L.; Carroll, A.L.; Régnière, J.; Langor, D.W.; Riel, W.G.; Shore, T.L.; Peter, B.; Cooke, B.J.; Nealis, V.G.; Taylor, S.W. Potential for range expansion of mountain pine beetle into the boreal forest of North America. *Can Entomol.* **2010**, *142*, 415-442.

89. Safranyik, L. Mountain pine beetle: biology overview. In: Symposium on the management of lodgepole pine to minimize losses to the mountain pine beetle. USDA Forest Service, Intermountain Forest and Range Experiment Station. **1989**, 9-12.

90. Paine, T.D.; Millar, J.G.; Hanlon, C.C.; Hwang, J.S. Identification of semiochemicals associated with Jeffrey pine beetle, *Dendroctonus jeffreyi. J Chem Ecol.* **1999**, 25, 433-353.

91. Krause, A.M.; Townsend, P.A.; Lee, Y.; Raffa, K.F. Predators and competitors of the mountain pine beetle *Dendroctonus ponderosae* (Coleoptera: Curculionidae) in stands of changing forest composition associated with elevation. *Agric For Entomol*. **2018**, *20*, 402-413.

92. Sambaraju, K.R.; Goodsman, D.W. Mountain pine beetle: an example of a climate-driven eruptive insect impacting conifer forest ecosystems. *CAB Rev*. **2021**,16, 1-8.

93. Safranyik, L.; Carroll, A.L. The biology and epidemiology of the mountain pine beetle in lodgepole pine forests, In: Safranyik L.Wilson B. (eds.), The mountain pine beetle: A synthesis of its biology, management and impacts on lodgepole pine. Natural Resources Canada, Canadian Forest Service, Pacific Forestry Centre, Victoria, Canada. **2006**. 3–66.

94. Reid, R.W. Biology of the mountain pine beetle, *Dendroctonus monticolae* Hopkins, in the East Kootenay Region of British Columbia I. Life Cycle, Brood Development, and Flight Periods1. *Can Entomol*. **1962**, *94*, 531-538.

95. Bleiker, K.P.; O'Brien, M.R.; Smith, G.D.; Carroll, A.L. Characterisation of attacks made by the mountain pine beetle (Coleoptera: Curculionidae) during its endemic population phase. *Can Entomol*. **2014**, *146*, 271–284.

96. Bleiker, K.P.; Van Hezewijk, B.H. Flight period of mountain pine beetle (Coleoptera: Curculionidae) in its recently expanded range. *Environ Entomol*. **2016**, *45*, 1561-1567.

97. Boone, C.K.; Aukema, B.H.; Bohlmann, J.; Carroll, A.L.; Raffa, K.F. Efficacy of tree defense physiology varies with bark beetle population density: a basis for positive feedback in eruptive species. *Can J For Res*. **2011**, *41*, 1174–1188.

98. Raffa, K.F.; Aukema, B.H.; Bentz, B.J.; Carroll, A.L.; Hicke, J.A.; Turner, M.G.; Romme, W.H. Cross-scale drivers of natural disturbances prone to anthropogenic amplification: dynamics of biome-wide bark beetle eruptions. *BioScience*. **2008**, *58*, 501–517.

99. Reeve, J.D.; Anderson, F.E.; Kelley, S.T. Ancestral state reconstruction for *Dendroctonus* bark beetles: evolution of a tree killer. *Environ Entomol*. **2012**, *41*, 723-730.

100.   Lee, S.; Kim, J.J.; Breuil, C. Diversity of fungi associated with mountain pine beetle, *Dendroctonus ponderosae*, and infested lodgepole pines in British Columbia. Natural Resources Canada, Canadian Forest Service, Pacific Forestry Centre, Victoria, Canada. **2006**, 1-22.

101.   Six, D.L. Ecological and evolutionary determinants of bark beetle—fungus symbioses. *Insects*. **2012**, *3*, 339-366.

102.   Harrington, T.C. Biology and taxonomy of fungi associated with bark beetles. In: Beetle pathogen interactions in conifer forest. Schowalter, T.D.; Filip, G.M. (eds) Academic Press, San Diego. USA. **1993**, 37-51.

103.   Harrington, T.C. Ecology and evolution of mycophagous bark beetles and their fungal partners. In: Insect-Fungal Associations: ecology and evolution. Vega F.E. (ed). Oxford University Press, Oxford, UK. **2005**, 257-291.

104.   Lee, S.; Kim, J.J.; Breuil, C. 2005. *Leptographium longiclavatum* sp. nov., a new species associated with the mountain pine beetle, *Dendroctonus ponderosae*. *Mycolog Res*. **2005**, *109*, 1162–1170.

105.   Wang, Y.; DiGuistini, S.; Wang, T.C.; Bohlmann, J.; Breuil, C. *Agrobacterium*-meditated gene disruption using split-marker in *Grosmannia clavigera*, a mountain pine beetle associated pathogen. *Curr Genet*. **2010**, *56*, 297-307.

106.   Hulcr, J.; Barnes, I.; De Beer, Z.W.; Duong, T.A.; Gazis, R.; Johnson, A.J.; Jusino, M.A.; Kasson, M.T.; Li, Y.; Lynch, S.; Mayers, C. Bark beetle mycobiome: collaboratively defined research priorities on a widespread insect-fungus symbiosis. *Symbiosis*. **2020**, *81*, 101-113.

107.   Rice, A.V.; Thormann, M.N.; Langor, D.W. Mountain pine beetle-associated blue-stain fungi are differentially adapted to boreal temperatures. *For Pathol*. **2008**, *38*, 113-123.

108.   Carroll, A.L.; Shore, T.L.; Safranyik, L. Direct control: theory and practice In: Safranyik L, Wilson B (eds) The mountain pine beetle: a synthesis of its biology, management and impacts on lodgepole pine. Natural Resources Canada, Canadian Forest Service, Pacific Forestry Centre, Victoria, British Columbia, **2006**, pp 155-172

109.   Coops, N.C.; Timko, J.A.; Wulder, M.A.; White, J.C.; Ortlepp, S.M. Investigating the effectiveness of mountain pine beetle mitigation strategies. *Int J Pest Manag*. **2008**, *54*, 151-165.

110.   Parker, T.J.; Clancy, K.M.; Mathiasen, R.L. Interactions among fire, insects and pathogens in coniferous forests of the interior western United States and Canada. *Agric For Entomol*. **2006**, *8*,167–189.

111.   Thompson, D.G.; Kreutzweiser, D.P. A review of the environmental fate and effects of natural" reduced-risk" pesticides in Canada. In: Felsot, A.S.; Racke, K.D. (eds) Crop protection products for organic agriculture. ACS Symposium Series, American Chemical Society, Washington, DC **2006**, 245-274.

112.   Thompson, D.G. Ecological impacts of major forest use pesticides. In: Sanchez-Bayo, F.; van den Brink, P.; Mann, R.M. (eds) Ecological impacts of toxic chemicals. Bentham Publishers. Sarjah, United Arab Emirates, **2011**, 88-110.

113.   Palma, L.; Muñoz, D.; Berry, C.; Murillo, J.; Caballero, P. *Bacillus thuringiensis* toxins: an overview of their biocidal activity. *Toxins*. **2014**, *6*, 3296-3325.

114.   Jouzani, G.S.; Valijanian, E.; Sharafi, R. *Bacillus thuringiensis*: a successful insecticide with new environmental features and tidings. *App Microbiol Biotechnol*. **2017**, *101*, 2691-711.

115.   Hellmich, R.L.; Hellmich, K.A. Use and impact of Bt maize. *Nature Education Knowledge*. **2012**, *3*, 1-4.

116.   Mendelsohn, M.; Kough, J.; Vaituzis, Z.; Matthews, K. Are Bt crops safe? *Nat Biotechnol.* **2003**, *21*, 1003-1009.

117.   Bravo, A.; Likitvivatanavong, S.; Gill, S.S.; Soberón, M. *Bacillus thuringiensis*: a story of a successful bioinsecticide. *Insect Biochem Mol Biol*. **2011**, *41*, 423-431.

118.   Pardo-Lopez, L.; Soberon, M.; Bravo, A. *Bacillus thuringiensis* insecticidal three-domain Cry toxins: mode of action, insect resistance and consequences for crop protection. *FEMS Microbiol Rev*. **2012**, *37*, 3-22.

119.   Djenane, Z.; Nateche, F.; Amziane, M.; Gomis-Cebolla, J.; El-Aichar, F.; Khorf, H.; Ferré, J. Assessment of the antimicrobial activity and the entomocidal potential of *Bacillus thuringiensis* isolates from Algeria. *Toxins*. **2017**, *9*, 1-19.

120.   Deepak, R.; Jayapradha, R. Lipopeptide biosurfactant from *Bacillus thuringiensis* pak2310: A potential antagonist against *Fusarium oxysporum*. J Mycol Med. **2015**, *25*, W15-W24.

121.   Stein, T. *Bacillus subtilis* antibiotics: structures, syntheses and specific functions. *Mol Microbiol*. **2005**, *56*, 845-57.

122.   Cochrane, S.A.; Vederas, J.C. Lipopeptides from *Bacillus* and *Paenibacillus* spp.: a gold mine of antibiotic candidates. *Med Res Rev*. **2016**, *36*, 4-31.

123.   Daas, M.S.; Rosana, A.R.R.; Acedo, J.Z.; Nateche, F.; Kebbouche-Gana, S.; Vederas, J.C.; Case, R.J. Draft genome sequences of *Bacillus cereus* E41 and *Bacillus anthracis* F34 isolated from Algerian salt lakes. *Genome Announc*. **2017**, *5*, e00383-17.

124.   Daas, M.S.; Acedo, J.Z.; Rosana, A.R.R.; Orata, F.D.; Reiz, B.; Zheng, Natache, F.; Case, R.J.; Kebbouche-Gana, S.; Vederas, J.C. *Bacillus amyloliquefaciens* ssp. *plantarum* F11 isolated from Algerian salty lake as a source of biosurfactants and bioactive lipopeptides. *FEMS Microbiol Lett*. **2017**, *365*, fnx248.

125.   Sumi, C.D.; Yang, B.W.; Yeo, I.C.; Hahm, Y.T. Antimicrobial peptides of the genus *Bacillus*: a new era for antibiotics. *Can J Microbiol*. **2014**, *61*, 93-103.

126.   Baumann, L.; Okamoto, K.; Unterman, B.M.; Lynch, M.J.; Baumann, P. Phenotypic characterization of *Bacillus thuringiensis* and *Bacillus cereus*. *J Invertebr Pathol*. **1984**, *44*, 329-341.

127.   Barjac, H.; Frachon, E. Classification of *Bacillus thuringiensis* strains. *BioControl*. **1990**, *35*, 233-340.

128.   Gibbons, N.E.; Murray, R.G. Proposals concerning the higher taxa of bacteria. *Int J Syst Evol Microbiol*. **1978**, *28*, 1-6.

129.   West, A.W.; Burges, H.; Dixon, T.J.; Wyborn, C.H. Survival of *Bacillus thuringiensis* and *Bacillus cereus* spore inocula in soil: effects of pH, moisture, nutrient availability and indigenous microorganisms. *Soil Biol Biochem*. **1985**, *17*, 657-665.

130.   Field, D.; Garrity, G.; Gray, T.; Morrison, N.; Selengut, J.; Sterk, P.; Tatusova, T.; Thomson, N.; Allen, M.J.; Angiuoli, S.V.; Ashburner, M. The minimum information about a genome sequence (MIGS) specification. *Nat Biotechnol*. **2008**, *26*, 541-547.

131.   Bertelli, C.; Laird, M.R.; Williams, K.P.; Simon Fraser University Research Computing Group; Lau, B.Y.; Hoad, G.; Winsor, G.L.; Brinkman, F.S. IslandViewer 4: expanded prediction of genomic islands for larger-scale datasets. *Nucleic Acids Res*. **2017**, *45*, W30-W35.

132.   Arndt, D.; Grant, J.R.; Marcu, A.; Sajed, T.; Pon, A.; Liang, Y.; Wishart, D.S. PHASTER: a better, faster version of the PHAST phage search tool. *Nucleic Acids Res*. **2016**, *44*, W16-W21.

133.   He, J.; Wang, J.; Yin, W.; Shao, X.; Zheng, H.; Li, M.; Zhao, Y.; Sun, M.; Wang, S.; Yu, Z. Complete genome sequence of *Bacillus thuringiensis* subsp. *chinensis* strain CT-43. *J Bacteriol*. **2011**, 193, 3407-3408.

134.   Murawska, E.; Fiedoruk, K.; Bideshi, D.K.; Swiecicka, I. Complete genome sequence of *Bacillus thuringiensis* subsp. *thuringiensis* strain IS5056, an isolate highly toxic to *Trichoplusia*. *Genome Announc*. **2013**, *1*, e00108-13.

135.   Wang, P.; Zhang, C.; Guo, M.; Guo, S.; Zhu, Y.; Zheng, J.; Zhu, L.; Ruan, L.; Peng, D.; Sun, M. Complete genome sequence of *Bacillus thuringiensis* YBT-1518, a typical strain with high toxicity to nematodes. *J Biotechnol*. **2014**, *171*, 1-2.

136.   Nicholson, W.L. Roles of *Bacillus endospores* in the environment. *Cell Mol Life Sci*. **2002**, *59*: 410-416.

137.   Abriouel, H.; Franz, C.M.; Ben-Omar, N.; Gálvez, A. Diversity and applications of *Bacillus* bacteriocins. *FEMS Microbiol Rev*. **2011**, *35*, 201-232.

138.   Angelini, T.E.; Roper, M.; Kolter, R.; Weitz, D.A.; Brenner, M.P. *Bacillus subtilis* spreads by surfing on waves of surfactant. *Proc Natl Acad Sci U S A*. **2009**, *106*, 18109-18113.

139.   Borriss, R.; Chen, X.H.; Rueckert, C.; Blom, J.; Becker, A.; Baumgarth, B.; Fan, B.; Pukall, R.; Schumann, P.; Spröer, C.; Junge, H. Relationship of *Bacillus amyloliquefaciens* clades associated with strains DSM 7T and FZB42T: a proposal for *Bacillus amyloliquefaciens* subsp. *amyloliquefaciens* subsp. nov. and *Bacillus amyloliquefaciens* subsp. *plantarum* subsp. nov. based on complete genome sequence comparisons. *Int J Syst Evol Microbiol*. **2011**, *61*, 1786-1801.

140.   Goris. J.; Konstantinidis, K.T.; Klappenbach, J.A.; Coenye, T.; Vandamme, P.; Tiedje, J.M. DNA-DNA hybridization values and their relationship to whole-genome sequence similarities. *Int J Syst Evol Microbiol*. **2007**, *57*, 81-91.

141.   Dunlap, C.A.; Kim, S.J.; Kwon, S.W.; Rooney, A.P. *Bacillus velezensis* is not a later heterotypic synonym of *Bacillus amyloliquefaciens*; *Bacillus methylotrophicus*, *Bacillus amyloliquefaciens* subsp. *plantarum* and '*Bacillus oryzicola*' are later heterotypic synonyms of *Bacillus velezensis* based on phylogenomics. *Int J Syst Evol Microbiol*. **2016**, *66*, 1212-1217.

142.   Fan, B.; Blom, J.; Klenk, H.P.; Borriss, R. *Bacillus amyloliquefaciens*, *Bacillus velezensis*, and *Bacillus siamensis* form an "Operational Group *B. amyloliquefaciens*" within the *B. subtilis* species complex. *Front Microbiol*. **2017**, *8*, 1-22.

143.   Singh, P.; Cameotra, S.S. Potential applications of microbial surfactants in biomedical sciences. *Trends Biotechnol*. **2004**, *22*, 142-146.

144.   Krepsky, N.; Da Silva, F.S.; Fontana, L.F.; Crapez, M.A. Alternative methodology for isolation of biosurfactant-producing bacteria. *Braz J Biol*. 2007, 67, 117-124.

145.   de Oliveira, D.W.; França, I.W.; Félix, A.K.; Martins, J.J.; Giro, M.E.; Melo, V.M.; Gonçalves, L.R. Kinetic study of biosurfactant production by *Bacillus subtilis* LAMI005 grown in clarified cashew apple juice. *Colloids Surf B Biointerfaces*. **2013**, *101*, 34-43.

146.   Ongena, M.; Jacques, P. *Bacillus* lipopeptides: versatile weapons for plant disease biocontrol. *Trends Microbiol*. **2008**, *16,* 115-125.

147.   Zhao, H.; Shao, D.; Jiang, C.; Shi, J.; Li, Q.; Huang, Q.; Rajoka, M.S.; Yang, H.; Jin, M. Biological activity of lipopeptides from *Bacillus*. *Appl Microbiol Biotechnol*. **2017**, *101*, 5951-5960.

148.   Hiradate, S.; Yoshida, S.; Sugie, H.; Yada, H.; Fujii, Y. Mulberry anthracnose antagonists (iturins) produced by *Bacillus amyloliquefaciens* RC-2. *Phytochemistry*. **2002**, *61*, 693-698.

149.   Arguelles-Arias, A.; Ongena, M.; Halimi, B.; Lara, Y.; Brans, A.; Joris, B.; Fickers, P. *Bacillus amyloliquefaciens* GA1 as a source of potent antibiotics and other secondary metabolites for biocontrol of plant pathogens. *Microb Cell Fact* **2009**, *8*, 1-2.

150.   Halimi, B.; Dortu, C.; Arguelles-Arias, A.; Thonart, P.; Joris B.; Fickers, P. Antilisterial activity on poultry meat of amylolysin, a bacteriocin from *Bacillus amyloliquefaciens* GA1. *Probiotics Antimicrob Proteins*. **2010**, *2*, 120-125.

151.   Vanittanakom, N.; Loeffler, W.; Koch, U.; Jung, G. Fengycin-a novel antifungal lipopeptide antibiotic produced by *Bacillus subtilis* F-29-3. *J Antibiot.* **1986**, *39*, 888-901.

152.	Lim, K.B.; Balolong, M.P.; Kim, S.H.; Oh, J.K.; Lee, J.Y.; Kang, D.K. Isolation and characterization of a broad spectrum bacteriocin from *Bacillus amyloliquefaciens* RX7. *Biomed Res Int.* **2016**, *2016*, 1-7.

153.	Carvalho, R.V.; Correa, T.L.R.; Da Silva, J.C.M.; Mansur, L.R.C.O.; Martins, M.L.L. Properties of an amylase from thermophilic *Bacillus* sp. *Braz J Microbiol*. **2008**, *39*, 102–107.

154.	Cordeiro, C.A.M.; Martins, M.L.L.; Luciano, A.B. Production and properties of alpha-amylase from thermophilic *Bacillus* sp. *Braz J Microbiol*. **2002**, *33*, 57-61.

155.	da Silva, C.R.; Delatorre, A.B.; Martins, M.L.L. Effect of the culture conditions on the production of an extracellular protease by thermophilic *Bacillus* sp and some properties of the enzymatic activity. *Braz J Microbiol.* **2007**, *38*, 253-258.

156.	Oliveira, L.R.; Barbosa, J.B.; Martins, M.L.; Martins, M.A. Extracellular production of avicelase by the thermophilic soil bacterium *Bacillus* sp. SMIA-2. *Acta Sci Biol Sci*. **2014,** *36*, 215-222.

157.	Costa, E.A.; Nunes, R.; Cruz, E.; Ladeira, S.A.; Carvalho, R.V.; Martins, M.L.L. Sugarcane bagasse and passion fruit rind flour as substrates for cellulase production by *Bacillus* sp. SMIA-2 strain isolated from Brazilian soil. *J Microbiol Biotechnol*. **2017**, *2*: e000115.

158.	Barbosa, J.B.; Ladeira, S.A.; Martins, M.L.L. Cheese whey and passion fruit rind flour as substrates for protease production by *Bacillus* sp SMIA-2 strain isolated from Brazilian soil. *Biocatal Biotransformation*. **2014**, *32*, 244-250.

159.	Cruz, E.; de Moraes, L.P.; Costa, E.A.; Barbosa, J.B.; Martins, M.L. Optimization of food-waste based culture medium for cellulase production by thermophilic *Bacillus* sp.

SMIA-2 and effect of divalent metal ions on activity and stability of the enzyme at higher temperatures. *Int J Adv Res Sci Eng Technol.* **2019**, *6*, 331-337.

160.   de Souza, A.N.; Martins, M.L. Isolation, properties and kinetics of growth of a thermophilic *Bacillus*. *Braz J Microbiol*. **2001**, *32*, 271-275.

161.   Ladeira, S.A.; Cruz, E.; Delatorre, A.B.; Barbosa, J.B.; Martins, M.L.L. Cellulase production by thermophilic *Bacillus* sp: SMIA-2 and its detergent compatibility. *Electronic J Biotechnol.* **2015**, *18*, 110-115.

162.   Read, T.D.; Peterson, S.N.; Tourasse, N.; Baillie, L.W.; Paulsen, I.T.; Nelson, K.E.; Tettelin, H.; Fouts, D.E.; Eisen, J.A.; Gill, S.R.; Holtzapple, E.K.; Okstad, O.A.; Helgason, E.; Rilstone, J.; Wu, M.; Kolonay, J.F.; Beanan, M.J.; Dodson, R.J.; Brinkac, L.M.; Gwinn, M.; DeBoy, R.T.; Madpu, R.; Daugherty, S.C.; Durkin, A.S.; Haft, D.H.; Nelson, W.C.; Peterson, J.D.; Pop, M.; Khouri, H.M.; Radune, D.; Benton, J.L.; Mahamoud, Y.; Jiang, L.; Hance, I.R.; Weidman, J.F.; Berry, K.J.; Plaut, R.D.; Wolf, A.M.; Watkins, K.L.; Nierman, W.C. The genome sequence of *Bacillus anthracis* Ames and comparison to closely related bacteria. *Nature*, **2003**, 423, 81– 86.

163.   Hotta, K.; Kim, C.Y.; Fox, D.T.; Koppisch, A.T. Siderophore-mediated iron acquisition in *Bacillus anthracis* and related strains. *Microbiology*. **2010**, *156*, 1918–1925.

164.   Xin, B.; Zheng, J.; Liu, H.; Li, J.; Ruan, L.; Peng, D.; Sajid, M.; Sun, M. Thusin, a novel two-component lantibiotic with potent antimicrobial activity against several Gram-positive pathogens. *Front Microbiol*. **2016**, *7*, e1115.

165.   Dunlap, C.A.; Kwon, S.W.; Rooney, A.P.; Kim, S.J. *Bacillus paralicheniformis* sp. nov., isolated from fermented soybean paste. *Int J Syst Evol Microbiol*. **2015**, *65*, 3487-3492.

166.   Koumoutsi, A.; Chen, X.H.; Henne, A.; Liesegang, H.; Hitzeroth, G.; Franke, P.; Vater, J.; Borriss, R. Structural and functional characterization of gene clusters directing nonribosomal synthesis of bioactive cyclic lipopeptides in *Bacillus amyloliquefaciens* strain FZB42. *J Bacteriol*. **2004**, *186*, 1084-1096.

167.   Veith, B.; Herzberg, C.; Steckel, S.; Feesche, J.; Maurer, K.H.; Ehrenreich, P.; Bäumer, S.; Henne, A.; Liesegang, H.; Merkl, R.; Ehrenreich, A. The complete genome sequence of *Bacillus licheniformis* DSM13, an organism with great industrial potential. *J Mol Microbiol Biotechnol*. **2004**, *7*, 204-211.

168.   Vetter, N.D.; Langill, D.M.; Anjum, S.; Boisvert-Martel, J.; Jagdhane, R.C.; Omene, E.; Zheng, H.; Van Straaten, K.E.; Asiamah, I.; Krol, E.S.; Sanders, D.A. A previously unrecognized kanosamine biosynthesis pathway in *Bacillus subtilis*. *J Am Chem Soc*. **2013**, 135, 5970-5973.

169.   Challis, G.L. 2005. A widely distributed bacterial pathway for siderophore biosynthesis independent of nonribosomal peptide synthetases. *Chem Bio Chem*. **2015**, *6*, 601-611.

170.   Blin, K.; Shaw, S.; Steinke, K.; Villebro, R.; Ziemert, N.; Lee, S.Y.; Medema, M.H.; Weber, T. antiSMASH 5.0: updates to the secondary metabolite genome mining pipeline. *Nucleic Acids Res. 2019, 47, W81-W87.*

171.   Rojas, S.M.; Rosana, A.R.R.; Montecillo, A.D.; Arboleda, M.D.; Nacorda, H.M.; Lantican, N.B. Draft genome sequences of six bacteria isolated from the Benham Bank, Philippine Rise, Philippines. *Microbiol Res Announc*. **2019**, *8*, e00777-19.

172.   Al-Ansari, M.; Alkubaisi, N.; Vijayaragavan, P.; Murugan, K. Antimicrobial potential of *Streptomyces* sp. to the Gram positive and Gram negative pathogens. *J Infect Public Health*. **2019**, *12*, 861–866.

173.   Chevrette, M.G.; Carlson, C.M.; Ortega, H.E.; Thomas, C.; Ananiev, G.E.; Barns, K.J.; Book, A.J.; Cagnazzo, J.; Carlos, C.; Flanigan, W.; Grubbs, K.J.; Horn, H.A.;Hoffmann, F.M.; Klassen, J.L.; Knack, J.J.; Lewin, G.R.; McDonald, B.R.; Muller, L.; Melo, W.G.P.; Pinto-Tomas, A.A.; Sschmitz, A.; Wendt-Pienkowski, E.; Wildman, S.; Zhao, M.; Zhang, F.; Bugni, T.S.; Andes, D.R.; Pupo, M.T.; Currie, C.R. The antimicrobial potential of *Streptomyces* from insect microbiomes. *Nat Commun*. **2019**, *10*, 1-11

174.   Braña, A.F.; Sarmiento-Vizcaíno, A.; Osset, M.; Pérez-Victoria, I.; Martín, J.; De Pedro, N.; De la Cruz, M.; Díaz, C.; Vicente, F.; Reyes, F.; García, L.A. Lobophorin K, a new natural product with cytotoxic activity produced by *Streptomyces* sp. M-207 associated with the deep-sea coral *Lophelia pertusa*. *Mar Drugs*. **2017**, *15*, 1-8.

175.   Davies, J.; Wang, H.; Taylor, T.; Warabi, K.; Huang, X.H.; Andersen, R.J. Uncialamycin, a new enediyne antibiotic. *Org Lett*. **2005**, *7*, 5233-5236.

176.   Williams, J.C.; Dutter, B.; Sheldon, J.; Imlay, H.; Skaar, E.; Sulikowski, G. The total synthesis of the siderophore coelichelin. In: Front. Chem. Conference of the National Organization for the Professional Advancement of Black Chemists and Chemical Engineers at the 45th Annual Conference. **2019.**

177.   Motohashi, K.; Takagi, M.; Yamamura, H.; Hayakawa, M.; Shin-Ya, K. A new angucycline and a new butanolide isolated from lichen-derived *Streptomyces* spp. *J Antibiot.* **2010,** *63,* 545-548.

178.   Law, J.W.; Letchumanan, V.; Tan, L.T.; Ser, H.L.; Goh, B.H.; Lee, L.H. The rising of "Modern Actinobacteria" era. *Prog Microbe Mol Biol*. **2020**, *3*, 1-6.

179.   Raymundo, A.K.; Reyes, G.D.; Zulaybar, T.O. Isolation and Identification of local streptomycin-producing actinomycetes. *Philipp Agri*. **1987**, *70*, 61-66.

180.   Papa, I.A.; Zulaybar, T.O.; Raymundo, A.K. Biological control of *Ralstonia solanacearum* and *Erwinia carotovora* by use of locally isolated bacteria. **2008**. Retrieved from https://agris.fao.org/ on February 20, 2021.

181.   Lin, Z.; Koch, M.; Pond, C.D.; Mabeza, G.; Seronay, R.A.; Concepcion, G.P.; Barrows, L.R.; Olivera, B.M.; Schmidt, E.W. Structure and activity of lobophorins from a turrid mollusk associated *Streptomyces* sp. *J Antibiot*. **2014**, *67*, 121–126.

182.   Parungao, M.M.; Maceda, E.B.; Villano, M.A.F. Screening of antibiotic-producing actinomycetes from marine, brackish and terrestrial sediments of Samal Island, Philippines. *J Res Sci Comp Eng*. **2007**, *4*, 29-38.

183.   Sabido, E.M.; Tenebro, C.P.; Suarez, A.F.; Ong, S.D.; Trono, D.J.; Amago, D.S.; Evangelista, J.E.; Reynoso, A.M.; Villalobos, I.G.; Alit, L.D.; Surigao, C.F. Villanueva, C.A.; Saludes, J.P.; Dalisay, D.S. Marine sediment-derived *Streptomyces* strain produces angucycline antibiotics against multidrug-resistant *Staphylococcus aureus* harboring SCCmec type 1 gene. *J Marine Sci Eng* **2020**, *8*, 1-19.

184.   De Leon, M.P.; Park, A.Y.; Montecillo, A.D.; Siringan, M.A.; Rosana, A.R.R.; Kim, S.G.Near-complete genome sequences of *Streptomyces* sp. strains AC1-42T and AC1-42W, isolated from bat guano from Cabalyorisa Cave, Mabini, Pangasinan, Philippines. *Microbiol Res Announc*. **2018**, *7*, e00904-18.

185.   Daquioag, J.E.L.; Penuliar, G.M. Isolation of actinomycetes with cellulolytic and antimicrobial activities from soils collected from an urban green space in the Philippines. *Int J Microbiol.* **2021**, *6699430*, 1-14

186.   Andayani, D.G.; Sukandar, U.; Sukandar, E.Y.; Adnyana, I.K.Antibacterial, antifungal, and anticancer activity of five strains of soil microorganisms isolated from Tangkuban Perahu Mountain by Fermentation. *Hayati J Biosci.* **2015**, *22,* 186-190.

187.   Um, S.; Choi, T.J.; Kim, H.; Kim, B.Y.; Kim, S.H.; Lee, S.K.; Oh, K.B.; Shin, J.; Oh, D.C. Ohmyungsamycins A and B: cytotoxic and antimicrobial cyclic peptides produced by *Streptomyces* sp. from a volcanic island. *J Org Chem.* **2013**, *78*, 12321-12329.

188.   Singh, R.; Dubey, A.K. Isolation and characterization of a new endophytic actinobacterium *Streptomyces californicus* strain ADR1 as a promising source of anti-bacterial, anti-biofilm and antioxidant metabolites. *Microorganisms.* **2020**, 8,(6): 1-18

189.   Kemung, H.M.; Tan, L.T.; Chan, K.G.; Ser, H.L.; Law, J.W.; Lee, L.H.; Goh, B.H. *Streptomyces* sp. strain MUSC 125 from mangrove soil in Malaysia with anti-MRSA, anti-biofilm and antioxidant activities. *Molecules.* **2020**, *15*, 1-20.

190.   Norouzi, H.; Khorasgani, M.R.; Danesh, A. Anti-MRSA activity of a bioactive compound produced by a marine streptomyces and its optimization using statistical experimental design. *Iranian J Basic Med Sci.* **2019**, *22*, 1073–1084.

191.   Naorungrote, S.; Chunglok, W.; Lertcanawanichakul, M.; Bangrak, P. Actinomycetes producing anti-methicillin resistant *Staphylococcus aureus* from soil samples in Nakhon Si Thammarat. *Walailak J Sci Technol.* **2011**, *8*, 131–138.

192.   Zin, N.M.; Al-Shaibani, M.M.; Jalil, J.; Sukri, A.; Al-Maleki, A.R.; Sidik, N.M. Profiling of gene expression in methicillin-resistant *Staphylococcus aureus* in response

to *cyclo*-(L-Val-L-Pro) and chloramphenicol isolated from *Streptomyces* sp., SUK 25 reveals gene downregulation in multiple biological targets. *Arch Microbiol*. **2020**, *202*, 2083–2092.

193. Kemung, H.M.; Tan, L.T.; Khan, T.M.; Chan, K.G.; Pusparajah, P.; Goh, B.H.; Lee, L.H. *Streptomyces* as a prominent resource of future anti-MRSA drugs. *Front Microbiol*. **2018**, *9*, 2221.

194. World Health Organization. Fact sheets on sustainable development goals: health targets. *Antimicrobial Resistance*. **2017**, Retrieved from https://www.euro.who.int/ on March 11 2021.

195. Ghahremani, M.; Jazani, N.H.; Sharifi, Y. Emergence of vancomycin-intermediate and-resistant *Staphylococcus aureus* among methicillin-resistant *S. aureus* isolated from clinical specimens in the northwest of Iran. *J Glob Antimicrob Resist*. **2018**, *14*, 4–9.

196. Roch, M.; Gagetti, P.; Davis, J.; Ceriana, P.; Errecalde, L.; Corso, A.; Rosato, A.E. Daptomycin resistance in clinical MRSA strains is associated with a high biological fitness cost. *Front Microbiol*. **2017**, *8*, 1-9.

197. De Dios-Caballero, J.; Pastor, M.D.; Vindel, A.; Máiz, L.; Yagüe, G.; Salvador, C.; Cobo, M.; Morosini, M.I.; del Campo, R.; Cantón, R.; GEIFQ Study Group. Emergence of *cfr*-mediated linezolid resistance in a methicillin-resistant *Staphyloccous aureus* epidemic clone isolated from patients with cystic fibrosis. *Antimicrob Agent Chemother*. **2016**, *60*, 1878-1882.

198. Suffness, M.; Pezzuto, J.M. Assays related to cancer drug discovery. In: Methods in plant biochemistry: assay for bioactivity. Hostettmann K ed. London: Academic Press. **1990**, 71–133.

199.   Bae, M.; An, J.S.; Hong, S.H.; Bae, E.S.; Chung, B.; Kwon, Y.; Hong, S.; Oh, K.B.; Shin, J.; Lee, S.K.; Oh, D.C. Donghaecyclinones A–C: New cytotoxic rearranged angucyclinones from a volcanic island-derived marine *Streptomyces* sp. *Mar Drugs.* **2020**, *18*, 1-13

200.   Hughes, C.C.; Macmillan, J.B.; Gaudencio, S.P. Jensen, P.R.; Fenical, W. Ammosamides: structures of cell cycle modulators from a marine-derived *Streptomyces* species. *Angew Chem Int Ed Engl*. **2009**, *48*, 725–727.

201.   Kornsakulkarn, J.; Saepua, S.; Srijomthong, K.; Rachtawee, P.; Thongpanchang, C. Quinazolinone alkaloids from actinomycete *Streptomyces* sp. BCC 21795. *Phytochem Lett*. **2015**, *12*, 6–8.

202.   Hohmann, C.; Schneider, K.; Bruntner, C. Caboxamycin, a new antibiotic of the benzoxazole family produced by the deep-sea strain *Streptomyces* sp. NTK 937. *J Antibiot*. **2019**, *62*, 99–104.

203.   Tan, L.T.; Chan, C.K.; Chan, K.G.; Pusparajah, P.; Khan, T.M.; Ser, H.L.; Lee, L.H.; Goh, B.H. *Streptomyces* sp. MUM256: A source for apoptosis inducing and cell cycle-arresting bioactive compounds against colon cancer cells. *Cancers*. **2019**, *11*, 1-25.

204.   Law, J.W.; Law, L.N.; Letchumanan, V.; Tan, L.T.; Wong, S.H.; Chan, K.G.; Ab Mutalib, N.S.; Lee, L.H. Anticancer drug discovery from microbial sources: The unique mangrove *Streptomycetes*. *Molecules.* **2020**, *25*, 1-18.

205.   Ravikumar, S.; Fredimoses, M.; Gnanadesigan, M. Anticancer property of sediment actinomycetes against MCF-7 and MDA-MB231 cell lines. *Asian Pac J Trop Biomed*. **2012**, *2*, 92-96.

206.   Ser, H.L.; Ab Mutalib, N.S.; Yin, W.F.; Chan, K.G.; Goh, B.H.; Lee, L.H. Evaluation of antioxidative and cytotoxic activities of *Streptomyces pluripotens* MUSC 137 isolated from mangrove soil in Malaysia. *Front Microbiol*. **2015**, *6*, 1-11.

207.   Sanjivkumar, M.; Babu, D.R.; Suganya, A.M.; Silambarasan, T.; Balagurunathan, R.; Immanuel, G. Investigation on pharmacological activities of secondary metabolite extracted from a mangrove associated actinobacterium *Streptomyces olivaceus* (MSU3). *Biocatal Agric Biotechnol*. **2016**, *6*, 82–90.

208.   Wayne, L.G. International committee on systematic bacteriology: announcement of the report of the ad hoc Committee on reconciliation of approaches to bacterial systematics. *Zentralbl Bakteriol Mikrobiol Hyg A*. **1988**, *268*, 433-434.

209.   Goris, J.; Konstantinidis, K.T.; Klappenbach, J.A.; Coenye, T.; Vandamme, P.; Tiedje, J.M. DNA-DNA hybridization values and their relationship to whole-genome sequence similarities. *Int J Syst Evol Microbiol*. **2007**, *57*, 81-91.

210.   Meier-Kolthoff, J.P.; Auch, A.F.; Klenk, H.P.; Göker, M. Genome sequence-based species delimitation with confidence intervals and improved distance functions. *BMC Bioinformatics*. **2013**, *14*, 1-14.

211.   Rodriguez-R, L.M.; Gunturu, S.; Harvey, W.T.; Rosselló-Mora, R.; Tiedje, J.M.; Cole, J.R.; Konstantinidis, K.T. The microbial genomes atlas (MiGA) webserver: taxonomic and gene diversity analysis of archaea and bacteria at the whole genome level. *Nucleic Acids Res*. **2015**, *46*, W282-W288.

212.   Hu, D.; Sun, C.; Jin, T.; Fan, G.; Mok, K.M.; Li, K.; Lee, S.M.Y. Exploring the potential of antibiotic production from rare actinobacteria by whole-genome sequencing and guided MS/MS analysis. *Front Microbiol*. **2020**, *11*, 1–12.

213.   Challis, G.L. Exploitation of the *Streptomyces coelicolor* A3 (2) genome sequence for discovery of new natural products and biosynthetic pathways. *J Ind Microbiol Biotechnol*. **2014**, *41*, 219–232.

214.   Maxwell, C.A.; Hartwig, U.A.; Joseph, C.M.; Phillips, D.A. A chalcone and two related flavonoids released from alfalfa roots induce *nod* genes of *Rhizobium meliloti*. *Plant Physiol*. **1989**, *91*, 842-847.

215.   Gürtler, H.; Pedersen, R.; Anthoni, U.; Christophersen, C.; Nielsen, P.H.; Wellington, E.M.; Pedersen, C.; Bock, K. Albaflavenone, a sesquiterpene ketone with a zizaene skeleton produced by a streptomycete with a new rope morphology. *J Antibiotics* **1994**, *47*, 434-439.

216.   Zhao, B.; Lin, X.; Lei, L.; Lamb, D.C.; Kelly, S.L.; Waterman, M.R.; Cane, D.E. Biosynthesis of the sesquiterpene antibiotic albaflavenone in *Streptomyces coelicolor* A3(2). *J Biol Chem*. **2008**, *283*, 8183–8189.

217.   Sadeghi, A.; Soltani, B.M.; Nekouei, M.K.; Jouzani, G.S.; Mirzaei, H.H.; Sadeghizadeh, M. Diversity of the ectoines biosynthesis genes in the salt tolerant *Streptomyces* and evidence for inductive effect of ectoines on their accumulation. *Microbiol Res*. **2014**, *169*, 699-708.

218.   Sánchez-Hidalgo, M.; González, I.; Díaz-Muñoz, C.; Martínez, G.; Genilloud, O. Comparative genomics and biosynthetic potential analysis of two lichen-isolated *Amycolatopsis* strains. *Front Microbiol*. **2018**, *9*, 1-6.

219.   Katsuyama, Y.; Kita, T.; Funa, N.; Horinouchi, S. Curcuminoid biosynthesis by two type III polyketide synthases in the herb *Curcuma longa*. *J Biol Chem*. **2009**, *284*, 11160–11170.

220. Schmerk, C.L.; Welander, P.V.; Hamad, M.A.; Bain, K.L.; Bernards, M.A.; Summons, R.E.; Valvano, M.A. Elucidation of the *Burkholderia cenocepacia* hopanoid biosynthesis pathway uncovers functions for conserved proteins in hopanoid-producing bacteria. *Environ Microbiol*. **2015**, *17*, 735-750

221. Sohlenkamp, C.; Geiger, O. Bacterial membrane lipids: diversity in structures and pathways. *FEMS Microbiol Rev*. 2016, 40, 133-159.

222. Chen, Z.; Washio, T.; Sato, M.; Suzuki, Y. Cytotoxic effects of several hopanoids on mouse leukemia L1210 and P388 cells. *Biol Pharm Bull*. **1995**, *18*, 421–423.

223. Moreau, R.A.; Hicks, K.B. Bacteriohopanetetrol and related compounds useful for modulation of lipoxygenase activity and anti-inflammatory applications. *US Patent* 6117415B1. **2001**.

224. Kishimoto, S.; Nishimura, S.; Kakeya, H. Total synthesis and structure revision of mirubactin, and its iron binding activity. *Chem Lett*. **2015**, *44*, 1303-1305

225. Pramanik, A.; Stroeher, U.H.; Krejci, J.; Standish, A.J.; Bohn, E.; Paton, J.C.; Autenrieth, I.B.; Braun, V. Albomycin is an effective antibiotic, as exemplified with *Yersinia enterocolitica* and *Streptococcus pneumoniae*. *Int J Med Microbiol*. **2007**, *297*, 459-469.

226. Sulochana, M.B.; Jayachandra, S.Y.; Kumar, S.A.; Parameshwar, A.B.; Reddy, K.M.; Dayanand, A. Siderophore as a potential plant growth-promoting agent produced by *Pseudomonas aeruginosa* JAS-25. *Appl Biochem Biotechnol*. **2014**, *174*, 297–308.

227. Wencewicz, T.A.; Möllmann, U.; Long, T.E.; Miller, M.J. Is drug release necessary for antimicrobial activity of siderophore-drug conjugates? Syntheses and biological studies

of the naturally occurring salmycin "Trojan Horse" antibiotics and synthetic desferridanoxamine-antibiotic conjugates. *Biometals*. **2009**, *22*, 633-648.

228.   Challis, G.L.; Ravel, J. Coelichelin, a new peptide siderophore encoded by the *Streptomyces coelicolor* genome: structure prediction from the sequence of its non-ribosomal peptide synthetase. *FEMS Microbiol Lett*. **2000**, *187*, 111-114.

229.   Williams, D.E.; Davies, J.; Patrick, B.O.; Bottriell, H.; Tarling, T.; Roberge, M.; Andersen, R.J. Cladoniamides A-G, tryptophan-derived alkaloids produced in culture by *Streptomyces uncialis*. *Org Lett*. **2008**, *10*, 3501-3504.

230.   Ma, J.; Huang, H.; Xie, Y.; Liu, Z.; Zhao, J.; Zhang, C.; Ju, J. Biosynthesis of ilamycins featuring unusual building blocks and engineered production of enhanced anti-tuberculosis agents. *Nat Commun*. **2017**, *8*, 1-10.

231.   Minami, Y.; Yoshida, K.I.; Azuma, R.; Urakawa, A.; Kawauchi, T.; Otani, T.; Komiyama, K.; Ōmura, S. Structure of cypemycin, a new peptide antibiotic. *Tetrahedron Lett*. **1994**, *65*, 8001-8004.

232.   Fredenhagen, A.; Fendrich, G.; Marki, F.; Marki, W.; Grunder, J.; Raschdorf, F.; Peter, H.H. Duramycin B and C, two new lanthionine-containing antibiotics as inhibitors of phospholipase A2. Structural revision of duramycin and cinnamycin. *J Antibiot*. **1990**, *43*, 1403–1412.

233.   Shiba, T.; Wakamiya, T.; Fukase, K.; Ueki, Y.; Teshima, T.; Nishikawa, M. Structure of the lanthionine peptides nisin, ancovenin and lanthiopeptin. In: Nisin and Novel Lantibiotics. Jung, G.; Sahl, H-G. eds. ESCOM Leiden. **1991**, 113–122.

234.   Amin, S.A.; Green, D.H.; Kupper, F.C.; Carrano, C.J. Vibrioferrin, an unusual marine siderophore: iron binding, photochemistry, and biological implications. *Inorg Chem*. **2009**, *48*, 11451-11458.

235.   Hagan, A.K.; Plotnick, Y.M.; Dingle, R.E.; Mendel, Z.I.; Cendrowski, S.R.; Sherman, D.H.; Tripathi, A.; Hanna, P.C.Petrobactin protects against oxidative stress and enhances sporulation efficiency in *Bacillus anthracis* Sterne. *mBio*. **2018**, *9*, e02079-18

236.   Banala S, Süssmuth RD. Thioamides in nature: in search of secondary metabolites in anaerobic microorganisms. *Chem Bio Chem*. **2010**, *11*, 1335-1337.

237.   Lu, J.; Wu, Y.; Li, J.; Zhang, Y.; Bai, Z.; Zheng, J.; Zhu, J.; Wang, H. Lanthipeptide synthetases participate in the biosynthesis of 2-aminovinyl-cysteine motifs in thioamitides. **2020**. bioRxiv doi.org/10.1101/2020.08.21.260323

238.   Robinson, S.L.; Christenson, J.K.; Wackett, L.P. Biosynthesis and chemical diversity of β-lactone natural products. *Nat Prod Rep*. **2019**, *36*, 458-475.

239.   Miller, B.R.; Gulick, A.M. Structural biology of non-ribosomal peptide synthetases. *Methods Mol Biol.* **2016**, *140*, 3-29.

240.   Soltani, J. Secondary metabolite diversity of the genus *Aspergillus*: Recent advances in new and future developments. In: Microbial Biotechnology and Bioengineering. 1st edition. Gupta VK ed. Amsterdam: Elsevier. **2016**, 293-301.

241.   Staunton, J. The extraordinary enzymes involved in erythromycin biosynthesis. *Angew Chem Int Ed Engl*. **1991**, *30*, 1302–1306.

242.   Katz, L.; Baltz, R.H. Natural product discovery: Past, present, and future. *J Ind Microbiol Biotechnol*. **2016**, *43*, 155–176.

243.   Erbilgin, N.; Ma, C.; Whitehouse, C.; Shan, B.; Najar, A.; Evenden, M. Chemical similarity between historical and novel host plants promotes range and host expansion of the mountain pine beetle in a naïve host ecosystem. *New Phytol*. **2014**, *201*, 940-950.

244.   Janes, J.K.; Li, Y.; Keeling, C.I.; Yuen, M.M.; Boone, C.K.; Cooke, J.E.; Bohlmann, J.; Huber, D.P.; Murray, B.W.; Coltman, D.W.; Sperling, F.A. How the mountain pine beetle (*Dendroctonus ponderosae*) breached the Canadian Rocky Mountains. *Mol Biol Evol*. **2014**, *31*,1803-1815.

245.   Cullingham, C.I.; Cooke, J.E.; Dang, S.; Davis, C.S.; Cooke, B.J.; Coltman, D.W. Mountain pine beetle host-range expansion threatens the boreal forest. *Mol Ecol*. **2011**, *20*, 2157-2171.

246.   Cooke, B.J.; Carroll, A.L. Predicting the risk of mountain pine beetle spread to eastern pine forests: considering uncertainty in uncertain times. *For Ecol Manage*. **2017**, *396*, 11–25.

247.   James, P.M.; Huber, D.P. TRIA-Net: 10 years of collaborative research on turning risk into action for the mountain pine beetle epidemic. *Can J For Res*. **2019**, *49*, 3-5.

248.   Erbilgin, N. Phytochemicals as mediators for host range expansion of a native invasive forest insect herbivore. *New Phytol*. **2019**, *221*, 1268-1278.

249.   Fettig, C.J.; Munson, A.S.; Grosman, D.M.; Bush, P.B. Evaluations of emamectin benzoate and propiconazole for protecting individual *Pinus contorta* from mortality attributed to colonization by *Dendroctonus ponderosae* and associated fungi. *Pest Manag Sci*. **2014**, *70*, 771-778.

250. Zhang, L.W.; Liu, Y.J.; Yao, J.; Wang, B.; Huang, B.; Li, Z.Z.; Fan, M.Z.; Sun, J.H. Evaluation of *Beauveria bassiana* (*Hyphomycetes*) isolates as potential agents for control of *Dendroctonus valens*. *Insect Sci*. **2011**, *18*, 209-216.

251. Kocacevik, S.; Sevim, A.; Eroglu, M.; Demirbag, Z.; Demir, I. Molecular characterization, virulence and horizontal transmission of *Beauveria pseudobassiana* from *Dendroctonus micans*. *J Appl Entomol*. **2015**, *139*, 381-389.

252. Davis, T.S.; Mann, A.J.; Malesky, D.; Jankowski, E.; Bradley, C. Laboratory and field evaluation of the entomopathogenic fungus *Beauveria bassiana* (*Deuteromycotina: Hyphomycetes*) for population management of spruce beetle, *Dendroctonus rufipennis* (*Coleoptera: Scolytinae*), in felled trees and factors limiting pathogen success. *Environ Entomol*. **2018**, *47*, 594-602.

253. Hallet, S.; Grégoire, J-C.; Coremans-Pelseneer, J. Prospects in the use of entomopathogenous fungus *Beauveria bassiana* (Bals.) Vuill. (*Deuteromycetes, Hyphomycetes*) to control the spruce bark beetle *Ips typographus* L. *Proc Int Symposium Crop Protection*, **1994**, 379–383.

254. Lutyk, P.; Swieczynska, H. Trials of control of the larger pine-shoot beetle *Tomicus piniperda* L. with the use of the fungus *Beauveria bassiana* (Bals.) Vuill. on piled wood. *Sylwan*, **1984**, *128*, 41–45.

255. Dembilio, Ó.; Moya, P.; Vacas, S.; Ortega-García, L.; Quesada-Moraga, E.; Jaques, J.A.; Navarro-Llopis, V. Development of an attract-and-infect system to control *Rhynchophorus ferrugineus* with the entomopathogenic fungus *Beauveria bassiana*. *Pest Manag Sci*. **2018**, *74*, 1861-1869.

256.   Hunt, D.W.; Borden, J.H.; Rahe, J.E.; Whitney, H.S. Nutrient-mediated germination of *Beauveria bassiana* conidia on the integument of the bark beetle *Dendroctonus ponderosae* (*Coleoptera: Scolytidae*). *J Invertebr* Pathol. **1984**, *44*, 304-314.

257.   Shipp, J.L.; Zhang, Y.; Hunt, D.W.; Ferguson, G. Influence of humidity and greenhouse microclimate on the efficacy of *Beauveria bassiana* (Balsamo) for control of greenhouse arthropod pests. *Environ Entomol*. **2003**, *32*, 1154-1163.

258.   Huang, B.F.; Feng, M.G. Comparative tolerances of various *Beauveria bassiana* isolates to UV-B irradiation with a description of a modeling method to assess lethal dose. *Mycopathologia*. **2009**, *168*, 145-152.

259.   Maurer, P.; Couteaudier, Y.; Girard, P.A.; Bridge, P.D.; Riba, G. Genetic diversity of *Beauveria bassiana* and relatedness to host insect range. *Mycol Res*. **1997**, *101*, 159-164.

260.   Sibao, W.A.; Xuexia, M.I.; Weiguo, Z.H.; Huang, B.; Meizhen, F.A.; Zengzhi, L.I.; Huang, Y. Genetic diversity and population structure among strains of the entomopathogenic fungus, *Beauveria bassiana*, as revealed by inter-simple sequence repeats (ISSR). *Mycol Res*. 2005, 109, 1364-1372.

261.   Gasmi, L.; Baek, S.; Kim, J.C.; Lee, M.R.; Kim, S.; Park, S.E.; Li, D.; Shin, T.Y.; Kim, J.S. Gene diversity shapes biological features of entomopathogenic *Beauveria bassiana*. Spring International. *Con KSAE.* **2019**, *1*, 57-58.

262.   Devi, K.U.; Reineke, A.; Reddy, N.N.; Rao, C.U.; Padmavathi, J. Genetic diversity, reproductive biology, and speciation in the entomopathogenic fungus *Beauveria bassiana* (Balsamo) Vuillemin. *Genome*. **2006**, *49*, 495-504.

263.   Rohrlich, C.; Merle, I.; Mze Hassani, I.; Verger, M.; Zuin, M.; Besse, S.; Robene, I.; Nibouche, S.; Costet, L. Variation in physiological host range in three strains of two species of the entomopathogenic fungus *Beauveria*. *PloS One*. **2018**, *13*, e0199199.

264.   Basyouni, S.H.E.; Brewer, D.; Vining, L.C. Pigments of the genus *Beauveria*. *Can J Bot*. **1968**, *46*, 441-448.

265.   Safavi, S.A.; Shah, F.A.; Pakdel, A.K.; Reza, R.G.; Bandani, A.R.; Butt, T.M. Effect of nutrition on growth and virulence of the entomopathogenic fungus *Beauveria bassiana*. *FEMS Microbiol Lett*. **2007**, *270*, 116-123

266.   Liu, H.P.; Skinner, M.; Brownbridge, M.; Parker, B.L. Characterization of *Beauveria bassiana* and *Metarhizium anisopliae* isolates for management of tarnished plant bug, *Lygus lineolaris* (*Hemiptera: Miridae*). *J Inver Pathol*. **2003**, *82*,139-147.

267.   Talaei-Hassanloui, R.; Kharazi-Pakdel, A.; Goettel, M.; Mozaffari, J. Variation in virulence of *Beauveria bassiana* isolates and its relatedness to some morphological characteristics. *Biocontrol Sci Technol*. **2006**, *16*, 525-534.

268.   Romon, P.; Hatting, H.; Goldarazena, A.; Iturrondobeitia, J.C. Variation in virulence of *Beauveria bassiana* and *B. pseudobassiana* to the pine weevil *Pissodes nemorensis* in relation to mycelium characteristics and virulence genes. *Fungal Biol*. **2017**, *121*,189-197.

269.   Kreutz, J.; Vaupel, O.; Zimmermann, G. Efficacy of *Beauveria bassiana* (Bals.) Vuill. against the spruce bark beetle, *Ips typographus* L., in the laboratory under various conditions. *J Appl Entomol*. **2004**, *128*, 384-389.

270.   Al Mazra'awi, M.S.; Shipp, J.L.; Broadbent, A.B.; Kevan, P.G. Dissemination of *Beauveria bassiana* by honeybees (*Hymenoptera: Apidae*) for control of tarnished plant bug (*Hemiptera: Miridae*) on canola. *Environ Entomol.* **2006**, *35*, 1569-1577.

271.   Al Mazra'awi, M.S.; Kevan, P.G.; Shipp, L. Development of *Beauveria bassiana* dry formulation for vectoring by honeybees *Apis mellifera* (*Hymenoptera: Apidae*) to the flowers of crops for pest control. *Biocontrol Sci Technol.* **2007**, *17*, 733-741.

272.   Butt, T.M.; Ibrahim, L.; Ball, B.V.; Clark, S.J. Pathogenicity of the entomogenous fungi *Metarhizium anisopliae* and *Beauveria bassiana* against crucifer pests and the honey bee. *Biocontrol Sci Technol.* **1994**, *4*, 207-214.

273.   Meikle, W.G.; Mercadier, G.; Holst, N.; Nansen, C.; Girod, V. Impact of a treatment of *Beauveria bassiana* (*Deuteromycota: Hyphomycetes*) on honeybee (*Apis mellifera*) colony health and on *Varroa destructor* mites (*Acari: Varroid*ae). *Apidolo*gie. **2008**, *39*, 247-259.

274.   Arathi, H.S.; Spivak, M. Influence of colony genotypic composition on the performance of hygienic behaviour in the honeybee, *Apis mellifera* L. *Ani Behav.* **2001**, *62*, 57-66.

275.   Brownbridge, M.; Costa, S.; Jaronski, S.T. Effects of in vitro passage of *Beauveria bassiana* on virulence to *Bemisia argentifolii. J Invertebr Pathol.* **2001**, *77*, 280-283.

276.   Wang, D.Y.; Fu, B.; Tong, S.M.; Ying, S.H.; Feng, M.G. Two photolyases repair distinct DNA lesions and reactivate UVB-inactivated conidia of an insect mycopathogen under visible light. *Appl Environ Microbiol.* **2019**, *85*, 1-16.

277. Mann, A.J.; Davis, T.S. Plant secondary metabolites and low temperature are the major limiting factors for *Beauveria bassiana* (Bals.-Criv.) Vuill. (*Ascomycota: Hypocreales*) growth and virulence in a bark beetle system. *Biol Control*. **2020**, *141*, 1-11.

278. Jirakkakul, J.; Cheevadhanarak, S.; Punya, J.; Chutrakul, C.; Senachak, J.; Buajarern, T.; Tanticharoen, M.; Amnuaykanjanasin, A. Tenellin acts as an iron chelator to prevent iron-generated reactive oxygen species toxicity in the entomopathogenic fungus *Beauveria bassiana*. *FEMS Microbiol Lett*. **2015**, *362*, 1-8.

279. Fernandes, E.K.; Rangel, D.E.; Moraes, Á.M.; Bittencourt, V.R.; Roberts, D.W. Variability in tolerance to UV-B radiation among *Beauveria* spp. isolates. *J Invertebr Pathol*. **2007**, *96*, 237-243.

280. Cagan, L.; Svercel, M. The influence of UV on pathogenicity of entomopathogenic fungus *Beauveria bassiana* (Balsamo) vuillemin to the European corn borer, *Ostrinia nubilalis* HBN. (*Lepidoptera: Crambidae*). *J Central Eur Agric.* **2001**, *2*, 228-234.

281. Kaiser, D.; Bacher, S.; Mène-Saffrané, L.; Grabenweger, G. Efficiency of natural substances to protect *Beauveria bassiana* conidia from UV radiation. *Pest Manag Sci*. **2018**, *75*, 556-563.

282. Chiu, C.C.; Keeling, C.I.; Bohlmann, J. Toxicity of pine monoterpenes to mountain pine beetle. *Sci Rep*. **2017**, *7*, 1-8.

283. Chiu, C.C.; Keeling, C.I.; Bohlmann, J. Monoterpenyl esters in juvenile mountain pine beetle and sex-specific release of the aggregation pheromone trans-verbenol. *Proc Natl Acad Sci U S A*. **2018**, *115*, 3652-3657.

284.   Chiu, C.C.; Keeling, C.I.; Bohlmann, J. The cytochrome P450 CYP6DE1 catalyzes the conversion of α-pinene into the mountain pine beetle aggregation pheromone trans-verbenol. *Sci Rep*. **2019**, *9*, 1-0.

285.   Jakus, R.; Blazenec, M. Treatment of bark beetle attacked trees with entomopathogenic fungus *Beauveria bassiana* (Balsamo) Vuillemin. *Folia For Pol Ser A For*. **2011**, *53*,150-155.

286.   Grodzki, W.; Kosibowicz, M. An attempt to use the fungus *Beauveria bassiana* (Bals.) Vuill. in forest protection against the bark beetle *Ips typographus* (L.) in the field. *For Res Papers*. **2015**, *76*, 5-17.

287.   Barta, M.; Kautmanová, I.; Čičková, H.; Ferenčík, J.; Florián, S.; Novotný, J.; Kozánek, M. The potential of *Beauveria bassiana* inoculum formulated into a polymeric matrix for a microbial control of spruce bark beetle. *Bio Sci Tech*. **2018**, *28*, 718-735.

288.   Rosana, A.R.R.; Pokorny, S.; Klutsch, J.G.; Ibarra-Romero, C.; Sanichar, R.; Engelhardt, D.; van Belkum, M.J.; Erbilgin, N.; Bohlmann, J.; Carroll, A.L.; Vederas, J.C. Selection of entomopathogenic fungus *Beauveria bassiana* (*Deuteromycotina: Hyphomycetes*) for the biocontrol of *Dendroctonus ponderosae* (*Coleoptera: Curculionidae, Scolytinae*) in Western Canada. *Appl Microbiol Biotechnol*. **2021**, *105*, 2541-2557.

289.   Posada-Flórez, F.J. Production of *Beauveria bassiana* fungal spores on rice to control the coffee berry borer, *Hypothenemus hampei*, in Colombia. *J Insect Sci*. **2008** *8*, 1-13.

290.   Das, P.; Hazarika, L.K.; Bora, D. Study on mass production of *Beauveria bassiana* (Bals.) Vuill. for the management of rice hispa, *Dicladispa armigera* (Olivier). *Cutt Res Agric Sci* **2021**, *11*, 100-107.

291.   Hunt, D.W.A. 1986 Absence of fatty acid germination inhibitors for conidia of *Beauveria bassiana* on the integument of the bark beetle *Dendroctonus ponderosae* (*Coleoptera: Scolytidae*). *Can Entomol*. **1986**, *118*, 837-838.

292.   Fan, Y.; Liu, X.; Keyhani, N.O.; Tang, G.; Pei, Y.; Zhang, W.; Tong, S. Regulatory cascade and biological activity of *Beauveria bassiana* oosporein that limits bacterial growth after host death. *Proc Natl Acad Sci U S A*. **2017**, *114*, 1578-1586.

293.   Feng, P.; Shang, Y.; Cen, K.; Wang, C. Fungal biosynthesis of the bibenzoquinone oosporein to evade insect immunity. *Proc Natl Acad Sci U S A*. **2015**, *112*, 11365-11370.

294.   Klutsch, J.G, Cale, J.A.; Whitehouse, C.; Kanekar, S.S.; Erbilgin, N. Trap trees: An effective method for monitoring mountain pine beetle activities in novel habitats. *Can J For Res*. **2017**, *47*, 1-6.

295.   Mayfield III, A.E.; Juzwik, J.; Scholer, J.; Vandenberg, J.D.; Taylor, A. Effect of bark application with *Beauveria bassiana* and permethrin insecticide on the walnut twig beetle (*Coleoptera: Curculionidae*) in black walnut bolts. *J Econ Entomol*. **2019**, *112*, 2493-2496.

296.   Chakraborty, A.; Modlinger, R.; Ashraf, M.Z.; Synek, J.; Schlyter, F.; Roy, A. Core mycobiome and their ecological relevance in the gut of five *Ips* bark beetles (*Coleoptera: Curculionidae: Scolytinae*). *Front Microbiol*. **2020**, 11, 1-16.

297.   Tsui, C.K.; Beauseigle, S.; Ojeda, Alayon, D.I.; Rice, A.V.; Cooke, J.E.; Sperling, F.A.; Roe, A.D.; Hamelin, R.C. Fine-scale genetic diversity and relatedness in fungi associated with the mountain pine beetle. *Can J Forest Res*. **2019**, 48, 933-941.

298.   Zipfel, R.D.; de Beer, Z.W.; Jacobs, K.; Wingfield, B.D.; Wingfield, M.J. Multi-gene phylogenies define *Ceratocystiopsis* and *Grosmannia* distinct from *Ophiostoma*. *Stud Mycol*. **2006**, *55*, 75–97.

299.   Plattner, A.; Kim, J.J.; DiGuistini, S.; Breuil, C. Variation in pathogenicity of a mountain pine beetle–associated blue-stain fungus, *Grosmannia clavigera*, on young lodgepole pine in British Columbia. *Can J Plant Pathol*. **2008**, *30*,457-466.

300.   Lee, S.; Kim, J.-J.; Breuil C. *Leptographium longiclavatum* sp. nov., a new species associated with the mountain pine beetle, *Dendroctonus ponderosae*. Mycol. Res. **2005**, *109*, 1162–1170.

301.   Rumbold, C.T. A blue stain fungus, *Ceratostomella m*ontiumn. sp., and some yeasts associated with two species of *Dendroctonus*. *J Agric Res*. **1941**, *62*, 589601.

302.   Khadempour, L.; LeMay, V.; Jack, D.; Bohlmann, J.; Breuil C. The relative abundance of mountain pine beetle fungal associates through the beetle life cycle in pine trees. *Microb Ecol*. **2012** *64,* 909–917.

303.   Cale, J.A.; Klutsch, J.G.; Dykstra, C.B.; Peters, B.; Erbilgin, N. Pathophysiological responses of pine defensive metabolites largely lack differences between pine species but vary with eliciting ophiostomatoid fungal species. *Tree Physiol*. **2019**, *39,* 1121-1135.

304.   Amin, G.A.; Youssef, N.A.; Bazaid, S.; Saleh, W.D. Assessment of insecticidal activity of red pigment produced by the fungus *Beauveria bassiana*. *World J Microbiol Biotechnol*. **2010**, *26*, 2263-2268.

305.	Eley, K.L.; Halo, L.M.; Song, Z.; Powles, H.; Cox, R.J.; Bailey, A.M.; Lazarus, C.M.; Simpson, T.J. Biosynthesis of the 2-pyridone tenellin in the insect pathogenic fungus *Beauveria bassiana*. *Chem Bio Chem*. **2007**, *8*, 289-297.

306.	Jeffs, L.B.; Khachatourians, G.G. Toxic properties of *Beauveria* pigments on erythrocyte membranes. *Toxicon*. **1997**, *35*, 1351-1356.

307.	Singh, D.; Son, S.Y.; Lee, C.H. Perplexing metabolomes in fungal-insect trophic interactions: A terr incognita of mycobiocontrol mechanisms. *Front Microbiol*. **2016**, 7, 1-13.

308.	Halo, L.M.; Marshall, J.W.; Yakasai, A.A.; Song, Z.; Butts, C.P.; Crump, M.P.; Heneghan, M.; Bailey, A.M.; Simpson, T.J.; Lazarus, C.M.; Cox, R.J. Authentic heterologous expression of the tenellin iterative polyketide synthase nonribosomal peptide synthetase requires coexpression with an enoyl reductase. *Chem Bio Chem*. **2008**, *9*, 585-594.

309.	Boettger, D.; Hertweck, C. Molecular diversity sculpted by fungal PKS– NRPS hybrids. *Chem Bio Chem*. **2013**, *14*, 28–42.

310.	Alurappa, R.; Bojegowda, M.R.; Kumar, V.; Mallesh, N.K.; Chowdappa, S. Characterisation and bioactivity of oosporein produced by endophytic fungus *Cochliobolus kusanoi* isolated from *Nerium oleander* L. *Nat Prod Res*. **2014**, *28*, 2217-2220.

311.	Da Costa Souza, P.N.; Grigoletto, T.L.; de Moraes, L.A.; Abreu, L.M.; Guimarães, L.H.; Santos, C.; Galvão LR, Cardoso, P.G. Production and chemical characterization of pigments in filamentous fungi. *Microbiol*. **2016**, *162*, 12-22.

312.	Mc Namara, L.; Dolan, S.K.; Walsh, J.M.; Stephens, J.C.; Glare, T.R.; Kavanagh, K.; Griffin, C.T. Oosporein, an abundant metabolite in *Beauveria caledonica*, with a

feedback induction mechanism and a role in insect virulence. *Fungal Biol*. **2019**, *123*, 601-610.

313.   Ávila-Hernández, J.G.; Carrillo-Inungaray, M.L.; De, R.; la Cruz-Quiroz, J.E.; Paz, D.B.; Parra, R.; Aguilar, C.N.; Aguilar-Zárate, P.; Huasteca, Z.; del Campo, R. *Beauveria bassiana* secondary metabolites: a review inside their production systems, biosynthesis, and bioactivities. *Mex J Biotechnol.* **2020**, *5*, 1-33.

314.   Daas, M.S.; Rosana, A.R.; Acedo, J.Z.; Douzane, M.; Nateche, F.; Kebbouche-Gana, S.; Vederas, J.C. Insights into the draft genome sequence of bioactives-producing *Bacillus thuringiensis* DNG9 isolated from Algerian soil-oil slough. *Stand Gen Sci*. **2018**, *13*, 1-10.

315.   Bernardo, S.P.; Rosana, A.R.R.; de Souza, A.N.; Chiorean, S.; Martins, M.L.; Vederas, J.C. Draft genome sequence of the thermophilic bacterium *Bacillus licheniformis* SMIA-2, an antimicrobial- and thermostable enzyme-producing isolate from Brazilian soil. *Microbiol Res Announc*. **2020**, *9*, e00106-20.

316.   Oliveros, K.M.; Rosana, A.R.R.; Montecillo, A.D.; Opulencia, R.B.; Jacildo, A.J.; Zulaybar, T.O.; Raymundo, A.K. Genomic insights into the antimicrobial and anticancer potential of *Streptomyces* sp. A1-08 isolated from the volcanic soils of Mount Mayon, Philippines. *Phil J Sci*. **2021**,*150*, 1351-1377.

317.   Clinical and Laboratory Standards Institute. Methods for Dilution Antimicrobial susceptibility tests for bacteria that grow aerobically; Approved Standard. 9th ed. Pennysylvania, USA: Clinical and Laboratory Standards Institute. **2012**. 1-19.

318.   Helgason, E.; Økstad, O.A.; Caugant, D.A.; Johansen, H.A.; Fouet, A.; Mock, M.; Hegna, I.; Kolstø, A.B. *Bacillus anthracis*, *Bacillus cereus*, and *Bacillus thuringiensis—*

one species on the basis of genetic evidence. *Appl Environ Microbiol*. **2000**, *66*, 2627-2630.

319.   Field, D.; Garrity, G.; Gray, T.; Morrison, N.; Selengut, J.; Sterk, P.; Tatusova, T.; Thomson, N.; Allen, M.J.; Angiuoli, S.V.; Ashburner, M. The minimum information about a genome sequence (MIGS) specification. *Nat Biotechnol*. **2008**, *26*, 541-547

320.   Rosana, A.R.R.; Chamot, D.; Owttrim, G.W. Autoregulation of RNA helicase expression in response to temperature stress in *Synechocystis* sp. PCC 6803. *PloS One*. **2012**, *7*, e48683.

321.   Woese, C.R.; Kandler, O.; Wheelis, M.L. Towards a natural system of organisms: proposal for the domains Archaea, Bacteria, and Eucarya. *Proc Natl Acad Sci USA*. **1990**, *87*, 4576-4579.

322.   Gibbons, N.E.; Murray, R.G. Proposals concerning the higher taxa of bacteria. *Int J Syst Evol Microbiol*. **1978**, *28*, 1-6.

323.   Ludwig, W.; Schleifer, K.H.; Whitman, W.B. Class I. Bacilliclass nov. *In*: De Vos, P.; Garrity, G.; Jones, D.; Krieg, N.R.; Ludwig, W. editors. Bergey's Manual of Systematic Bacteriology New York: Springer-Verlag **2009**. 19–20.

324.   Prévot, A.R. *In*: Hauderoy, P.; Ehringer, G.; Guillot, G.; Magrou, J.; Prévot, A.R.; Rosset, D.; Urbain, A. editors. Dictionnaire des Bactéries Pathogènes. Paris: Masson et Cie; **1953**, 1–692.

325.   Logan, N.A.; Berge, O.; Bishop, A.H.; Busse, H.J.; De Vos, P.; Fritze, D.; Heyndrickx, M.; Kämpfer, P.; Rabinovitch, L.; Salkinoja-Salonen, M.S.; Seldin, L. Proposed minimal standards for describing new taxa of aerobic, endospore-forming bacteria. *Int J Syst Evol Microbiol*. **2009**, *59*, 2114-2121.

326.   Skerman, V.B.; McGowan, V.; Sneath, P.H. Approved lists of bacterial names. *Int J Syst Evol Microbiol*. **1980**, *30*, 225-420.

327.   Berliner, E. Über die Schlaffsucht der Mehlmottenraupe (Ephestia kühniella Zell.) und ihren Erreger *Bacillus thuringiensis* n. sp. *J Appl Entomol*. **1915**, *2*, 29-56.

328.   Barjac, H.; Frachon, E. Classification of *Bacillus thuringiensis* strains. *BioControl*. **1990**, *35*, 233-340.

329.   West, A.W.; Burges, H.; Dixon, T.J.; Wyborn, C.H. Survival of *Bacillus thuringiensis* and *Bacillus cereus* spore inocula in soil: effects of pH, moisture, nutrient availability and indigenous microorganisms. *Soil Biol Biochem*. **1985**, *17*, 657-665.

330.   Vilas-Boas, G.T.; Peruca, A.P.; Arantes, O.M. Biology and taxonomy of *Bacillus cereus*, *Bacillus anthracis*, and *Bacillus thuringiensis*. *Can J Microbiol*. **2007**, *53*, 673-687.

331.   Schnepf, E.; Crickmore, N.V.; Van Rie, J.; Lereclus, D.; Baum, J.; Feitelson, J.; Zeigler, D.R.; Dean, D. *Bacillus thuringiensis* and its pesticidal crystal proteins. *Microbiol Molec Biol Rev*. **1998**, *62*, 775-806.

332.   Ashburner, M.; Ball, C.A.; Blake, J.A.; Botstein, D.; Butler, H.; Cherry, J.M.; Davis, A.P.; Dolinski, K.; Dwight, S.S.; Eppig, J.T.; Harris, M.A. Gene Ontology: tool for the unification of biology. *Nat Genet*. **2000**, *25*, 25-29.

333.   Tatusova, T.; DiCuccio, M.; Badretdin, A.; Chetvernin, V.; Nawrocki, E.P.; Zaslavsky, L.; Lomsadze, A.; Pruitt, K.D.; Borodovsky, M.; Ostell, J. NCBI prokaryotic genome annotation pipeline. *Nucleic Acids Res*. **2016**, *44*, 6614-6624.

334.   Chen, I.M.; Markowitz, V.M.; Chu, K.; Palaniappan, K.; Szeto, E.; Pillay, M.; Ratner, A.; Huang, J.; Andersen, E.; Huntemann, M.; Varghese, N. IMG/M: integrated

genome and metagenome comparative data analysis system. *Nucleic Acids Res*. **2017,** *45*, D507-D516.

335.   Hyatt, D.; Chen, G.L.; LoCascio, P.F.; Land, M.L.; Larimer, F.W.; Hauser, L.J. Prodigal: prokaryotic gene recognition and translation initiation site identification. *BMC Bioinformatics*. **2010**, *11*, e19.

336.   Aziz, R.K.; Bartels, D.; Best, A.A.; DeJongh, M.; Disz, T.; Edwards, R.A. Formsma, K.; Gerdes, S.; Glass, E.M.; Kubal, M.; Meyer, F. The RAST Server: rapid annotations using subsystems technology. *BMC Genomics*. **2008**, *9*, e75.

337.   Van Domselaar, G.H.; Stothard, P.; Shrivastava, S.; Cruz, J.A.; Guo, A.; Dong, X.; Lu, P.; Szafron, D.; Greiner, R.; Wishart, D.S. BASys: a web server for automated bacterial genome annotation. *Nucleic Acids Res*. **2005**, *33*, W455-W459.

338.   Grissa, I.; Vergnaud, G.; Pourcel, C. CRISPRFinder: a web tool to identify clustered regularly interspaced short palindromic repeats. *Nucleic Acids Res*. **2007**, *35*, W52-W57.

339.   Galardini, M.; Biondi, E.G.; Bazzicalupo, M.; Mengoni, A. CONTIGuator: a bacterial genomes finishing tool for structural insights on draft genomes. *Source Code Biol Med*. **2011**, *6*, e11.

340.   Bosi, E.; Donati, B.; Galardini, M.; Brunetti, S.; Sagot, M.F.; Lió, P.; Crescenzi, P.; Fani, R.; Fondi, M. MeDuSa: a multi-draft based scaffolder. *Bioinformatics*. **2015**, *31*, 2443-2451.

341.   Grant, J.R.; Stothard, P. The CGView Server: a comparative genomics tool for circular genomes. *Nucleic Acids Res*. **2008**, *36*, W181-W184.

342.   Varghese, N.J.; Mukherjee, S.; Ivanova, N.; Konstantinidis, K.T.; Mavrommatis, K.; Kyrpides, N.C.; Pati, A. Microbial species delineation using whole genome sequences. *Nucleic Acids Res*. **2015**, *43*, 6761-6771.

343.   Rosana, A.R.R.; Whitford, D.S.; Fahlman, R.P. Owttrim, G.W. Cyanobacterial RNA helicase CrhR localizes to the thylakoid membrane region and cosediments with degradosome and polysome complexes in *Synechocystis* sp. strain PCC 6803. *J Bacterio*l. **2016**, *198*, 2089-2099.

344.   Schaeffer, A.B.; Fulton, M.D. A simplified method of staining endospores. *Science*. **1993**, *77*, 194.

345.   Aziz, R.K.; Bartels, D.; Best, A.A.; DeJongh, M.; Disz, T.; Edwards, R.A.; Formsma, K.; Gerdes, S.; Glass, E.M.; Kubal, M.; Meyer, F.; Olsen, G.J.; Olson, R.; Osterman, A.L.; Overbeek, R.A.; McNeil, L.K.; Paarmann, D.; Paczian, T.; Parrello, B.; Pusch, G.D.; Reich, C.; Stevens, R.; Vassieva, O.; Vonstein, V.; Wilke, A.; Zagnitko, O. The RAST server ver 2.0: rapid annotations using subsystems technology. *BMC Genomics*. **2008**, *9*, e75

346.   Richter, M.; Rosselló-Móra, R. Shifting the genomic gold standard for the prokaryotic species definition. *Proc Natl Acad Sci U S A*. **2009**, *106*: 19126-19131.

347.   Weber, T.; Blin, K.; Duddela, S.; Krug, D.; Kim, H.U.; Bruccoleri, R.; Lee, S.Y.; Fischbach, M.A.; Müller, R.; Wohlleben, W.; Breitling, R.; Takano, E.; Medema, M.H. antiSMASH 3.0—a comprehensive resource for the genome mining of biosynthetic gene clusters. *Nucleic Acids Res*. **2015**, *43*, W237-W243.

348. van Heel, A.J.; de Jong, A.; Montalbán-López, M.; Kok, J.; Kuipers, O.P. BAGEL3: automated identification of genes encoding bacteriocins and (non-)bactericidal posttranslationally modified peptides. *Nucleic Acids Res* **2013**, *41*, W448 –W453.

349. Markowitz, V.M.; Chen, I.M.; Palaniappan, K.; Chu, K.; Szeto, E.; Pillay, M.; Ratner, A.; Huang, J.; Woyke, T.; Huntemann, M.; Anderson, I. IMG 4 version of the integrated microbial genomes comparative analysis system. *Nucleic Acids Res*. **2013**, *42*, D560-D567.

350. Blin, K.; Wolf, T.; Chevrette, M.G.; Lu, X.; Schwalen, C.J.; Kautsar, S.A.; Duran, S.; Hernando, G.; de los Santos, E.L.; Kim, H.U.; Nave, M. antiSMASH 4.0— improvements in chemistry prediction and gene cluster boundary identification. *Nucleic Acids Res*. **2017**, *45*, W36-W41.

351. Peng, Y.; Leung, H.C.; Yiu, S.M.; Chin, F.Y. IDBA-UD: a de novo assembler for single-cell and metagenomic sequencing data with highly uneven depth. *Bioinformatics*. **2012**, *28*, 1420-1428.

352. Yoon, S.H.; Ha, S.M.; Lim, J.M.; Kwon, S.J.; Chun, J. A large-scale evaluation of algorithms to calculate average nucleotide identity. *Antonie van Leeuwenhoek*. **2017**, *110*, 1281–1286.

353. Chaudhari, N.M.; Gupta, V.K.; Dutta, C. BPGA- an ultra-fast pan-genome analysis pipeline. *Sci Rep*. **2016**, *6*, 1-10.

354. Larkin, M.A.; Blackshields, G.; Brown, N.P.; Chenna, R.; McGettigan, P.A.; McWilliam, H.; Valentin, F.; Wallace, I.M.; Wilm, A.; Lopez, R.; Thompson, J.D. Clustal W and Clustal X version 2.0. *Bioinformatics*. **2007**, *23*, 2947-2948.

355.	Kearse, M.; Moir, R.; Wilson, A.; Stones-Havas, S.; Cheung, M.; Sturrock, S.; Buxton, S.; Cooper, A.; Markowitz, S.; Duran, C.; Thierer, T. Geneious Basic: an integrated and extendable desktop software platform for the organization and analysis of sequence data. *Bioinformatics*. **2012**, *28*, 1647-1649.

356.	Stamatakis, A. RAxML version 8: a tool for phylogenetic analysis and post-analysis of large phylogenies. *Bioinformatics*. **2014**, 30, 1312-1313.

357.	Grant, J.R.; Arantes, A.S.; Stothard, P. Comparing thousands of circular genomes using the CGView Comparison Tool. *BMC Genomics.* **2012**, *13*, 1-8.

358.	Altschul, S.F.; Gish, W.; Miller, W.; Myers, E.W.; Lipman, D.J. Basic local alignment search tool. *J Mol Biol.* **1990**, *215*, 403-410.

359.	Das, M.; Das, S.K.; Mukherjee, R.K. Surface active properties of the culture filtrates of a *Micrococcus* species grown on n-alkanes and sugars. *Biores Technol.* **1998**, *63*, 231-235.

360.	Bodour, A.A.; Miller-Maier, R.M. Application of a modified drop-collapse technique for surfactant quantitation and screening of biosurfactant-producing microorganisms *J Microbiol Methods*. **1998**, *32*, 273-280.

361.	Youssef, N.H.; Duncan, K.E.; Nagle, D.P.; Savage, K.N.; Knapp, R.M.; McInerney, MJ. Comparison of methods to detect biosurfactant production by diverse microorganisms. *J Microbiol Methods*. **2004**, *56*, 339-347.

362.	Morikawa, M.; Hirata, Y.; Imanaka, T. A study on the structure-function relationship of lipopeptide biosurfactants. *Biochim Biophys Acta*. **2000**, 1488: 211-218.

363.	Shirling, E.B.; Gottlieb, D. Methods, classification, identification and description of genera and species. *Int J Syst Bacteriol*. **1966**, *2*, 61–292.

364.   Zulaybar, T.O.; Raymundo, A.K.; Casyao, J.M. Effect of gamma irradiation on the tylosin yield of *Streptomyces fradiae* No. 93. *Philipp J Biotechnol*. **1997**, *8*, 31-38.

365.   Zulaybar, T.O.; Marfori, E.C.; Papa, I.A.; Perez, M.T.M. Structural characterization of bioactive compounds from Philippine microorganisms: Part 1. Antimicrobial compound from locally isolated *Streptomyces* sp. **2011**, Retrieved from https://agris.fao.org/ on February 22, 2021.

366.   Mosmann, T. Rapid colorimetric assay for cellular growth and survival: Application to proliferation and cytotoxicity assays. *J Immunol Meth*. **1983**, 65, 55-63.

367.   Newberry, C.J.; Webster, G.; Cragg, B.A.; Parkes, R.J.; Weightman, A.J.; Fry, J.C. Diversity of prokaryotes and methanogenesis in deep subsurface sediments from the Nankai Trough, Ocean Drilling Program Leg 190. *Environ Microbiol*. **2004**, *6*, 274-287.

368.   Muyzer, G.; Teske, A.; Wirsen, C.O.; Jannasch, H.W. Phylogenetic relationships of *Thiomicrospira* species and their identification in deep-sea hydrothermal vent samples by denaturing gradient gel electrophoresis of 16S rDNA fragments. ***Arch Microbiol.* 1995,** *164*, 165-172.

369.   Andrews, S. FastQC: a quality control tool for high throughput sequence data. **2010** Retrieved from https://www.bioinformatics.babraham.ac.uk/projects/fastqc on April 11 2021.

370.   Bushnell,   B.   BBTools   software.   **2014**, package.https://sourceforge.net/projects/bbmap/

371.   Bankevich, A.; Nurk, S.; Antipov, D.; Gurevich, A.A.; Dvorkin, M.; Kulikov, A.S.; Lesin, V.M.; Nikolenko, S.I.; Pham, S.; Prjibelski, A.D.; Pyshkin, A.V. SPAdes: a new

genome assembly algorithm and its applications to single-cell sequencing. *J Comput Biol*. **2012**, *19*, 455-477.

372.   Gurevich, A.; Saveliev, V.; Vyahhi, N.; Tesler, G. QUAST: quality assessment tool for genome assemblies. *Bioinformatics.* **2013**, *29*, 1072–1075.

373.   Stothard, P.; Wishart, D.S. Circular genome visualization and exploration using CG view. *Bioinformatics*. **2005**, *21*, 537-539.

374.   Seemant, T. Prokka: rapid prokaryotic genome annotation. *Bioinformatics*. **2014**, *30*, 2068-2069.

375.   Meier-Kolthoff, J.P.; Göker, M. TYGS is an automated high-throughput platform for state-of-the-art genome-based taxonomy. *Nature Commun*. **2019**, *10*, 1-10.

376.   Meier-Kolthoff, J.P.; Hahnke, R.L.; Petersen, J.; Scheuner, C.; Michael, V.; Fiebig, A.; Rohde, C.; Rohde, M.; Fartmann, B.; Goodwin, L.A.; Chertkov, O. Complete genome sequence of DSM 30083[T], the proposal for delineating subspecies in microbial taxonomy. *Stand Genomic Sci*. **2014**, *9*, 1–19.

377.   Lefort, V.; Desper, R.; Gascuel, O. FastME 2.0: A comprehensive, accurate, and fast distance-based phylogeny inference program. *Molec Biol Evol.* **2015**, *32*, 2798–2800.

378.   Kreft, L.; Botzki, A.; Coppens, F.; Vandepoele, K.; Van Bel, M. PhyD3: A phylogenetic tree viewer with extended phyloXML support for functional genomics data visualization. *Bioinformatics*. **2017**, *33*, 2946–2947.

379.   Blin, K.; Shaw, S.; Kloosterman, A.M.; Charlop-Powers, Z.; van Wezel, G.P.; Medema, M.H.; Weber, T. antiSMASH 6.0: improving cluster detection and comparison capabilities. *Nucleic Acids Res*. **2021**, *1*, 1-6.

380.   Kautsar, S.A.; Blin, K.; Shaw, S.; Navarro-Muñoz, J.C.; Terlouw, B.R.; van der Hooft, J.J.; Van Santen, J.A.; Tracanna, V.; Suarez Duran, H.G.; Pascal Andreu, V.; Selem-Mojica, N. MIBiG 2.0: a repository for biosynthetic gene clusters of known function. *Nucleic Acids Res*. 2020, 48, D454-458.

381.   Skinnider, M.A.; Johnston, C.W.; Gunabalasingam, M.; Merwin, N.J.; Kieliszek, A.M.; MacLellan, R.J.; Li, H.; Ranieri, M.R.; Webster, A.L.; Cao, M.P.; Pfeifle, A. 2020. Comprehensive prediction of secondary metabolite structure and biological activity from microbial genome sequences. *Nat Com*. **2020**, *11*, 1-9.

382.   Laatsch, H. AntiBase: the natural compound identifier. Weinheim: Wiley-Vch. **2017**, 220 p.

383.   Flissi, A.; Ricart, E.; Campart, C.; Chevalier, M.; Dufresne, Y.; Michalik, J.; Jacques, P.; Flahaut, C.; Lisacek, F.; Leclère, V.; Pupin, M. Norine: update of the nonribosomal peptide resource. *Nucleic Acids Res*. **2020**, *48*, D465-D469.

384.   Zhang, L.B.; Tang, L.; Ying, S.H.; Feng, M.G. Regulative roles of glutathione reductase and four glutaredoxins in glutathione redox, antioxidant activity, and iron homeostasis of *Beauveria bassiana*. *Appl Microbiol Biotechnol*. **2016**, *100*, 5907-5917.

385.   Burke, J.L.; Carroll, A.L. Breeding matters: Natal experience influences population state-dependent host acceptance by an eruptive insect herbivore. *PloS One*. **2017**, *12*, e0172448.

386.   Burke, J.L.; Carroll, A.L. The influence of variation in host tree monoterpene composition on secondary attraction by an invasive bark beetle: implications for range expansion and potential host shift by the mountain pine beetle. *Forest Ecol Manag*. **2016**, *359*, 59-64.

387.   Mori, K. Synthesis of optically pure (+)-trans-verbenol and its antipode, the pheromone of *Dendroctonus* bark beetles. *Agric Biol Chem*. **1976**, *40*, 415-418.

388.   Mayr-Harting, A.; Hedges, A.J.; Berkeley, R.C.W. Methods for studying bacteriocins. In Bergen, T.; Norris, J.R. (eds) Methods in Microbiology. London: Academic Press. **1972**, 315-422.

389.   Lyon, R.L. A useful secondary sex character in *Dendroctonus* bark beetles. *Can Entomol*. **1985**, *90*, 582–584.

390.   Klutsch, J.G.; Najar, A.; Cale, J.; Erbilgin, N. Direction of interaction between mountain pine beetle (*Dendroctonus ponderosae*) and resource-sharing wood-boring beetles depends on plant parasite infection. *Oecologia*. **2016**, *182*, 1-12.

391.   R Core Team. R: A language and environment for statistical computing. R Foundation for Statistical Computing, Vienna, Austria. **2019**.

392.   Teshler, Miron.; Todorova, S.I. Compacted pesticide formulations. Anatis Bioprotection, Inc. US Patent US2015272129A1. **2015**.

393.   Ullah, A.; Klutsch, J.G.; Erbilgin, N. Production of complementary defense metabolites reflects a co-evolutionary arms race between a host plant and a mutualistic bark beetle-fungal complex. *Plant Cell Environ*. **2021**, *44*, 3064–3077

394.   Hussain, A.; Rodriguez-Ramos, J.C.; Erbilgin, N. Spatial characteristics of volatile communication in lodgepole pine trees: Evidence of kin recognition and intra-species support. *Sci Total Environ*. **2019**, *692*, 127-135.

395.   Guevara-Rozo, S.; Hussain, A.; Cale, J.A.; Klutsch, J.G.; Rajabzadeh, R.; Erbilgin, N. Nitrogen and ergosterol concentrations varied in live jack pine phloem following

inoculations with fungal associates of mountain pine beetle. *Front Microbiol*. **2020**, *11*, 1-10.

396.   Schneider, C.A.; Rasband, W.S.; Eliceiri, K.W. NIH Image to ImageJ: 25 years of image analysis. *Nat Methods*. **2012**, *9*, 671–675.

397.   Chevrette, M.G.; Aicheler, F.; Kohlbacher, O.; Currie, C.R.; Medema, M.H. SANDPUMA: ensemble predictions of nonribosomal peptide chemistry reveal biosynthetic diversity across Actinobacteria. *Bioinformatics*. **2017**, *33*, 3202-3210.